



THE HONG KONG  
POLYTECHNIC UNIVERSITY

香港理工大學

Pao Yue-kong Library

包玉剛圖書館

---

## Copyright Undertaking

This thesis is protected by copyright, with all rights reserved.

**By reading and using the thesis, the reader understands and agrees to the following terms:**

1. The reader will abide by the rules and legal ordinances governing copyright regarding the use of the thesis.
2. The reader will use the thesis for the purpose of research or private study only and not for distribution or further reproduction or any other purpose.
3. The reader agrees to indemnify and hold the University harmless from and against any loss, damage, cost, liability or expenses arising from copyright infringement or unauthorized usage.

### IMPORTANT

If you have reasons to believe that any materials in this thesis are deemed not suitable to be distributed in this form, or a copyright owner having difficulty with the material being included in our database, please contact [lbsys@polyu.edu.hk](mailto:lbsys@polyu.edu.hk) providing details. The Library will look into your claim and consider taking remedial action upon receipt of the written requests.

**The Hong Kong Polytechnic University**

**Institute of Textiles and Clothing**

**NANO FUNCTIONAL SCAFFOLDS FOR  
TISSUE ENGINEERING**

by  
**Li Lin**

A Thesis Submitted in Partial Fulfillment of the Requirements for the  
Degree of Doctor of Philosophy

**March 2010**

## CERTIFICATE OF ORIGINALITY

I hereby declare that this thesis is my own work and that, to the best of my knowledge and belief, it reproduces no material previously published or written, nor material that has been accepted for the award of any other degree or diploma, except where due acknowledgement has been made in the text.

\_\_\_\_\_ (Signed)

Li Lin (Name of student)

## ABSTRACT

### **Nano Functional Scaffolds for Tissue Engineering**

Li Lin

**Supervisors:** Prof. Yi Li, Prof. Frank Ko, Prof. Ling Qin, Prof. Arthur FT Mak

Scaffolds for tissue engineering should have good biocompatibility and antibacterial properties to reduce the risk of infection and improve healing. Poly-L-Lactide (PLLA), which is biocompatible, biodegradable, and an immunologically inert synthetic polymer was selected for the fabrication of tissue engineering scaffolds in this study. Silver and its compounds have been studied for many years because of their strong antibacterial activity and low toxicity. It has been found that its toxicity was related to the individual silver species rather than total silver concentration. Furthermore the toxicity of silver mainly depends on the active, free  $\text{Ag}^+$  concentration. Therefore, the cytotoxicity and antibacterial property of PLLA scaffolds composed with silver nanoparticles (Ag/PLLA scaffolds) were studied. Wool keratin has been reported as being suitable for long-term cell cultivation with a high cell density. Therefore the cytotoxicity and cell proliferation of PLLA/keratin (Pk) scaffolds composed with wool keratin were explored as well.

In this study, PLLA scaffolds were prepared in two forms, films and electrospun fibrous membranes. Films were prepared with nano silver particles with weight ratios of nano silver particles to PLLA of 0.5%, 2.5%, 5%, 7.5% and 10% produced by an evaporation method. Fibrous membranes were fabricated from PLLA with silver

nanoparticles or wool keratin by an electrospinning technique.

*In vitro* cytotoxicity, cell proliferation and antibacterial tests were performed. The results implied that Ag/PLLA scaffolds can be used as non-toxic scaffolds for tissue engineering with antibacterial property. On the other hand, PLLA/keratin membranes were fabricated with different weight ratios at 2:1, 1:1, 1:2, 1:4 and 1:8 (Pk21, Pk11, Pk12, Pk14 and Pk18). The physical properties and degradability of the PLLA/keratin membranes were firstly tested. It was found that, although the tensile strength and elongation decreased, after being composited with keratin particles, the PLLA/keratin membranes became more hydrophilic than the pure PLLA membranes. This result suggested that the proportion of keratin particles within the membranes can affect the hydrophilicity of PLLA/keratin membranes. Furthermore, the releasing rate of keratin from the membranes was detected by fourier transform infrared (FTIR) after the PLLA/keratin membranes were degraded in PBS up to 4 weeks. Although more than half of the keratin was removed from the PLLA/keratin membrane in the first few hours of degradation, some keratin particles were still embedded in the PLLA fibers which were expected to enhance cell attachment and their proliferation on the PLLA.

Then, cytotoxicity and cell proliferation of PLLA/keratin membranes were studied. High concentrations of wool keratin showed cytotoxicity, and the concentration of the wool keratin particles significantly influenced the cell adhesion on the PLLA/keratin membranes. Pk21 increased cell proliferation compared to PLLA,

while the other PLLA/keratin membranes decreased it. Furthermore, the cytotoxicity of the Pk membranes had a close relationship with the tensile property and moisture content of the scaffolds, as, basically, it was most correlated to the wool keratin concentration. So, the raw materials and the properties of the scaffolds are two main factors which affect the cytotoxicity, but the specific mechanism of the scaffold cytotoxicity still needs further study.

It can be concluded that Ag/PLLA is a good matrix for containing and gradually releasing antibacterial substance, while PLLA/keratin membranes can give good support for cell proliferation. Therefore, Ag/PLLA scaffolds can be used as non-cytotoxic antibacterial scaffolds for tissue engineering. PLLA/keratin fibrous membranes can provide a good matrix for cell proliferation. Combining these two kinds of compositions may produce antibacterial TE scaffolds with biomechanical properties that would enable them to play an important role as a skin substitute in the wound healing process.

## PUBLICATIONS

### Conference papers

1. Li Y., Hu JY, El-Khamy D, Li L and Ko F. Electrospun nano fibers with wool keratin and PEO. 22nd Annual Technical Conference of the American Society for Composites, Washington, September 17-19, 2007. (Oral Presentation)
2. Li L, Li Y, Li JS, Yao L, Mak AFT, Ko F, Qin L. Antibacterial and nontoxic nano silver PLLA composites for tissue engineering. International conference on Multi-functional Materials and Structures, Hong Kong. 28 July-31 July, 2008. *Advanced Materials Research* 47-50: 849-852, 2008. (Oral Presentation)
3. Li JS, Li Y, Li L, Mak AFT, Ko F and Qin L. Fabrication of poly (L-lactic acid) scaffolds with wool keratin for osteoblast cultivation. International conference on Multi-functional Materials and Structures, Hong Kong. 28 July-31 July, 2008. *Advanced Materials Research*, 47-50: 845-848, 2008. (Oral Presentation)
4. Li L, Li Y, Li JS, Mak AFT, Ko F, Qin L. The effects of PLLA/keratin composite fibrous scaffolds on the proliferation of osteoblasts. International Symposium of Textile Bioengineering and Informatics, Hong Kong, China, 2008, *Proceedings of TBIS*, pp 696-699, 2008. (Oral Presentation)
5. Li JS, Li Y, Li L, Mak AFT, Ko F and Qin L. Preparation and degradation of PLLA/keratin electrospun membranes. International Symposium of Textile Bioengineering and Informatics, Hong Kong, China, 2008, *Proceedings of TBIS*, pp 654-658, 2008. (Oral Presentation)
6. Lv R, Li Y, Li JS, Li L. Mechanical and physical properties of PLLA/keratin electrospun nonwoven fibrous membrane. *TBIS Proceedings*, International Symposium of Textile Bioengineering and Informatics, Hong Kong, China, 2008, *Proceedings of TBIS*, pp 685-691, 2008. (Oral Presentation)
7. Li L, Li Y, Li JS, Mak AFT, Ko F, Qin L. Cytotoxicity and cell adhesion of PLLA/keratin composite fibrous scaffolds. 13th International Conference on Biomedical Engineering, Singapore, ICBME 2008, *Proceedings* 23, pp 1492–1495, 2009. (Oral Presentation).
8. Li JS, Li Y, Li L, Chen AZ. PLLA/Danggui oil nonwoven fabric for tissue engineering. *TBIS Proceedings*, International Symposium of Textile Bioengineering and Informatics, Hong Kong, China, 2009. (Oral Presentation)

9. Liu X, Li L, Li Y. Cytotoxicity of the wool hydrolyzed polypeptides on human fibroblasts. TBIS, Hong Kong, China, 2009, Proceedings of TBIS, pp 43-46, 2009. (Oral Presentation)

### **Journal papers**

1. Li L, Li Y, Li JS, Yao L, Mak AFT, Ko F, Qin L. Antibacterial properties of nano silver PLLA fibrous membranes. Journal of Nanomaterials. Vol 2009, 2009. doi:10.1155/2009/168041.
2. Li JS, Li Y, Li L, Mak AFT, Ko F and Qin L. Fabrication of poly (L-lactic acid) scaffolds with wool keratin for osteoblast cultivation. Composites Part B: Engineering. Vol 40 (7), 2009, 664-667.
3. Li JS, Li Y, Li L, Mak AFT, Ko F and Qin L. Preparation and biodegradation of electrospun PLLA/keratin nonwoven fibrous membrane. Polymer Degradation and Stability. Vol 94 (10), 2009, 1800-1807.
4. Li JS, Chen Y, Mak AFT, Tuan RS, Li L, Li Y. A one-step method to fabricate PLLA scaffolds with deposition of bioactive hydroxyapatite and collagen using ice-based microporogens. Acta Biomaterialia. Vol 6 (6), 2010, 2013-2019.
5. Li L, Li Y, Li JS, Yao L, Mak AFT, Ko F, Qin L. Cytotoxicity and antibacterial properties of nano silver PLLA composite membranes. (In submission)
6. Li L, Li Y, Li JS, Mak AFT, Ko F, Qin L. Effects of PLLA/keratin composite fibrous scaffolds on cell proliferation. (In preparation)

### **Patents**

1. Li Y, Li JS, Hu JY, Li L. Biomaterial scaffolds with keratin for tissue engineering. US 2010/0008969 A1.
2. Li Y, Li JS, Hu JY, Li L. Biodegradable and/or bioabsorbable biomaterials and keratins fibrous articles for medical applications. US 2010/0009488 A1.

## ACKNOWLEDGEMENTS

I would like to sincerely thank my chief supervisor, Professor Li Yi for his kind guidance, constructive and creative comments and all his ongoing support in this project.

I also express my gratitude to my co-supervisors, Professor Frank Ko, Professor Qin Ling and Professor Arthur Mak for their prompt and kind feedback, and encouragement throughout this project.

As well, I owe a great deal of thanks to my colleagues, Dr. Yao Lei, Dr. Hu Jun Yan, Dr. Li Jiashen, Ms. Lv Ru, Dr. Lin Yinglei, Dr. Guo Yueping, Dr. Chen Dong, and Miss Liu Xuan for their kind help and comments. I would also like to thank all my colleagues for their precious friendship.

I am very grateful to Dr. Yang Mo and Dr. Polly Leung for allowing me to use the labs in the department of Health Technology and Information (HTI) and thank them for their time and insightful comments from a researcher's perspective. I would also like to thank Dr. Yu Jin Jiang, Mr. Brian Pow from HTI and Mr. Yeung Man Nin from the Materials Research Center for their kind assistance.

Finally, I would like to give my most sincere thanks to my husband, my parents and my daughter for their love and moral support, particularly in the periods of frustration and confusion. Thanks, also, to all my friends and everyone who welcomed me so warmly during the years I spent in Hong Kong, making this unforgettable experience so rewarding.

## TABLE OF CONTENTS

Abstract.....	i
Publications.....	iv
Acknowledgements.....	vi
Table of Contents.....	vii
Acronyms.....	xii
List of Tables.....	xiii
List of Figures.....	xiv

### **Chapter 1: Introduction**

1.1 Motivation and objectives of research.....	1
1.2 Original contributions.....	4
1.3 Scope and outline of thesis.....	5

### **Chapter 2: Literature Review**

2.1 Introduction to skin tissue engineering.....	8
2.2 Applications.....	12
2.3 Fabrication.....	17
2.4 Properties.....	27
2.5 Cytotoxicity.....	36
2.6 Cell proliferation.....	38
2.7Antibacterial activity.....	39
2.8 Research gap.....	42
2.9 Summary of literature review.....	43

### **Chapter 3: Fabrication**

3.1 Materials and equipments.....	46
3.1.1 Materials.....	46
3.1.2 Main equipments.....	49

3.2 Fabrication of PLLA and Ag/PLLA composed films.....	49
3.3 Electrospinning of PLLA and Ag/PLLA fibers.....	51
3.4 Preparation of wool keratin particles.....	53
3.4.1 Preparation of wool keratin emulsion.....	53
3.4.2 Preparation of wool keratin particles.....	54
3.5 Electrospinning of wool keratin-PEO fibers.....	57
3.5.1 FTIR of the electrospun wool keratin-PEO fibers.....	57
3.5.2 Effect of keratin concentration on fiber diameter.....	58
3.5.3 Effect of PEO concentration on fiber diameter.....	60
3.6 Electrospinning of PLLA/keratin fibers.....	62
3.6.1 Scanning electron microscopy.....	63
3.6.2 FTIR of PLLA and PLLA/keratin fibers.....	64

#### **Chapter 4: Physical Properties**

4.1 Introduction.....	66
4.2 Morphology.....	66
4.3 Hydrophilicity.....	67
4.3.1 Method.....	67
4.3.2 Results and discussion.....	68
4.4 Tensile property.....	73
4.4.1 Method.....	73
4.4.2 Results and discussion.....	73
4.5 Moisture related properties.....	77
4.5.1 Moisture content.....	77
4.5.2 Water vapor permeability.....	80
4.5.3 Moisture management property.....	82
4.6 Conclusions.....	89

#### **Chapter 5: *In Vitro* Degradation**

5.1 Introduction.....	91
-----------------------	----

5.2 Process of <i>in vitro</i> degradation.....	91
5.2.1 Materials and instrument.....	91
5.2.2 Process of <i>in vitro</i> degradation.....	91
5.3 Degradation of PLLA/keratin fibrous membranes.....	92
5.3.1 Keratin releasing rate.....	92
5.3.2 Morphological change.....	95
5.3.3 Discussion.....	98
5.3.4 Conclusions.....	99

## **Chapter 6: Cytotoxicity**

6.1 Introduction.....	100
6.2 Cytotoxicity test.....	100
6.3 Statistical analysis.....	101
6.4 Cytotoxicity of the Ag/PLLA films and fibrous membranes.....	102
6.4.1 Cell line.....	102
6.4.2 Results.....	102
6.4.3 Discussion.....	114
6.4.4 Conclusions.....	117
6.5 The cytotoxicity of the PLLA/keratin fibrous membranes.....	118
6.5.1 Cell line.....	118
6.5.2 Cell adhesion.....	118
6.5.3 Scanning electron microscopy.....	118
6.5.4 Results.....	118
6.5.5 Discussion.....	122
6.5.6 Conclusions.....	126

## **Chapter 7: Cell Adhesion and Proliferation**

7.1 Ag/PLLA films.....	127
7.1.1 Cell proliferation.....	127
7.1.2 Statistical analysis.....	128

7.1.3 Results.....	128
7.1.4 Discussion.....	132
7.1.5 Conclusions.....	134
7.2 PLLA/keratin fibrous membranes.....	134
7.2.1 Cell proliferation.....	135
7.2.2 Scanning electron microscopy.....	135
7.2.3 Statistical analysis.....	135
7.2.4 Results.....	135
7.2.5 Discussion.....	141
7.2.6 Conclusions.....	146

## **Chapter 8: Antibacterial Activity**

8.1 Introduction.....	147
8.2 Antibacterial activity of Ag/PLLA films.....	148
8.2.1 Preparation of PLLA and Ag/PLLA films.....	148
8.2.2 Antibacterial test.....	148
8.2.3 Scanning electron microscopy.....	149
8.2.4 Statistical analysis.....	150
8.2.5 Results.....	150
8.3 Antibacterial activity of Ag/PLLA fibrous membranes.....	152
8.3.1 Electrospinning of PLLA and Ag/PLLA fibrous membranes.....	152
8.3.2 Antibacterial test.....	153
8.3.3 Scanning electron microscopy.....	154
8.3.4 Statistical analysis.....	154
8.3.5 Results.....	154
8.4 Discussion.....	158
8.5 Conclusions.....	160

## **Chapter 9: Conclusions and Suggestions for Future Research**

9.1 Conclusions.....	161
----------------------	-----

9.2 Suggestions for Future research.....	164
9.2.1 Cell proliferation and antibacterial function.....	164
9.2.2 Composing TCM into scaffolds.....	165
9.2.3 Animal model experiment.....	166
<b>References.....</b>	<b>167</b>

## ACRONYMS

Ag NPs	Silver nano particles
DE	Dermal equivalent
DMEM	Dulbecco's modified eagle's medium
ES	Electrospinning
FBS	Fetal bovine serum
FTIR	Fourier transform infrared spectroscopy
MTS	CellTiter 96 AQueous non-radioactive cell proliferation assay
Pk	PLLA/keratin
PLLA	Poly (L-lactic acid)
RH	Relative humidity
SC	Stratum corneum
SEM	Scanning electron microscopy
TE	Tissue engineering

## LIST OF TABLES

<b>Table 2.1</b> Commercially available epidermal/dermal skin substitutes for clinical use .....	15
<b>Table 2.2</b> Nano particle scaffold materials.....	18
<b>Table 2.3</b> Nano fibrous scaffold materials.....	19
<b>Table 4.1</b> The contact angle of the films.....	69
<b>Table 4.2</b> Contact angle values of the PLLA and Pk fibrous membranes measured before sterilization.....	70
<b>Table 4.3</b> Contact angle values of the sterilized PLLA and Pk fibrous membranes..	72
<b>Table 4.4</b> Cross-sectional area of the PLLA and Pk fibrous membranes.....	76
<b>Table 6.1</b> The concentration of the Ag NPs for each immersed scaffold.....	115
<b>Table 8.1</b> Assessment of the antibacterial activity of the extractions of the Ag/PLLA films.....	150
<b>Table 8.2</b> Assessment of the antibacterial activity of the extractions of the Ag/PLLA membranes.....	156

## LIST OF FIGURES

<b>Figure 1.1</b> Structure of thesis. ....	5
<b>Figure 2.1</b> The typical tissue engineering approach.....	9
<b>Figure 2.2</b> Structure of human skin .....	10
<b>Figure 2.3</b> Hydrogel wound dressing.....	13
<b>Figure 2.4</b> Structure of nano scaffolds.....	21
<b>Figure 2.5</b> TEM images of A) Al <sub>2</sub> O <sub>3</sub> –ZrO <sub>2</sub> composite nanoparticles, B) collagen, and C) grafted collagen. SEM images of hybrid nanocomposites with a composite nanoparticle content of D) 1.2 wt% and E) 7.3 wt %. [Cao et al, 2006].....	22
<b>Figure 2.6</b> SEM images of foam scaffolds in axial direction: (a) plain PLGA, (b) PLGA + 5 wt% TiO <sub>2</sub> and (c) PLGA + 20 wt% TiO <sub>2</sub> . Some TiO <sub>2</sub> agglomerates are seen in the 20 wt% foam. [Torres et al, 2007].....	22
<b>Figure 2.7</b> SEM images of alginate–PEO nanofibers: A–C) survey images of the nanofibers spun from solutions with alginate/PEO ratios of 70:30, 80:20, and 90:10, respectively. The insets show the fiber size distributions. A'–C') High-magnification images of A–C, respectively. All polymer solutions were prepared with 0.5 wt% Triton X-100 surfactant and 5 wt% DMSO cosolvent. [Bhattarai et al, 2006].....	24
<b>Figure 2.8</b> Typical electrospinning setup. $Q$ , flow rate; $d$ , distance between plate and needle; $V$ , applied voltage. ( <a href="http://www.liebertonline.com/ten">www.liebertonline.com/ten</a> ).....	25
<b>Figure 2.9</b> SEM micrographs of electrospun PLLA (A), PLGA 85:15 (B), 75:25 (C), and 50:50 (D) scaffolds prior to implantation [Blackwood et al, 2008].....	26
<b>Figure 2.10</b> SEM photographs of MG-63 cells cultured on the (a) dense, (b) porous, (c) particulate PLLA membranes after 1 d incubation. [Liu et al, 2004].....	28

<b>Figure 2.11</b> Morphological changes in an electrospun nanofibrous matrix and a microfibrinous matrix. A. Electrospun nanofibrous matrix; B. Microfibrinous [Noh et al, 2006].....	29
<b>Figure 2.12</b> Diagrammatic sketch of air-pockets .....	34
<b>Figure 2.13</b> Selected SEM images of (a) pre-neutralized as-spun chitosan nanofibrous membrane from 7% chitosan solution in 70:30 v/v TFA/DCM, chitosan nanofibrous membrane after neutralization with (b) 5 M NaOH or (c) 5 M Na <sub>2</sub> CO <sub>3</sub> aqueous solution, and (d) chitosan nanofibrous membrane in panel c after submersion in PBS for 12 weeks. [Sangsanoh et al, 2006].....	35
<b>Figure 2.14</b> Phase-contrast micrographs of HT-1080 cells: (A) unexposed cells; (B–F) 24 h after the cultures were exposed to 3.12, 6.25, 12.5, 25 and 50µg/mL SNP, respectively (magnification 200×). [Arora et al, 2008].....	37
<b>Figure 2.15</b> Antibiotic released from electrospun scaffolds demonstrate the same activity as the pure drug form, indicating that the processing is not damaging to the drug. Incubation of bacteria directly with drug loaded scaffolds demonstrates that the drug is able to diffuse from the scaffold and inhibit bacterial proliferation.....	40
<b>Figure 2.16</b> Flow chart for wound healing strategy.....	45
<b>Figure 3.1</b> Wool fibers purchased from Nanjing Wool Market.....	47
<b>Figure 3.2</b> SEM images of silver nanoparticles (20kV). Silver nanoparticles are grey and white color with an average particle size of 35nm.....	48
<b>Figure 3.3</b> Scheme of PLLA and Ag/PLLA membrane preparation. (0) PLLA (1) 0.5% Ag/PLLA (2) 2.5% Ag/PLLA (3) 5% Ag/PLLA (4) 7.5% Ag/PLLA (5) 10% Ag/PLLA.....	50
<b>Figure 3.4</b> Topographical SEM images of PLLA and 5% Ag/PLLA film surfaces.....	50

<b>Figure 3.5</b> Scheme of electrospinning process.....	52
<b>Figure 3.6</b> SEM images of PLLA and Ag/PLLA fibrous membranes at x1000 magnification. (20kV).....	53
<b>Figure 3.7</b> Preparation of wool keratin powder. (A) Wool keratin emulsion (B) Wool keratin powder.....	55
<b>Figure 3.8</b> SEM images of wool keratin particles (20kV). Particles are white color and agglomerated.....	55
<b>Figure 3.9</b> SEM images of non-dialyzed wool keratin particles. (20kV).....	56
<b>Figure 3.10</b> Fourier transform infrared spectroscopy (FTIR) of electrospun PEO/keratin fibers.....	58
<b>Figure 3.11</b> Morphology of fibers at different wool concentrations of 4%, 8% and 12%. The average, standard deviation, maximum and minimum values of the fiber diameters are also given in this figure.....	59
<b>Figure 3.12</b> Relationship between the wool keratin concentration and the fiber diameter.....	60
<b>Figure 3.13</b> Morphology of fibers at different PEO concentrations at 0.5%, 1% and 3%. The average, standard deviation, maximum and minimum values of the fiber diameter are also given in this figure.....	61
<b>Figure 3.14</b> Relationship between the PEO concentration and the fiber diameter.....	62
<b>Figure 3.15</b> SEM images of PLLA and PLLA/keratin electrospun fibers.....	63
<b>Figure 3.16</b> FTIR spectra of the PLLA, keratin and PLLA/keratin membranes. For the PLLA/keratin composite membrane, two peaks appeared at 1630 cm <sup>-1</sup> and 1550 cm <sup>-1</sup> (indicated by the red arrows) which corresponded to the keratin.....	64

<b>Figure 4.1</b> Sketch of contact angle ( $\theta$ ). the contact angle is the angle at which a liquid droplet (the blue part) interface meets the solid surface.....	68
<b>Figure 4.2</b> Contact angles of the PLLA and Ag/PLLA films prepared with different silver nanoparticle concentrations. For the Ag/PLLA membranes, the higher the silver nanoparticle concentration, the greater was the contact angle.....	69
<b>Figure 4.3</b> Contact angles of the PLLA/keratin fibrous membranes measured before sterilization.....	71
<b>Figure 4.4</b> The droplet shape changed as during the measurement of the contact angles of the sterilized PLLA/keratin fibrous membranes until it was absorbed thoroughly. All the contact angles of the PLLA/keratin fibrous membranes (Pk21, Pk11, Pk12, Pk14, Pk18) were $0^\circ$ .....	72
<b>Figure 4.5</b> Maximum Load of the PLLA and PLLA/keratin membranes: with increasing of keratin concentration the maximum load of the membranes decreased gradually.....	74
<b>Figure 4.6</b> Maximum strains of the PLLA and PLLA/keratin membranes: the maximum strain of the membranes decreased gradually as the keratin concentration increased.....	75
<b>Figure 4.7</b> Tensile strength of the PLLA and Pk membranes: with increasing keratin concentration showing that the tensile strength of the membranes decreased gradually.....	77
<b>Figure 4.8</b> Moisture content of the PLLA and PLLA/keratin membranes: with increasing keratin proportion showing that the moisture content of the Pk membranes increased. The moisture content of membranes became relatively stable as the proportion of Pk12.....	79
<b>Figure 4.9</b> Water vapor permeability of the PLLA and PLLA/keratin membranes: no	

significant differences were observed between the PLLA membranes with different ratios of keratin particles.....81

**Figure 4.10** Wetting times of the PLLA and PLLA/keratin membranes: the wetting time of the bottom surface of the PLLA membrane was 120s, which meant that the bottom surface was not wet; top surface of Pk21 membrane was almost dry. For the other PLLA/keratin membranes, both top and bottom surfaces became wet in a short time (less than 30s).....84

**Figure 4.11** Max absorption rates of the PLLA and PLLA/keratin membranes: the water absorption rates of the membrane top surfaces were quite low, especially for the Pk21 membrane. However, the water absorption rates of the membrane bottom surfaces were very high except for the PLLA membrane.....85

**Figure 4.12** Max wetted radiuses of the PLLA and PLLA/keratin membranes: the wetted radius of the PLLA bottom surface was zero; all the water transported to the Pk21 bottom surface, so the wetted radius of the top surface was zero; except for the PLLA and Pk21 membranes, the top and bottom surfaces of the membranes had similar wetted radii; the Pk18 membrane had the largest wetted radius.....86

**Figure 4.13** Spreading speed of the PLLA and PLLA/keratin membranes: the spreading speed of the PLLA bottom surface was zero; the spreading speed of the Pk21 top surface was zero; the spreading speed of both the top and bottom surfaces of the Pk11, Pk12, Pk14 were similar; the spreading speed on the Pk18 bottom surface was higher than the top surface.....87

**Figure 4.14** Accumulative one-way transport index (AOWTI) of PLLA and Pk membranes: the PLLA membrane had lowest AOWTI; adding keratin to membrane improved the AOWTI; Pk21 membrane had the highest AOWTI.....88

**Figure 5.1** Sketch of the *in vitro* degradation experiment which proceeded in a 37 °C water bath. The time intervals were 3hr, 1d, 3d, 7d, 14d and 28d.....92

<b>Figure 5.2</b> FTIR spectra of the electrospun PLLA/keratin membranes during the degradation period. The amplitude of the characteristic peaks of keratin ( $1630\text{cm}^{-1}$ and $1550\text{cm}^{-1}$ indicated by arrows) decreased correspondingly.....	94
<b>Figure 5.3</b> Percentage of keratin in the electrospun PLLA/keratin plotted against degradation time.....	94
<b>Figure 5.4</b> SEM of an electrospun PLLA/keratin fibrous membrane which shows that the keratin particles were encapsulated by the PLLA to form PLLA/keratin composite fibers.....	96
<b>Figure 5.5</b> SEM image of the electrospun PLLA/keratin fibrous membrane after 3 hrs degradation. Some keratin particles were lost (directed by white arrows) and some were still embedded in the PLLA (directed by black arrows).....	97
<b>Figure 5.6</b> Macroscopic observation of the <i>in vitro</i> degradation of the keratin fibrous membranes. (A) Before submersion; (B) After submersion in PBS for 5 days.....	98
<b>Figure 6.1</b> Flowchart for the cytotoxicity test of materials.....	101
<b>Figure 6.2</b> Inverted microscopic images of cells cultured with (A) Culture medium; (B) 0.5% Ag/PLLA extraction for 1h; (C) 0.5% Ag/PLLA extraction for 1d (x100).....	103
<b>Figure 6.3</b> Inverted microscopic images of cells cultured with (A) Culture medium; (B) 2.5% Ag/PLLA extraction for 1h; (C) 2.5% Ag/PLLA extraction for 1d (x100).....	103
<b>Figure 6.4</b> Inverted microscopic images of cells cultured with (A) Culture medium; (B) 5% Ag/PLLA extraction for 1h; (C) 5% Ag/PLLA extraction for 1d (x100) .....	104
<b>Figure 6.5</b> Inverted microscopic images of cells cultured with (A) Culture medium; (B) 7.5% Ag/PLLA extraction for 1h; (C) 7.5% Ag/PLLA extraction for 1d	

(x100) .....104

**Figure 6.6** Inverted microscopic images of cells cultured with (A) Culture medium;  
(B) 10% Ag/PLLA extraction for 1h; (C) 10% Ag/PLLA extraction for 1d  
(x100) .....105

**Figure 6.7** Inverted microscopic images of cells cultured with (A) Culture medium;  
(B) PLLA extraction for 1h; (C) PLLA extraction for 1d (x100) .....105

**Figure 6.8** Inverted microscopic images of cells cultured with (A) Culture medium  
(B) 0.5% Ag/PLLA extraction for 1d (C) 0.5% Ag/PLLA extraction for 3d  
(x100).....106

**Figure 6.9** Inverted microscopic images of cells cultured with (A) Culture medium  
(B) 2.5% Ag/PLLA extraction for 1d (C) 2.5% Ag/PLLA extraction for 3d  
(x100) .....107

**Figure 6.10** Inverted microscopic images of cells cultured with (A) Culture medium  
(B) 5% Ag/PLLA extraction for 1d (C) 5% Ag/PLLA extraction for 3d  
(x100) .....107

**Figure 6.11** Inverted microscopic images of cells cultured with (A) Culture medium  
(B) 7.5% Ag/PLLA extraction for 1d (C) 7.5% Ag/PLLA extraction for 3d  
(x100) .....108

**Figure 6.12** Inverted microscopic images of cells cultured with (A) Culture medium  
(B) 10% Ag/PLLA extraction for 1d (C) 10% Ag/PLLA extraction for 3d  
(x100).....108

**Figure 6.13** Inverted microscopic images of cells cultured with (A) Culture medium  
(B) PLLA extraction for 1d (C) PLLA extraction for 3d (x100).....109

**Figure 6.14** Morphological changes of cells cultured with different extractions after  
one day's culture. (A) PLLA (B) 0.5% Ag/PLLA (C) 2.5% Ag/PLLA (D) 5%

Ag/PLLA (E) 7.5% Ag/PLLA (F) 10% Ag/PLLA. Morphological changes and detachment of the cells were observed in the extractions 7.5% and 10% Ag/PLLA films (x100).....109

**Figure 6.15** MTS assay results of cell proliferation with different extractions (492nm). The 7.5% and 10% Ag/PLLA film extractions inhibited cell proliferation, while the 5% Ag/PLLA extraction increased the cell number significantly ( $P < 0.05$ ).....110

**Figure 6.16** Inverted microscopic images of cells cultured with different extractions: (A) PLLA; (B) 0.5% Ag/PLLA membranes; (C) 2.5% Ag/PLLA membranes; (D) 5% Ag/PLLA membranes; (E) 7.5% Ag/PLLA membranes; (F) 10% Ag/PLLA membranes. (G) Before adding extractions of Ag/PLLA fibrous membranes (x100) .....112

**Figure 6.17** Cell viability of the cells cultured with the extractions of the PLLA and Ag/PLLA membranes.....113

**Figure 6.18** The linear relationship between the contact angle values and the absorbance of cell proliferation in the extractions of the PLLA and Ag/PLLA films ( $r = -0.981, P < 0.05$ ).....116

**Figure 6.19** Morphological changes of cells cultured with different extractions of PLLA/keratin fibrous membranes. Morphological changes and detachment of the cells were observed in the extractions of Pk12, Pk14 and Pk18 membranes through an inverted microscope.....119

**Figure 6.20** MTS assay results for cell adhesion on the PLLA and PLLA/keratin fibrous membranes. Pk21 cell adhesion is significantly higher than that of the other PLLA/keratin membranes and there is no significant difference between the Pk21 and PLLA membranes.....120

**Figure 6.21** SEM images of PLLA/keratin fibrous membranes with cells cultured for

three days. Cells can be seen stretched and spread like translucent films on the PLLA, Pk21 and Pk11 membranes (arrows), few cells can be seen on the Pk12, Pk14 and Pk18 membranes.....121

**Figure 6.22** The linear relationship between the wool keratin concentration and the cell adhesion of the PLLA and Pk fibrous membranes (  $r = -0.906$ ,  $P < 0.05$ ).....122

**Figure 6.23** The linear relationship between the max load and the cell adhesion of the PLLA and Pk fibrous membranes (  $r = 0.966$ ,  $P < 0.05$ ).....123

**Figure 6.24** The linear relationship between the max strain and cell adhesion of the PLLA and Pk fibrous membranes (  $r = 0.915$ ,  $P < 0.05$ ).....124

**Figure 6.25** The linear relationship between the moisture content and cell adhesion of the PLLA and Pk fibrous membranes (  $r = -0.777$ ,  $P < 0.05$ ).....124

**Figure 6.26** The linear relationship between the water vapor permeability and the absorbance of cell adhesion of PLLA and Pk fibrous membranes (  $r = 0.274$ ,  $P > 0.05$ ).....125

**Figure 7.1** Cell adhesion after 1 day culture: (a) Normal plate; (b) PLLA film; (c) Ag/PLLA film.....128

**Figure 7.2** Cell proliferation after 7 days culture: (a) Normal plate; (b) PLLA film; (c) Ag/PLLA film.....129

**Figure 7.3** Effects of Ag/PLLA films on cell proliferation. Cell proliferation was assessed with MTS reagent and measurement of absorbance at 492nm. The 5% Ag/PLLA film showed slightly higher cell proliferation compared to the other Ag/PLLA films, but there were no significant differences ( $P > 0.05$ ).....130

**Figure 7.4** SEM images of cell layers on different films after 14 days of culture. Cells already covered the whole films with several layers. (A) PLLA film; (B) 5%Ag/PLLA film.....131

<b>Figure 7.5</b> The relationship between the contact angle values and the absorbance of cell proliferation in the extractions of the PLLA and Ag/PLLA films ( $r = -0.357$ , $P > 0.05$ ).....	133
<b>Figure 7.6</b> SEM images of cells cultured on the PLLA fibrous membrane for 3d, 7d, 14d and 21d. The cells highly proliferated until 21d, and covered the whole membrane.....	136
<b>Figure 7.7</b> SEM images of cells cultured on the Pk21 fibrous membrane for 3d, 7d, 14d and 21d. Cells had obviously proliferated at 21d and were observed on almost the whole membrane.....	136
<b>Figure 7.8</b> SEM images of cells cultured on the Pk11 fibrous membrane for 3d, 7d, 14d and 21d. Cells had obviously proliferated at 21d and were observed on almost the whole membrane.....	137
<b>Figure 7.9</b> SEM images of cells cultured on the Pk12 fibrous membrane for 3d, 7d, 14d and 21d. Cells proliferated gradually, and covered almost the whole membrane at 21d.....	137
<b>Figure 7.10</b> SEM images of cells cultured on the Pk14 fibrous membrane for 3d, 7d, 14d and 21d. The proliferation of cells was hardly observed until 14d, only some of the confluent cells could be observed on the membrane after 21d.....	138
<b>Figure 7.11</b> SEM images of cells cultured on Pk18 fibrous membrane for 3d, 7d, 14d and 21d. The proliferation of cells was hardly observed until 14d, only some of the confluent cells could be found scattered on membrane after 21d.....	138
<b>Figure 7.12</b> SEM images of cells cultured on the PLLA and Pk fibrous membrane for 21d.....	139
<b>Figure 7.13</b> MTS assay results for the cell proliferation on the PLLA and Pk fibrous membranes.....	140

**Figure 7.14** The relationship between the maximum load and the 3 days cell proliferation of the PLLA and Pk fibrous membranes ( $r = -0.562$ ,  $P < 0.05$ ).....142

**Figure 7.15** The linear relationship between the max load and the 14 days cell proliferation of the PLLA and Pk fibrous membranes ( $r = 0.865$ ,  $P < 0.05$ ).....143

**Figure 7.16** The relationship between the moisture content and the 3 days cell proliferation of the PLLA and Pk fibrous membranes ( $r = 0.334$ ,  $P > 0.05$ ).....143

**Figure 7.17** The linear relationship between the moisture content and the 14 days cell proliferation of the PLLA and Pk fibrous membranes ( $r = -0.848$ ,  $P < 0.05$ )...144

**Figure 7.18** The relationship between the water vapor permeability and the 3 days cell proliferation of the PLLA and Pk fibrous membranes ( $r = -0.312$ ,  $P > 0.05$ )...144

**Figure 7.19** The relationship between the water vapor permeability and the 14 days cell proliferation of the PLLA and Pk fibrous membranes ( $r = 0.236$ ,  $P > 0.05$ )....145

**Figure 8.1** Results of the antibacterial activity for the extraction of the 2.5% Ag/PLLA film using Staph. at different bacteria concentrations:  $10^1$ ,  $10^2$ ,  $10^3$ ,  $10^4$  and  $10^5$  CFU/mL after 24hr incubation at  $37^\circ\text{C}$ . The highest concentration of Staph. which could be inhibited by the original extraction of the 2.5% Ag/PLLA film was  $10^1$  CFU/mL.....151

**Figure 8.2** Results of the antibacterial activity for the extraction of the 5% Ag/PLLA film using Staph. at different bacteria concentrations:  $10^1$ ,  $10^2$ ,  $10^3$ ,  $10^4$  and  $10^5$  CFU/mL after 24hr incubation at  $37^\circ\text{C}$ . The highest concentration of Staph. which could be inhibited by the original extraction of the 5% Ag/PLLA film was  $10^3$  CFU/mL.....151

**Figure 8.3** Antibacterial test results for the Ag/PLLA using Staphylococcus (Left) and E. coli (right). Bacteria inhibited, clear zones for both the E.coli and Staph. can be observed around the Ag/PLLA membranes (lower specimen) with an average

width of 5mm after 24hr incubation.....155

**Figure 8.4** Antibacterial activity of the Ag/PLLA fibrous membrane (lower specimen) was reduced after exposure in the air for 8 weeks. The average width of the E.coli and Staph. inhibition clear zones decreased to 1.2mm and 1.5mm respectively after 24hr incubation.....156

**Figure 8.5** SEM images showing Staph. on the PLLA and Ag/PLLA fibrous membrane magnified 20 thousand times (20kV). (1) The number of Staph. on the PLLA membranes were more than that on the Ag/PLLA membrane. (2) Staph. on the PLLA membrane had a smooth surface, whereas those on the Ag/PLLA membrane were not very smooth.....157

## CHAPTER 1: INTRODUCTION

1.1 Motivation and objectives of research .....	1
1.2 Original contributions .....	4
1.3 Scope and outline of thesis.....	5

### 1.1 Motivation and objectives of research

Tissue engineering is a promising new therapy for patients who need implantations or medical devices to improve their quality of life or to save their lives. In the development of skin tissue engineering, noticeable progress has been made for the *in vitro*-engineered substitutes that mimic human skin, which can be used for repairing skin damage, especially for partial-thickness burns. These are used either as grafts for the replacement of lost skin or for the establishment of human-based *in vitro* skin models [Groeber F *et al*, 2011]. This artificial skin, which performs as a biodegradable template for the synthesis of neodermal tissue is applicable for not only short-term acute use, but also long-term, chronic use [Yannas IV and Burke JF, 1980]. Biodegradation is the process whereby materials are broken down by nature either through hydrolytic mechanisms without the help of enzymes and/or enzymatic mechanisms. It is loosely associated with the terms absorbable, erodible, and resorbable [Wong and Bronzino, 2007, pp6-16].

Individuals who suffer extensive loss of skin are commonly in danger of massive infection [Groeber F *et al*, 2011]. Consequently, the risk of infection requires

tissue engineering scaffolds to have antibacterial properties [Walder *et al*, 2002; Lai *et al*, 2002; Crabtree *et al*, 2003; Gaonkar *et al*, 2003; Alt *et al*, 2004; Li *et al*, 2006]. Yannas IV and Burke JF have previously described the physicochemical, biochemical and mechanical considerations that form the basis for the design of artificial skin useful as an experimental wound closure [Yannas IV and Burke JF, 1980]. Thus, an appropriately engineered skin scaffold with the capability of cell proliferation and antibacterial activity and possessing skin mechanical properties will have a very promising application in burns treatment.

Biomaterials are synthetic materials used to replace either part of a living system or to function in intimate contact with living tissues [Wong and Bronzino, 2007, pp3-20]. Hard keratins have been the subject of biomaterial investigations for many years. According to previous findings, keratins have been demonstrated to have excellent compatibility in biological systems [Hill P *et al*, 2010]. This compatibility is defined as “biocompatibility”, which is the complete acceptance of an artificial implant by the surrounding tissues. In this respect, the implant should be compatible with tissues in terms of mechanical, chemical surface, and pharmacological properties [Wong and Bronzino, 2007, pp3-20]. In 1998, Yamauchi *et al* found that, on wool keratin composed films, fibroblast cells could adhere, spread and grow rapidly. Wool keratin scaffolds have also been reported as being good scaffolds for cell adhesion, spreading and growth [Tachibana *et al*, 2002]. Thus, wool keratin is considered to be a useful natural protein, biomaterial suitable for tissue engineering scaffolds. Therefore, in this study, the fabrication,

biocompatibility and biomechanics of wool keratin fibrous scaffolds have been primarily investigated by characterizing the physical properties, degradability, cytotoxicity, cell proliferation of the scaffolds.

Silver and its compounds have been studied for many years not only for their low cytotoxicity, but also for their antibacterial activity [Galeano *et al*, 2003; Furno *et al*, 2004; Thomas *et al*, 2007; Chen and Schluesener, 2008; Li *et al*, 2011]. With the development of nanotechnology, some researchers have found that the toxic concentration of silver nanoparticles (Ag NPs) is significantly higher than that of ionic silver [Kvitek L *et al*, 2011]. Nanoparticles are particles which are sized between 1 and 100 nanometers. Consequently, in this study, the feasibility of using Ag NPs composite films and fibrous membranes by evaluating their cytotoxicity and antimicrobial capability was also investigated. *In vitro* cytotoxicity tests and cell proliferation experiments were employed to study the functions of Ag/PLLA scaffolds.

To obtain a comprehensive understanding of the procedures involved and previous research, an extensive literature review was undertaken, and is reported in Chapter 2, which identified a number of knowledge gaps. To fill the knowledge gaps, the objectives of this study were defined and summarized as follows.

- 1) To characterize the physical properties of tissue engineered scaffolds and study the relationship between their properties and the ratio of wool keratin to

PLLA constituents.

- 2) To examine the *in vitro* degradation of PLLA and PLLA/keratin (Pk) membranes.
- 3) To evaluate the scaffolds by testing the cytotoxicity of Ag/PLLA films, Ag/PLLA and PLLA/keratin fibrous membranes, and the relationship between their properties and the cytotoxicity.
- 4) To explore the relationship between the cell proliferation, the properties, and raw material concentration of the Ag/PLLA films and Pk fibrous membranes.
- 5) To investigate the bacterial activity and mechanism of Ag NPs composed scaffolds.

## **1.2 Original contributions**

This study has tried to narrow the research gap which exists in wound healing, especially skin healing, by studying the possibility of combining cell proliferation and antibacterial activity into tissue engineered skin scaffolds constructed from wool keratin and Ag NPs with respect to the biomechanical properties of the scaffolds. The scientific understanding and technologies developed from this project will be transferred to the textile industry and the medical device industry for the purpose of saving lives and improving the quality of life for patients.

In this study, the physical properties and degradability of electrospun Pk fibrous membranes were initially characterized; secondly, the cytotoxicity and cell proliferation of Pk scaffolds and Ag NPs composed PLLA scaffolds (Ag/PLLA scaffolds) were investigated and the relationship between the properties, cytotoxicity and cell proliferation of the scaffolds were explored; finally, the antibacterial activity of Ag/PLLA was studied, primarily to assess the potential antibacterial function of the scaffolds in the hope that this could provide justification and evidence for further research into antibacterial artificial skin.

### 1.3 Scope and outline of thesis

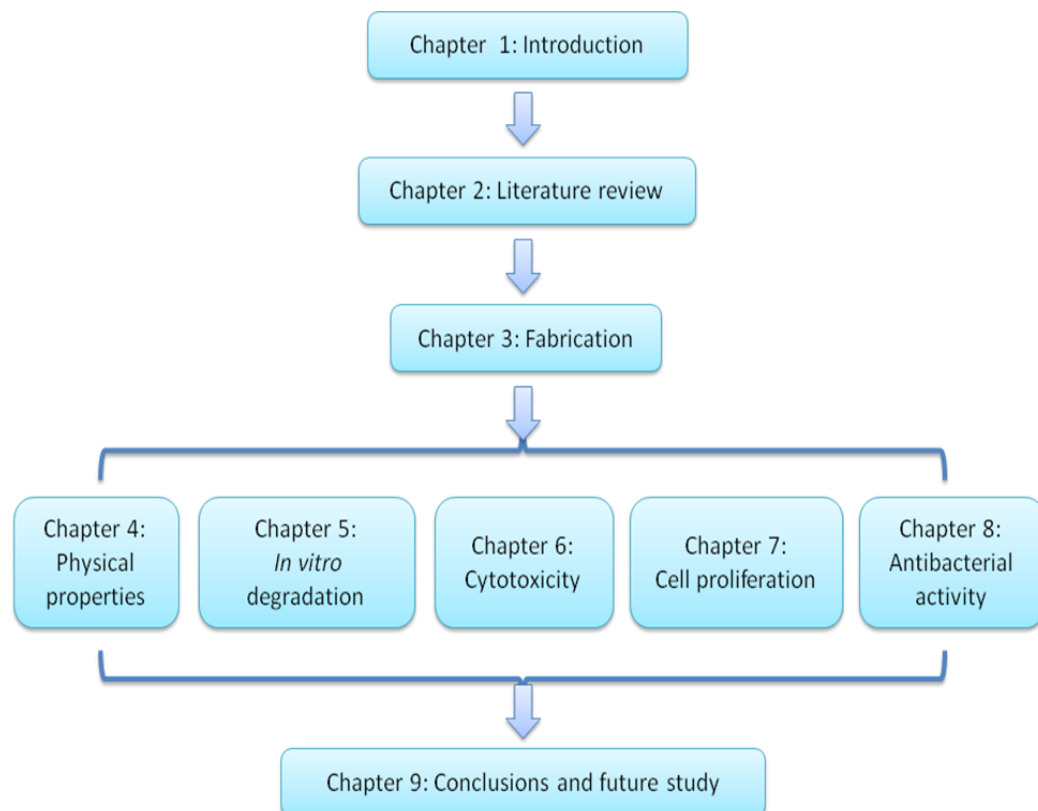


Figure 1.1. Structure of thesis.

This research work comprises four sections focusing on scaffolds: fabrication,

characterization, cell experiments, and antibacterial tests. Cell experiments included cytotoxicity tests, cell adhesion, and cell proliferation experiments.

This thesis is divided into nine chapters:

Chapter 1 introduces the research and presents an overview of the thesis, including its originality, objectives and scope.

Chapter 2 reviews literature related to this research work. Skin tissue engineering, skin tissue engineering scaffolds, their applications, fabrication, properties, cytotoxicity, cell proliferation, and antibacterial activity together with the research gaps identified will be presented.

Chapter 3 describes the process for the fabrication of Ag/PLLA films and Ag/PLLA and Pk fibrous membranes. The materials and methods used in the fabrications of the films and electrospun fibres will be introduced.

Chapter 4 studies the relationship between the physical properties of Pk scaffolds and the ratios of keratin to PLLA, including the characterization of their morphology, the hydrophilicity, tensile properties and moisture related properties of the scaffolds.

Chapter 5 describes the process and presents the results of the *in vitro* degradation of Pk fibrous membranes and analyzes the relationship between the physical properties and the *in vitro* degradation of the scaffolds.

Chapter 6 introduces the cytotoxicity tests, explores the mechanism of the cytotoxicity of Pk fibrous membranes, Ag/PLLA films and fibrous membranes, and the relationship between the properties and the cytotoxicity of the scaffolds.

Chapter 7 describes the procedures and the results of the cell adhesion and proliferation of Pk fibrous membranes and Ag/PLLA films together with an analysis of the relationship between the properties and the cell proliferation of the scaffolds.

Chapter 8 investigates the mechanism of the antibacterial activity of Ag/PLLA films and fibrous membranes.

Chapter 9 summarizes the conclusions drawn from the study, together with suggestions for future research work.

## CHAPTER 2: LITERATURE REVIEW

2.1 Introduction to skin tissue engineering .....	8
2.2 Applications .....	12
2.3 Fabrication .....	17
2.4 Properties .....	27
2.5 Cytotoxicity.....	36
2.6 Cell proliferation .....	38
2.7 Antibacterial activity .....	39
2.8 Research gap .....	42
2.9 Summary of literature review .....	43

### 2.1 Introduction to skin tissue engineering

#### 2.1.1 Tissue engineering

Tissue engineering (TE) was probably first defined by Langer and Vacanti who stated it to be "an interdisciplinary field that applies the principles of engineering and life sciences towards the development of biological substitutes that restore, maintain, or improve tissue function or a whole organ" [Langer and Vacanti, 1993]. MacArthur and Oreffo (2005) defined TE as "understanding the principles of tissue growth, and applying this to produce functional replacement tissue for clinical use".

As shown in Figure 2.1, the typical TE approach includes five main steps: remove cells, expand the cell number, seed cells on a scaffold with growth factor, place the scaffolds into a culture medium, and re-implant. To regenerate

biologically functional tissue, TE requires the design and fabrication of ideal scaffolds to provide temporary templates for cell seeding, invasion, proliferation and differentiation [Jayaraman, 2004].

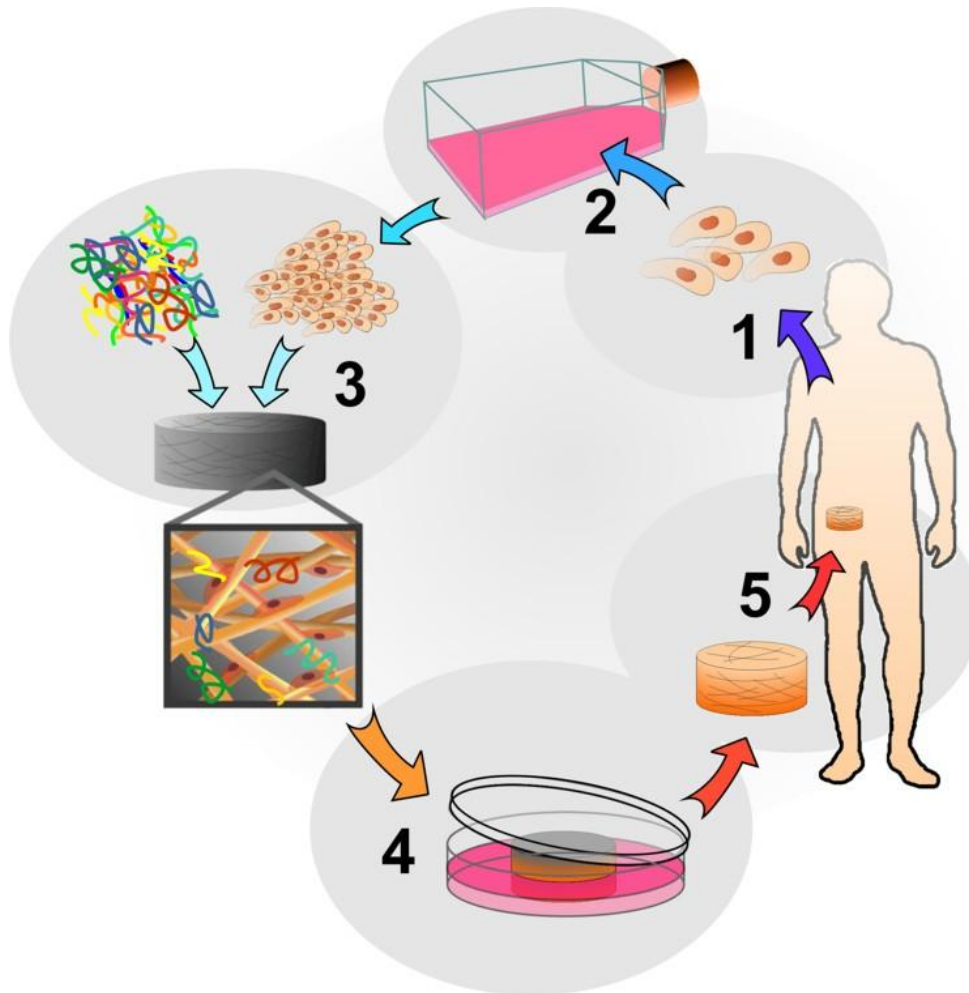


Figure 2.1 The typical tissue engineering approach.

(<http://www.centropede.com/UKSB2006/ePoster/background.html>)

### 2.1.2 Skin tissue engineering

As the largest organ in mammals, skin serves as a protective barrier between the human body and the surrounding environment. If the skin is damaged, the underlying organs will not be protected against pathogens and microorganisms.

In the past two decades or more, great efforts have been made to create substitutes that mimic human skin [MacNeil et al, 2007].

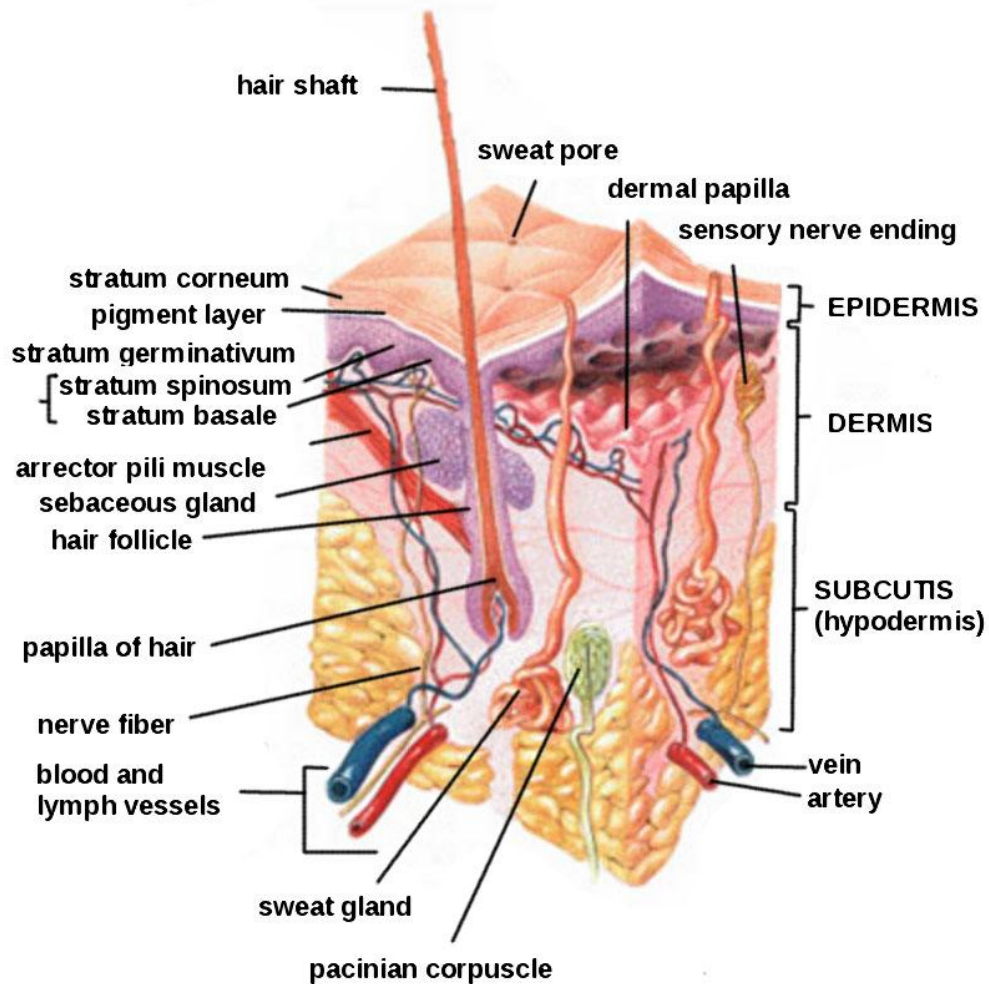


Figure 2.2 Structure of human skin.

(<http://upload.wikimedia.org/wikipedia/commons/e/e8/HumanSkinDiagram.jpg>)

As shown in Figure 2.2, the two main protective layers of human skin are the epidermis and the dermis. Although the epidermis is relatively thin, usually around 0.1–0.2 mm in depth, this keratinized epidermal layer provides the barrier layer which resists bacterial entry and prevents the loss of fluid and electrolyte, while the dermal part is much thicker, and the thickness of these two layers

varies at the different body sites. The dermis is composed primarily of collagen I, with dermal inclusions of hair shafts and sweat glands, which are lined under epidermal keratinocytes. The dermal part is also well vascularized and contains receptors for touch, temperature and pain [Shier D, 1999].

As a part of TE, skin TE combines various biological and synthetic materials with in vitro cultured cells to generate functional tissue substitutes. Most skin TE scaffolds, for example, artificial skin, are created by proliferating skin cells in the laboratory and using them to restore skin biofunction. Other uses include accelerating healing, reducing pain in superficial burns etc. Skin needs to be capable of regeneration, for short-term or longer-term healing [Sheila M, 2007]. Skin consists of several different cell types, including keratinocytes which form the surface barrier layer, as well as fibroblasts which form the dermal layer and provide strength and resilience. So, skin TE mainly applies human keratinocytes and fibroblasts to in vitro seed onto a suitable scaffold. For a full-thickness skin substitute, the fibroblasts and the matrix are initially used to establish the dermal part. The keratinocytes are then cultured on the top of the dermis to form the epidermal part of the skin substitute. These skin TE scaffolds can be employed as a skin graft or a human cell-based in vitro test system [Groeber et al, 2011]. The following section presents the applications for skin TE scaffolds.

## **2.2 Applications**

Skin TE scaffolds can be used for skin damage caused in a variety of ways. So, the main applications for skin TE scaffolds include wound dressings and skin substitutes, where they are used for wound healing and as alternatives to real skin in *in vitro* test systems. With the development of nano manufacturing techniques and progress in the development of nano biomaterials, nano skin TE scaffolds will become more widely used for these applications. These main applications viz. wound dressing and skin substitutes, will now be considered in more detail.

### **2.2.1 Wound dressing**

Wound healing is a complex process. Besides tissue regeneration, wounds often require treatment with antibiotics and suitable wound dressings. Katti et al(2004) reported the initial development of a biodegradable polymeric nanofiber-based antibiotic delivery system. The functions of such a system would be to serve as biodegradable gauze and antibiotic delivery system. They demonstrated that electrospinning is a sound technique for the fabrication of nanofibers produced from biodegradable polymers such as PLAGA. Noh et al (2006) found that the degradation rate of nanofibers is faster than microfibers, which indicated that electrospun nano fibers possess the potential for wound healing. It is loosely associated with terms such as absorbable, erodible, and resorbable [Wong and Bronzino, 2007, pp6-16].

## Hydrogel Wound Dressing

The Japan Science and Technology Corporation contracts research on this material to the private sector.

**Merits**

1. Speeds healing
2. Painless removal of the dressing
3. No residue
4. Transparency enables observing the healing process



**Product**



**Example of treatment**

Use: ① Skin burns ② Bedsores ③ Pharmaceutical chemical for wet cloth ④ Facial pack

Figure 2.3 Hydrogel wound dressing.

(<http://ciscpyon.tokai-sc.jaea.go.jp/english/ff/ff46/tech01.html>)

Figure 2.3 shows a wound dressing product produced by The Japan Science and Technology Corporation. This hydrogel wound dressing has many valuable clinical merits, such as fast healing, painless removal of the dressing, no residue and transparency which enables observation of the healing process. This product can be used for the treatment of skin burns and bedsores or as a pharmaceutical chemical for a wet cloth or facial pack.

However, sometimes the wound is deep and large penetrating through all the skin layers. In this case, it is not suitable to be treated simply by a wound dressing. Currently, the clinical gold standard for the treatment of a full-thickness skin

wound is autologous skin transplantation. Autologous split skin grafts (SSGs) are produced by detaching the epidermis and a superficial part of the dermis by a dermatome. The residual dermis of the donor site will re-grow an epidermis [Andreassi et al, 2005; Converse et al, 1975]. Although every donor site can be harvested up to 4 times, each harvest may cause heavier scars as well as increasing the risk of infection. Moreover, if the skin damage is more extensive, the availability of donor sites will become extremely limited, which exposes patients to a more dangerous situation. In this case, another possibility is allografts. However, these have potential disadvantages viz.: a tendency to complications, immune response, no enough source and they are also associated with ethical and safety issues. Consequently, skin substitutes provide a more permanent and acceptable solution.

### **2.2.2 Skin substitutes**

#### ***In vivo applications***

Skin damage can be categorised into four levels according to the depth of the wound: I) epidermal, II) superficial partial-thickness, III) deep partial-thickness, IV) full-thickness skin wounds [Papini, 2004]. Wound levels I to III can self-heal by stimulating keratinocyte regeneration which migrate from the remaining dermis at the wound edges [Blanpain et al, 2004; Tumber et al, 2004; Tumber, 2006]. It was found that any loss of full-thickness skin of more than 4 cm in diameter will not heal well without a graft [Herndon, 1989]. When the wound

area of the skin is too large to be treated in time with any convenient technique, even death may occur. When the wound is very deep, ideally, the optimal graft, that will not induce an immune response, should be readily available, to cover and protect the wound bed, accelerate the wound healing, reduce pain for the patient with little or no scar formation [Groeber et al, 2011]. As an alternative, particularly where there is a shortage of donor grafts skin substitutes, either with or without cells, may provide a possible optimal solution with lower manufacturing costs.

There are mainly three kinds of skin substitutes: epidermal substitutes, dermal substitutes and epidermal/dermal substitutes. Of these substitutes, the most advanced and sophisticated for clinical use are the epidermal/dermal substitutes, which can mimic both epidermal and dermal skin layers. These substitutes are composed of autologous or allogeneic keratinocytes and fibroblasts. The commercially available products of these cell-seeded skin substitutes for temporary clinical use are listed in Table 2.1 [Groeber et al, 2011].

Table 2.1 Commercially available epidermal/dermal skin substitutes for clinical use.

<b>Brand name</b>	<b>Manufacturer</b>	<b>Cell source</b>	<b>Matrix</b>
<b>Apligraf</b>	Organogenesis Inc., Canton, Massachusetts, CA, USA	Allogeneic keratinocyte and fibroblasts	Bovine collagen
<b>OrCel</b>	Ortec International, Inc., New York, NY, USA	Allogeneic keratinocyte and fibroblasts	Bovine collagen
<b>PolyActive</b>	HC Implants BV, Leiden, The Netherlands	Autologous keratinocyte and fibroblasts	PEO/PBT

<b>TissueTech Autograft System (Laserskin and Hyalograft 3D)</b>	Fidia Advanced Biopolymers, Abano Terme, Italy	Autologous keratinocyte and fibroblasts	HA
--	--	---	----

PEO: polyethylene oxide terephthalate.

PBT: polybutylene terephthalate.

HA: hyaluronic acid.

The skin substitutes shown in Table 3 make long-term grafting possible, but, because of the immunogenic tolerance of the host, applying allogeneic fibroblasts is controversial [Clark et al, 2007; Campoccia et al, 1998; Caravaggi et al, 2003; Uccioli, 2003; Myers et al, 1997; Nomi et al, 2002; George et al, 2000]. To date, only the microperforated HA membranes, on which the autologous fibroblasts and keratinocytes are grown, designed by Fidia Advanced Biopoly, can achieve permanent wound closure [Campoccia et al, 1998; Caravaggi et al, 2003; Uccioli, 2003.]. However, this skin substitute still cannot be considered to be a ‘real’ epidermal-dermal skin substitute, because, unlike normal skin, it has no antibacterial function.

### ***In vitro applications***

In addition to the in vivo applications mentioned above, in vitro applications have appeared for skin substitutes as in vitro test systems [Ponec, 2002]. Using these skin substitutes as an alternative to actual skin, means that investigations into both the fundamental processes of the skin and the toxicity of substances that may be used on the skin may be undertaken, without having to use animal models. These substitutes are currently applied in pharmacological and basic

research. In pharmacological research, skin substitutes are employed as dependable models to confirm irritative, toxic or corrosive properties of chemical agents designed for use on human skin [Robinson, 1999]. In basic studies, skin substitutes can help to explore the fundamental processes of wound healing, infection [Xie et al, 2010; Welss, 2004] and other skin-related processes.

Another in vitro application of skin substitutes is in the provision of diseased skin models, including psoriasis skin models, wound healing models and in vitro infection models [Andrei et al, 2010; Coolen et al, 2008; Green, 2004; Martin and Leibovich, 2005; Saiag et al, 1985]. This application has become more and more popular because of its obvious merits. However in vitro skin substitutes are not easily produced and stored, because these kinds of substitutes need to be highly customized and they also face the risk of contamination. If there are other substances that can improve cell proliferation, so that fewer autologous skin donors are needed, and, if the skin substitutes can be made to have an antibacterial property, they must be more acceptable for clinical applications.

### **2.3 Fabrication**

TE scaffolds are capable of supporting two or three-dimensional tissue formation. These scaffolds are often critical, both in vitro and in vivo, to allowing cells to influence their own microenvironments. Such devices are usually referred to as scaffolds or membranes. Various materials have been used for different purposes.

### 2.3.1 Materials and Methods

The raw materials needed for the production of TE scaffolds fall into two categories viz. biocompatible components and essential laboratory equipments. Both natural and synthesized materials, such as metals, polymers and proteins are used in the preparation of nano scaffolds,.

As shown in Table 2.2, many kinds of nanoparticles have been used to fabricate nano scaffolds. For example, titanium dioxide (TiO<sub>2</sub>) [Torres et al, 2007], hydroxyapatite (HA) [Cheng et al, 2007; Kong et al, 2005; Ramay et al, 2005; Sachlos et al, 2006], gold nanoparticles [Jordan et al, 2006; Liu et al, 2008; Singh et al, 2007], zirconia (ZrO<sub>2</sub>) [Zong et al, 2006], magnetite nanoparticles [Shimizu et al, 2006] and Silver sulfadiazine [Choi et al, 1999]. As reported by Cao et al (2006), composite nanoparticles have been synthesized and then anchored onto the grafted collagen or other matrix. Although the nano particles have been used for TE scaffolds, they seldom find application for skin TE scaffolds.

Table 2.2 Nanoparticle scaffold materials

Nanoparticle	Matrix	Remarks
TiO <sub>2</sub>	PLGA	An increase in storage modulus.
HA	PDLLA	Has good adhesion tendency to chondrocytes.
Gold	Spider silk	A promising candidate for the development of materials for vapor-sensing applications.
Ap-gold	PDMS	Provides an efficient means to functionalize three-dimensional (3-D) protein microstructures.

<b>ZrO<sub>2</sub></b>	Collagen	Provides an excellent matrix for protein immobilization and biosensor preparation.
<b>Magnet</b>	Collagen, PLA	Significantly enhances cell-seeding efficiency.
<b>Al<sub>2</sub>O<sub>3</sub>-ZrO<sub>2</sub></b>	Collagen	Enhances the mechanical properties of triple helices of collagen.
<b>HA</b>	Chitosan	Shows better biocompatibility than pure chitosan scaffolds.
<b>HA</b>	Chitosan-alginate	Better proliferated cells than the scaffolds without nano HA or with micro-sized HA.
<b>Silver sulfadiazine</b>	Gelatin-alginate	Good wound healing effect.

As summarized in Table 2.3, biodegradable polymers are extensively used to develop nano fibrous scaffolds. Different methods are employed to produce nano fibrous scaffolds. These include using Facio, a 3-D graphics program, employing Tinker with a charm 19 force field parameter [Nagai et al, 2006], or a double diffusion technique [Manjubala et al, 2006]. However electrospinning has become more and more popular because it generates nanoscale properties and technologies [Langer and Vacanti, 1993].

Table 2.3 Nano fibrous scaffold materials.

<b>Materials</b>	<b>Remarks</b>
<b>Fibronectin, PLLC</b>	Fn grafted on PLLC scaffold greatly promotes epithelium regeneration.
<b>Collagen</b>	Aligned collagen nano fibrous scaffold can be very useful for engineering different specific tissues or organs.
<b>Alginate, PEO</b>	Exhibits good uniformity, structural integrity, and cellular compatibility.

<b>Fibroin silk</b>	The concentration of regenerated silk solution is the most dominant parameter to produce uniform and continuous fibers.
<b>Collagen, GAG</b>	May potentially provide a better environment for tissue formation/biosynthesis compared to the traditional scaffolds.
<b>RADA16, hydrogel</b>	Release profiles can be tailored by controlling nanofiber-diffusant molecular level interactions.
<b>Hydroxyapatite, collagen, PLLA</b>	Could decrease the degradation rate in vitro.
<b>PLA, PLGA</b>	Hydrophilicity influenced by nano fibrous scaffolds has a considerable effect on neurite extension.
<b>Carbon</b>	Provides a high-surface-area.
<b>Chitin, silk fibroin</b>	Has excellent cell attachment and spreading for normal human fibroblasts.
<b>PGA, chitin</b>	Has both biomimetic three-dimensional structure and excellent cell attachment and spreading.
<b>HA, HA/gelatin</b>	HA/gelatin nanofibrous membranes are expected to be used as novel scaffolds for biomedical applications.

As shown above, many kinds of polymers such as Poly-L-Lactide (PLLA), Polyglycolic acid (PGA), Poly (lactide-co-glycolide) (PLGA), Polymethyl methacrylate (PMMA) are often used in the fabrication of scaffolds, not only at the micro-scale but also at the nano-scale [Sangsanoh and Supaphol, 2006; Sukigara et al, 2003; Ye et al, 2006]. Besides natural biomaterials, such as silk, protein and collagen are also used to fabricate the scaffolds [Sukigara et al, 2003, 2004; Putthanarat et al, 2006]. To explore substitutes for skin, some researchers have studied PLLA, PLGA, collagen, hyaluronic acid (HA), gelatin and alginate as the main components of skin TE scaffolds [Blackwood et al, 2008; Campoccia

et al, 1998; Choi et al, 1999; Kubo and Kuroyanagi, 2003; Li et al, 2005; Yannas et al, 1980].

### 2.3.2 Structures

As mentioned earlier, there are mainly two kinds of scaffold structures, nanoparticle scaffolds and nano fibrous scaffolds, as shown in Figure 2.4. Each structure will be introduced separately.

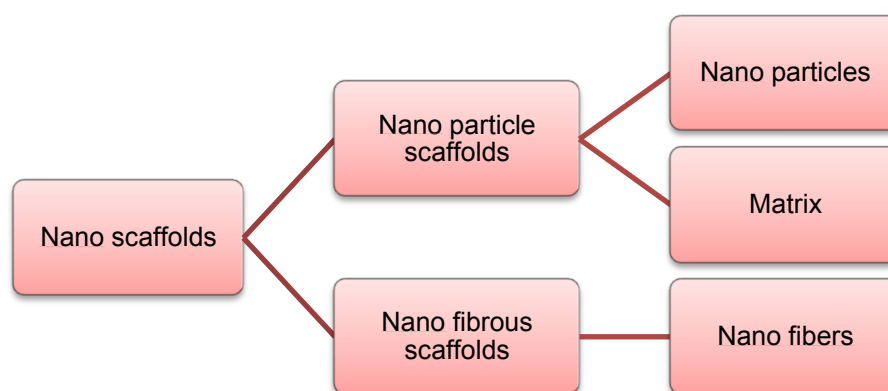


Figure 2.4 Structure of nano scaffolds.

#### *Nano particle scaffolds*

A simple way to explain the structure of nanoparticle scaffolds is that nanoparticle scaffolds are composed of nanoparticles blended or coated with matrices. Various surface modification techniques have been developed for patterning the nano scaffolds by using different nanoparticles. Cao et al(2006) used  $\text{Al}_2\text{O}_3\text{-ZrO}_2$  composite nanoparticles to enhance the mechanical properties of triple helices of collagen (Figure 2.5).

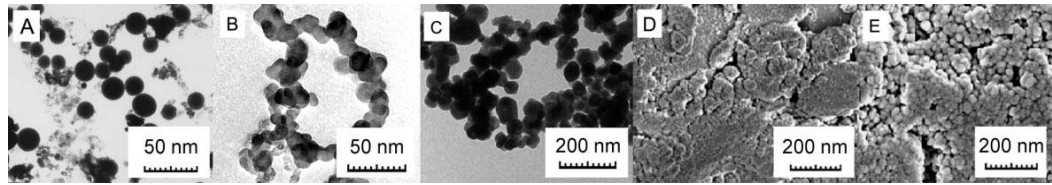


Figure 2.5 TEM images of A)  $\text{Al}_2\text{O}_3\text{-ZrO}_2$  composite nanoparticles, B) collagen, and C) grafted collagen. SEM images of hybrid nanocomposites with a composite nanoparticle content of D) 1.2 wt% and E) 7.3 wt % [Cao et al, 2006].

Torres et al(2007) filled PLGA foam with titanium dioxide ( $\text{TiO}_2$ ) nanoparticles to obtain tubular macropores which were interconnected by a network of micropores (Figure 2.6).

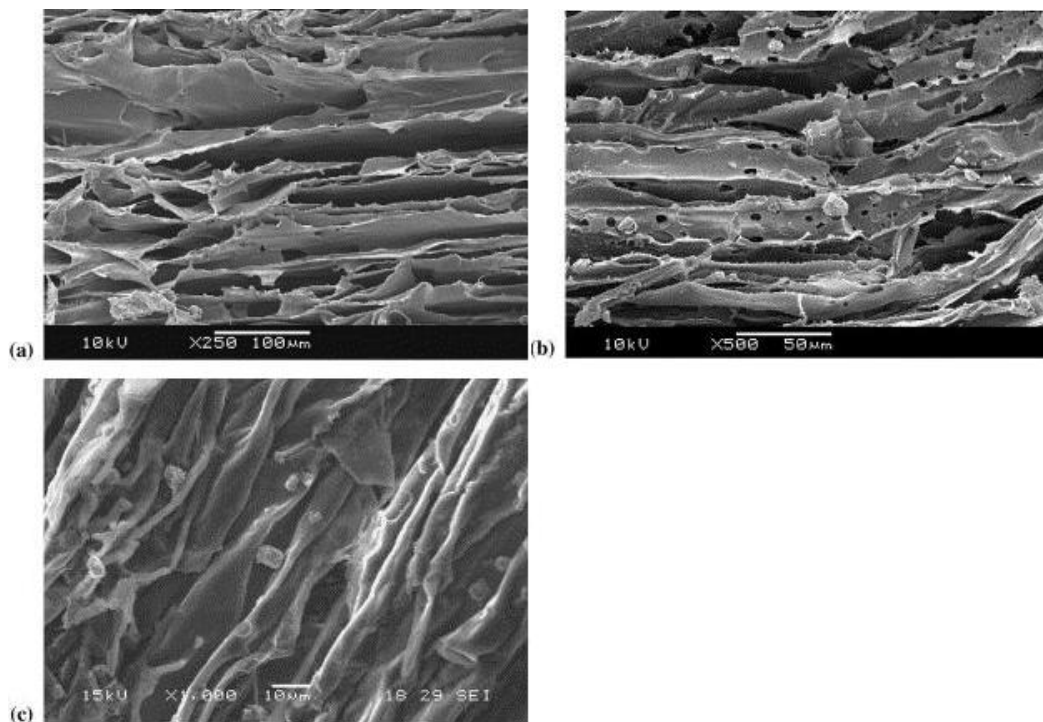


Figure 2.6 SEM images of foam scaffolds in axial direction: (a) plain PLGA, (b) PLGA + 5 wt%  $\text{TiO}_2$  and (c) PLGA + 20 wt%  $\text{TiO}_2$ . Some  $\text{TiO}_2$  agglomerates are seen in the 20 wt% foam [Torres et al, 2007].

Based on these studies, the composing particle is found to be one of the important factors that affects the properties of the scaffolds and cell viability. Ramay et al (2005) incorporated nano- and micro-hydroxyapatite (HA) particles into chitosan-alginate porous scaffolds. The results suggested that the nano-sized HA scaffold generated better mechanical and biological properties than either the micro-sized HA or scaffolds without HA. So, it may be anticipated that nano scale technology elicits more advanced techniques for not only material science but also TE.

### **Nano fibrous scaffolds**

In terms of good penetrability, fibrous scaffolds have been investigated for many years. Researchers have been trying to apply different materials and methods to fabricate appropriate nano scaffolds for both biological and medical applications [Ellis-Behnke et al, 2006; Hosseinkhania et al, 2006; Ji et al, 2006; Liang et al, 2005; Park et al, 2006; Tan and Lim, 2006; Wei et al, 2006; Yoon et al, 2006; Zhong et al, 2005]. If fibrous scaffolds are mainly constructed using nano-scale fibers, the penetrability of the scaffolds would be higher. So, more research work into nano fibrous scaffolds has been done recently. For example, Woodfield et al found that tissue formation was supported well by three dimensional fibrous scaffolds in vitro and in vivo [Woodfield et al, 2004]. On the basis of the findings above, it can be concluded that the most acceptable method for the fabrication of skin TE scaffolds is probably electrospinning (Figure 2.7).

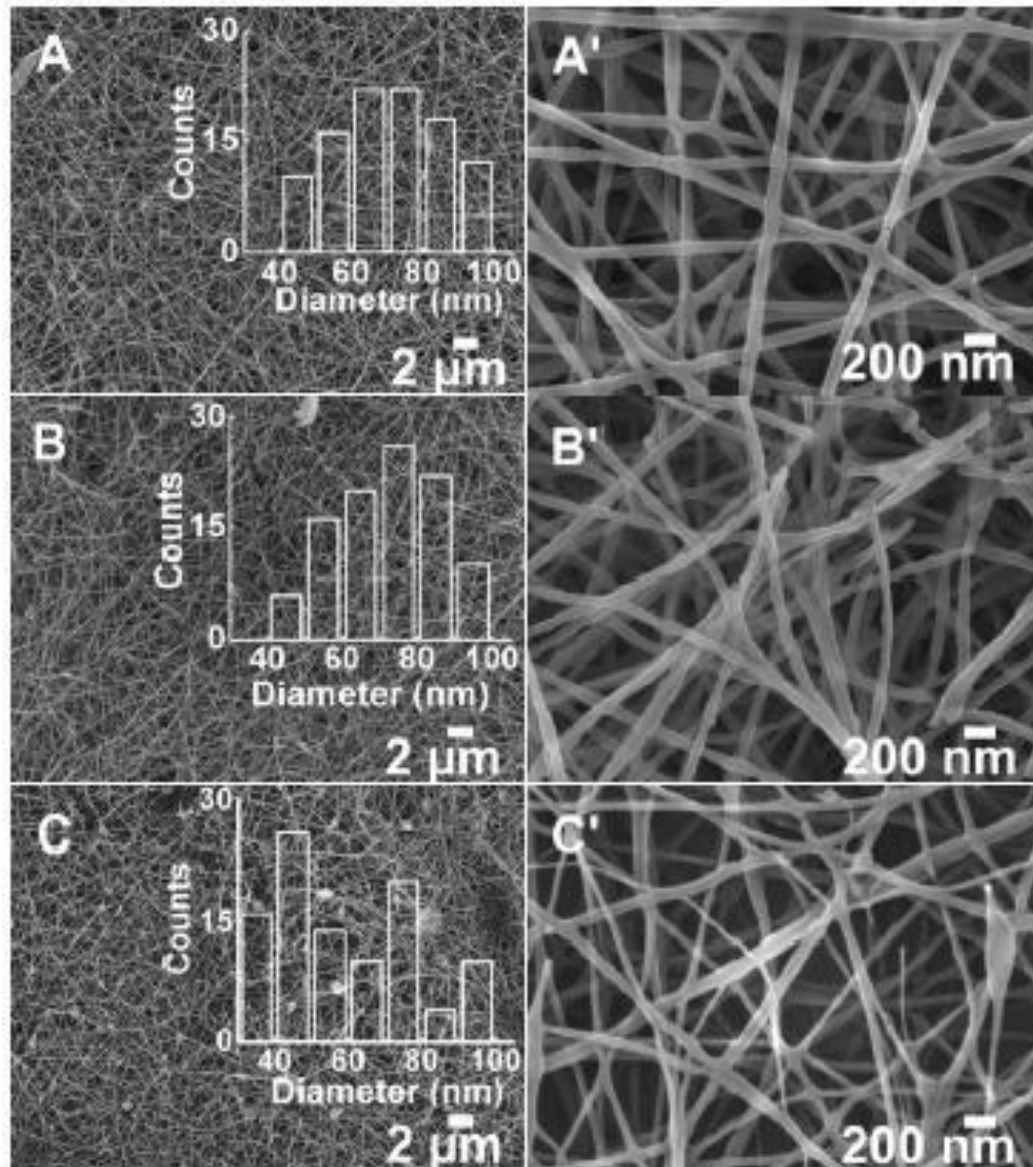


Figure 2.7 SEM images of alginate-PEO nanofibers: A-C) survey images of the nanofibers spun from solutions with alginate/PEO ratios of 70:30, 80:20, and 90:10, respectively. The insets show the fiber size distributions. A'-C') High-magnification images of A-C, respectively. All polymer solutions were prepared with 0.5 wt% Triton X-100 surfactant and 5 wt% DMSO cosolvent. [Bhattarai et al, 2006].

Electrospinning is used to fabricate nano fibrous matrices [Li et al, 2002]. Noh et al(2006) found that the attachment and spreading of the cells cultured on electrospun chitin nano fibers were higher than that for cells cultured on micro

fibers. This may be as a consequence of the higher surface area available for cell attachment due to their three-dimensional features and high surface area-to-volume ratios, which are favorable parameters for cell attachment, growth, and proliferation. These kinds of porous scaffolds are good for delivering nutrients to cells proliferated in the scaffolds, whilst the products of metabolism can be transferred out at the same time.

The basic electrospinning setup consists of a high voltage source, a syringe pump and a collector (Figure 2.8) [Pham et al, 2006]. The setup is simple and inexpensive, but it has the potential to provide more precise control for cells' behavior such as proliferation, attachment and migration. The process of electrospinning involves the use of a polymer, a protein, a polymer/protein, or any blended solution, a syringe and a high voltage. All these parameters affect the fabrication of nano scaffolds [Ye et al, 2006; Doshi and Reneker 1995; Reneker and Chun 1996; Shin et al, 2001; Yarin et al, 2001; Senador et al, 2001].

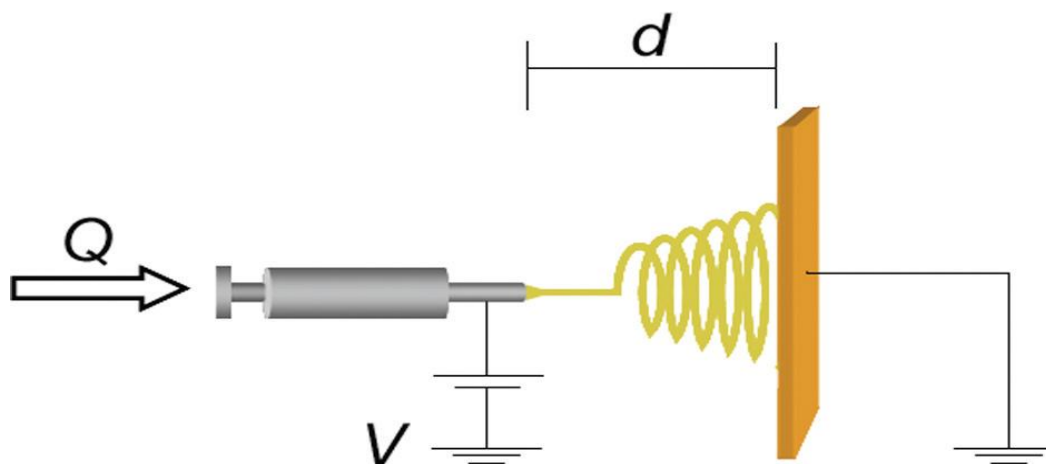


Figure 2.8 Typical electrospinning setup.  $Q$ , flow rate;  $d$ , distance between plate and needle;  $V$ , applied voltage. ([www.liebertonline.com/ten](http://www.liebertonline.com/ten)).

Sukigara et al (2003) studied the effect of electrospinning parameters on the morphology and fiber diameter of regenerated *Bombyx mori* silk . They found that the silk concentration was the most important parameter in producing uniform cylindrical fibers less than 100 nm in diameter. On the other hand, the proportion of the components in the electrospinning solution is also very important factor to fabricate the nano fibers, not only for controlling the diameter of the electrospun fibers, but also for the possibility of obtaining straight and even fibers.

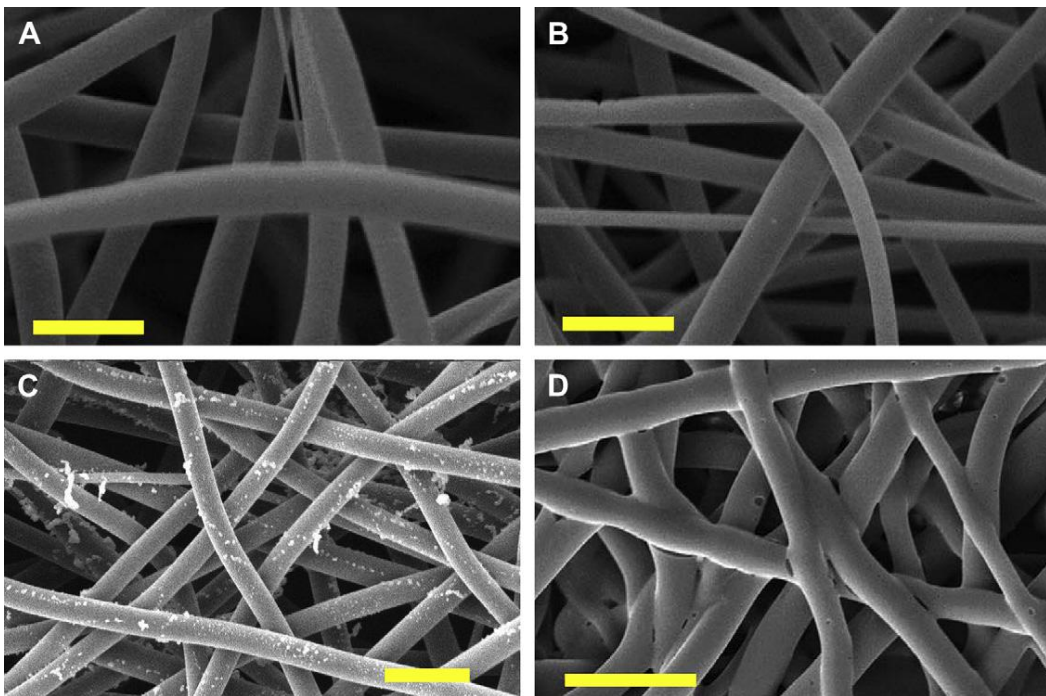


Figure 2.9 SEM micrographs of electrospun PLLA (A), PLGA 85:15 (B), 75:25 (C), and 50:50 (D) scaffolds prior to implantation [Blackwood et al, 2008].

As shown in Figure 2.9, this characterization of the scaffolds seems more applicable for skin TE scaffolds which can be used as substitutes for the dermal and epidermal parts of skin [Blackwood et al, 2008].

Over the last two decades, there has been an increasing number of studies of electrospun scaffolds. Designing nano featured TE scaffolds by applying the electrospinning technique is even regarded as art [Ramalingam and Seeram, 2006]. Thus, electrospinning is a promising technique for making polymeric flexible nano fibrous structures, and it can possibly be used for fabricating large sheets of scaffolds as dermal substitutes [Agić et al, 2010].

## **2.4 Properties**

The properties of nano scaffolds generally depend on their constituent materials and their structures, and the treatments applied to scaffolds will affect the properties of nano scaffolds markedly. This finding helps to provide a scientific basis for fabricating more suitable scaffolds for biomedical applications. In this section, some major properties of nano scaffolds including their morphology, tensile properties, hydrophilicity, moisture-related properties and degradability will be discussed.

### **2.4.1 Morphology**

The morphology of nano scaffolds including their diameter, porosity and two- or three-dimensional structures should be studied as well as the sequent research on the physical and mechanical properties of the scaffolds. Liu et al (2004) found that the particulate membrane not only improved cell adhesion and growth, but also regulated osteoblastic phenotype. Cells cultured on the porous and

particulate membrane can be considered to be completely flattened and well spread (Figure 2.10).

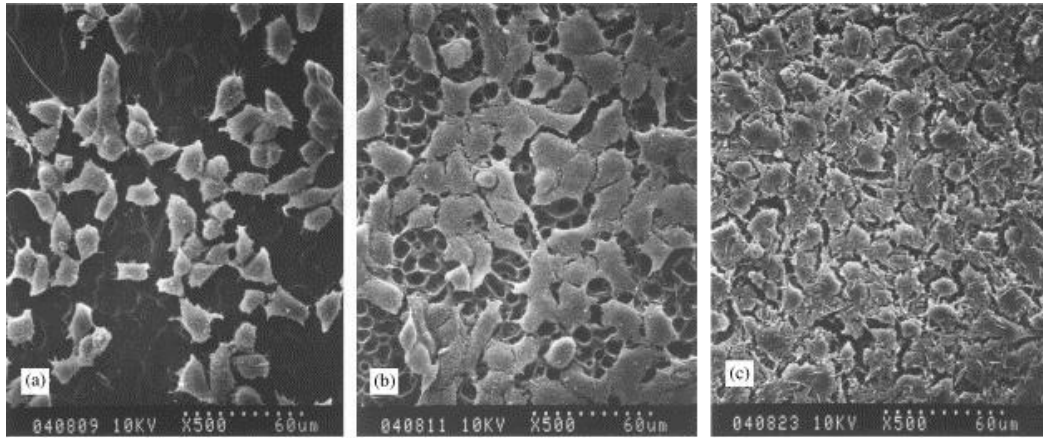


Figure 2.10 SEM photographs of MG-63 cells cultured on the (a) dense, (b) porous, (c) particulate PLLA membranes after 1 d incubation. [Liu et al, 2004].

The surface and structural changes of the scaffolds can be observed through scanning electron microscopy (SEM) micrographs (Figure 2.11) [Noh et al, 2006, Manjubala et al, 2006].

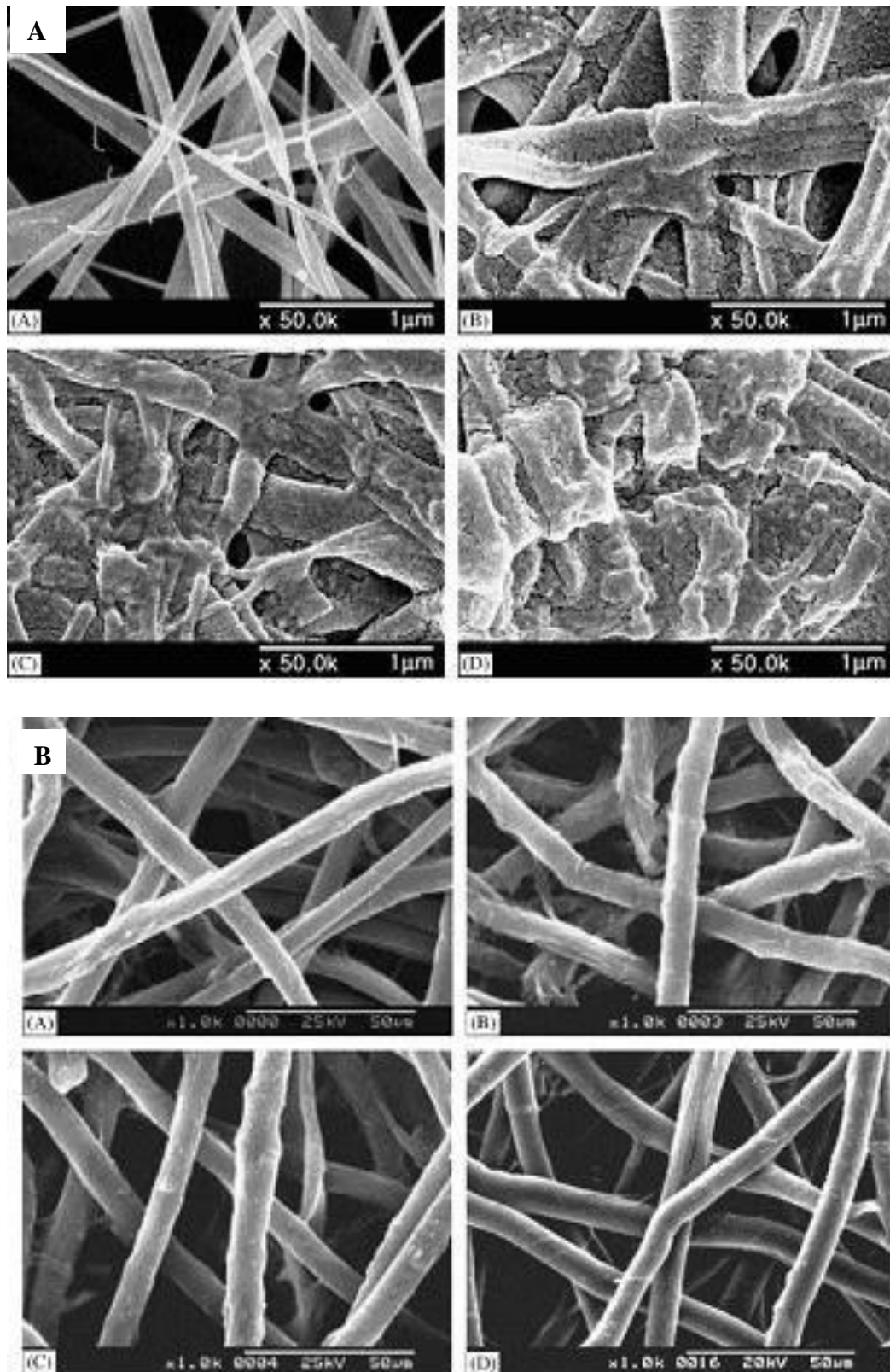


Figure 2.11 Morphological changes in an electrospun nanofibrous matrix and a microfibrillar matrix. A. Electrospun nanofibrous matrix; B. Microfibrillar [Noh et al, 2006].

The fibrous structure, which can be described as porous, shown in Figure 2.11 showed the morphological changes of the fibrous structure. It can be seen that the nanofibrous scaffolds decayed more obviously than the microfibrinous one. This may be important evidence for fabricating biodegradable TE scaffolds. On the other hand, some researchers found that the morphology also influences the mechanical properties of the skin TE scaffolds, such as their friction coefficients [Derler and Gerhardt, 2011].

#### **2.4.2 Tensile property**

There are many mechanical properties of the skin, which give it its protective functions against mechanical trauma, such as extensibility and recovery, compression, friction, impact resistance, and shear strength. This raises the question - for skin, what are the most important properties? From a medical point of view, the tensile property is the most important mechanical property of the skin with respect to its protective function. Usually, the tensile property of skin is described in terms of its tensile strength (ultimate load divided by cross-sectional area), which ranges from 5-30N/mm<sup>2</sup>. Its maximum value is about 21N/mm<sup>2</sup> reached at 8 years of age. It then starts to decline to about 17 N/mm<sup>2</sup> at 95 years. Furthermore, when the skin is stretched, the ultimate strain, the extension before rupture, changes from about 35% to 115% [Edwards and Marks, 1995]. The skin referred to above includes the epidermal and dermal layers. As an important part of the skin layers, the dermal layer, helps to provide mechanical protection and a

base for cell proliferation to form the skin equivalent (SE). In 1995, Lafrance et al tried to measure the tensile property of the dermal equivalent (DE). Their result showed that the cell culture period on the DE may influence the tensile property and the DE structure became stable after four days of cell culture [Lafrance et al, 1995]. In 2010, the mechanical properties of excised human skin were studied by Annaidh et al. They concluded that the mean ultimate tensile strength was  $21.5 \pm 8.4 \text{MPa (N/mm}^2\text{)}$  [Annaidh et al, 2010]. Hendriks found, from tensile tests, that the maximum Young's modulus and maximum strain of the skin were 4MPa and 32% respectively [Hendriks, 2005]. However, there is no definitive information about the mechanical properties of the individual skin layers, especially *in vivo*. Thus, there needs to be further study of the mechanical properties of skin layers.

### **2.4.3 Hydrophilicity**

Hydrophilicity is measured by the water contact angle  $\theta$ . A lower degree of contact angle means a higher hydrophilicity, and vice versa. Kim et al (2003) demonstrated that a higher contact angle scaffold surface did not spread cell solution well. They attempted to control the degradation rate of the scaffolds by incorporating a hydrophilic catalyst (lactide) in the nanofiber in order to accelerate the hydrolytic reaction, so a PLA-b-PEG-b-PLA triblock copolymer was used to “entrap” the hydrophilic lactide because of its amphiphilic nature. This copolymer modified the hydrophobicity of the scaffolds.

In Aroca et al's study (2004), poly (2-hydroxyethyl acrylate) hydrophilic coatings were grafted onto macroporous poly (methyl methacrylate) by adsorbing monomer vapor and subsequent plasma-induced polymerisation without the need for thermal or photoinitiators. By means of this particular protocol it was possible to graft hydrophilic polymers onto hydrophobic scaffolds whilst maintaining their initial porosity. This composite material was able to form a resistant polymer hydrogel when water was absorbed. Thus, hydrophobicity plays a key role in the function of nano scaffolds. So, the modification of hydrophilicity is another key factor influencing the function of nano scaffolds.

Generally, cells tend to adhere and grow more on hydrophilic materials than hydrophobic ones. So, hydrophilicity of the materials and modifying this property become very important in the preparation of skin substitutes.

#### **2.4.4 Moisture-related properties**

Individuals who lose skin extensively, for example in serious burns, are in danger of not only massive infection, but also severe fluid loss [Yannas and Burke, 1980]. This means that, besides the infection risk, the moisture-related properties are also very important in the design of skin TE scaffolds. Under normal conditions, the stratum corneum (SC) which, is the most outer layer of the epidermal skin, receives moisture from the fluids around underneath the skin

layers. SC also receives moisture from the sweat glands when they are active. However, the sweat glands are active only at temperatures above 30°C to aid in the body heat removal. Usually the moisture from the sweat glands is not included in studies of skin moisture, because different sites of the skin have various numbers of sweat glands. On the uncovered areas of skin, water will be evaporated from the SC into the surrounding atmosphere. The loss of water from the surface of skin is related to the surrounding temperature, relative humidity and air flow. When the conditions are maintained at a temperature around 23°C, a relative humidity of 40 to 50% RH in quiet air, water from the full thickness of abdominal skin is lost at the rate of 0.1 to 0.2 mg/cm<sup>2</sup>/hr, and the dermal part of the skin loses water at a rate of 10.0 to 15.0 mg/cm<sup>2</sup>/hr [Blank, 1952]. Furthermore, it has been found that the skin equivalent with an RH of 30% has the highest tensile strength [Park and Baddiel, 1972].

On the other hand, Yannas and Burke (1980) mentioned in their study that air-pockets appeared at the graft-wound bed interface, which are also named "dead space", and these often become the place for bacterial proliferation (Figure 2.12). So, appropriate moisture content of the wound bed is necessary for the graft to contact and spread over the wound area and displace the air-pockets from the interface. Also, an appropriate rate of moisture flux through the skin TE scaffold is required by the effective wound closure. If the moisture flux through the scaffold is very slow, water accumulates at the interface between the scaffold and the wound bed and causes edema. When the moisture passes through the

scaffold at a high rate of flux, the scaffold loses its ability to keep the wound bed wet, so that it fails to maintain an air-free interface. Therefore, its moisture management property is also a very important property for a skin TE scaffold.

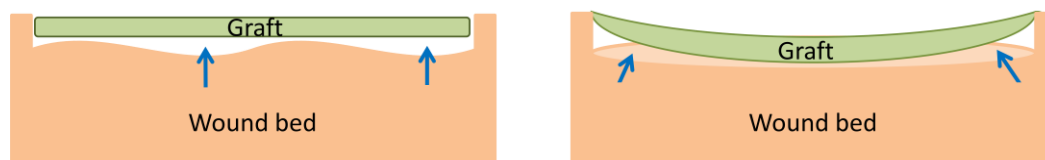


Figure 2. 12 Diagrammatic sketch of air-pockets (indicated by arrows).

Thus, with compatible mechanical and moisture-related properties, a skin TE scaffold can provide a good skin substitute. Therefore, in this study, the moisture-related properties of skin TE scaffolds including moisture content, water vapor permeability and moisture management properties will be investigated.

#### 2.4.5 Degradability

As mentioned above, when the skin TE scaffolds are used in a human body for wound treatment degradability is quite significant for the different tissue substitutes. Quite a few studies into the degradation of materials have been undertaken [Kwon et al, 2005; Chen et al, 2006; Shum and Mak, 2003; Kim et al, 2003]. Sangsanoh et al (2006) observed the degradation of electrospun chitosan nano fibrous membranes in neutral or weak basic aqueous solutions. They found that electrospun chitosan nano fibrous membranes, after neutralization in the  $\text{Na}_2\text{CO}_3$  aqueous solution, could maintain their fibrous structure even after

continuous submersion in phosphate buffer saline (pH = 7.4) or distilled water for 12 weeks (Figure 2.13). Kim et al (2003) demonstrated that the biodegradation rate, as well as the hydrophilicity of the electrospun nano scaffolds, could be finely tuned using different material compositions.

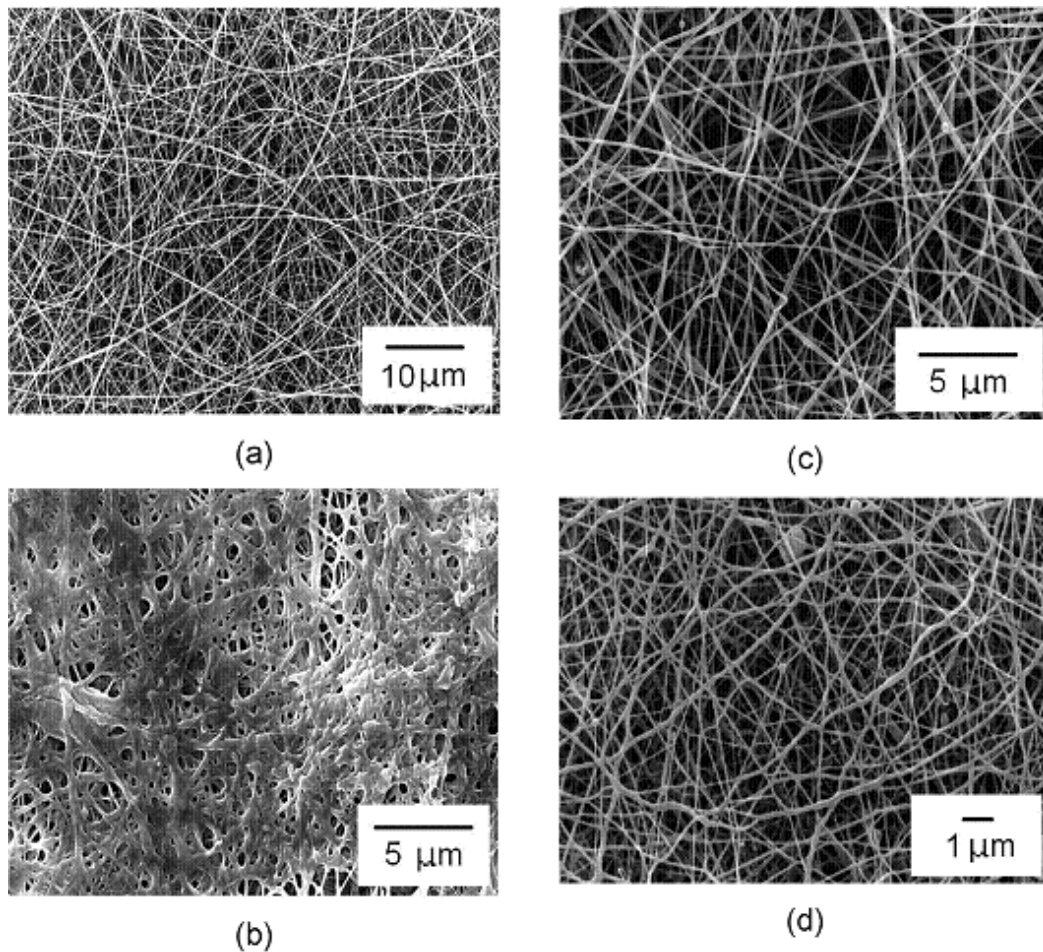


Figure 2.13 Selected SEM images of (a) pre-neutralized as-spun chitosan nanofibrous membrane from 7% chitosan solution in 70:30 v/v TFA/DCM, chitosan nanofibrous membrane after neutralization with (b) 5 M NaOH or (c) 5 M Na<sub>2</sub>CO<sub>3</sub> aqueous solution, and (d) chitosan nanofibrous membrane in panel c after submersion in PBS for 12 weeks. [Sangsanoh et al, 2006]

The degradability of the scaffolds was tested according to the techniques developed by Shum and Mak, Li and Mak, and Yuan (2003; 2005; 2002, 2003).

Nano scaffolds were immersed in phosphate buffered saline to test their degradability. After some time, the scaffolds were tested at different time points. Samples of degraded scaffolds were characterized in terms of weight loss, dimensional changes, morphology (using SEM) and chemical structure analysis (using Fourier Transform Infrared Spectroscopy (FTIR)).

Characterising the degradability of nano scaffolds is quite pivotal to obtain optimal scaffolds for biomedical purposes. Neither too fast degradability nor too slow degradability are suitable for TE biomaterials. If they degrade too quickly, it will be impossible to culture cells on the scaffolds, whereas if they degrade too slowly, they will easily cause other problems in the human body such as rejection or inflammatory responses to the scaffolds. So, to characterize and modify the degradability of electrospun nano scaffolds is an essential requirement. For the wound healing process, degradability is highly desirable, because a single treatment for a wound can markedly reduce pain for the patients.

All the many different properties of the scaffolds are interdependent, so, exploring this interdependence is another aspect of nano scaffold research for skin TE.

## **2.5 Cytotoxicity**

Many kinds of synthesized materials have been investigated for their potential biomedical applications. Without question, cytotoxicity testing is a fair predictor

of biocompatibility. This method is useful for screening materials as a basic part of biomaterial compatibility evaluation [ISO 10993]. For instance, silver (Ag) which is known as an anti bacterial agent and is widely studied for medical applications has been investigated for its cytotoxicity. Arora et al (2008) tried to define a safe range of Ag NPs as a topical antimicrobial agent. Figure 2.14 shows that the concentration of Ag NPs influenced the cell culture significantly.

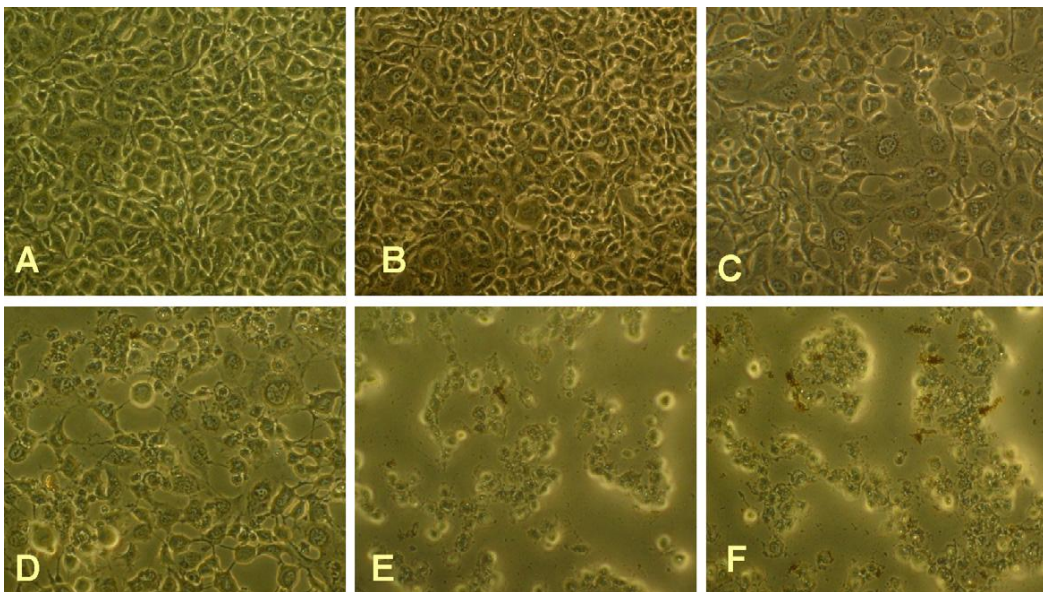


Figure 2.14 Phase-contrast micrographs of HT-1080 cells: (A) unexposed cells; (B–F) 24 h after the cultures were exposed to 3.12, 6.25, 12.5, 25 and 50 $\mu$ g/mL SNP, respectively (magnification 200 $\times$ ). [Arora et al, 2008]

Alt et al (2004) found that a scaffold loaded with silver salts was cytotoxic, but Ag NPs composed bone cement was free of in vitro cytotoxicity. The cells grown on Ag NPs bone cement were mainly vital and revealed similar behavior as the control cells. This result implied that the silver particle size was an important parameter for reducing the cytotoxic effects of biomaterials. On the other hand,

this experiment also supported the feasibility of the application of Ag NPs composed scaffolds for skin TE.

Hence, cytotoxicity testing is a primary and necessary step for further investigation of biomaterials, but the results should be combined with those from other tests to establish biocompatibility .

## **2.6 Cell proliferation**

Tissue regeneration is a popular research area for medical applications. When tissue defects such as burns and wounds occur, immediate and proper tissue regeneration is vitally important. Since the nano scaffolds have specific properties with good potential biocompatibility, they definitely become the desirable choice for supporting tissue regeneration. Kong et al (2006) found that there were more cells on a nano composite scaffold than on a scaffold without nano-HA. They concluded that the addition of nano-HA to a chitosan scaffold improved its bone bioactivity, which could develop the use of chitosan in bone TE.

In terms of cell proliferation, nano scaffolds have often been studied to improve the regeneration of bone, muscle, skin and axon [Hosseinkhani et al, 2007; Tuan, 2006; Ellis-Behnke et al, 2006; Pattison et al, 2006] sometimes by controlled release of protein from a 3-D tissue engineered nano-scaffold or through a nano fiber hybrid scaffold.

Until now, the most successful achievement in tissue regeneration research has been skin regeneration, such as the development of artificial skin. The most valuable application of cell lines for skin substitutes are fibroblasts and keratinocytes [Flasza-Baron et al, 2008; Myers et al, 1997; Noh et al, 2006; Saiag et al, 1985; Venugopal et al, 2006]. Usually, after culturing fibroblasts on the dermal part of the matrix, the keratinocytes will be seeded on it and then proliferated for a desired period before being used as skin substitutes.

Zacchi et al (1998) mentioned that a skin equivalent might be useful in the treatment of both burns and chronic wounds. Holder et al (1998) previously tried to apply poly-L-lactide (PLLA) and polyglycolide as skin matrices for implantation subcutaneously in a rat. Liu et al (2003) found that artificial derm built by acellular dermis, collagen membrane and collagen gel as scaffolds is a preferable structure as an ideal substitute for skin. While transplant medicine has made rapid progress, the development of optimal artificial skin grafts received more attention, especially for those patients who have suffered from burns and wounds. As the most advanced biomaterials, nano scaffolds will become the best choice to pursue this objective.

## **2.7 Antibacterial activity**

Drug delivery is another effective way to accelerate wound healing and avoid infection. As a carrier, a nano scaffold represents a good structure for bio-factor

delivery [Li et al, 2005; Nagai et al, 2006]. This kind of wound dressing may be used as a promising method to control the release of antibiotic by incorporating antibiotic into a nano fibrous scaffold (Figure 2.15) [Chiu et al, 2005; Kim et al, 2004].

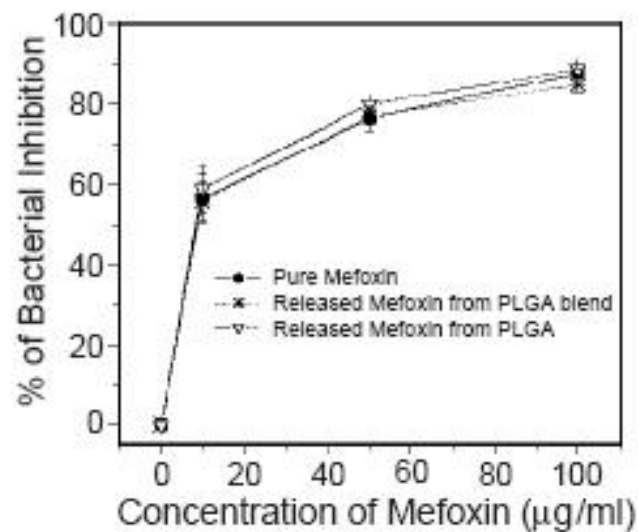


Figure 2.15 Antibiotic released from electrospun scaffolds demonstrate the same activity as the pure drug form, indicating that the processing is not damaging to the drug. Incubation of bacteria directly with drug loaded scaffolds demonstrates that the drug is able to diffuse from the scaffold and inhibit bacterial proliferation.

If the rate of drug release can be controlled, it can solve many clinical problems.

For example, frequent changes of the wound dressing can be avoided before

wound recovery. Consequently only one or two pieces of nano scale fibrous gauze may be enough for complete wound repair. On the other hand, during the treatment of a wound, infection is a common risk which needs to be prevented for good healing of the wound. Thus, the optimal scaffold for medical applications requires the TE scaffold to have antibacterial properties [Chen et al, 2008]. As mentioned earlier, due to their strong antibacterial properties and low toxicity, silver and its compounds have been studied for many years not only for their low toxicity, but also for their antibacterial activity [Alt et al, 2004; Crabtree et al, 2003; Chaloupka 2010; Furno et al, 2004; Galeano et al, 2003; Kidambi et al 2005; Lai and Fontecchio, 2002; Thomas et al, 2007]. Yeo et al (2003) found that fibers containing silver showed excellent antibacterial property. Alt et al (2004) demonstrated that nano particulate silver loaded bone cement revealed high antibacterial activity.

On the other hand, , some materials have an inherent antibacterial property, . Chitosan, for example. Eaton et al(2008) studied the antibacterial effects of chitosan on *Escherichia coli* (E.coli) and *Staphylococcus aureus* (Staph.), and found that these effects were related to the molecular weight of chitosan. Therefore, for example, if a scaffold included an antibacterial matrix incorporating chitosan and Ag NPs, such a skin TE scaffold may be more efficient in reducing the possibility of infections.

## 2.8 Research gap

The challenge in developing scaffolds suitable for TE is to find the appropriate materials and methods to fabricate the scaffolds with optimized physical and biological properties and functions, so that these scaffolds are able to be applied as tissue substitutes or medical devices. However, there is still a large gap in knowledge to fill to satisfy these research aims.

Although research into nano scaffolds has been proceeding, the only, almost successful, application is in skin substitutes, which indicates that there is a long way to go to translate basic research into commercialized products. Despite the nano- or micro- scaffolds, there are few acceptable substitutes for tissue regeneration which can be used in clinical applications.

Although antibacterial coatings on TE scaffolds have been researched, there are no optimal skin substitutes with both accelerated cell proliferation and relatively long lasting antibacterial effects. Furthermore, the control of the release of the antibacterial component through scaffolds is still a big challenge in this research area. Antibacterial activity would be an optimizing characteristic for skin TE scaffolds, but the quality and quantity of antibacterial biomaterials need to be studied more. If scaffolds can be made of antibacterial materials, how should their cytotoxicity and cell proliferation aspects be considered?

The different properties of nano scaffolds have been studied for many years, but it is still unclear how to control the properties to achieve the optimal scaffolds for TE. In other words, the relationship between their morphology, tensile properties, hydrophilicity, moisture-related properties and biodegradability needs more in-depth studies, and the optimization of the specifications for the fabrication of nano scaffolds has yet to be realised.

All these research gaps have started to be addressed by many researchers by far. However, there is still a long way to go to identify the optimal nano scaffolds for skin TE.

## **2.9 Summary of literature review**

Tissue defects, whether congenital or acquired in origin, need reconstruction. TE scaffolds are becoming an important medium to benefit the replacement, repair or enhancement of the biological functions at the level of a tissue or an organ. Compared to micro scale scaffolds, nano scaffolds have a huge potential to provide more precise and flexible structures for biomedical purposes. Thus, the realization of nano scaffolds in TE becomes a new frontier in biotechnology to develop new artificial skin, reconstructed tissue and wound treatments.

Usually, nano scaffolds can be categorized into two different types: one is a nanoparticle scaffold composed of various functional nanoparticles; the other is a nano fibrous scaffold which is mainly produced by electrospinning. Since a

number of natural and synthesized materials are used to generate the nano scaffolds, it is crucial to perform cytotoxicity test before systematically studying the parameters influencing the properties of the nano scaffolds, and subsequent cell responses to the scaffolds. With further developments in nanotechnology and TE, tissue regeneration, wound healing and drug delivery become frontier biomedical research areas. In this area, the study of artificial tissue and devices for wound treatments plays a key role with attractive potential. However there are still many research gaps that need to be filled.

When a piece of skin is lost, whether it is full skin thickness or not, the risk of infection and water loss is hard to avoid and sometimes these risks may even cause death. So, to apply a quick cell proliferation and an antibacterial protective skin substitute would be very effective. If the wound bed is large, the proper biomechanical properties of skin substitute are important for the recovery of the wound and restoring the normal biofunction to the wound area. On the other hand, for example, when skin burns are incurred, protein will also be lost, so, if the protein can be incorporated into the skin TE scaffold, it may provide some valuable nutrient for the wound healing.

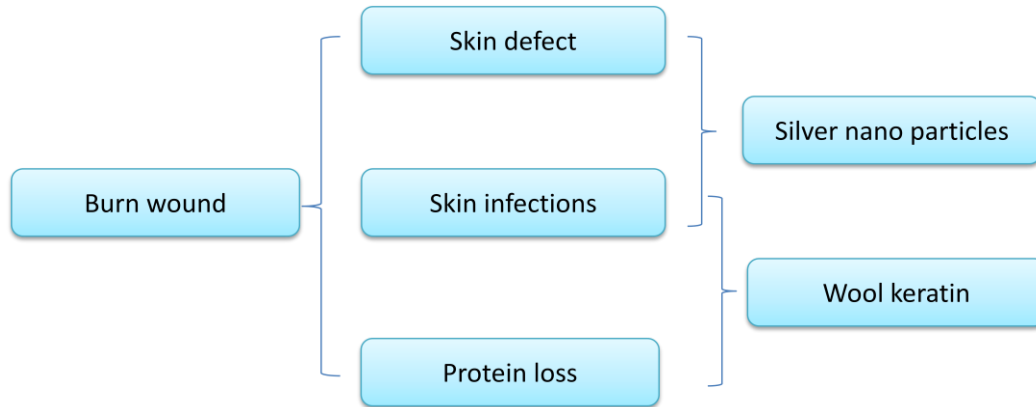


Figure 2.16 Flow chart for wound healing strategy.

As shown in Figure 2.16, there are mainly three after-effects of burns: skin defects, infections and protein loss. If these three effects can be treated properly, the potential risks to wound recovery must reduce significantly.

As mentioned earlier, maintaining the correct moisture condition for the wound bed can effectively decrease the chance of infection. Since wool keratin has a good moisture retention property, this protein can be helpful in controlling the relative humidity in skin substitutes. Therefore, this study will focus on the cell proliferation and antibacterial activity of skin TE scaffolds using wool keratin and Ag NPs. The aim will be to establish their ability to produce skin TE scaffolds that have both high cell proliferation and an antibacterial property.

## CHAPTER 3: FABRICATION

3.1 Materials and equipments .....	46
3.2 Fabrication of PLLA and Ag/PLLA composed films .....	49
3.3 Electrospinning of PLLA and Ag/PLLA fibers .....	51
3.4 Preparation of wool keratin particles .....	53
3.5 Electrospinning of wool keratin-PEO fibers .....	57
3.6 Electrospinning of PLLA/keratin fibers.....	62

### 3.1 Materials and equipments

In this chapter, the main materials, equipments and methods used in the research will be introduced. The methods include the fabrication of PLLA and Ag/PLLA composed films and fibers, preparation of wool keratin particles, and electrospinning of wool keratin composed fibers.

#### 3.1.1 Materials

**Poly-L-Lactide (PLLA):** PLLA with an inherent viscosity of 7.0 dl/g was purchased from PURAC, Netherlands.

**Wool fibers:** Wool fibers were purchased from the Nanjing Wool Market (Figure 3.1).



Figure 3.1 Wool fibers purchased from Nanjing Wool Market.

**Silver nanoparticles (Ag NPs):** Silver nanoparticles with particle sizes ranging from 1-100nm with 99.9% purity and a 35nm average particle size (Figure 3.2) were purchased from the Shenzhen Junye Nano Material Co. Ltd.

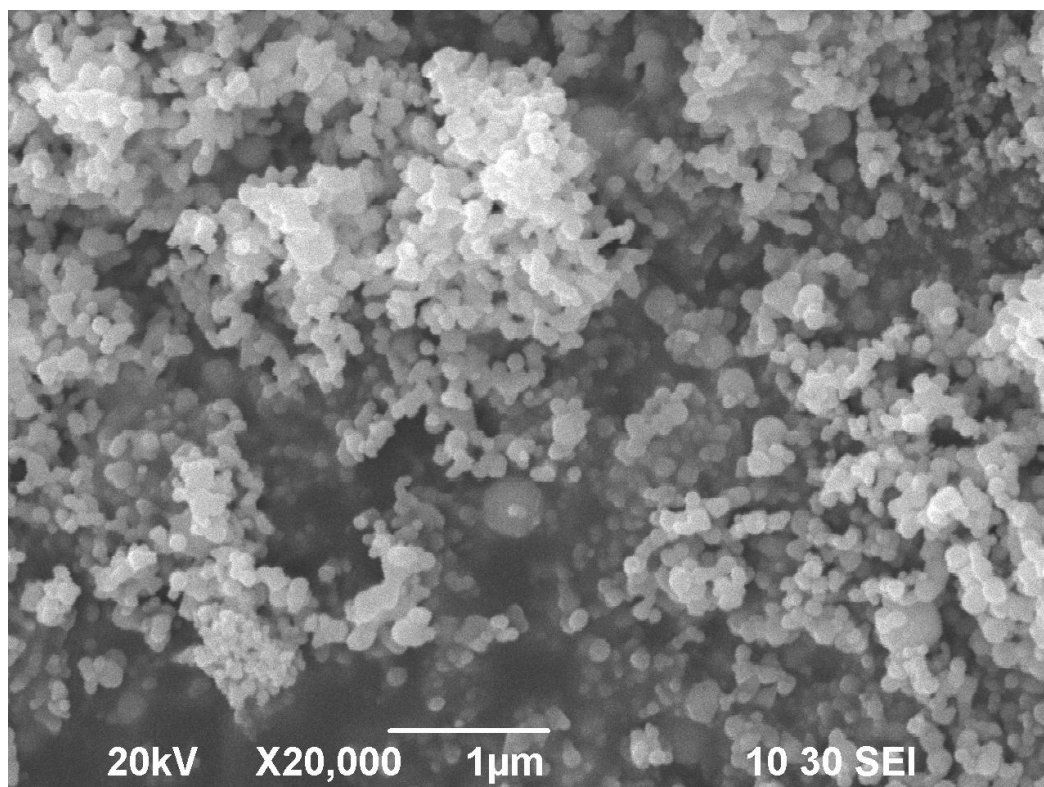


Figure 3.2 SEM images of Ag NPs (20kV). Ag NPs are grey and white color with an average particle size of 35nm.

**N, N-dimethylformamide (DMF):** DMF was purchased from Acros (Belgium).

**Chloroform:** Chloroform was purchased from Advanced Technology & Industrial Co. LTD, Hong Kong.

**Sodium hydroxide (NaOH):** NaOH was purchased from Advanced Technology & Industrial Co. LTD, Hong Kong.

**Hydrochloric acid (HCl):** HCl was purchased from Advanced Technology & Industrial Co. LTD, Hong Kong.

**Polyethylene oxide (PEO):** PEO was purchased from Aldrich Chemical Company.

**Formic acid:** Formic acid was purchased from Aldrich Chemical Company.

### **3.1.2 Main equipments**

**Mini spray drier:** BUCHI Labortechnik AG, B-290, Switzerland.

**Nanofiber electrospinning unit:** NEU-010, KES KATO TECH Co. LTD, Japan.

**Scanning electron microscopy (SEM):** JEOLJSM-6335F and LEICA, Stereoscan 440. The specimens were coated with gold using a sputter coater and their morphology was observed under the SEM at an acceleration voltage of 20kV.

**Fourier transform infrared spectroscopy (FTIR):** Perkin-Elmer System 2000.

### **3.2 Fabrication of PLLA and Ag/PLLA composed films**

PLLA was added into chloroform (an organic solvent) at a concentration of 2% in weight by volume (m/v) (2g of PLLA were added to 100ml of chloroform), and stirred for 4 hours to obtain PLLA-chloroform solution. Ag NPs were added into the PLLA-chloroform solution at different weight ratios to the PLLA to obtain 0.5%, 2.5%, 5%, 7.5%, and 10% Ag/PLLA solution.

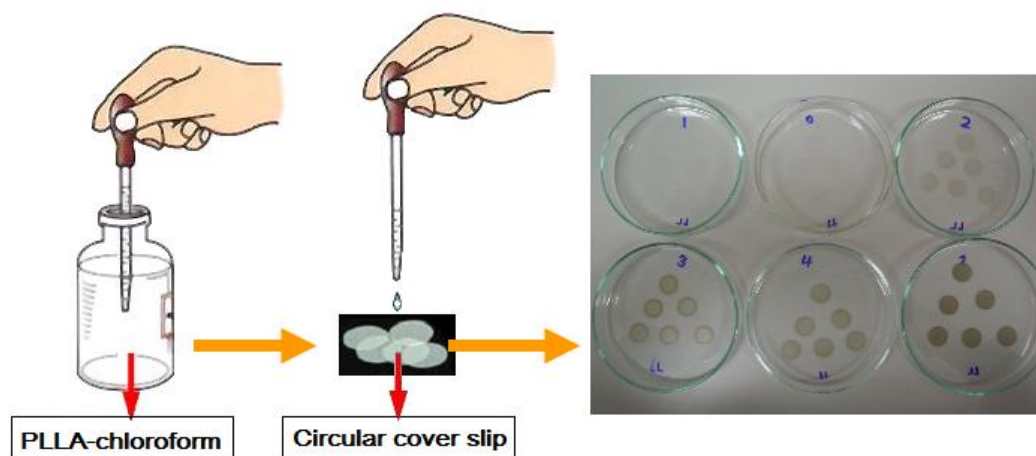


Figure 3.3 Scheme of PLLA and Ag/PLLA membrane preparation. (0) PLLA (1) 0.5% Ag/PLLA (2) 2.5% Ag/PLLA (3) 5% Ag/PLLA (4) 7.5% Ag/PLLA (5) 10% Ag/PLLA.

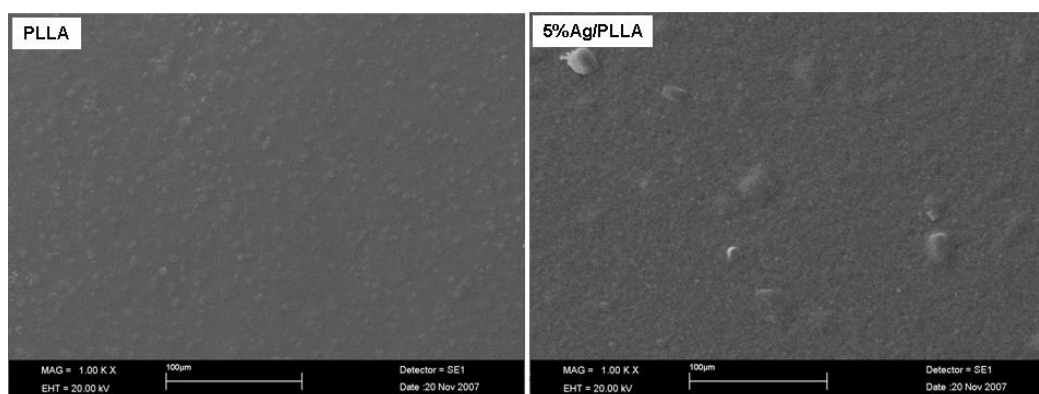


Figure 3.4 Topographical SEM images of PLLA and 5% Ag/PLLA film surfaces.

The PLLA-chloroform solution and the Ag/PLLA-chloroform solution were stirred gently at room temperature ( $20 \pm 2^\circ\text{C}$ ) until the Ag NPs had dispersed evenly. 200  $\mu\text{l}$  of the PLLA and Ag/PLLA solution were dropped onto separate circular cover slips (13mm diameter,) slowly and gently, to avoid producing any bubbles, and allowed to evaporate to form PLLA and Ag/PLLA films (Figure 3.3). The silver content of the Ag/PLLA films (from 10% Ag/PLLA to 0.5% Ag/PLLA) was  $300\mu\text{g}/\text{cm}^2$ ,  $225\mu\text{g}/\text{cm}^2$ ,  $150\mu\text{g}/\text{cm}^2$ ,  $75\mu\text{g}/\text{cm}^2$ ,  $15\mu\text{g}/\text{cm}^2$  respectively.

As shown in Figure 3.3, the higher the concentration of Ag NPs the darker was the shade of the membranes. The topography of the PLLA and Ag/PLLA was observed using scanning electron microscopy (SEM). Figure 3.4 shows that there was little difference in appearance between the PLLA and the Ag/PLLA films. Although only the 5% Ag/PLLA film is shown in Figure 3.4, other silver concentrations in the Ag/PLLA films had similar topographical images.

### **3.3 Electrospinning of PLLA and Ag/PLLA fibers**

The electrospinning method was performed following the procedure used in an earlier study by the author [Li et al, 2009]. In this study, a nanofiber electrospinning unit purchased from KES KATO TECH Co. LTD, Japan was used. Electrospinning is receiving more attention currently as a new way to produce nanofibers. As shown in Figure 3.5, electrospinning is a method whereby a polymer fluid is subjected to a high positive voltage (10-40kV) to, and the solution is sprayed through a syringe, into which a flattip stainless needle is inserted, onto a target that is charged negatively. When the fluid is ejected from the needle tip, it is fiberized by evaporation of the solvent. This process produces fibers with diameters at the nano scale.

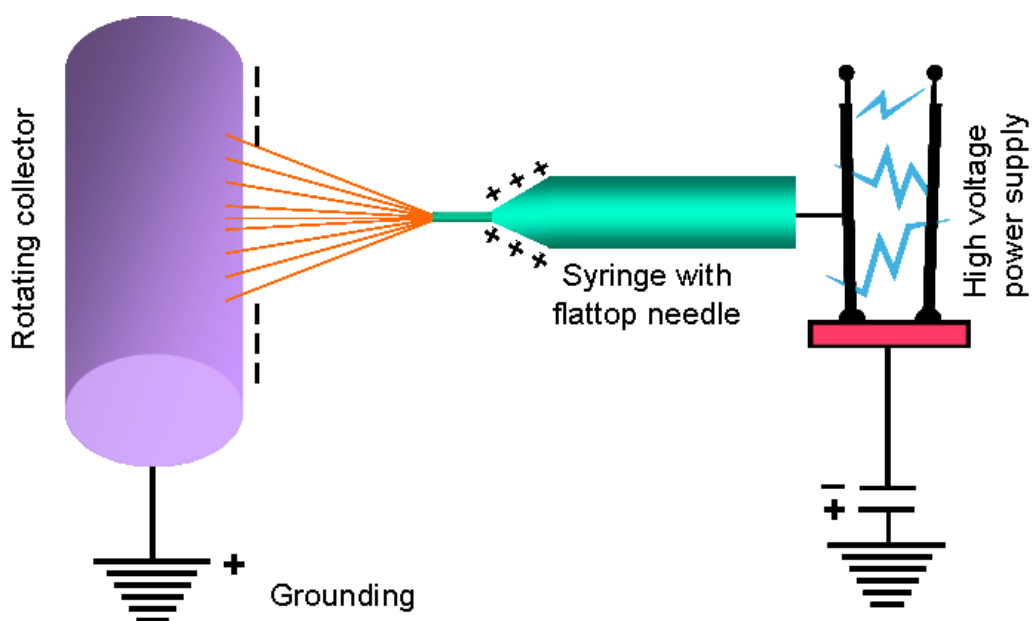


Figure 3.5 Scheme of electrospinning process.

To produce the PLLA and Ag/PLLA nano fibers, PLLA was dissolved at a weight ratio of 1% in chloroform, and N, N-dimethylformamide (DMF) (10:1, w/w) was added and stirred to obtain PLLA solution. Ag NPs were then added to the solution and stirred evenly to prepare an Ag/PLLA solution for electrospinning. The PLLA and Ag/PLLA solutions were then inserted into a syringe with a blunt needle, and then ejected by depressing the syringe plunger to deliver the fibre solution at a feeding rate of 0.3 mL/min. A grounded metal rotating drum, wrapped with aluminum foil, was located at a fixed distance of 10 cm away from the tip of the needle to collect the fibers. A high voltage (13 kV) electric field was applied to the stream of droplets as they emerged from the needle tip. This led to the creation of continuous fibers which formed, in turn, a fibrous membrane as they collected on the surface of the rotating drum.

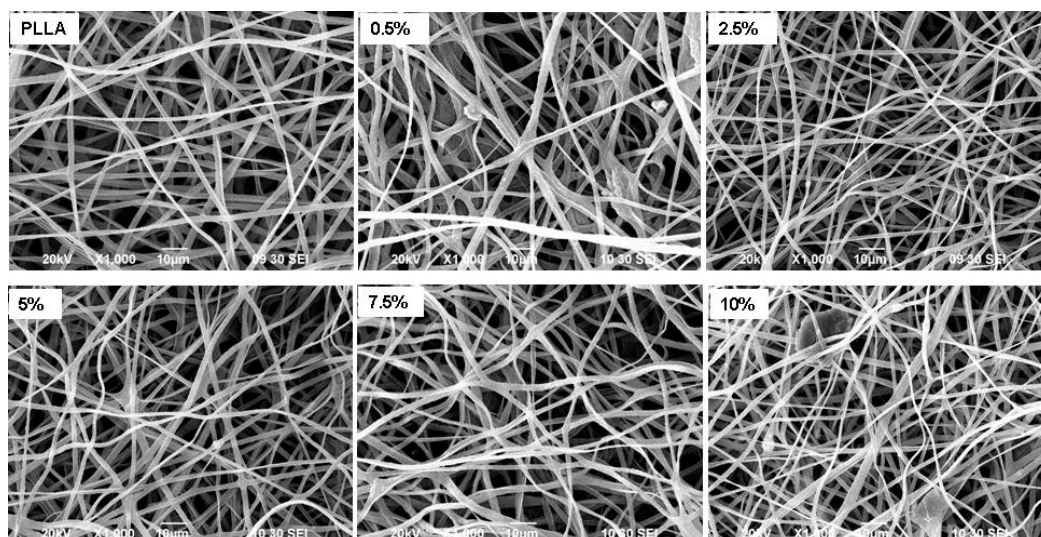


Figure 3.6 SEM images of PLLA and Ag/PLLA fibrous membranes at x1000 magnification. (20kV)

As shown in Figure 3.6, there were no obvious morphological differences between the PLLA and Ag/PLLA fibers. The diameter ( $d$ ) and length ( $l$ ) of the target drum was 100mm 330mm respectively, so the area ( $\pi dl$ ) of the electrospun fiber membrane was around 1000 cm<sup>2</sup>.

Because every sample produced contained 40mL of 1% PLLA, the weight of the PLLA membrane and each of the Ag/PLLA fibrous membrane was about 400µg/cm<sup>2</sup>. Thus, the silver content of the Ag/PLLA fibrous membranes (from 10% Ag/PLLA to 0.5% Ag/PLLA) was 40µg/cm<sup>2</sup>, 30µg/cm<sup>2</sup>, 20µg/cm<sup>2</sup>, 10µg/cm<sup>2</sup>, 2µg/cm<sup>2</sup> respectively.

### 3.4 Preparation of wool keratin particles

Wool keratin particles were prepared by spray drying wool keratin emulsion

#### 3.4.1 Preparation of wool keratin emulsion

Wool keratin emulsion was prepared according to a patent pending technique [Li et al, 2004]. Wool fibers were immersed and stirred into a 5% NaOH (w/v)/distilled water solution at a ratio of 5% weight by volume at 100°C to dissolve them. After the wool fibers had completely dissolved, 3.7% HCl (w/v) was added, slowly, to neutralize the wool keratin solution until its pH value reached a value of 6.92. After any impurity and precipitant were removed from the solution by centrifugation, the solution containing wool keratin was thoroughly dialyzed with distilled water for seven days at 22°C to obtain an aqueous wool keratin emulsion (Figure 3.7A).

#### **3.4.2 Preparation of wool keratin particles**

Wool keratin emulsion was spray dried using a Mini Spray Dryer (BUCHI Labortechnik AG, B-290, Switzerland) to obtain wool keratin particles (Figure 3.7B).



Figure 3.7 Preparation of wool keratin powder. (A) Wool keratin emulsion (B) Wool keratin powder.

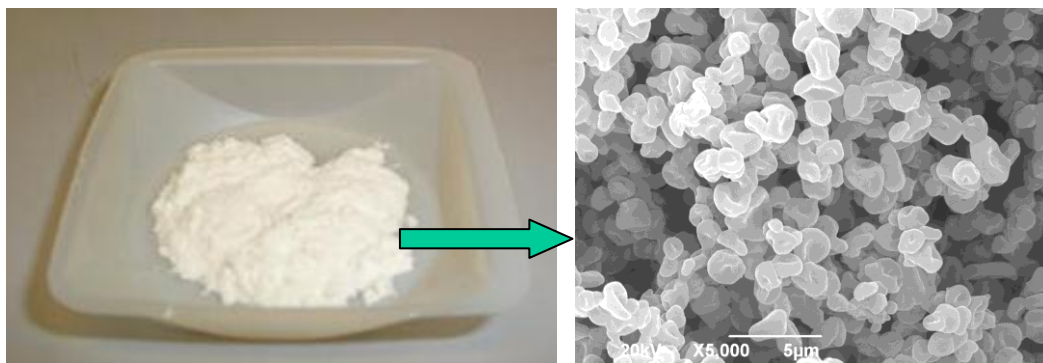


Figure 3.8 SEM images of wool keratin particles (20kV). Particles are white color and agglomerated.

The particles were observed using SEM. As shown in Figure 3.8, the particles were white in color and agglomerated. Although the wool keratin emulsion had been dialyzed, some components, such as NaCl, may have remained to make the particle larger than the original size. This possibility can be more easily understood from the SEM images of the non-dialyzed wool keratin particles (Figure 3.9).

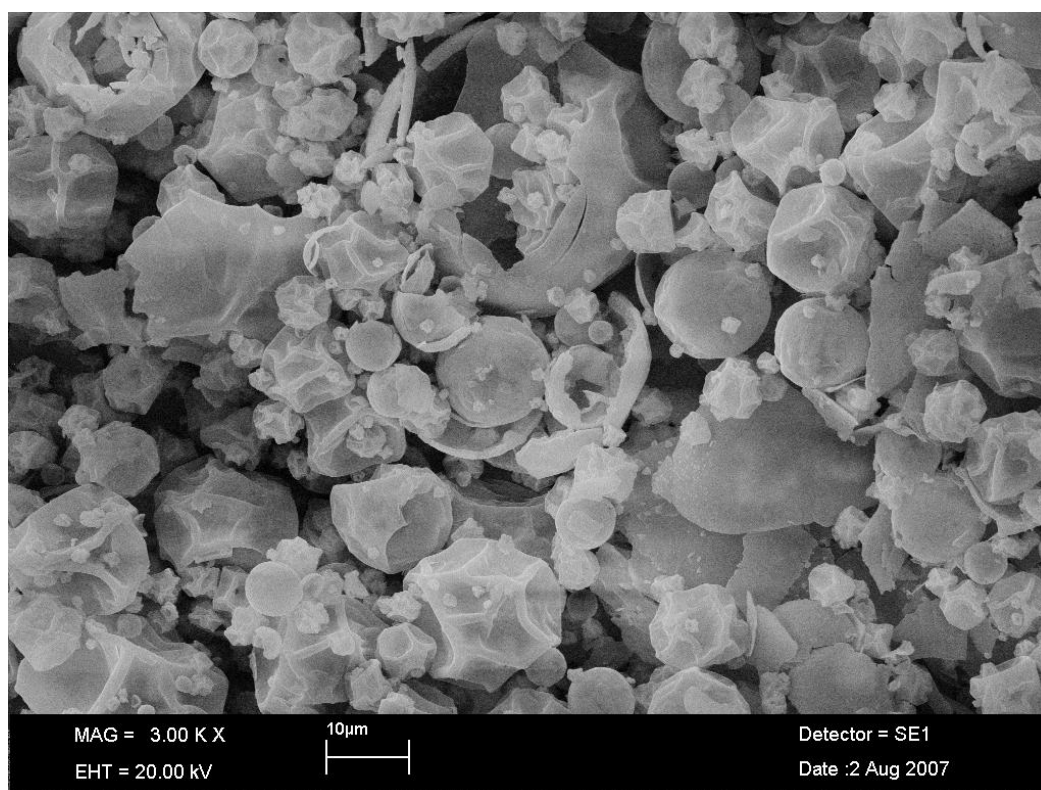


Figure 3.9 SEM images of non-dialyzed wool keratin particles. (20kV)

As shown in Figure 3.9, the diameters of the non-dialyzed wool keratin particles were observed to vary from less than 1µm to about 10µm. Also, some large particles were hollow and contained smaller particles inside them. This finding indicated that the non-dialyzed emulsion may have retained some other

components which made the particle size much larger than the dialyzed one.

Thus, dialysis was a necessary process for producing wool keratin particles.

### **3.5 Electrospinning of wool keratin-PEO fibers**

Electrospinning was performed according to the procedure essentially as detailed by Li et al (2002). The wool keratin particles were dissolved in 1% PEO formic acid solution thoroughly to obtain wool keratin-PEO-formic solutions with different wool keratin concentrations. Then, the solutions were inserted into a 20ml syringe and ejected as nanofibers onto a rotating drum as described in section 3.3 The electric potential between the aluminum foil covered target drum roller and the needle tip was about 30 kV. The distance between the needle tip and the metal target roller was about 10 cm.

#### **3.5.1 FTIR of the electrospun wool keratin-PEO nanofibers**

The IR absorption spectrum of the wool keratin-PEO nanofiber structure prepared in this study was compared with a spectrum obtained from the original wool fibers to determine the identity of the nanofibers using the Perkin-Elmer System 2000.

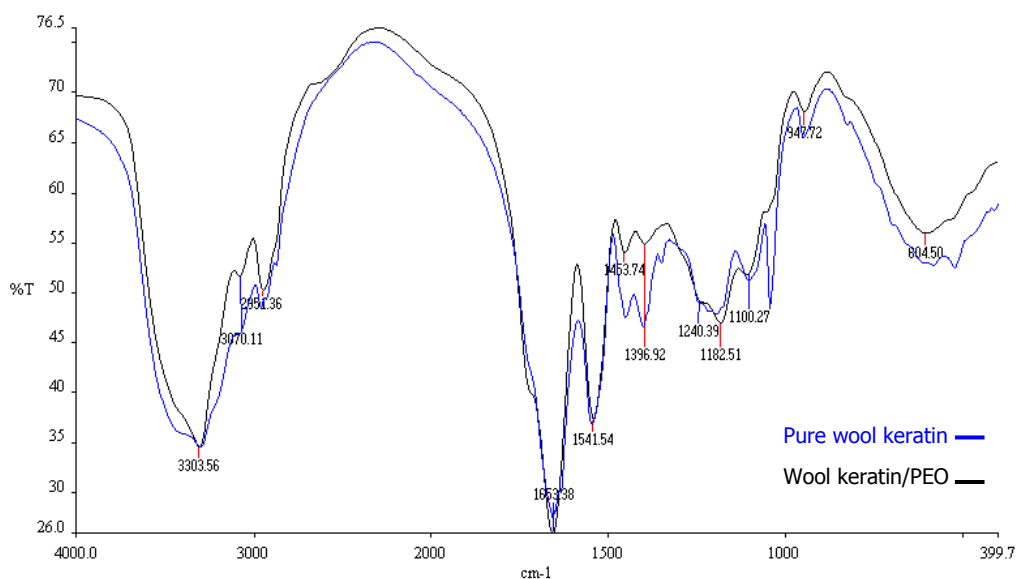


Figure 3.10 Fourier transform infrared spectroscopy (FTIR) of electrospun PEO/keratin fibers.

It can be seen in Figure 3.10 that all the characteristic peaks in the spectra for the original natural wool fibers and the wool keratin-PEO fibers were similar, indicating that the chemical compositions of the electrospun fibers were very similar to those of the original wool fibers. This showed that no new chemical bonds were produced in the electrospun wool-PEO fibers. This was because, adding polyethylene oxide to the wool keratin powder should have resulted in the formation of  $\text{CH}_2\text{OH}$  bonds that were originally present in the serine amino acid in the wool structure.

### 3.5.2 Effect of keratin concentration on fiber diameter

The morphology of the electrospun PEO/keratin fibers were observed using SEM (JEOLJSM-6335F).

Figure 3.11 shows the SEM images of the wool-PEO composite fibers with different wool keratin concentrations. By decreasing the concentration of wool in the formic acid and 1% PEO solution from 12% to 4%, the average diameter of the wool fibers was reduced from  $281 \pm 29$  nm to  $140 \pm 8$  nm respectively. However, although the average diameter of the 4% wool fiber concentration was only 140 nm, there were some beads on the fibers and the fibers were not straight and even. Conversely, the shapes of the 8% and 12% wool nano keratin fibers were straight and even, as shown in the SEM photos. However, the 12% wool fibers were fragmented.

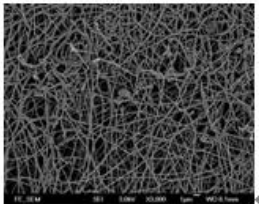
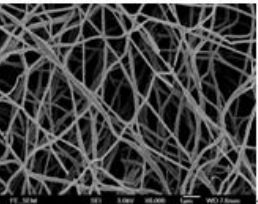
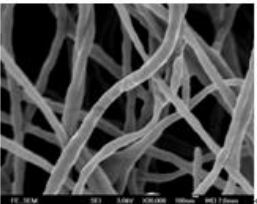
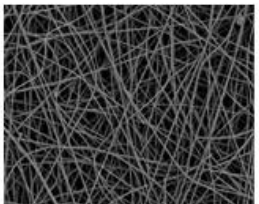
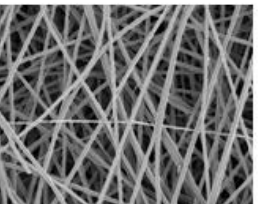
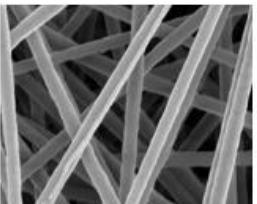
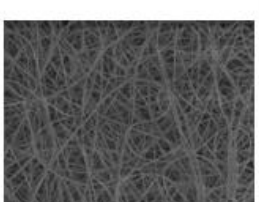
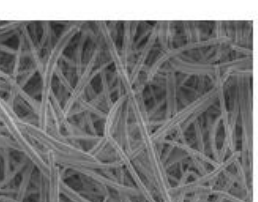
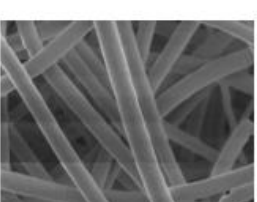
Wool	Magnification			Fiber diameter (nm)
	3000×	8000×	30000×	
4%				AV: 140 STDV: 8 Max: 154 Min: 127
8%				AV: 243 STDV: 25 Max: 272 Min: 206
12%				AV: 281 STDV: 29 Max: 329 Min: 255

Figure 3.11 Morphology of fibers at different wool concentrations of 4%, 8% and 12%. The average, standard deviation, maximum and minimum values of the fiber diameters are also given in this figure.

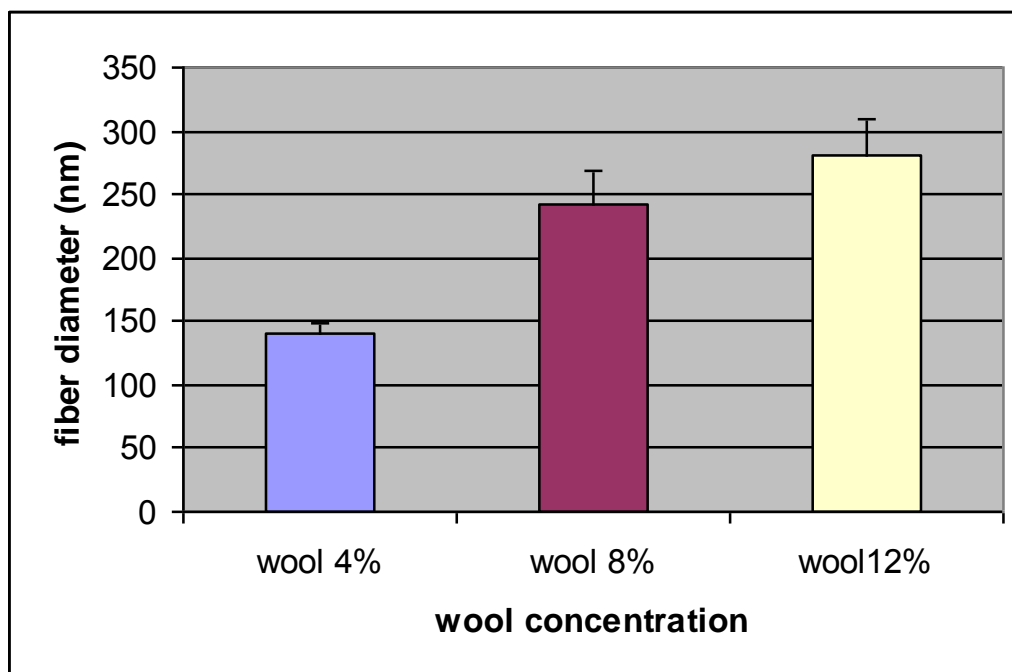


Figure 3.12 Relationship between the wool keratin concentration and the fiber diameter.

Figure 3.12 shows the relationship between the wool keratin concentration and the diameters of the nano keratin fibers. As the concentration of the wool keratin increased, the diameters of the nano fibers increased linearly.

### 3.5.3 Effect of PEO concentration on fiber diameter

The diameters of the electrospun wool keratin fibers were also affected by the concentration of the PEO. Here, the 8% wool solution was used for the experiments according to the previous results.

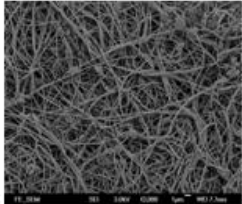
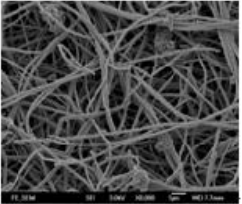
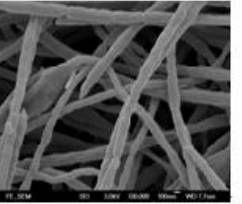
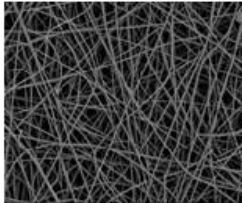
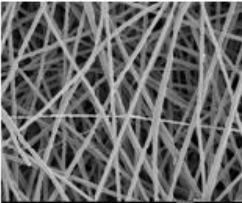
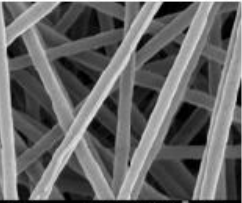
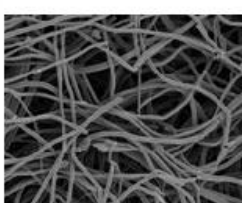
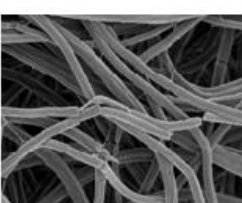
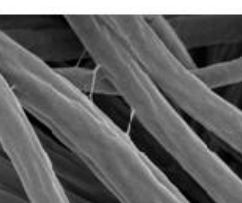
PEO	Magnification			Fiber diameter (nm)
	3000×	8000×	30000×	
0.5%				AV: 153 STDV:10 Max: 172 Min: 134
1%				AV: 243 STDV:25 Max: 272 Min: 206
3%				AV: 500 STDV:26 Max: 561 Min: 463

Figure 3.13 Morphology of fibers at different PEO concentrations at 0.5%, 1% and 3%. The average, standard deviation, maximum and minimum values of the fiber diameters are also given in this figure.

As shown in Figure 3.13, as the PEO concentration decreased from 3% to 0.5%, the average diameter of the fibers also decreased from  $500 \pm 26$  nm to  $153 \pm 10$  nm respectively. At 3%, the average diameter of the wool fiber was significantly larger than the 0.5% and 1% PEO wool keratin fibers and the fibers were fragmented. When the concentration of PEO decreased to 0.5%, the wool keratin fibers were not only fragmented but also exhibited many beads.

Figure 3.14 shows the relationship between the PEO concentration and the diameters of the nano keratin fibers. As the concentration of the PEO increased, the diameters of the nano keratin fibers increased correspondingly.

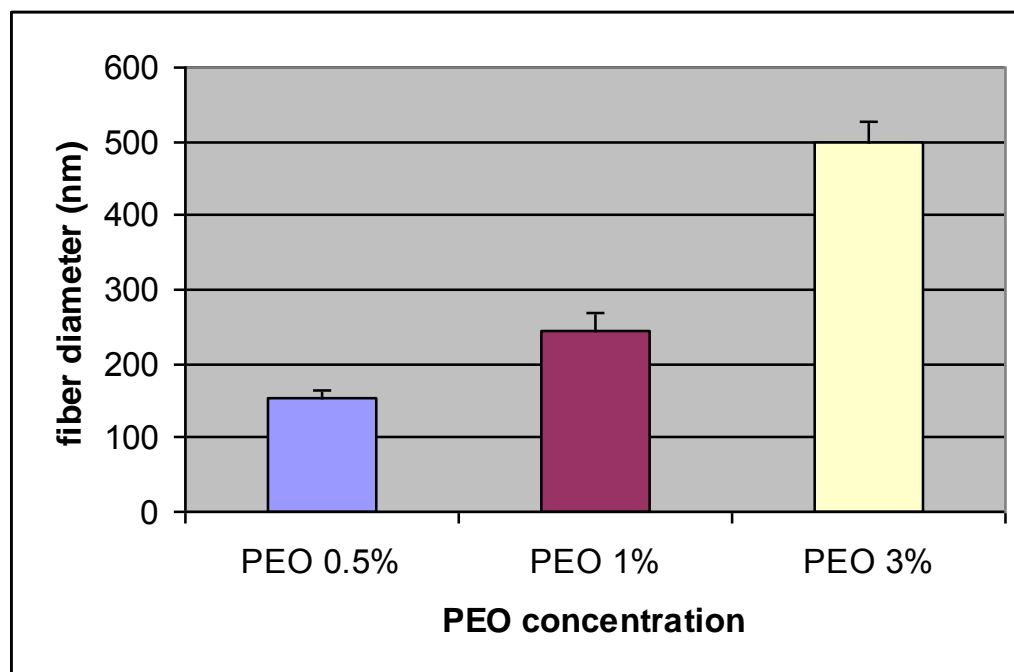


Figure 3.14 Relationship between the PEO concentration and the fiber diameter.

The electrospinning of wool keratin-PEO in formic acid was performed and fiber diameters ranging 125 nm to 560 nm were obtained depending on the wool or PEO concentrations. As the concentration of the wool keratin or PEO increased, the diameters of the electrospun wool keratin-PEO composite fibers increased. Also, the wool keratin-PEO composite fibers had similar chemical compositions to the original wool fibers. There were no chemical bonds formed in the composite fibers.

### 3.6 Electrospinning of PLLA/keratin fibers

PLLA was dissolved completely at a concentration of 1.0 % (w/w) in chloroform, N, N-dimethylformamide (DMF) (10:1, w/w) was added and stirred evenly to obtain PLLA solution for electrospinning. Then, different weights of wool keratin particles were dispersed gently into the PLLA solution to form

PLLA/keratin (2:1, 1:1, 1:2, 1:4 and 1:8, w/w) suspensions. The PLLA and PLLA/keratin suspensions were placed in the syringe respectively and ejected by a syringe pump at a feeding rate of 0.3 mL/min. A grounded rotating drum, wrapped with aluminum foil, was located at a fixed distance of 10 cm away from the syringe needle tip. The needle was connected to a high voltage power applying 13 kV.

### 3.6.1 Scanning electron microscopy

The morphologies of the wool keratin particles and the electrospun fibrous membranes were examined using (SEM) (LEICA, Stereoscan 440).

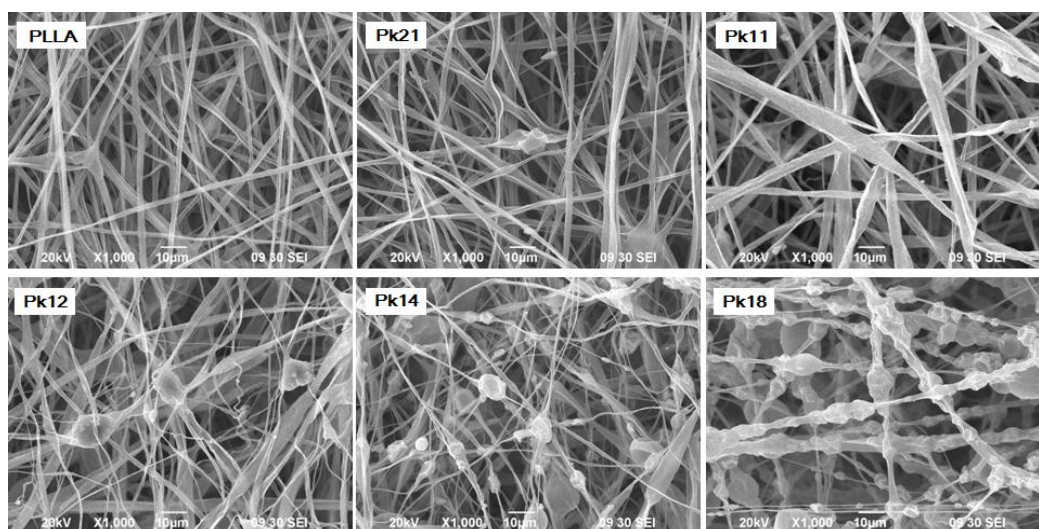


Figure 3.15 SEM images of PLLA and PLLA/keratin electrospun fibers.

As shown in Figure 3.15, more beads appeared on the fibers as the concentration of wool keratin particles increased. Furthermore, the beads that were formed were covered with PLLA.

### 3.6.2 FTIR of PLLA and PLLA/keratin fibers

FTIR spectra of the PLLA and PLLA/keratin membranes were examined with reference to pure wool keratin as the control.

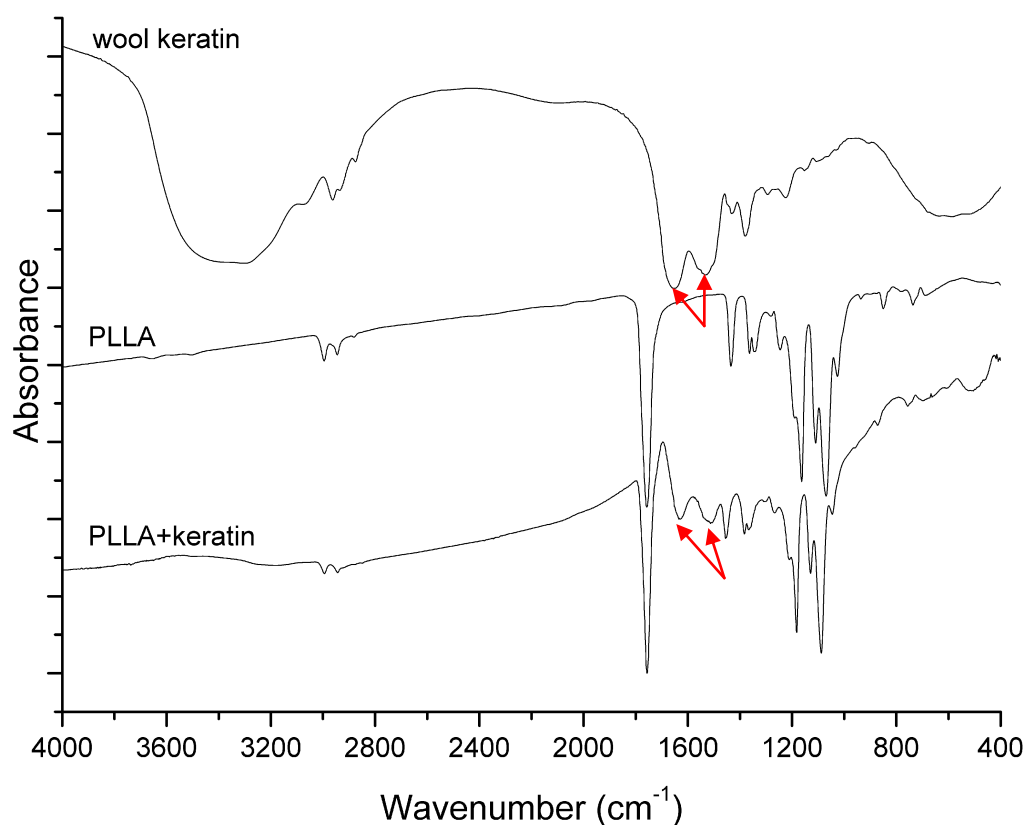


Figure 3.16 FTIR spectra of the PLLA, keratin and PLLA/keratin membranes. For the PLLA/keratin composite membrane, two peaks appeared at  $1630\text{ cm}^{-1}$  and  $1550\text{ cm}^{-1}$  (indicated by the red arrows) which correspond to the keratin.

It can be seen from Figure 3.16 that the FTIR spectra of the PLLA had no peaks from  $1700$  to  $1500\text{ cm}^{-1}$ , but for the PLLA/keratin fibers two peaks appeared at  $1630\text{ cm}^{-1}$  and  $1550\text{ cm}^{-1}$  which corresponded to the keratin. For the characteristic peaks of PLLA and keratin do not overlap, they could be used to calculate the ratio of PLLA and keratin after the composite was degraded.

The films and nano fibrous membranes developed in this chapter will be used as skin TE scaffolds for further study in subsequent chapters to meet the objectives of this research set out in chapter 1.

## CHAPTER 4: PHYSICAL PROPERTIES

4.1 Introduction .....	66
4.2 Morphology.....	66
4.3 Hydrophilicity .....	67
4.4 Tensile properties .....	73
4.5 Moisture related properties .....	77
4.6 Conclusions .....	89

### 4.1 Introduction

Chapter 4 aims to fulfill the first objective, by studying the relationship between the physical properties of the PLLA/keratin scaffolds and the ratios of keratin to PLLA. The morphology, hydrophilicity, tensile properties, moisture content, water vapor permeability, and moisture management properties of the scaffolds were characterized as the first step of this project.

### 4.2 Morphology

The morphology of scaffolds was observed using SEM (JEOLJSM-6335F and LEICA, Stereoscan 440). Details of the Ag/PLLA films, the Ag/PLLA, the wool keratin-PEO and the PLLA/keratin fibrous membranes have already been presented in Chapter3. The main feature of the film surface was its lumpiness, - the higher the Ag concentration, the lumpier it was. Furthermore the main characteristic of fibrous membranes was their porosity. The fibrous structure, which consists of many fibers, has a larger surface area than that of the film.

Consequently, the larger surface area and the porosity are the main structural differences between the fibrous membranes and the films.

### **4.3 Hydrophilicity**

The hydrophilicity of the scaffolds was determined by measuring the water contact angles of the scaffold surfaces. A smaller contact angle is indicative of a greater hydrophilicity.

#### **4.3.1 Method**

In this study, the hydrophilicity of scaffolds was tested by measuring the contact angle ( $\theta$ , Figure 4.1) using a contact angle goniometer purchased from Ramé-hart Instrument Company and a Tantec model CAM-MICRO contact angle meter.

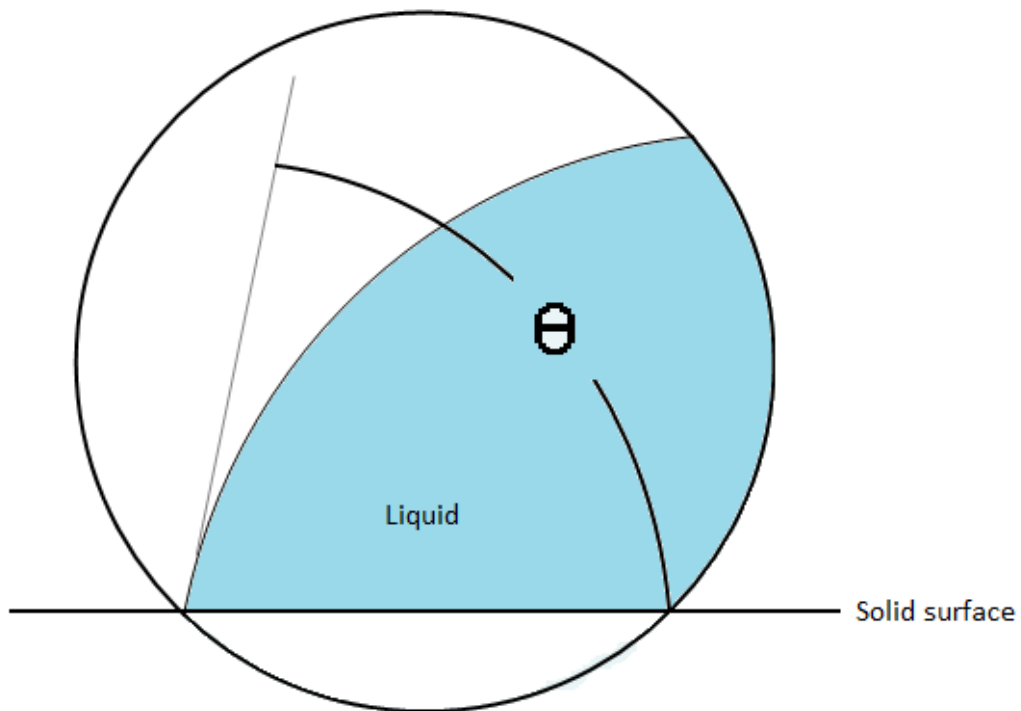


Figure 4.1 Sketch of contact angle ( $\theta$ ). The contact angle is the angle at which a liquid droplet (the blue part) interface meets the solid surface.

Six samples for each group of the scaffolds were measured. Statistical values were expressed as means  $\pm$  standard deviations. Statistical differences were determined by one-way Analysis of Variance (ANOVA).  $P$  values of less than 0.05 were considered to be statistically significant.

### 4.3.2 Results and discussion

#### PLLA and Ag/PLLA films

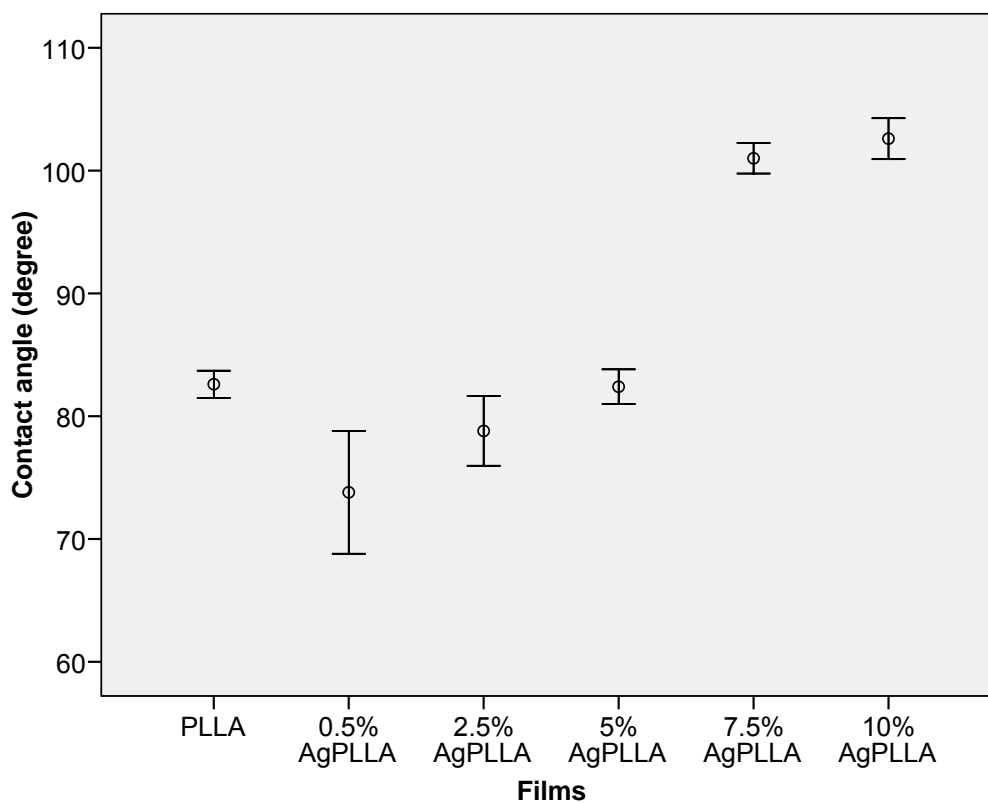


Figure 4.2 Contact angles of the PLLA and Ag/PLLA films prepared with different silver nanoparticle concentrations. For the Ag/PLLA membranes, the higher the silver nanoparticle concentration, the greater was the contact angle.

As shown in figure 4.2, the contact angles of the Ag/PLLA films increased with the Ag nanoparticle concentration. The average value of the contact angles of the films were shown in Table 4.1.

Table 4.1 The contact angles of the films.

Film	PLLA	0.5% Ag/PLLA	2.5% Ag/PLLA	5% Ag/PLLA	7.5% Ag/PLLA	10% Ag/PLLA
<b>Mean (°)</b>	82.6	73.8	78.8	82.4	101.0	102.6

However, compared to the PLLA films, the contact angle of the 5% Ag/PLLA films decreased slightly, while the contact angles of the 0.5% and 2.5%

Ag/PLLA films significantly decreased, and the 7.5% and 10% Ag/PLLA films significantly increased.

PLLA and PLLA/keratin fibrous membranes

The hydrophilicity of the electrospun PLLA and PLLA/keratin fibrous membranes was also characterized by measuring their water contact angles. The PLLA/keratin (2:1, 1:1, 1:2, 1:4 and 1:8, w/w) fibrous membranes are abbreviated as Pk21, Pk11, Pk12, Pk14 and Pk18. Because cell proliferation test will be performed on the membranes, the contact angles of both the non-sterilization and sterilization membranes were measured.

Table 4.2 Contact angle values of the PLLA and Pk fibrous membranes measured before sterilization.

Membrane	PLLA	PK21	PK11	PK12	PK14	PK18
Mean (°)	127.5±0.5	110.8±3.9	120.6±3.5	118.7±7.8	113.2±3.4	102.7±8.7

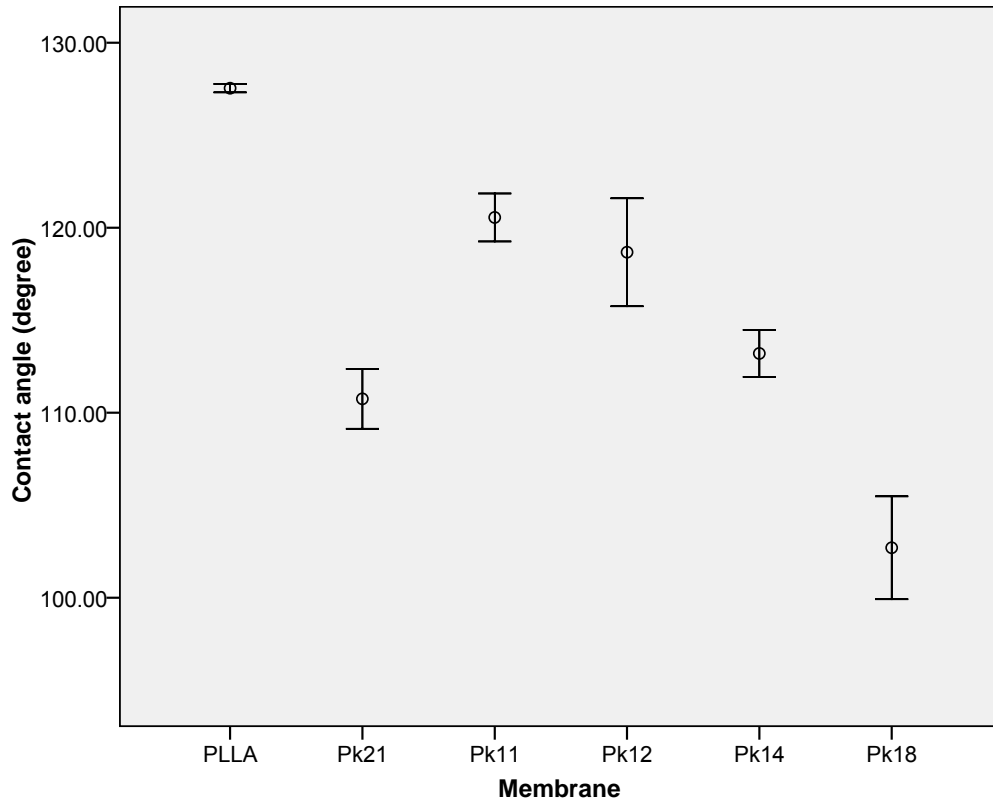


Figure 4.3 Contact angles of the PLLA/keratin fibrous membranes measured before sterilization.

From Table 4.2 and Figure 4.3, it can be seen that before sterilization, adding wool keratin particles into the PLLA caused a reduction in the contact angles of the membranes. As the proportion of keratin increased, the contact angle values decreased except for Pk21. Compared with the PLLA, the contact angle values for all the groups of the Pk membranes were significantly lower than those of the PLLA. Among the Pk membranes, there was no significant difference between Pk21 and Pk14, as well as Pk11 and Pk12.

Table 4.3 Contact angle values of the sterilized PLLA and PLLA/keratin fibrous membranes.

Membrane	PLLA	Pk21	Pk11	Pk12	Pk14	Pk18
Mean (°)	126.7±2.4	0	0	0	0	0

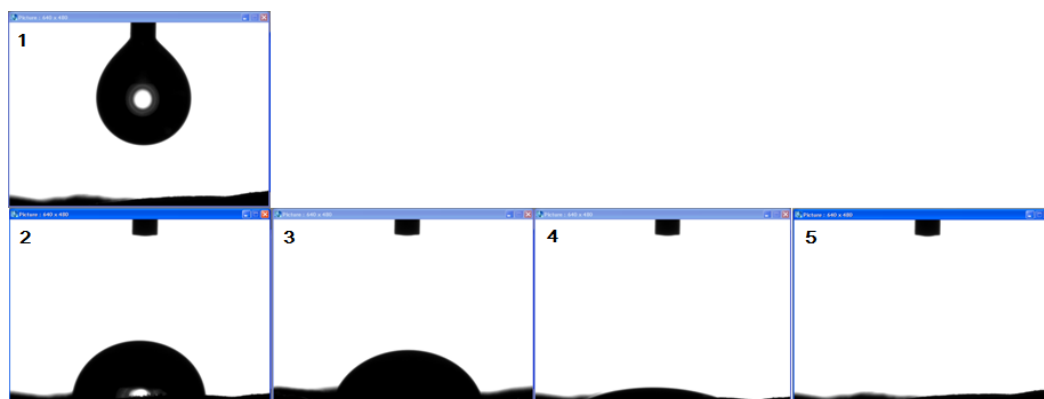


Figure 4.4 The droplet shape changed during the measurement of the contact angles of the sterilized PLLA/keratin fibrous membranes until it was absorbed thoroughly. All the contact angles of the Pk fibrous membranes (Pk21, Pk11, Pk12, Pk14, Pk18) were 0°.

All of the membranes were sterilized by ultraviolet irradiation for 20 minutes after being immersed in 70% ethanol for 1 hour. However, as shown in Table 4.3 and Figure 4.4, after sterilization, the contact angle values for all the PLLA/keratin membranes were 0°, which meant that they were completely hydrophilic. This result confirmed that the process of sterilization was an important factor that affected the hydrophilicity of the scaffolds, especially the ethanol. As an organic solvent, ethanol can dissolve liposoluble substances. Consequently it probably dissolved the liposoluble substances that adhered to the PLLA/keratin membranes. Furthermore, after being immersed in the alcohol, the fibers became denser, which have may caused a stronger capillary absorption during the contact angle measurement. On the other hand, this result implies that

the hydrophilicity will not make much difference to the properties for the different Pk fibrous membranes.

#### **4.4 Tensile properties**

The ability of a biomaterial to resist breaking under tensile stress is one of the most important properties for the skin substitutes. This property indicates how the skin substitute will react to tensile forces.

##### **4.4.1 Method**

The specimen size was set at 10mm×80mm before measuring the tensile properties. The specimen was clamped and extended by the two clamps of a tensile tester (Instron 4411 tensile tester). The distance between the top and bottom clamps was set to 50mm. The rate of extension was 10 mm/min. The tests were performed under standard temperature and humidity testing conditions viz. 21±1°C 60±3% R.H.

Three samples for each group of membranes were measured for the tests of the tensile properties and moisture related properties. And statistical values were expressed as means ± standard deviations. Statistical differences were determined by one-way Analysis of Variance (ANOVA). *P* values of less than 0.05 were considered to be statistically significant.

##### **4.4.2 Results and discussion**

The tensile properties measured included two indices – the maximum load and maximum strain. As shown in Figure 4.5 and Figure 4.6, the tensile strength and elongation of the Pk membranes were significantly influenced by the keratin content. When the keratin concentration increased, the maximum load and maximum strain of the Pk membranes decreased significantly. When the mass proportion of the PLLA to keratin reached 1:8, the maximum load and strain were reduced to about 29.5% and 7.5% of the pure PLLA membrane respectively.

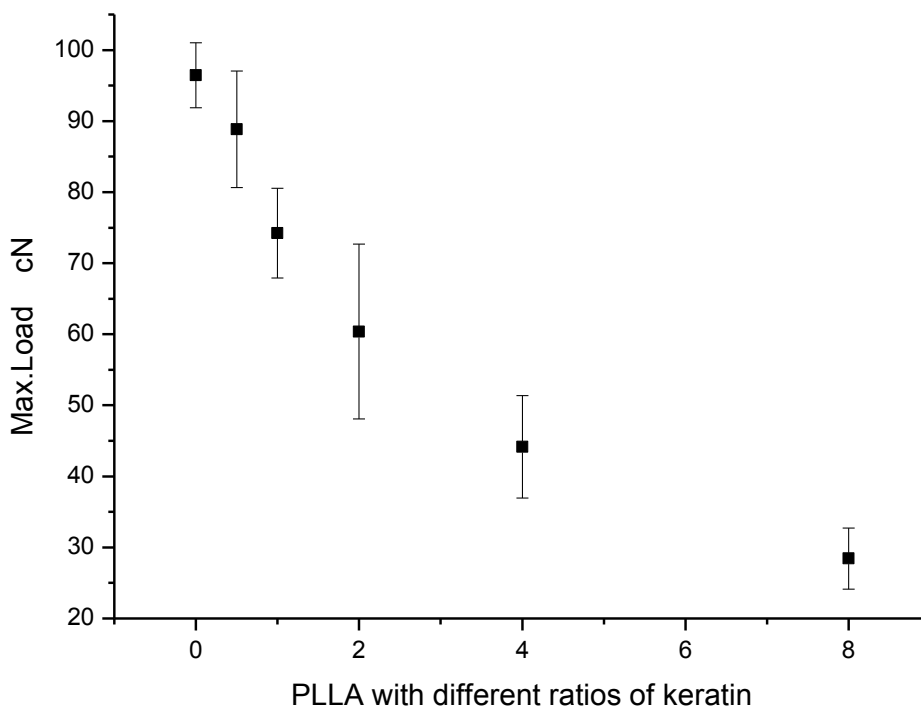


Figure 4.5 Maximum Load of the PLLA and Pk membranes: with increasing keratin concentration the maximum load of the membranes decreased gradually.

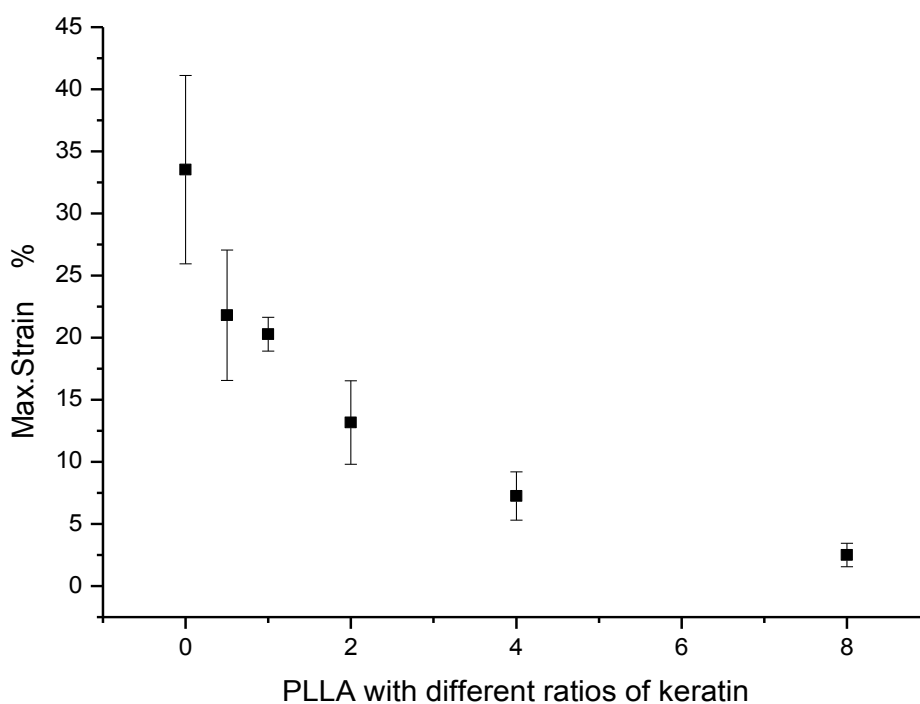


Figure 4.6 Maximum strains of the PLLA and Pk membranes: the maximum strain of the membranes decreased gradually as the keratin concentration increased.

Figures 4.5 and 4.6, also showed that the PLLA membrane exhibited the highest maximum load and maximum strain. From the SEM images shown in Chapter 3, it can be seen that the electrospun PLLA fibers were continuous and smooth (Figure 3.15). However, as the proportion of keratin particles increased an increasing number of beads formed along the PLLA fibers. The PLLA part of the fiber which covered the keratin particles became much thinner than that of the pure PLLA fibers, which were unable to envelop the particles completely. These findings confirm that the tensile strength of the Pk membranes principally depended upon the proportion of PLLA, and the inclusion of the keratin cause the PLLA fibers to have thinner places and hence make the fibers weaker.

Therefore, with an increasing keratin particle concentration, the tensile properties decreased significantly.

Table 4.4 Cross-sectional area of the PLLA and Pk fibrous membranes.

Membranes	PLLA	Pk21	Pk11	Pk12	Pk14	Pk18
<b>maximum load (cN)</b>	96.4±2.3	88.8±4.2	74.2±3.3	60.4±6.2	44.2±3.9	28.4±2.2
<b>Cross-sectional area (mm<sup>2</sup>)</b>	2.0±0.4	3.3±0.2	4.2±0.3	4.0±0.2	3.5±0.2	3.4±0.2
<b>Tensile strength (N/ mm<sup>2</sup>)</b>	48.2±7.1	26.7±0.6	17.8±0.5	15.1±0.8	12.5±0.6	8.3±0.4
<b>maximum strain (%)</b>	33.5±3.9	21.8±2.7	20.3±0.8	13.2±1.9	7.3±1.0	2.5±0.5

In Chapter 2, the tensile properties were shown to also be defined in terms of their tensile strength, which is the ultimate load divided by the cross-sectional area. As shown in Table 4.4, the maximum loads of the PLLA and Pk fibrous membranes were converted to their tensile strength.

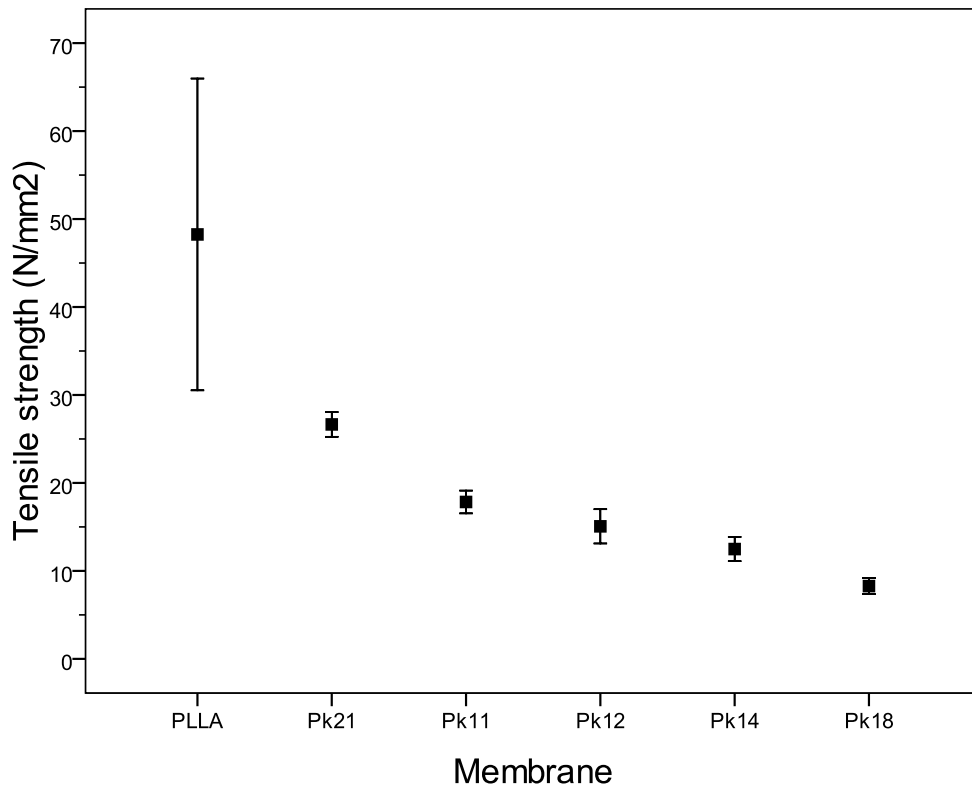


Figure 4.7 Tensile strength of the PLLA and Pk membranes: with increasing keratin concentration showing that the tensile strength of the membranes decreased gradually.

From Figure 4.7, it can be seen that, as the keratin proportion increased, the tensile strength decreased from 48.2-8.3  $\text{N/mm}^2$ . According to the previous research, the tensile strength of skin ranges from 5 $\text{N/mm}^2$  to 30 $\text{N/mm}^2$  [Edwards and Marks, 1995]. Thus, the tensile strength of the Pk fibrous membranes (8.3-26.7 $\text{N/mm}^2$ ), was just within the limits of normal skin tensile strength. This finding suggested that the Pk fibrous membranes had suitable tensile strength mechanical properties to be used as a an acceptable matrix for skin substitutes.

## 4.5 Moisture related properties

### 4.5.1 Moisture content

Individuals who lose skin extensively are often in danger of fluid loss [Yannas and Burke, 1980]. This means that the moisture-related properties are also very important to the design of skin TE scaffolds. So, for the characterization of the moisture-related properties, the moisture content, water vapor permeability, moisture management properties were tested respectively for the PLLA and Pk fibrous membranes.

### **Method**

The moisture content of the electrospun PLLA and Pk membranes was measured by drying them in an oven (Balance). The membranes were dried at 80 °C for more than 24 hours until they had constant mass. This mass was designated as  $m_0$ . Then, the dried specimens were put into a standard atmosphere for more than 24 hours until the specimens were mass-constant and this mass was marked as  $m_t$ .

The moisture content was calculated using equation 4.1:

$$\text{Moisture content} = (m_0 - m_t)/m_0 \times 100\% \quad (\text{eq. 4.1})$$

### **Results and discussion**

The moisture content of the Pk membranes was affected significantly by the keratin concentration.

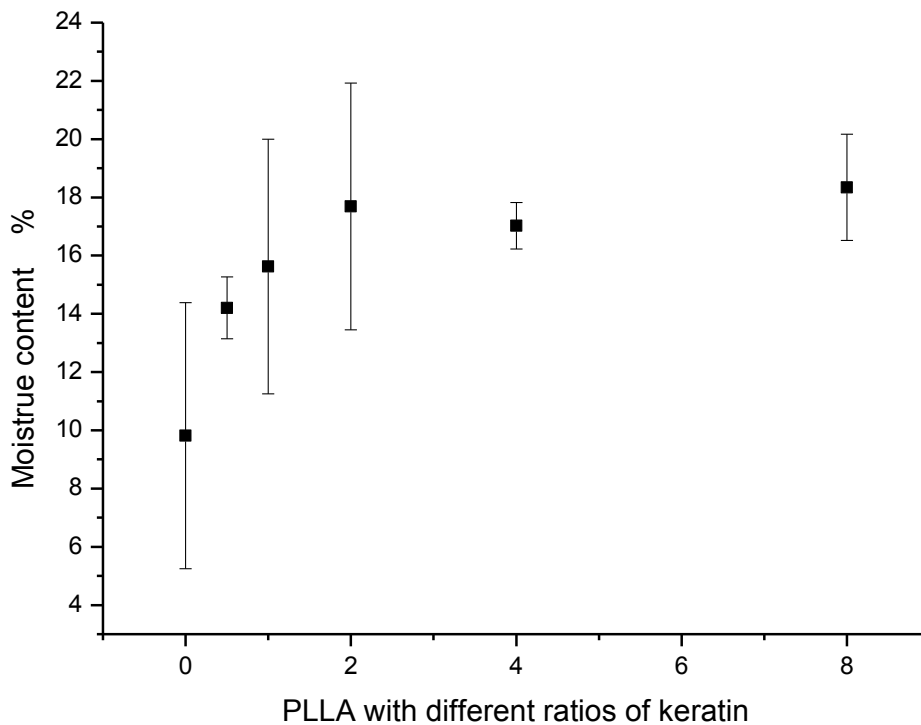


Figure 4.8 Moisture content of the PLLA and Pk membranes: with increasing keratin proportion showing that the moisture content of the Pk membranes increased. The moisture content of the membranes became relatively stable as the proportion of Pk12.

As shown in Figure 4.8, as the proportion of keratin particles increased, the moisture content of the Pk membranes increased. This may imply a direct contribution of the keratin particles which are known to absorb moisture from the air. After the proportion of the PLLA/keratin reached 1:2, the moisture content of the membranes was almost constant indicating that this concentration of keratin particles seemed to make the moisture content of the membranes become relatively stable, at around 1.5 times the PLLA membrane moisture content. Thus, these results confirmed that the main factor which affected the moisture content of the membranes was the proportion of keratin particles in the Pk membranes.

### **4.5.2 Water vapor permeability**

Water vapor permeability is the rate of water vapor transmission per unit area per unit of vapor pressure differential under test conditions. The Pk membranes exhibited a good moisture content level, however, it was not known how much they could retain the moisture under a normal operating environment. Normal human skin has the ability to control its water vapor permeability in balance, according to the surrounding conditions. So, water vapor permeability is naturally another important parameter to consider when designing skin TE scaffolds.

#### **Method**

The water vapor permeability of the PLLA and Pk membranes were measured employing a Balance, wide-mouthcups. Water vapor permeability was expressed in terms of the mass-loss per unit area of water vapor permeated from the membranes during 24 hours in a standard atmosphere.

#### **Results and discussion**

It is evident from Figure 4.9 that there were no significant differences in the moisture vapor transmission between the PLLA and Pk membranes with different ratios of keratin particles.

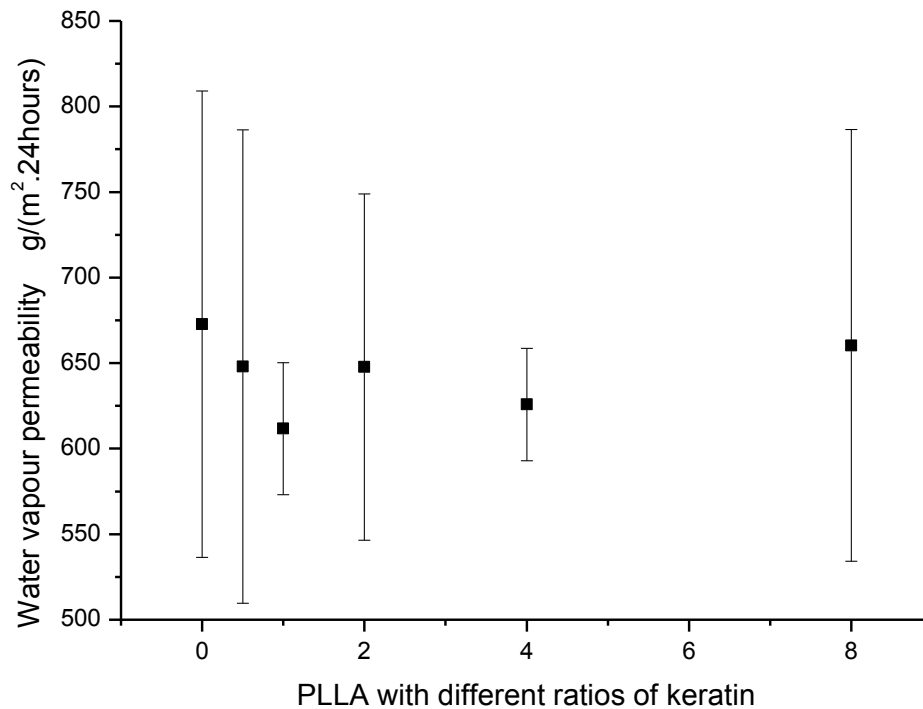


Figure 4.9 Watervapor permeability of the PLLA and Pk membranes: no significant differences were observed between the PLLA membranes with different ratios of keratin particles.

Since water vapor permeability has a close relationship with the porosity of materials, these results implied that the porosity of Pk membrane may have not changed much with an increase in the keratin proportion, although the keratin particles could enlarge the gaps formed between the fibers. Once a membrane is formed, its function is affected by the structural and morphological properties of the membrane such as porosity, pore size and distribution, transmembrane pressure and thickness [Gopal et al. 2006]. The membrane was composed of fibers randomly deposited in a mat with many layers. This may have caused the Pk membranes to have a similar porosity to the PLLA membranes. Consequently,

the water permeability of the PLLA and Pk membranes did not show a significant difference.

When the vironmental conditions are maintained at a temperature around 23° C and a relative humidity of 40 to 50% RH in still air, water is lost at a rate of 0.1 to 0.2 mg/cm<sup>2</sup>/hr from the full thickness of abdominal skin, and the dermal part of the skin loses water at the rate of 10.0 to 15.0 mg/cm<sup>2</sup>/hr [Blank, 1952]. According to the results from these tests, the water vapor permeability values of the PLLA and Pk fibrous membranes ranged from 2.6 to 2.8 mg/cm<sup>2</sup>/hr. This finding implied that these fibrous membranes potentially possessed good water permeability. So, it can be supposed that, after culturing enough skin cells until they covered the whole membrane, it should be possible to obtain an ideal skin scaffold with good permeability.

#### **4.5.3 Moisture management property**

The moisture management property is the fabric liquid moisture transport property in multiple dimensions. This property significantly influences human perceptions of moisture sensations. Thus, biomaterials which are going to be used on the human body require good moisture transport properties.

#### **Method**

Moisture management testing consists of dropping definite water on specimen top surface and calculating the relative indices of the spreading status of water on

both the top and bottom surfaces. A specimen with an excellent moisture management capacity will transport all the dropped water from the top to bottom, and keep the top surface dry.

The moisture management property of the PLLA and Pk membranes was characterized by using a new MMT Tester reported in Hu et al's study (2005).

The specimens were cut into 80mm × 80mm squares. The pumping time of the testing water was 20 seconds and the measuring time was 120 seconds (120s).

### **Results and discussion**

The moisture management property principally characterized the moisture absorption, spreading and one-way transport properties of the Pk membranes.

The property was mainly evaluated by the following indices: moisture wetting time on the top and bottom surface; the maximum moisture absorption rate on the top and bottom surface; the maximum wetted radius on the top and bottom surface; the moisture spreading speed on the top and bottom surface and the accumulative one-way transport index. All the results are shown in Figures 4.10 to Figure 4.14.

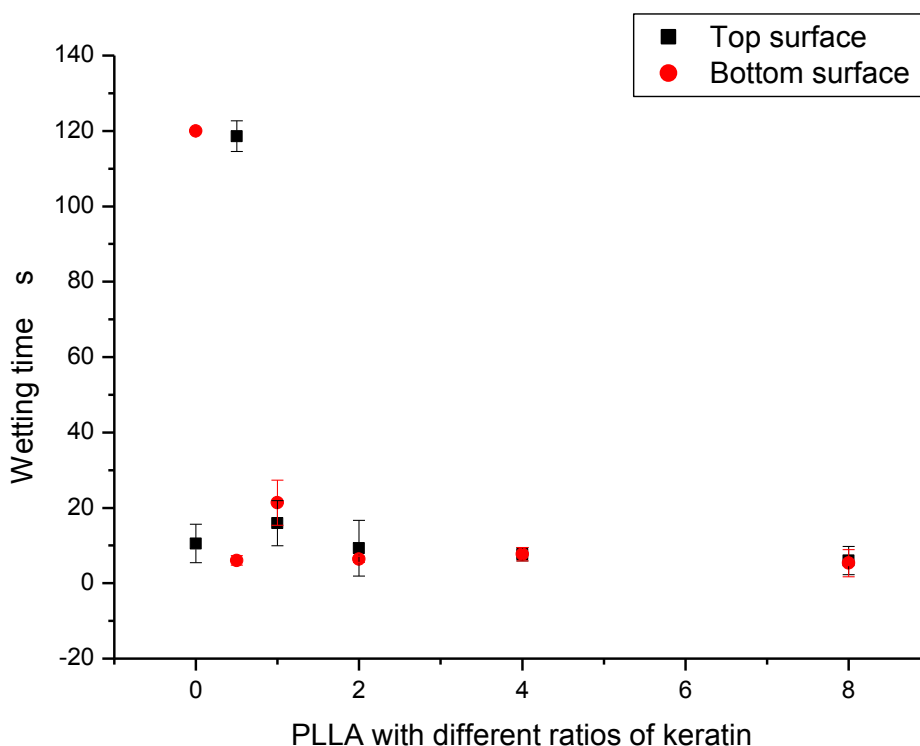


Figure 4.10 Wetting times of the PLLA and Pk membranes: the wetting time of the bottom surface of the PLLA membrane was 120s, which meant that the bottom surface was not wet; the top surface of the Pk21 membrane was almost dry. For the other Pk membranes, both top and bottom surfaces became wet in a short time (less than 30s).

Figure 4.10 shows the wetting times of the PLLA and Pk membranes. The wetting time of the bottom surface of the PLLA membrane was 120s, this result meant that the bottom surface of the PLLA membrane did not become wet. The top surface of the Pk21 membrane was almost dry, this means that the water transfer was very fast and complete from the top to the bottom surface. For the other Pk membranes, both the top and bottom surfaces became wet in less than 30s.

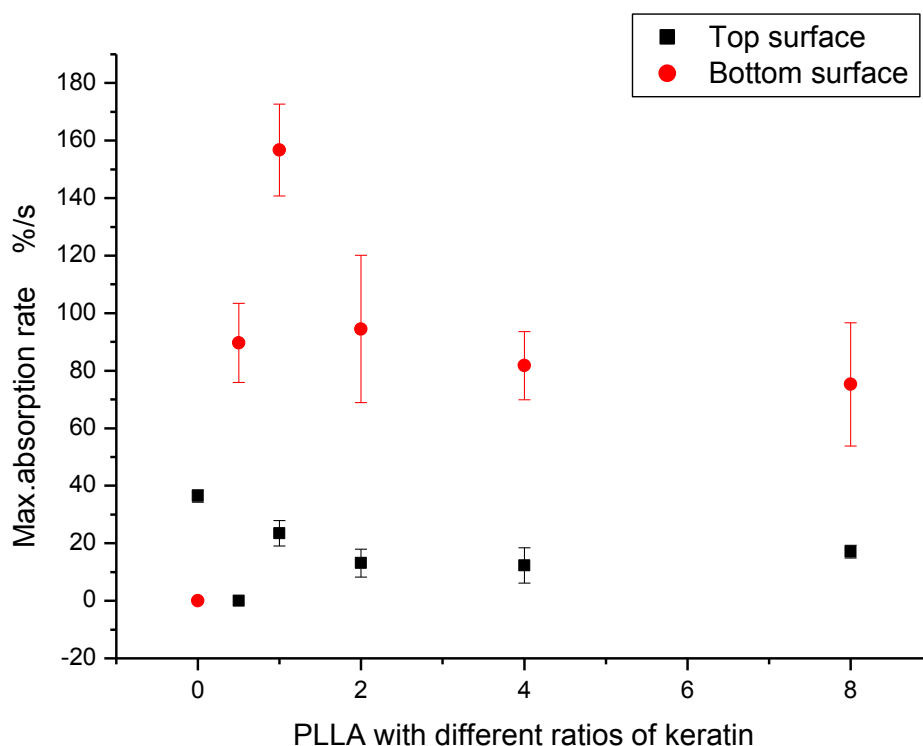


Figure 4.11 Max absorption rates of the PLLA and Pk membranes: the water absorption rates of the membrane top surfaces were quite low, especially for the Pk21 membrane. However, the water absorption rates of the membrane bottom surfaces were very high except for the PLLA membrane.

As shown in Figure 4.11, the maximum absorption rates of the membrane top surfaces were very low, especially for the Pk21 membrane. Conversely, the water absorption rates of the membrane bottom surfaces were very high except for the PLLA membrane. However, there were no significant differences between any of the membranes.

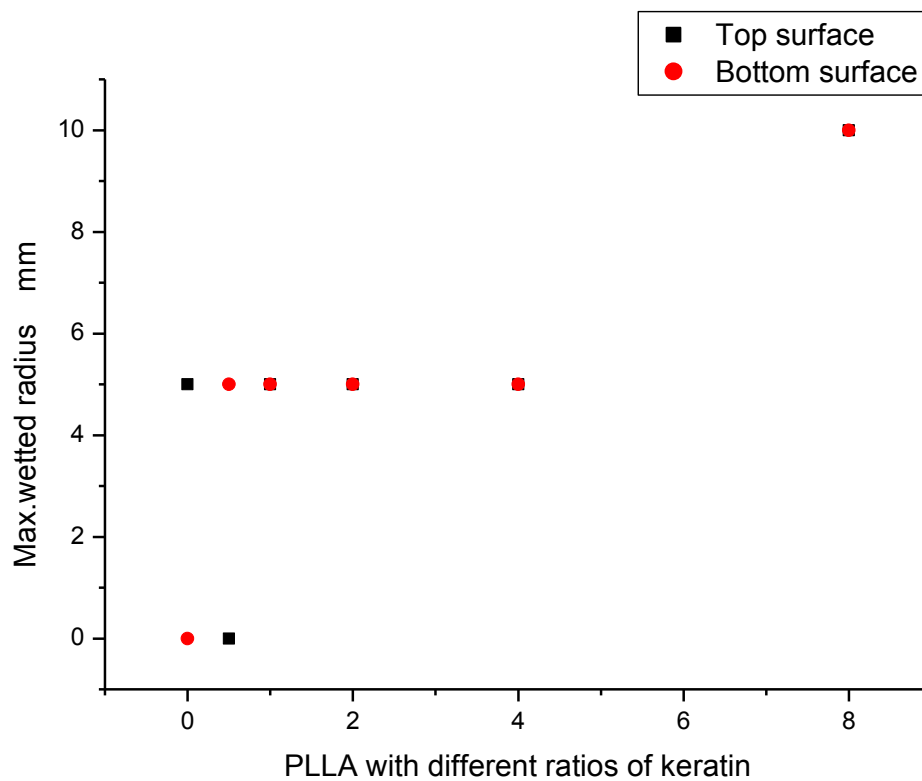


Figure 4.12 Max wetted radiuses of the PLLA and Pk membranes: the wetted radius of the PLLA bottom surface was zero; all the water transported to the Pk21 bottom surface, so the wetted radius of the top surface was zero; except for the PLLA and Pk21 membranes, the top and bottom surfaces of the membranes had similar wetted radii; the Pk18 membrane had the largest wetted radius.

Keratin particles are hydrophilic, those membranes containing keratin particles were more hydrophilic than the PLLA membrane; for the Pk21 membrane, water shifted from the top to bottom surface quickly even without spreading on the top surface. Apart from the Pk11, the membranes were hydrophilic and water was absorbed and spread on both the top and bottom surfaces. The Pk18 membrane indicated the largest max wetted radius and spreading speed value (Figure 4.12 and Figure 4.13).

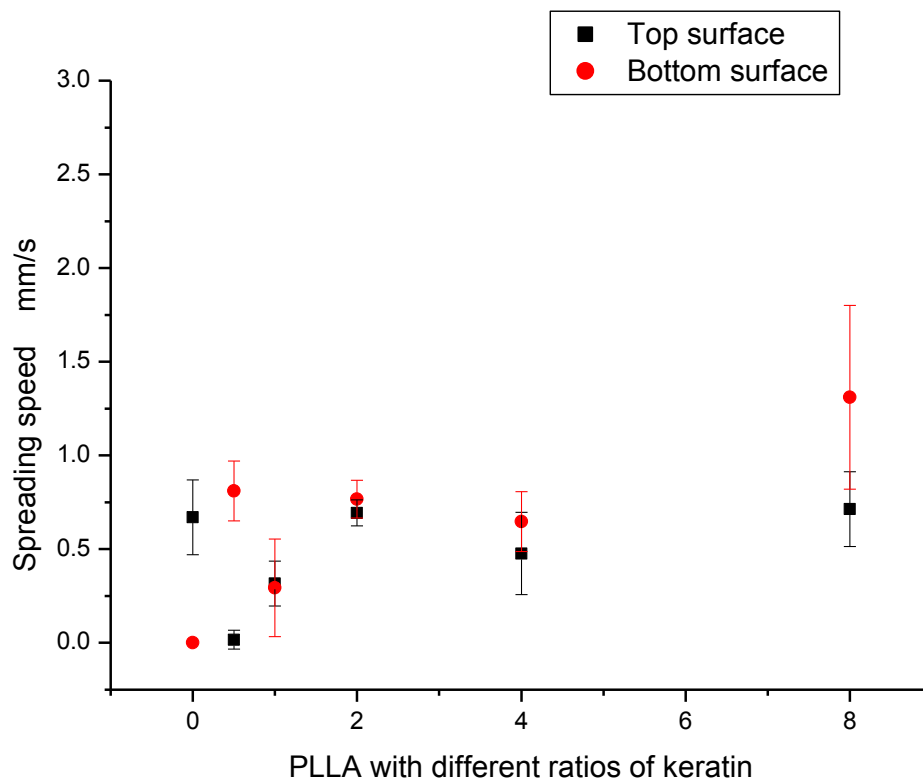


Figure 4.13 Spreading speed of the PLLA and Pk membranes: the spreading speed of the PLLA bottom surface was zero; the spreading speed of the Pk21 top surface was zero; the spreading speed of both the top and bottom surfaces of the Pk11, Pk12, Pk14 were similar; however the spreading speed on the Pk18 bottom surface was higher than the top surface.

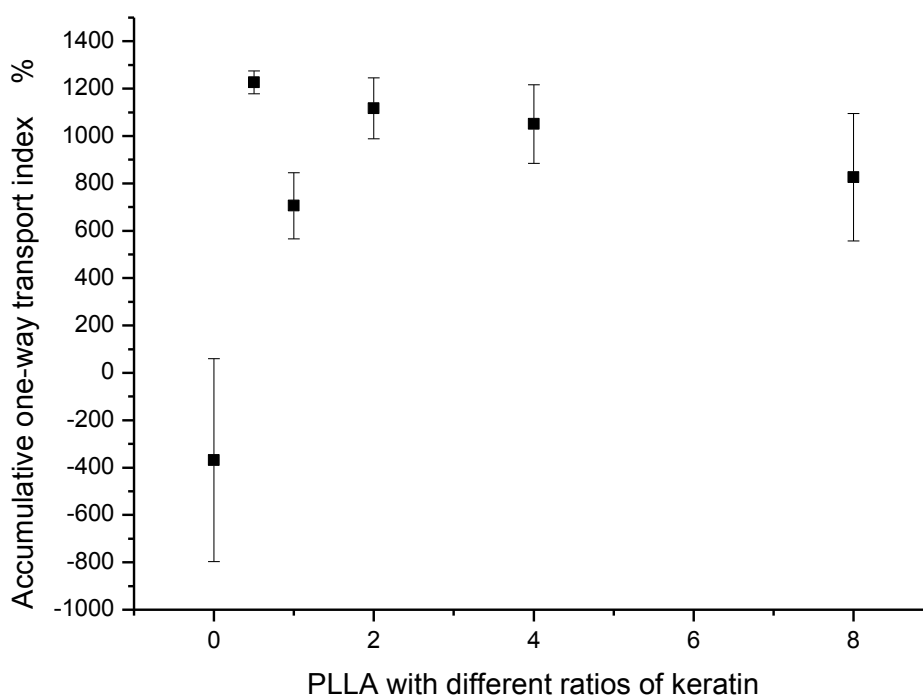


Figure 4.14 Accumulative one-way transport index (AOWTI) of PLLA and Pk membranes: the PLLA membrane had the lowest AOWTI; adding keratin to the membrane improved the AOWTI; Pk21 membrane had the highest AOWTI.

The PLLA membrane was hydrophobic and water drops could not be absorbed from the top to the bottom surface. Therefore, the pure PLLA membrane's top surface showed a specific wetting time, a maximum absorption rate, a maximum wetted radius and spreading speed value, but the bottom surface did not show any values. Thus, because of its hydrophobic property, PLLA membrane had the weakest moisture one-way transport property. Accordingly, adding keratin particles to PLLA improved the one-way transport index of the membranes. However, the one-way transport properties were not increased proportionally, as shown in Figure 4.14, Pk21 showed the highest one-way transport index.

To avoid infection, an appropriate moisture content in the wound bed is necessary for a graft to contact and spread over the wound area and displace the air-pockets from the interface [Yannas and Burke, 1980]. Therefore, an appropriate rate of moisture flux through the skin TE scaffold is required by the effective wound closure. In this respect, the Pk fibrous membranes showed relevant moisture related potential.

#### **4.6 Conclusions**

In this chapter, the first objective was fulfilled by characterizing the physical properties of the Ag/PLLA films and the Pk membranes. As the Ag NPs concentration increased, the contact angles increased. For the Pk fibrous membranes with an increasing proportion of keratin particles, the tensile strength and elongation decreased, while their moisture content increased. Their water vapor permeability was not significantly influenced by the keratin content. Thus, it can be concluded that the Pk membranes were more hydrophilic than the PLLA membranes, because of the keratin particles that they contained. Furthermore, these fibrous membranes potentially possessed good water permeability. So, it can be postulated that, after culturing enough skin cells until they covered the whole membrane, it should be possible to create an ideal skin scaffold with good permeability. Thus, based on the results of the tests, especially the tensile properties and moisture related properties, it can be

suggested that the Pk fibrous membranes with a suitable proportion of keratin particles can possibly provide an optimal matrix for skin substitutes.

**CHAPTER 5: *IN VITRO* DEGRADATION**

5.1 Introduction .....	91
5.2 Process of <i>in vitro</i> degradation .....	91
5.3 Degradation of PLLA/keratin fibrous membranes .....	92

**5.1 Introduction**

This Chapter aims to complete the second objective: To examine the *in vitro* degradation of PLLA and PLLA/keratin (Pk) membranes. According to the results obtained in this process and the physical properties of the scaffolds described in Chapter 4, the relationship between them will be analyzed.

**5.2 Process of *in vitro* degradation**

The PLLA and PLLA/keratin membranes were studied for *in vitro* degradation. Firstly the process of *in vitro* degradation will be introduced, then, the degradation of PLLA/keratin fibrous membranes will be discussed and explained.

**5.2.1 Materials and instrument**

This experiment mainly used phosphate buffer saline (PBS, pH=7.4) purchased from Invitrogen, and a water bath. In this study, the Pk11 fibrous membrane was selected for the *in vitro* degradation experiment.

**5.2.2 Process of *in vitro* degradation**

Six groups of electrospun PLLA/keratin membranes (15mm×15mm) were prepared with six samples in each group. Each sample was immersed in 50mL PBS contained in a wide mouth ampoule.

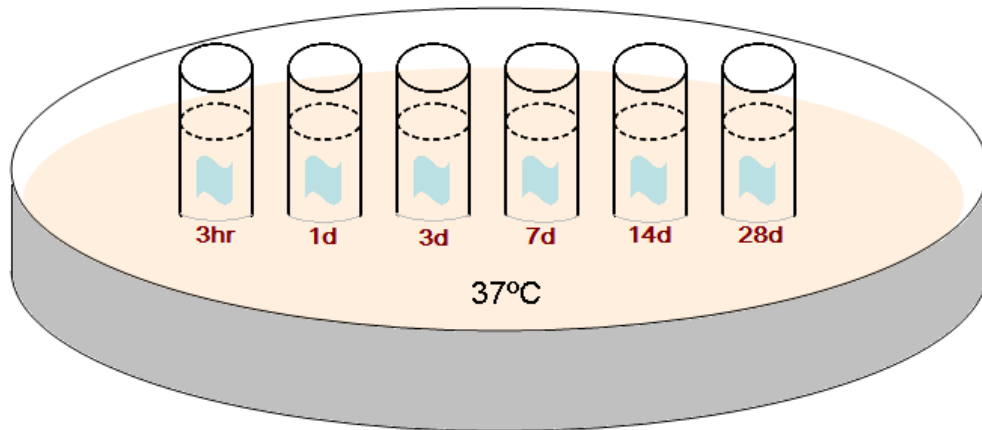


Figure 5.1 Sketch of the *in vitro* degradation experiment which proceeded in a 37 °C water bath. The time intervals were 3hr, 1d, 3d, 7d, 14d and 28d.

As shown in Figure 5.1, the ampoules with the samples and the PBS were put in a vibrating water bath set at 37°C of temperature for 4 weeks. The PBS in the ampoules was changed daily for the first week, then changed once at the tenth day and fourteenth day respectively, and finally changed weekly for the rest of the remaining period. Each sample was removed from the PBS, rinsed with distilled water, and vacuum dried for 24 hours at each appropriate time point as shown in Figure 5.1. Then, the dried samples were tested to measure the keratin releasing rate to evaluate the degradation of the membrane.

### 5.3 Degradation of PLLA/keratin fibrous membranes

#### 5.3.1 Keratin releasing rate

The PLLA/keratin samples were analysed using Fourier Transform Infrared spectroscopy (FTIR, Nicolet 5700, Thermo Co. USA) before and after degradation. As described in Chapter 3 (Figure 3.16), the FTIR spectra of pure PLLA had no peaks from 1700 to 1500  $\text{cm}^{-1}$ . For the PLLA and keratin composite membrane's FTIR spectrum, two peaks were evident at 1630  $\text{cm}^{-1}$  and 1550  $\text{cm}^{-1}$  corresponding to the keratin. The characteristic peaks of PLLA and keratin do not overlap, so they can be employed to evaluate the ratio of PLLA and keratin in the composite membranes.

The characteristic peaks of the PLLA and keratin were used to calculate their ratios after different degradation periods. Samples with different ratios of PLLA and keratin were tested by FTIR to determine the ratio of their absorption coefficients ( $k$ ). Then, the percentage of PLLA ( $C_p$ ) and keratin ( $C_k$ ) were calculated using the following equations 5.1:

$$C_p = \frac{R}{k + R} \times 100\% \quad , \quad C_k = \frac{k}{k + R} \times 100\% \quad (\text{eq. 5.1})$$

where  $R$  is the ratio of the absorbances of the PLLA ( $A_p$ ) and the keratin ( $A_k$ ):

$$R = \frac{A_p}{A_k} .$$

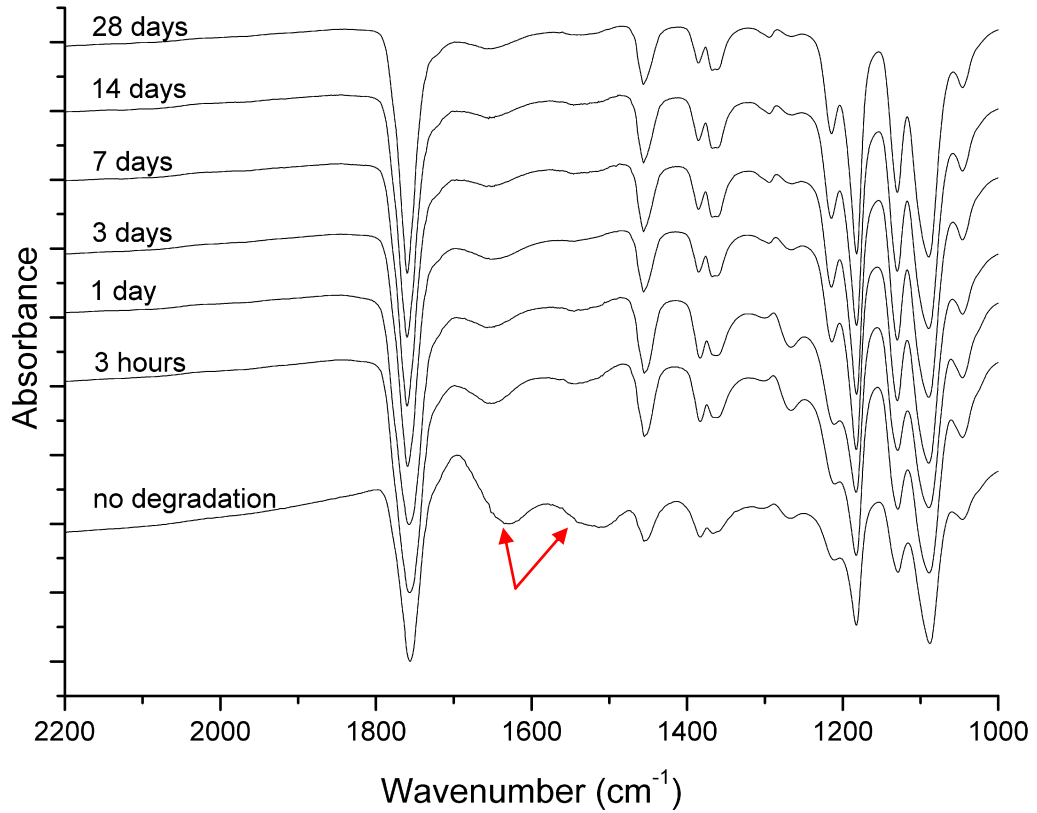


Figure 5.2 FTIR spectra of the electrospun PLLA/keratin membranes during the degradation period. The amplitude of the characteristic peaks of keratin ( $1630\text{cm}^{-1}$  and  $1550\text{cm}^{-1}$  indicated by arrows) decreased correspondingly.

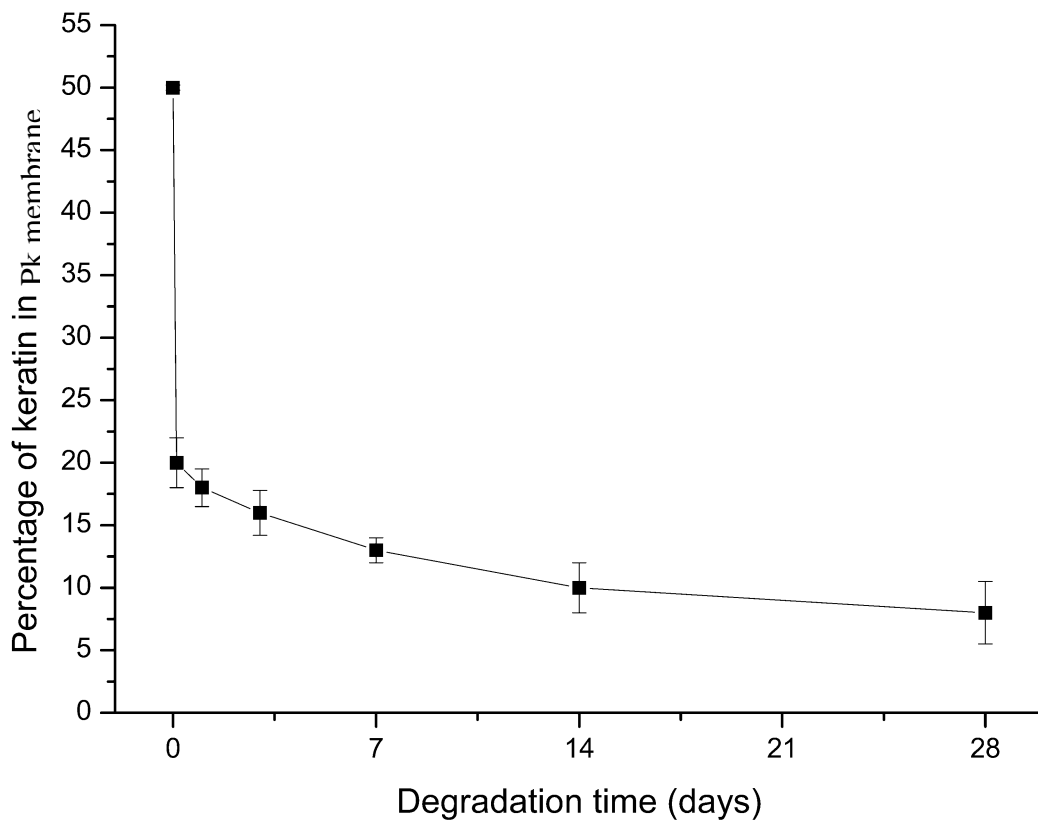


Figure 5.3 Percentage of keratin in the electrospun PLLA/keratin plotted against degradation time.

As Figure 5.2 shows, during the degradation period, the amplitude of the characteristic peaks of the keratin decreased correspondingly. According to the reduction in the absorbance shown in the FTIR spectra, the percentage of keratin in the composite was calculated using the equations 5.1. As shown in Figure 5.3, after the first three hours of degradation, more than half of the keratin particles were lost from the membrane. During the subsequent periods of degradation, the rate of keratin release slowed down. After 28 days of degradation, there remained only about 8% keratin particles in the PLLA/keratin membrane.

### **5.3.2 Morphological change**

The morphological change in the PLLA/keratin fibers was observed using SEM. The average diameter of the keratin particles used for the electrospinning was  $1.5\pm 0.3\mu\text{m}$ . The average diameter of the PLLA fibers was  $1.1\pm 0.6\mu\text{m}$  which was randomly evaluated from 100 measurements according to the SEM images. As shown in Figure 5.4, keratin particles were encapsulated in the PLLA fibers which formed PLLA/keratin fibers with evenly distributed keratin particle beads.

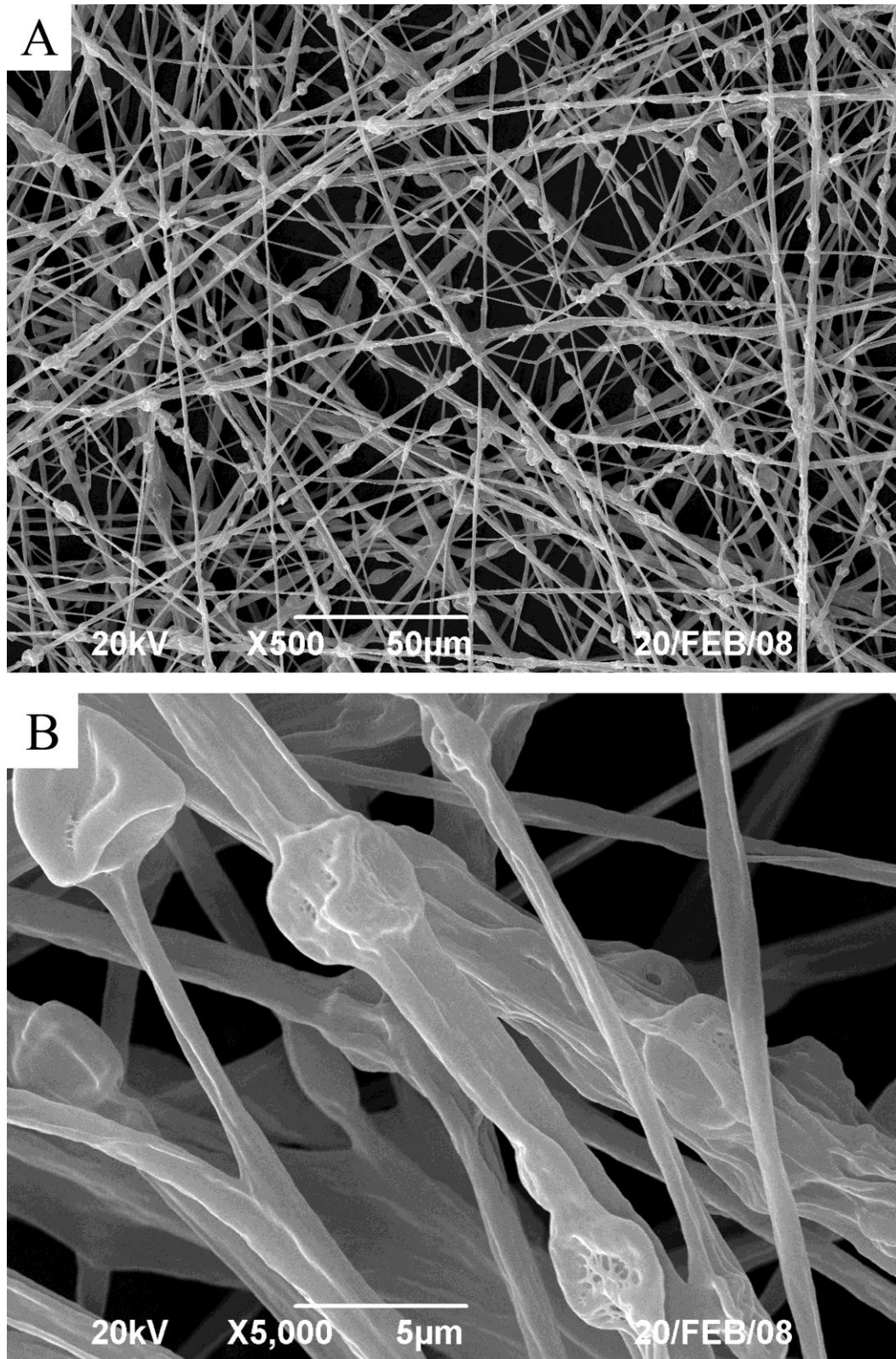


Figure 5.4 SEM of an electrospun PLLA/keratin fibrous membrane Which shows that the keratin particles were encapsulated by the PLLA to form PLLA/keratin composite fibers.

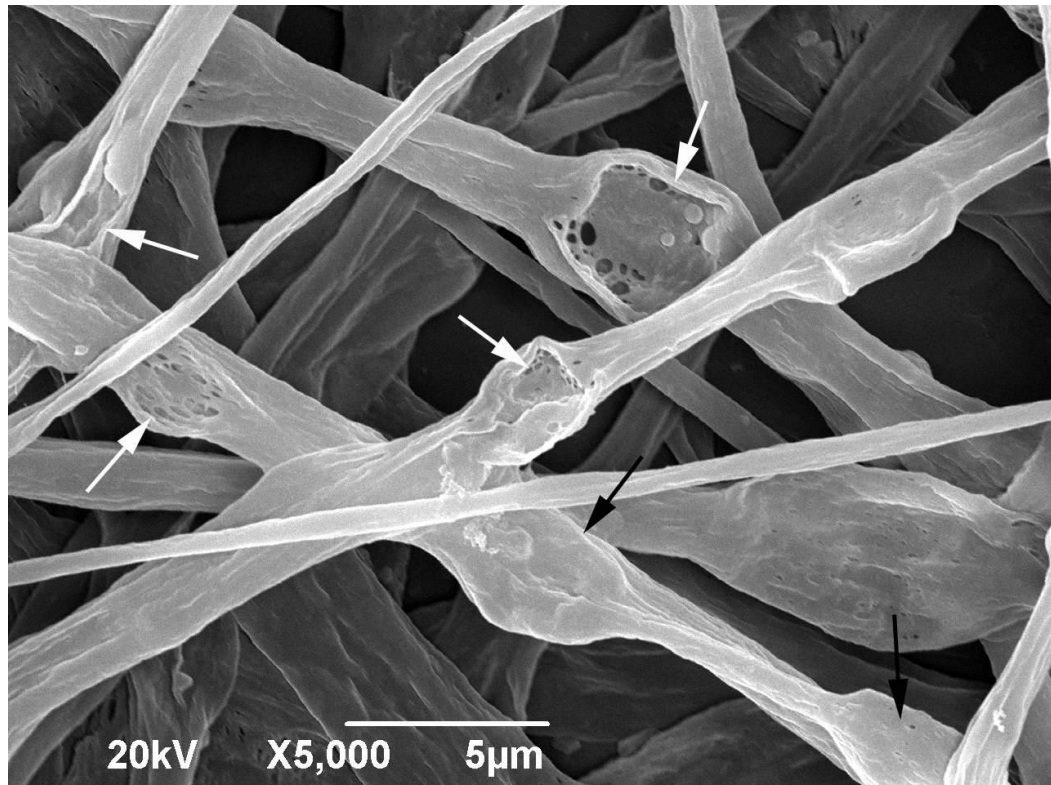


Figure 5.5 SEM image of the electrospun PLLA/keratin fibrous membrane after 3 hrs degradation. Some keratin particles were lost (directed by white arrows) and some were still embedded in the PLLA (directed by black arrows).

As a composite membrane, the releasing performance of the keratin from the PLLA fibers was anticipated to be an important factor that would affect subsequent cell attachment and proliferation. The FTIR results showed that more than half of the keratin particles were lost from the PLLA/keratin membrane within a few hours of *in vitro* degradation. This fast release may be related to two factors. Firstly, because the particle size was larger than the diameter of PLLA fibers, the keratin particles were only covered with a very thin PLLA layer or, in some cases, not even completely encapsulated, so that these particles could be easily peeled off as indicated by the white arrows in Figure 5.5. Secondly, the keratin particles were water-soluble and gradually dissolved in the PBS (Figure 5.6).

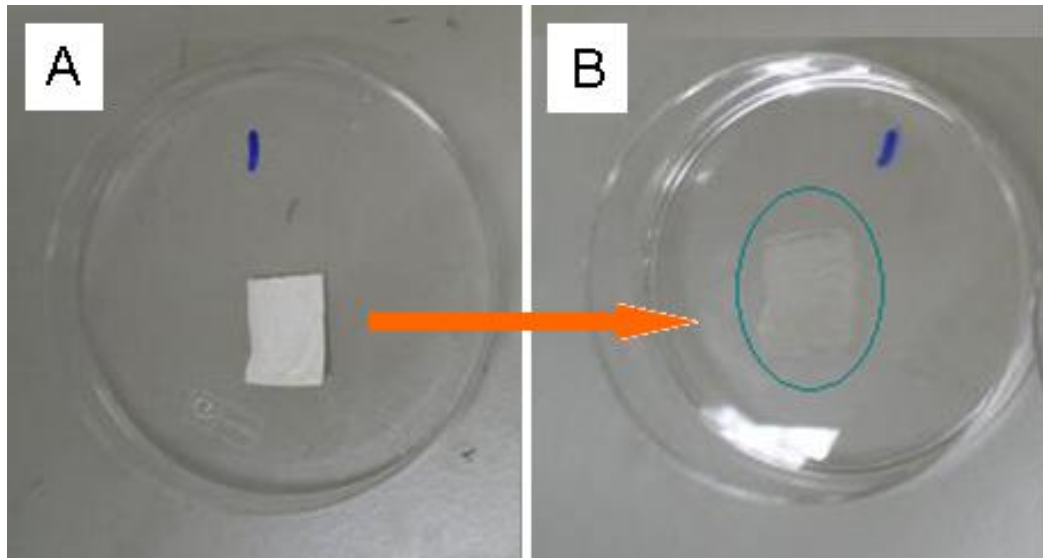


Figure 5.6 Macroscopic observation of the *in vitro* degradation of the keratin fibrous membranes. (A) Before submersion; (B) After submersion in PBS for 5 days.

The smaller diameter keratin particles were completely encapsulated in PLLA so that they were not initially exposed to the PBS (indicated by the black arrows in Figure 5.5). These keratin particles were expected to be gradually exposed and released with the degradation of the PLLA. This kind of PLLA/keratin structure would help to provide sufficient keratin to continuously support the cell affinity for the PLLA fibers during long term cell culture.

### 5.3.3 Discussion

This chapter considered the *in vitro* degradation of electrospun PLLA/keratin composite membranes. As a candidate material for *in vivo* tissue regeneration, this study showed that it was possible to produce PLLA membranes incorporating keratin particles that were still biodegradable. Although more than half of the keratin particles were released during the initial degradation stage, there were still some keratin particles entrapped in the PLLA fibers after 4 weeks, which may remain the releasing during a long time to assist in the cell

proliferation and the degradation controllable. On the basis of the results for the physical properties of the PLLA/keratin membranes, it can be suggested that the hydrophilicity should affect the *in vitro* degradation of the scaffolds. In other words, as the proportion of wool keratin in the PLLA/keratin membranes increased, they became more hydrophilic, which enhanced the ability of the PLLA/keratin fibrous membranes to absorb water. On the other hand, the inclusion of the keratin particles reduced the tensile strength and elongation; this may cause faster fracture of the PLLA/keratin fibers to enhance the biodegradability of the membranes.

#### **5.3.4 Conclusions**

In this Chapter, the second objective was achieved by examining the *in vitro* degradation. The study indicates that the keratin encapsulated within the PLLA structure would affect the degradability of the PLLA/keratin fibrous membrane. Furthermore the decreasing tensile strength and elongation with the increasing proportion of keratin particles may cause faster degradation of the PLLA/keratin fibers.

## CHAPTER 6: CYTOTOXICITY

6.1 Introduction .....	100
6.2 Cytotoxicity test .....	100
6.3 Statistical analysis .....	101
6.4 Cytotoxicity of the Ag/PLLA films and fibrous membranes .....	102
6.5 The Cytotoxicity of the PLLA/keratin fibrous membranes .....	118

### 6.1 Introduction

Chapter 6 aims to fulfill the third objective by testing the cytotoxicity of the Ag/PLLA films, the Ag/PLLA and the PLLA/keratin fibrous membranes, and exploring the relationship between their properties and their cytotoxicity.

The consideration of cytotoxicity must be taken into account when evaluating the safety of TE scaffolds. So, the cytotoxicity test is an important screening process for tissue engineering scaffolds. In this study, the MTS method was applied to test the cytotoxicity of the Ag/PLLA films, Ag/PLLA and the PLLA/keratin fibrous membranes. To explore the mechanism of the cytotoxicity of the scaffolds, the relationship between the properties and the cytotoxicity has been evaluated by analyzing the correlation between them.

### 6.2 Cytotoxicity test

According to the standard, EN ISO 10993-12:2007, sterilized membranes were rinsed with PBS three times, then immersed in a culture medium at a ratio of  $6\text{cm}^2/\text{mL}$  for films and  $0.1\text{g}/\text{mL}$  for fibrous membranes. This culture medium was kept in an incubator at  $37^\circ\text{C}$  for 24 hours to produce the extractions. The extraction is the term used for the culture medium that contains the substances released from the scaffolds in one day. This medium can help to test not only the cytotoxicity of the immersed scaffolds, but also the probable release rate of the

raw materials. The extractions of the films and membranes were subsequently used for cell culturing (Figure 6.1). The PLLA extraction was used as a reference control.

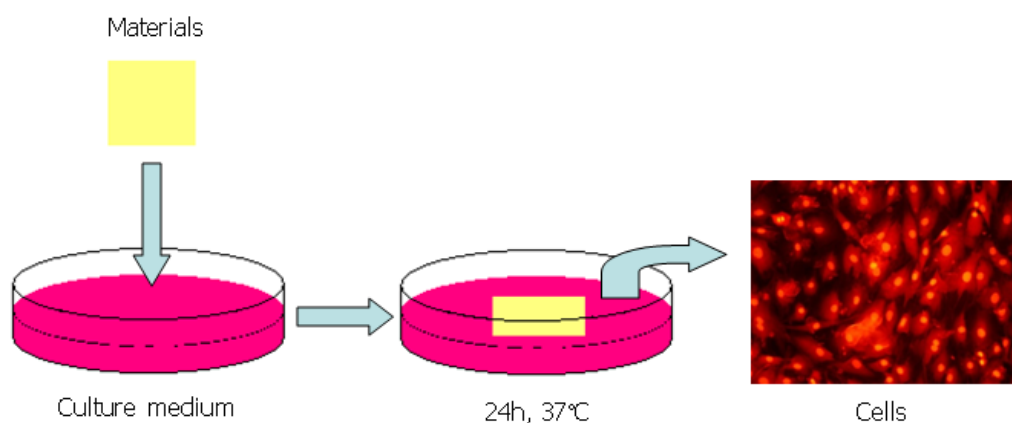


Figure 6.1 Flowchart for the cytotoxicity test of materials.

Cells ( $25\mu\text{L}$ ) at a density of  $4\times 10^5$  cells/mL were seeded in a 96-well plate, to which membrane extraction and normal culture medium were added. The medium was changed every two days. Morphological changes of the cells were observed through an inverted microscope and the cell viability was determined by MTS assay at an optical density measurement of 492nm. For morphological observation, the cells were seeded at a density of  $2\times 10^4$  cells/well in a 24-well plate.

### 6.3 Statistical analysis

Values were expressed as means  $\pm$  standard deviations. Statistical differences were determined by one-way Analysis of Variance (ANOVA). *P* values of less than 0.05 were considered to be statistically significant.

## 6.4 Cytotoxicity of the Ag/PLLA films and fibrous membranes

To determine the cytotoxic effects of the Ag/PLLA films and fibers, cytotoxicity tests were performed using the extractions of films and fibrous membranes.

### 6.4.1 Cell line

Human foreskin fibroblasts (HFF-1, ATCC) were used in this study. The cytotoxicity tests followed the steps described in section 6.2 *Cytotoxicity test*.

### 6.4.2 Results

#### *Cytotoxicity of Ag/PLLA films*

Human foreskin fibroblasts were cultured at a density of  $1 \times 10^4$  cells/well (Figures 6.2 to 6.7) and  $2 \times 10^4$  cells/well (Figures 6.8 to 6.14) respectively to study the effects of cell seeding number on cell morphological changes. The cells were then seeded in 24-well plates in the extractions of: PLLA, 0.5% Ag/PLLA, 2.5% Ag/PLLA, 5% Ag/PLLA, 7.5% Ag/PLLA and 10% Ag/PLLA films. Cell morphology was observed after the cells had been immersed in the extractions for one hour and one day respectively.

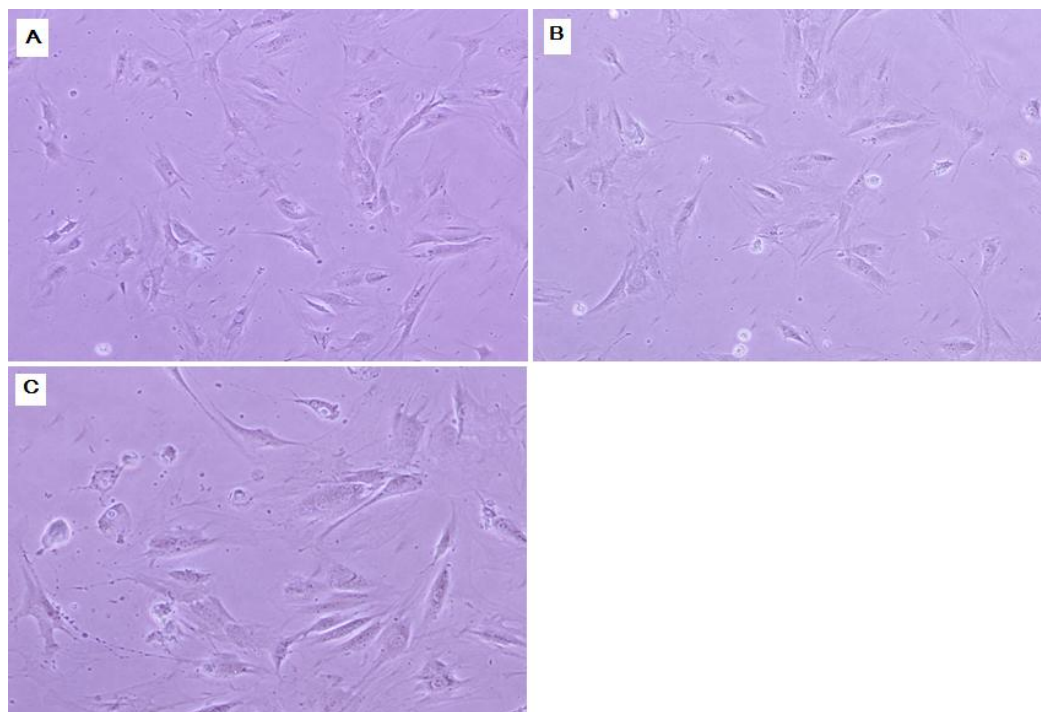


Figure 6.2 Inverted microscopic images of cells cultured with (A) Culture medium; (B) 0.5% Ag/PLLA extraction for 1h; (C) 0.5% Ag/PLLA extraction for 1d (x100).

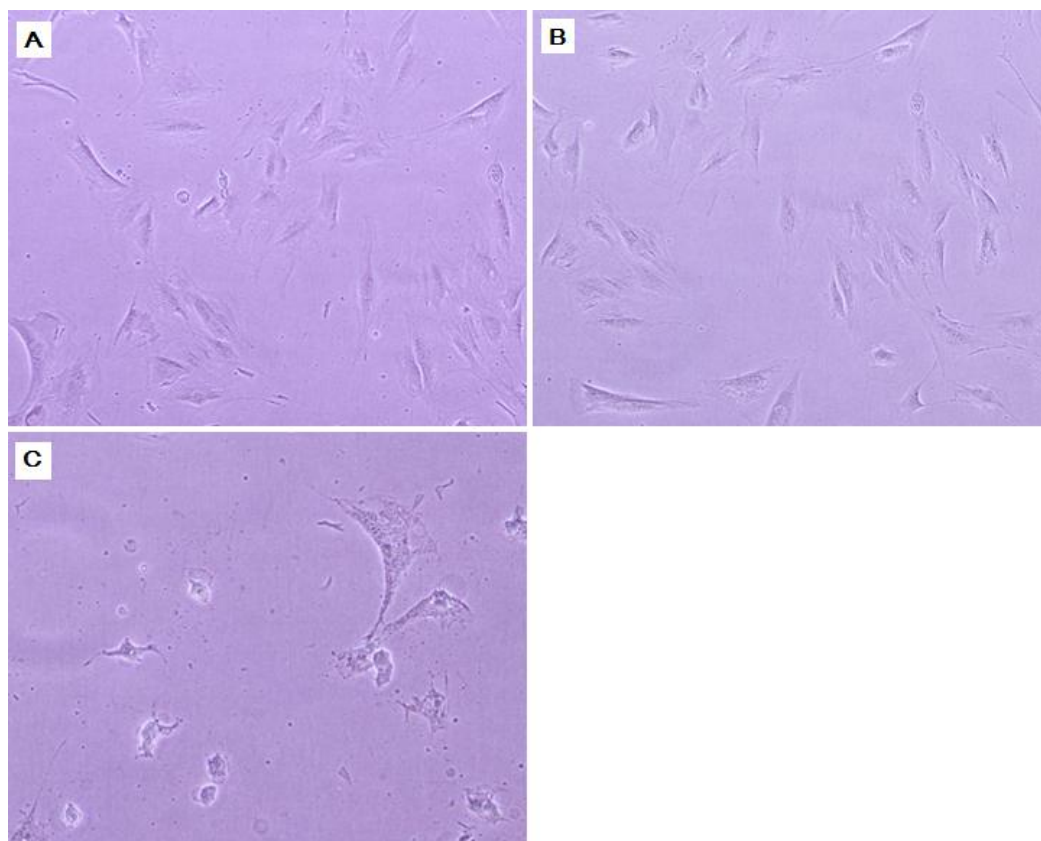


Figure 6.3 Inverted microscopic images of cells cultured with (A) Culture medium; (B) 2.5% Ag/PLLA extraction for 1h; (C) 2.5% Ag/PLLA extraction for 1d (x100).

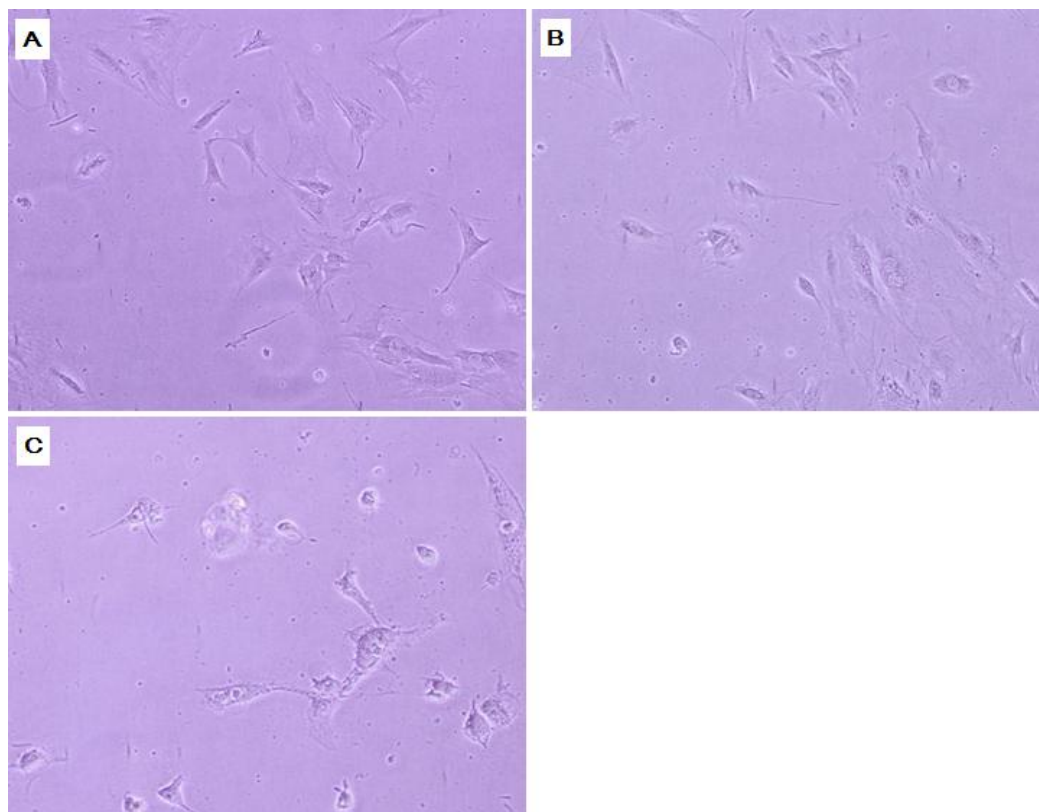


Figure 6.4 Inverted microscopic images of cells cultured with (A) Culture medium; (B) 5% Ag/PLLA extraction for 1h; (C) 5% Ag/PLLA extraction for 1d (x100).

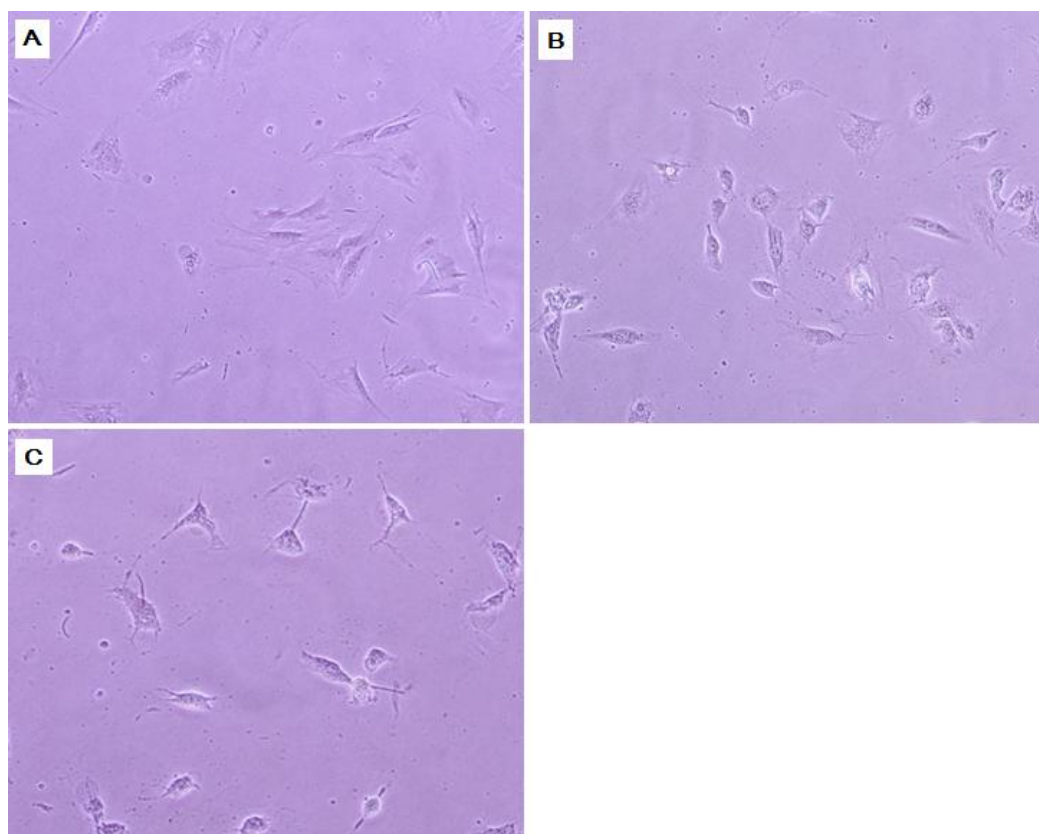


Figure 6.5 Inverted microscopic images of cells cultured with (A) Culture medium; (B) 7.5% Ag/PLLA extraction for 1h; (C) 7.5% Ag/PLLA extraction for 1d (x100).

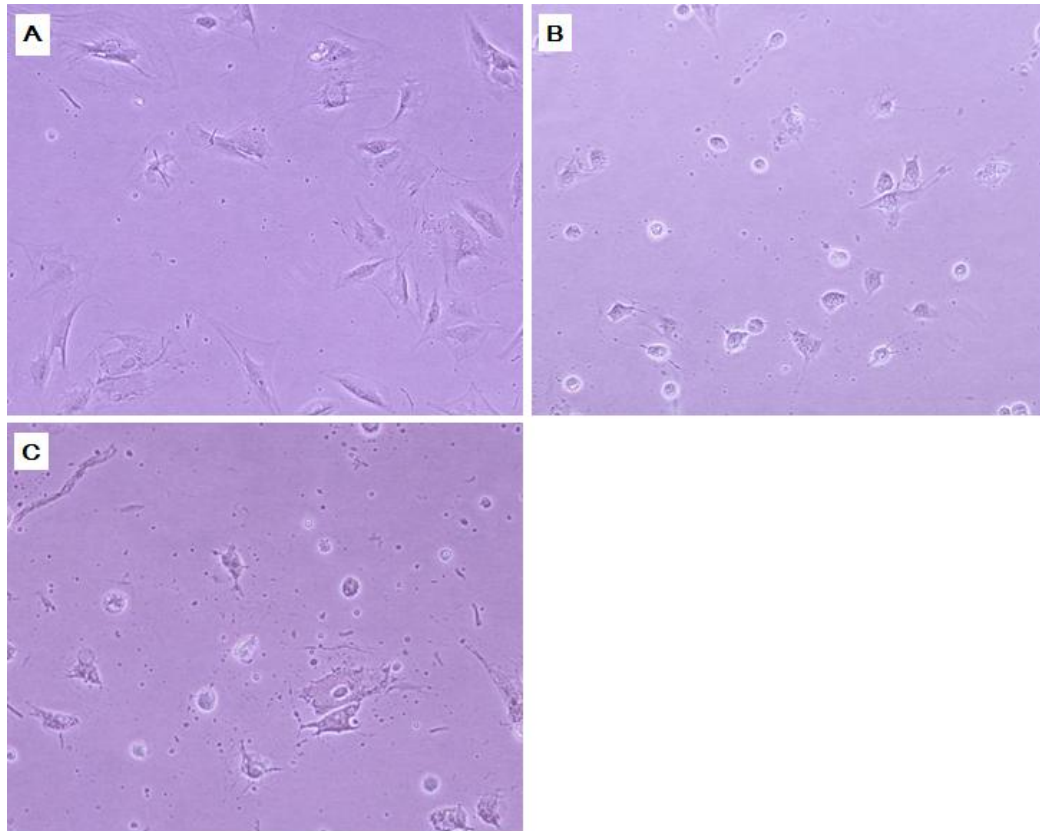


Figure 6.6 Inverted microscopic images of cells cultured with (A) Culture medium; (B) 10% Ag/PLLA extraction for 1h; (C) 10% Ag/PLLA extraction for 1d (x100).

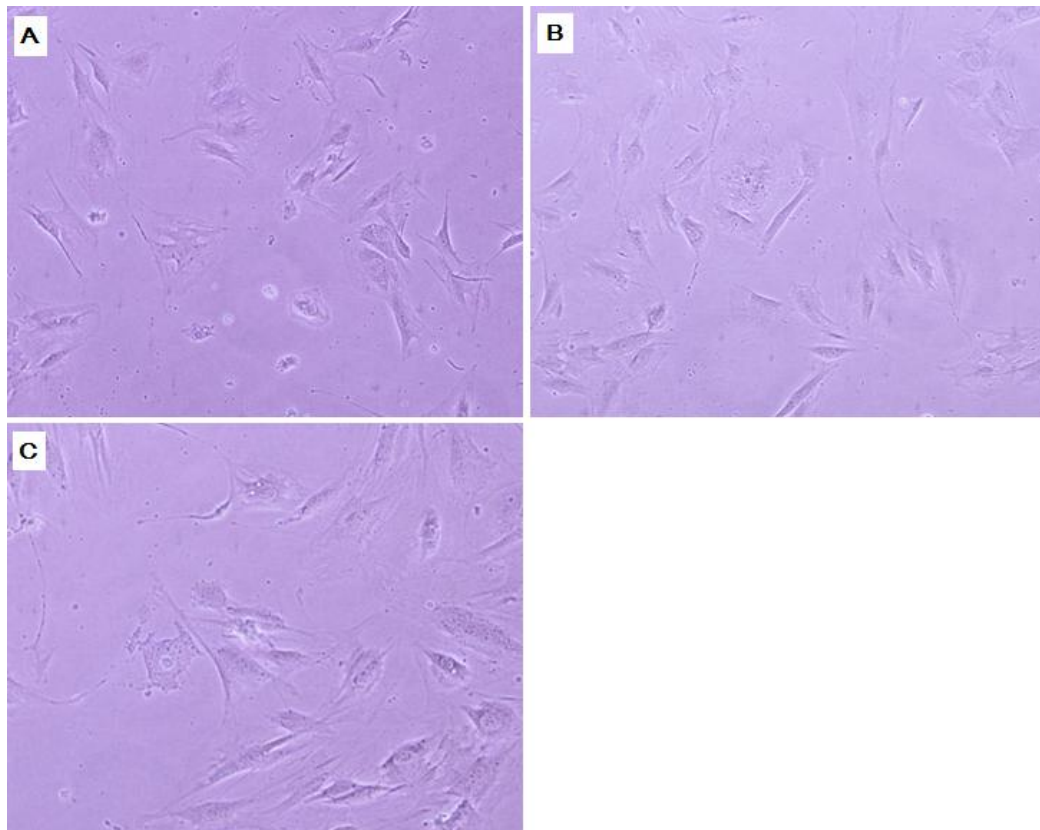


Figure 6.7 Inverted microscopic images of cells cultured with (A) Culture medium; (B) PLLA extraction for 1h; (C) PLLA extraction for 1d (x100).

As shown in Figures 6.2 to 6.7, the cytotoxic effects had already started after one hour's culture, and became worse in one day, especially in the extractions of the 7.5% Ag/PLLA and 10% Ag/PLLA films. However, in the extraction of the 5% Ag/PLLA film, although the cell morphology was changed, some stretched cells, which indicated them to be highly viable could still be observed. In the extractions of the PLLA, 0.5% Ag/PLLA, 2.5% Ag/PLLA films there were no obvious changes in the cell shapes.

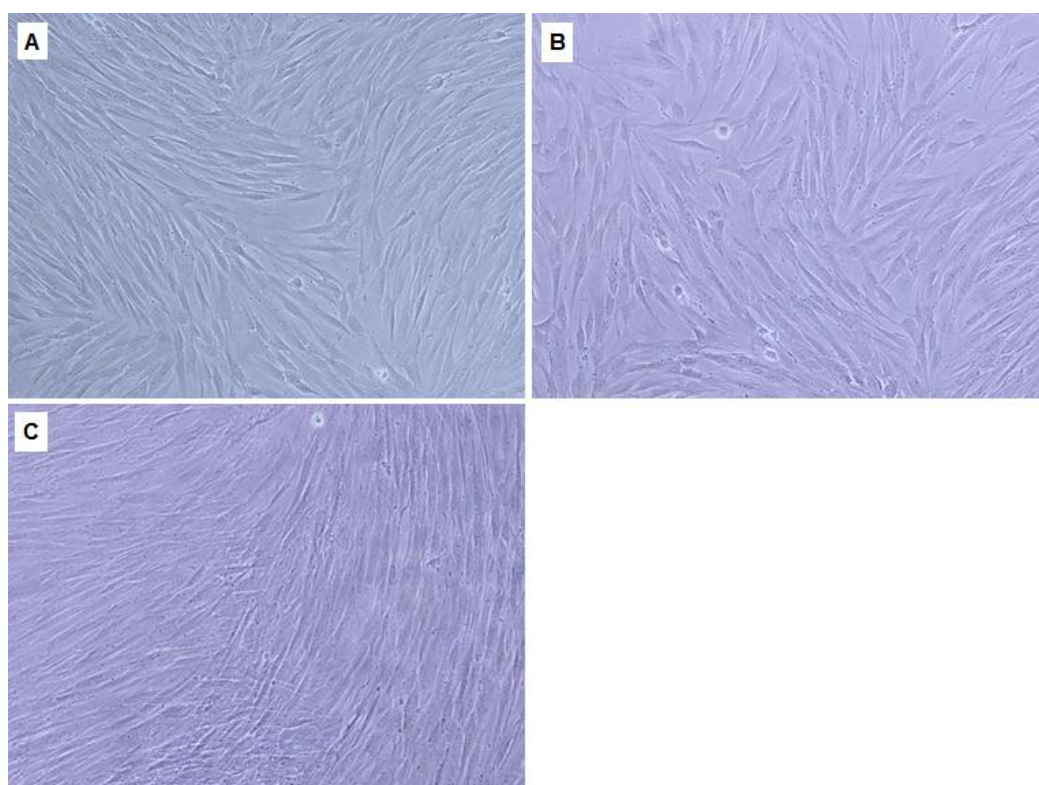


Figure 6.8 Inverted microscopic images of cells cultured with (A) Culture medium (B) 0.5% Ag/PLLA extraction for 1d (C) 0.5% Ag/PLLA extraction for 3d (x100).

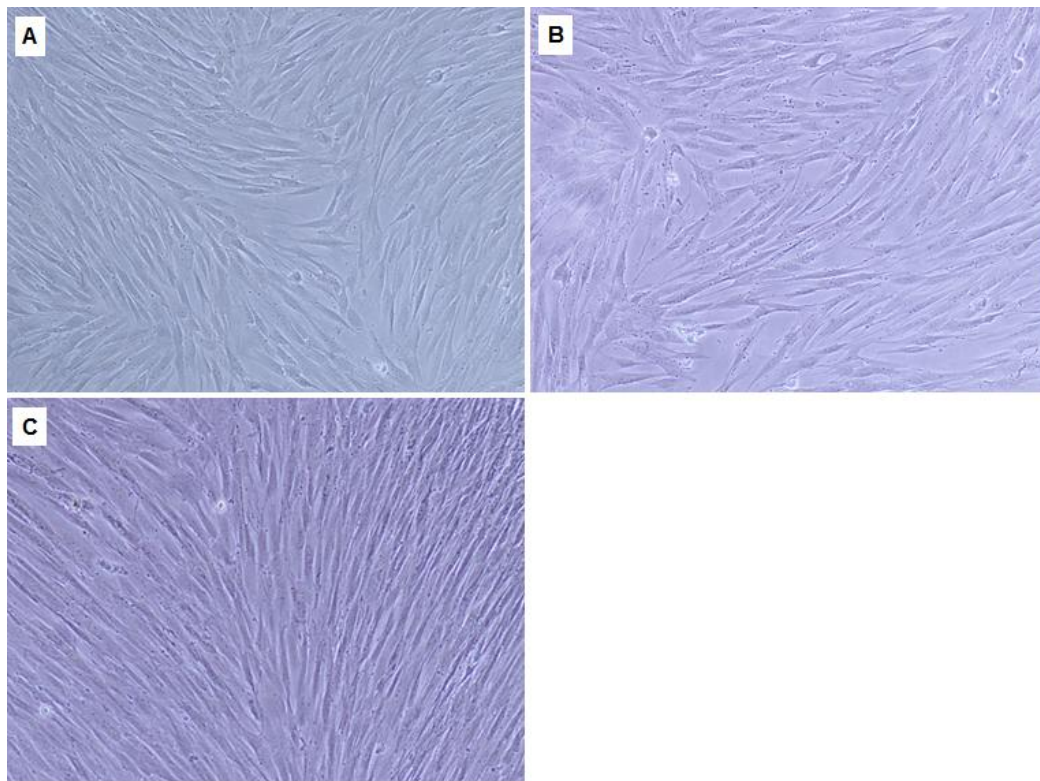


Figure 6.9 Inverted microscopic images of cells cultured with (A) Culture medium (B) 2.5% Ag/PLLA extraction for 1d (C) 2.5% Ag/PLLA extraction for 3d (x100).

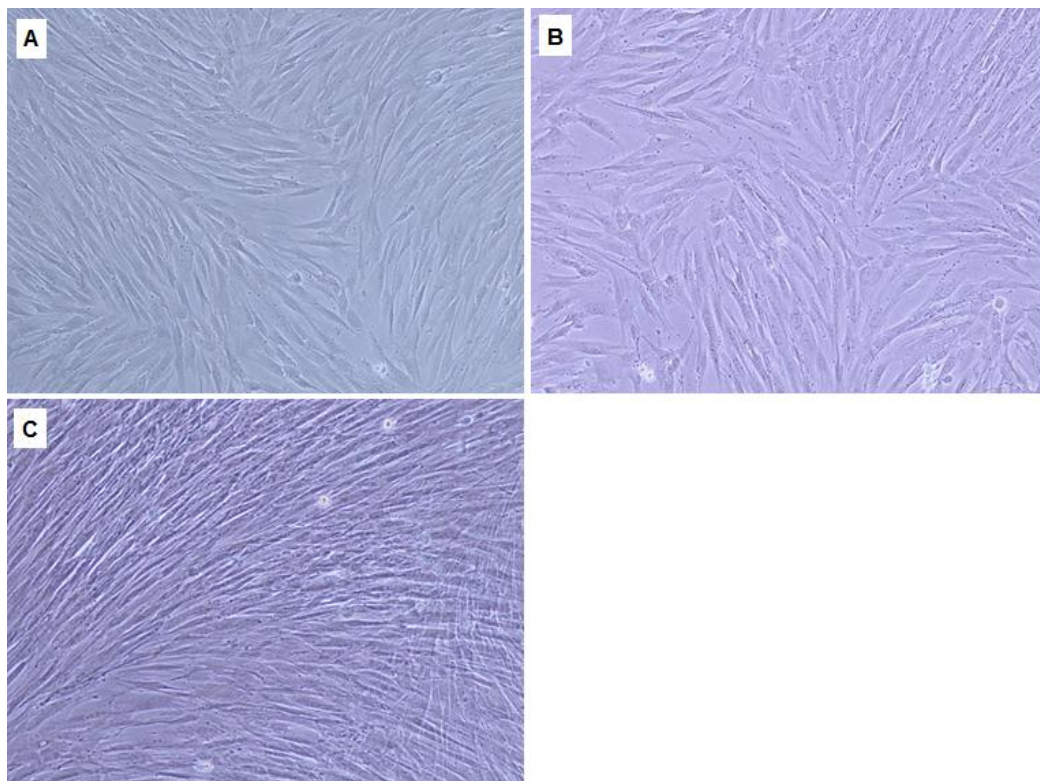


Figure 6.10 Inverted microscopic images of cells cultured with (A) Culture medium (B) 5% Ag/PLLA extraction for 1d (C) 5% Ag/PLLA extraction for 3d (x100).

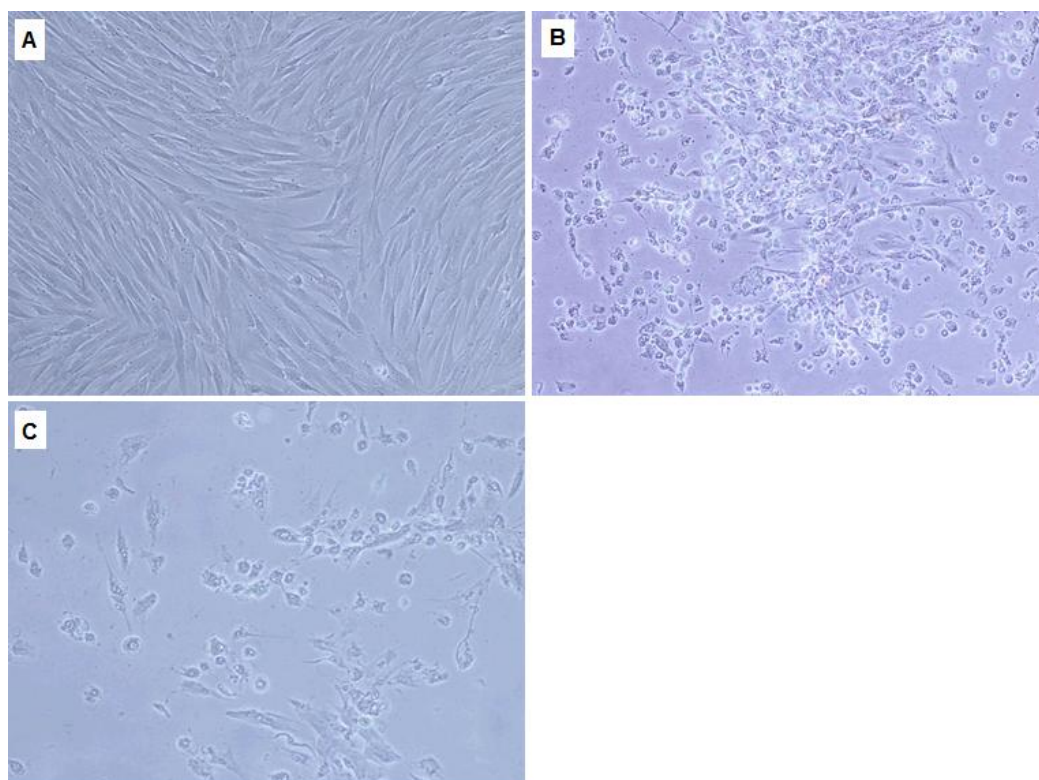


Figure 6.11 Inverted microscopic images of cells cultured with (A) Culture medium (B) 7.5% Ag/PLLA extraction for 1d (C) 7.5% Ag/PLLA extraction for 3d (x100).

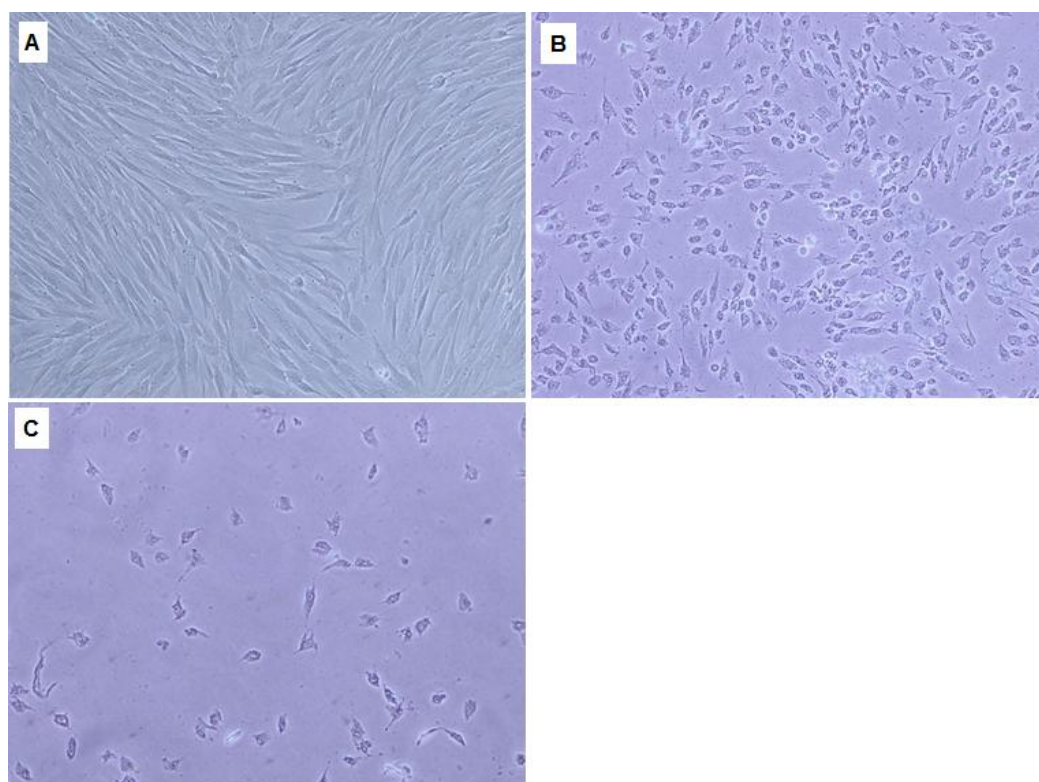


Figure 6.12 Inverted microscopic images of cells cultured with (A) Culture medium (B) 10% Ag/PLLA extraction for 1d (C) 10% Ag/PLLA extraction for 3d (x100).

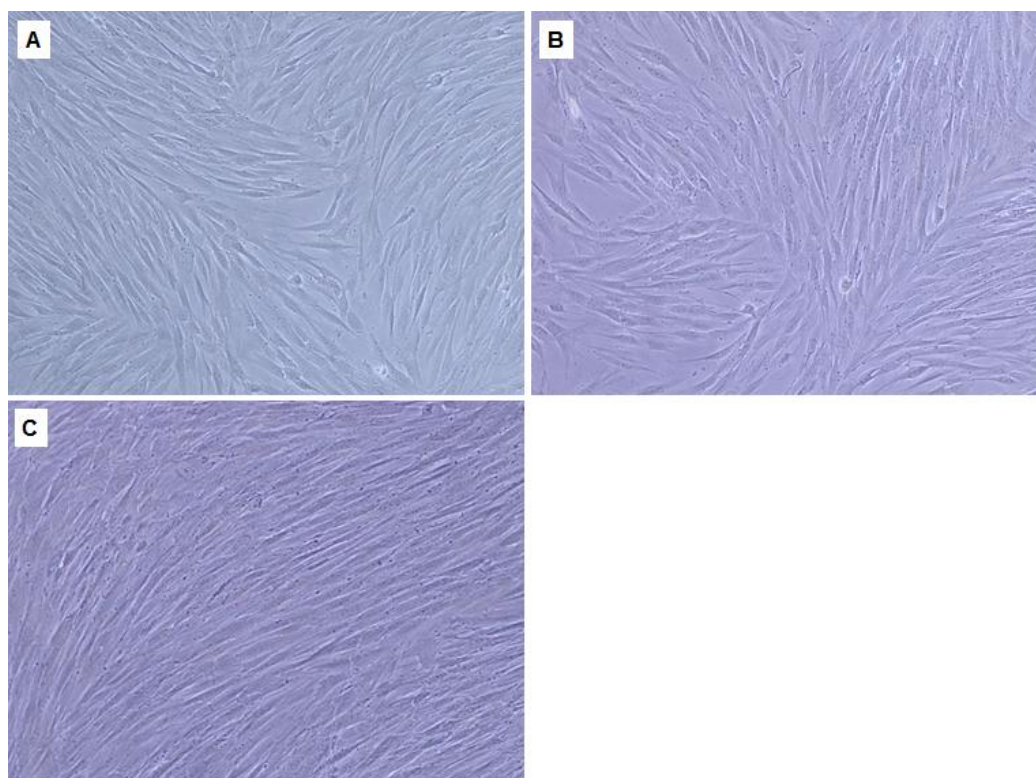


Figure 6.13 Inverted microscopic images of cells cultured with (A) Culture medium (B) PLLA extraction for 1d (C) PLLA extraction for 3d (x100).

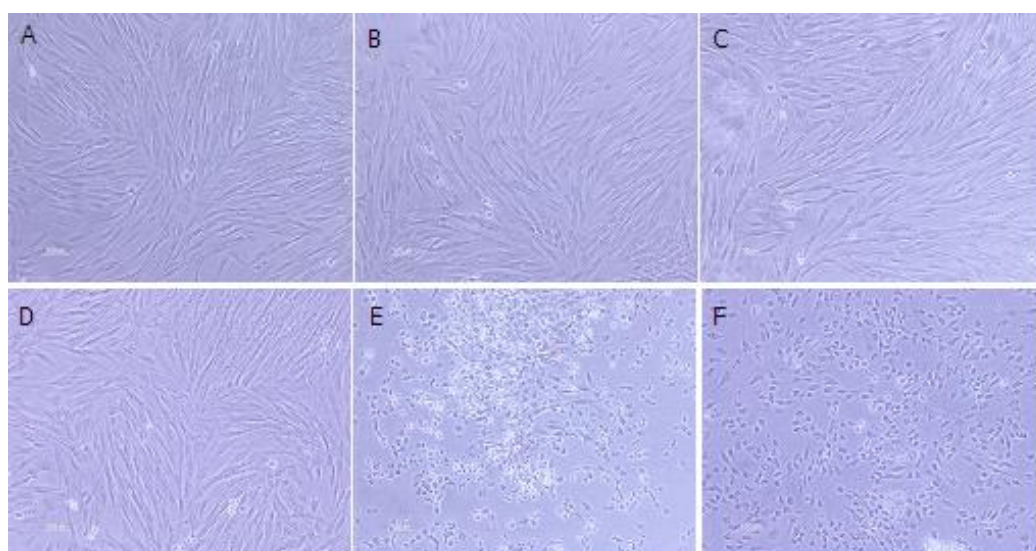


Figure 6.14 Morphological changes of cells cultured with different extractions after one day's culture. (A) PLLA (B) 0.5% Ag/PLLA (C) 2.5% Ag/PLLA (D) 5% Ag/PLLA (E) 7.5% Ag/PLLA (F) 10% Ag/PLLA. Morphological changes and detachment of the cells were observed in the extractions 7.5% and 10% Ag/PLLA films (x100).

As Figures 6.8 to 6.14 show, the morphology of cells cultured in the extractions of the 7.5% Ag/PLLA and 10% Ag/PLLA films was remarkably changed.

Conversely no or little changes were evident in the cells cultured in the PLLA, 0.5% Ag/PLLA, 2.5% Ag/PLLA and 5% Ag/PLLA after one day's culture. Furthermore, the cells cultured in these extractions were highly proliferated after three days. From the results shown above, it can be seen that as the number of cells seeded increased, the cell viability increased. As shown in Figure 6.14, the detached cells indicated that the 7.5% and 10% Ag/PLLA films were toxic to the cells.

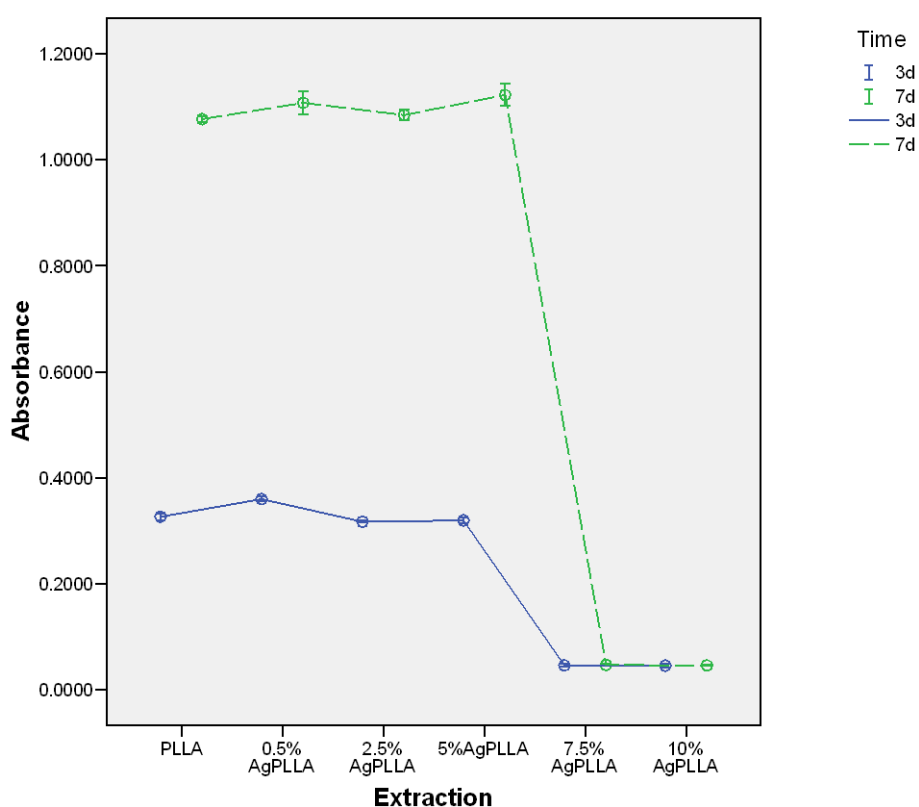


Figure 6.15 MTS assay results of cell proliferation with different extractions (492nm). The 7.5% and 10% Ag/PLLA film extractions inhibited cell proliferation, while the 5% Ag/PLLA extraction increased the cell number significantly ( $P < 0.05$ ).

In accord with the results shown in Figure 6.14, the results shown in Figure 6.15 indicate that the 7.5% and 10% Ag/PLLA film extractions inhibited cell proliferation, while the 5% Ag/PLLA extraction increased the cell number significantly. These results implied that only the 0.5%, 2.5% and 5% Ag/PLLA

film extractions were safe to use with the cells. So, these films were selected for the subsequent antibacterial and cell proliferation tests.

### *Cytotoxicity of Ag/PLLA fibrous membranes*

The cytotoxicity of the Ag/PLLA fibrous membranes was also tested using the extractions of the membranes by following the procedure described in section 6.2.

From Figure 6.16, it could be concluded that, compared with the cells cultured in the extractions of the Ag/PLLA films, the cells cultured in the extractions of the Ag/PLLA fibrous membranes showed more morphological damage. Dead cells were observed in the extractions of the 2.5% Ag/PLLA, 5% Ag/PLLA, 7.5% Ag/PLLA, and 10% Ag/PLLA membranes. Furthermore, in the extractions of the 7.5% Ag/PLLA and the 10% Ag/PLLA membranes, no living cells could be observed at all. In the extraction of the 5% Ag/PLLA, although there were not many, there were still a few stretched living cells visible, and more were seen in the extractions of the 2.5% Ag/PLLA and the 0.5% Ag/PLLA membranes. In the extraction of the 0.5% Ag/PLLA membrane, the number and shape of living cells were almost the same as the cells cultured in the PLLA extraction.

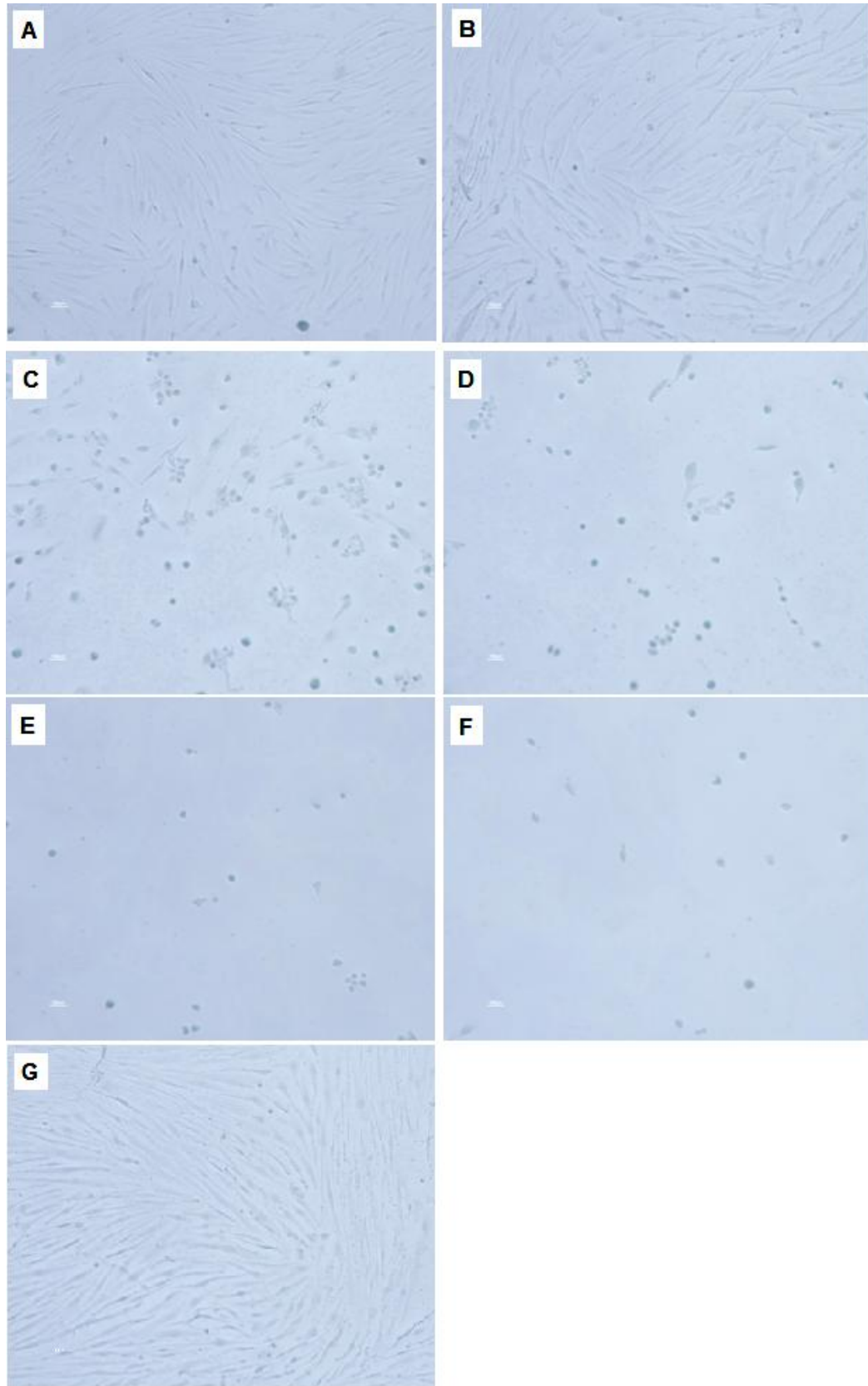


Figure 6.16 Inverted microscopic images of cells cultured with different extractions: (A) PLLA; (B) 0.5% Ag/PLLA membranes; (C) 2.5% Ag/PLLA membranes; (D) 5% Ag/PLLA membranes; (E) 7.5% Ag/PLLA membranes; (F) 10% Ag/PLLA membranes. (G) Before adding extractions of Ag/PLLA fibrous membranes (x100).

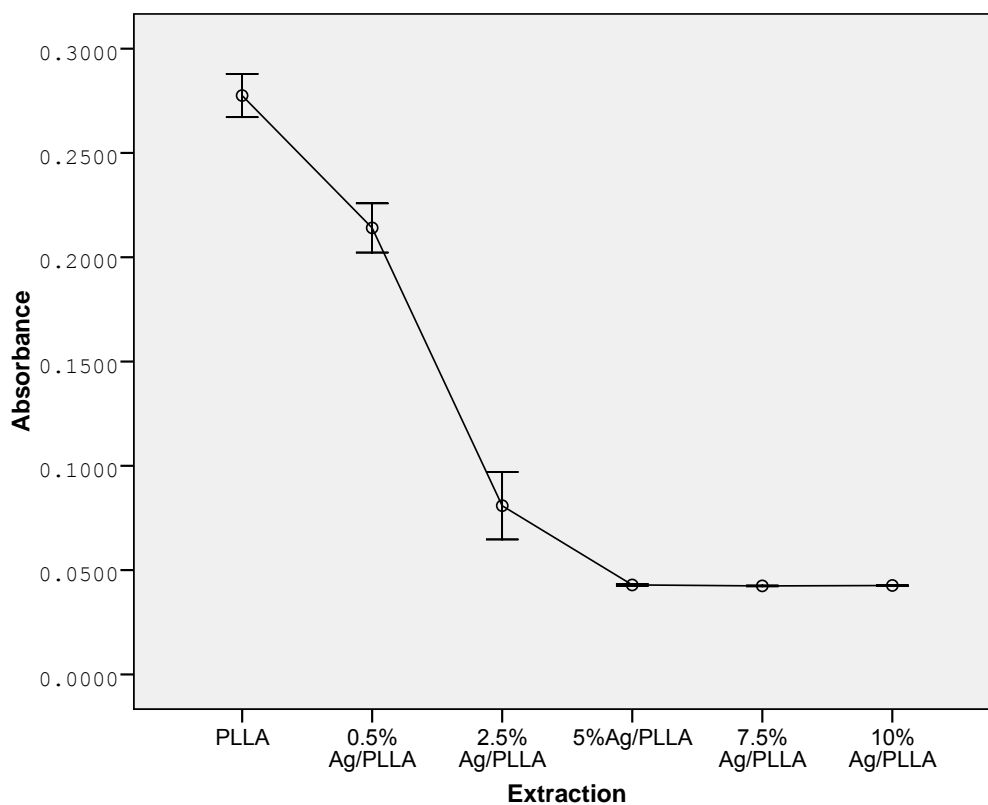


Figure 6.17 Cell viability of the cells cultured with the extractions of the PLLA and Ag/PLLA membranes.

Similar to the findings in Figure 6.16, the results for cell viability tested by MTS assay shown in Figure 6.17, indicated that, although the viability was significantly lower than that of the cells cultured in the PLLA extraction, the viability of the cells cultured in the 0.5% Ag/PLLA and the 2.5% Ag/PLLA extractions was significantly higher than that of the cells in the other extractions (Figure 6.17). These results supported the thought that the fibers probably released more Ag NPs from the Ag/PLLA fibrous membranes than were released from the Ag/PLLA films. Consequently, the membranes would need fewer Ag NPs than the films to have a similar cytotoxicity level. From the opposite point of view, this also implied that the Ag/PLLA fibrous membranes would be more efficient and economical for antibacterial activity.

### 6.4.3 Discussion

Tissue engineering scaffolds for medical applications have to fulfill two preconditions: They must be both non-cytotoxic and effective in reducing the possibility of infections [Gaonkar et al, 2003; Li et al, 2006; Morris and Stickler, 1998; Shan et al, 2008; Walder et al, 2002;]. This chapter has mainly discussed the cytotoxicity property of the scaffolds. The antibacterial test will be considered in Chapter 8.

The cytotoxicity of Ag NPs has been studied extensively during the last decade. Braydich-Stolle et al studied the cytotoxicity of nanoparticles in the germ line in vitro, and found that 15nm Ag NPs induced dramatic changes in the cells at concentrations of 10 $\mu$ g/mL and above, where the cells were observed to be necrotic and detached from the culture dishes [Braydich-Stolle et al, 2005]. Also, smaller Ag NPs were more toxic than larger particles. Xiong et al found that, when the diameter of the Ag NP was less than 100nm, over 50 $\mu$ g/mL of Ag NPs caused obvious morphological changes [Xiong et al, 2007]. Another study showed that when the cells were exposed to Ag NPs at 5-50  $\mu$ g/mL, mitochondrial function decreased significantly [Hussain et al, 2005]. Kim et al found that more than 300 mg/kg (300 $\mu$ g/mL) of Ag NPs might cause slight liver damage [Kim et al, 2008]. Consequently, when the morphological changes occurred, the Ag NPs concentration of the extractions was probably more than 50 $\mu$ g/mL.

As described in the cytotoxicity tests, the extractions were obtained by immersing the scaffolds in a culture medium at a ratio of 6cm<sup>2</sup>/mL for films, and 0.1g/mL for fibrous membranes. The concentrations of Ag NPs for each

immersed scaffold are shown in Table 6.1 derived according to the calculation of the Ag NPs content described in Chapter 3.

Table 6.1 The concentration of the Ag NPs for each immersed scaffold.

<b>Film</b>	<b>Ag NPs content (µg/mL)</b>	<b>Fibrous membrane</b>	<b>Ag NPs content (µg/mL)</b>
10% Ag/PLLA	1800	10% Ag/PLLA	10000
7.5% Ag/PLLA	1350	7.5% Ag/PLLA	7500
5% Ag/PLLA	900	5% Ag/PLLA	5000
2.5% Ag/PLLA	450	2.5% Ag/PLLA	2500
0.5% Ag/PLLA	90	0.5% Ag/PLLA.	500

According to the data shown in Table 6.1 and the cells' morphological changes shown in the figures above, it may be assumed that the concentration of the Ag NPs in the 5% Ag/PLLA film and the 0.5%Ag/PLLA fibrous membrane extractions would be around 50µg/mL. Consequently, it could be calculated that, after 24 hours immersing in the culture medium, the Ag NPs release rate of these two scaffolds would be 5.6% ( $50\mu\text{g/mL} / 900\mu\text{g/mL} \times 100\% \approx 5.6\%$ ) for the 5% Ag/PLLA film, and 10% for the 0.5% Ag/PLLA fibrous membrane. Based on this calculation, it may be inferred that the fibrous membranes released about twice the Ag NPs than the films. In other words, compared with the films, the Ag/PLLA fibrous membranes with the same Ag NPs concentration had more cytotoxic effects on the cells.

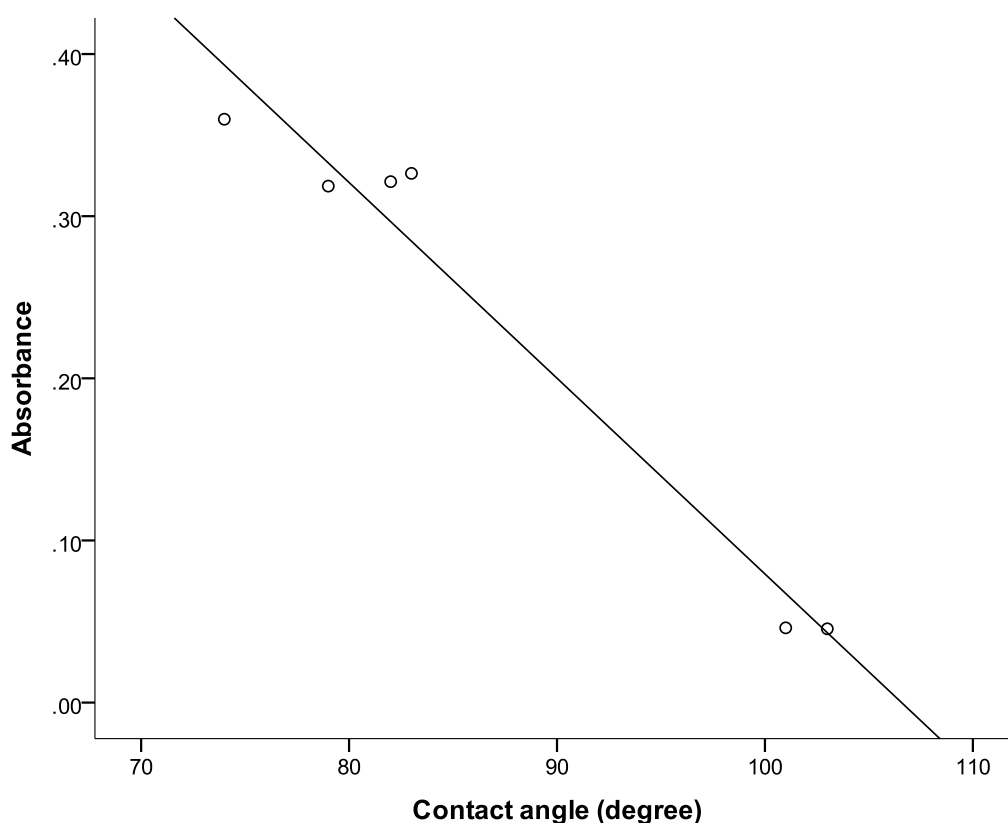


Figure 6.18 The linear relationship between the contact angle values and the absorbance of cell proliferation in the extractions of the PLLA and Ag/PLLA films ( $r = -0.98$ ,  $P < 0.05$ ).

As shown in Figure 6.18, the value of the linear correlation coefficient between the contact angle and the absorbance of cell proliferation on the Ag/PLLA films was  $-0.981$ . Consequently, the contact angle values and cell proliferation had a strong negative linear correlation. This meant as the hydrophobicity of the scaffolds increased, the number of cells that grew on the scaffolds decreased. In other words, as the contact angle values increased, the Ag/PLLA films become more cytotoxic. The understanding of the precise mechanism of this phenomenon remains to be further explored.

#### 6.4.4 Conclusions

In this part, the third objective was partially achieved by analyzing the cytotoxicity and the relationship between the cytotoxicity and hydrophilicity of the scaffolds. On the basis of the observations, it could be concluded that the concentration of the Ag NPs affected the cytotoxicity of the scaffolds in a proportional relationship. The cytotoxicity of the scaffolds increased as the concentration of the Ag NPs increased. Furthermore, the hydrophilicity and cell proliferation of the scaffolds had a strong negative linear correlation. Consequently, the optimal proportion of the Ag NPs and the PLLA for non-cytotoxicity was considered to be 5% (w/w) for the films, and 0.5% (w/w) for the Ag/PLLA fibrous membranes. In the extraction of the 2.5% Ag/PLLA membrane, there were some living cells that could be seen, and in the extraction of the 5% Ag/PLLA membrane, although there were not many, there were still a few stretched living cells visible. Consequently, it was concluded that the Ag NPs concentration of the Ag/PLLA membranes should be less than 5% (w/w) at most.

The probable release rate of the Ag NPs from the different scaffolds was also found. The Ag/PLLA fibrous membranes had a much higher release rate of Ag NPs than the Ag/PLLA films. This implied that, compared with the films, the Ag/PLLA fibrous membranes would use less Ag NPs for a comparable antibacterial activity with the same level of cytotoxic effects on the cells. This finding would provide the evidence to determine the Ag NPs dosage to fabricate the scaffolds for medical applications. Meanwhile, the actual mechanism of the

Ag NPs' action on the cells was not been elucidated. Therefore, further investigation into the effects of Ag NPs on cells is necessary.

## **6.5 The Cytotoxicity of the PLLA/keratin fibrous membranes**

### **6.5.1 Cell line**

Mouse osteoblasts (MC3T3, ATCC) were used for this study. The cytotoxicity tests followed the steps described in section 6.2 *Cytotoxicity test*.

### **6.5.2 Cell adhesion**

Osteoblasts (MC3T3, ATCC) used in this study were maintained in Dulbecco's Modified Eagle's Medium (DMEM) with 10% fetal bovine serum (FBS, Invitrogen, USA) in a 37°C and 5% CO<sub>2</sub> incubator. The medium was replaced twice weekly. All of the membranes were sterilized by ultraviolet irradiation for 20 minutes after being immersed in 70% ethanol for 1 hour. Each membrane was seeded with  $2 \times 10^4$  cells and kept in the incubator for one day. An MTS assay was employed to assess the cell adhesion on the membranes.

### **6.5.3 Scanning electron microscopy (SEM)**

Electrospun fibrous membranes with cells were coated with gold and then their morphologies were observed by scanning electron microscopy (JEOLJSM-6335F, 20kV).

### **6.5.4 Results**

To determine the cytotoxic effects of the Pk fibrous membranes, cytotoxicity tests were performed using the membrane extractions.

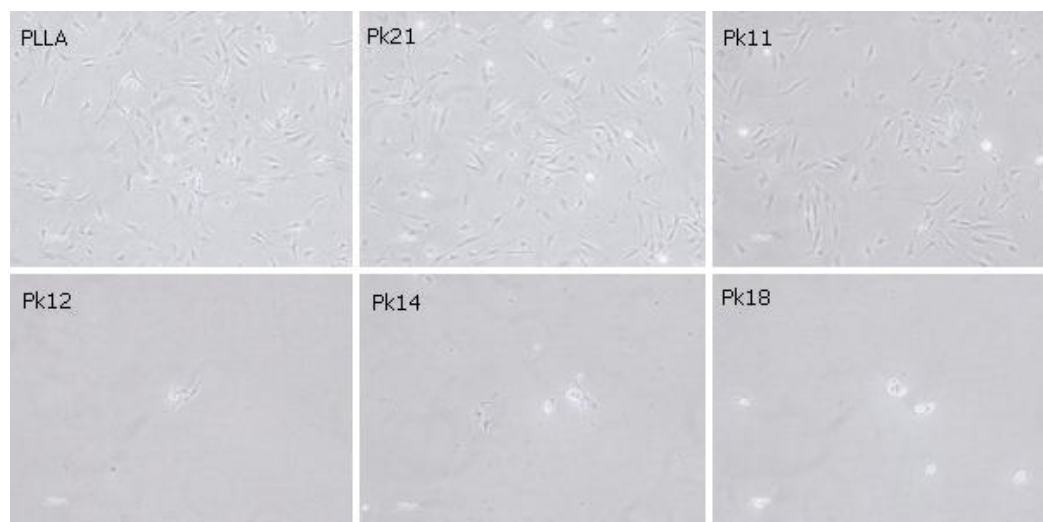


Figure 6.19 Morphological changes of cells cultured with different extractions of Pk fibrous membranes. Morphological changes and detachment of the cells were observed in the extractions of Pk12, Pk14 and Pk18 membranes through an inverted microscope.

The morphological changes and detachment of the cells were observed through an inverted microscope. As shown in Figure 6.19, the extractions of the Pk12, Pk14 and Pk18 membranes inhibited cell proliferation, whereas the extractions of the Pk21 and Pk11 membranes did not change the cell morphology significantly, which implied that these two membranes were suitable for cell proliferation.

Cell adhesion was also observed as a direct method for testing the cytotoxicity of the Pk membranes. Cells were cultured on the PLLA and Pk membranes for one day before applying an MTS assay for checking the cell adhesion (Figure 6.20).

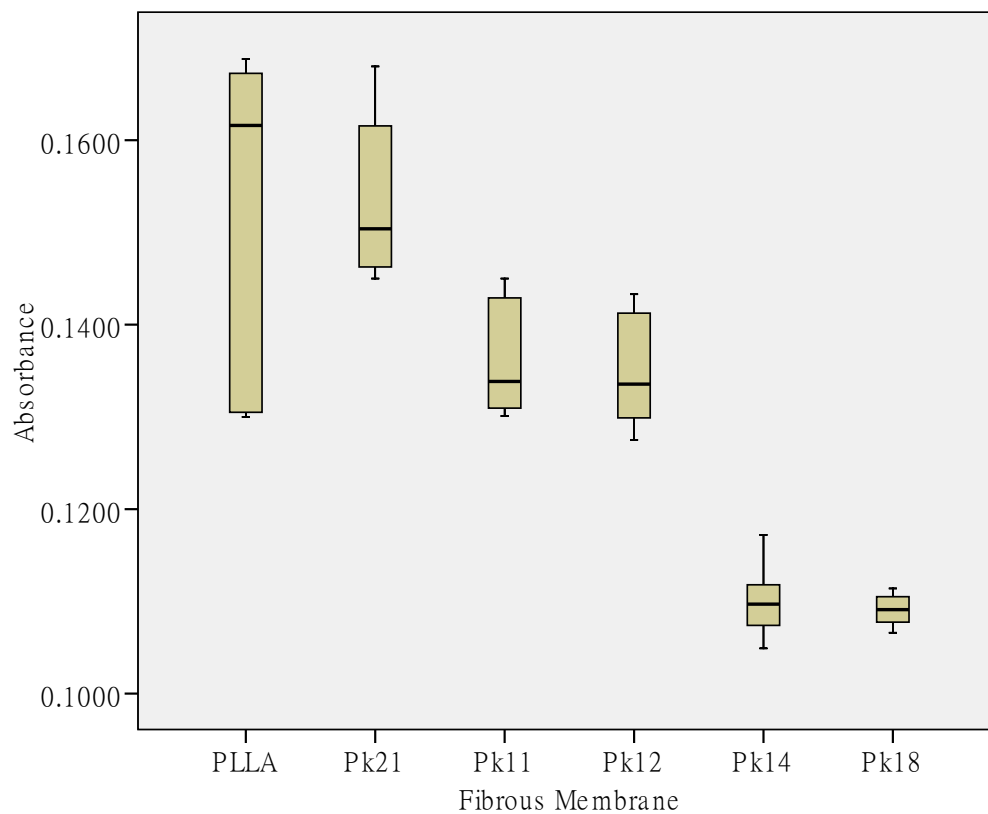


Figure 6.20 MTS assay results for cell adhesion on the PLLA and Pk fibrous membranes. Pk21 cell adhesion was significantly higher than that of the other Pk membranes and there was no significant difference between the Pk21 and PLLA membranes.

As shown in Figure 6.20, the cell adhesion of Pk21 was significantly higher than that of the other Pk membranes and there was no significant difference between the Pk21 and the PLLA membranes.

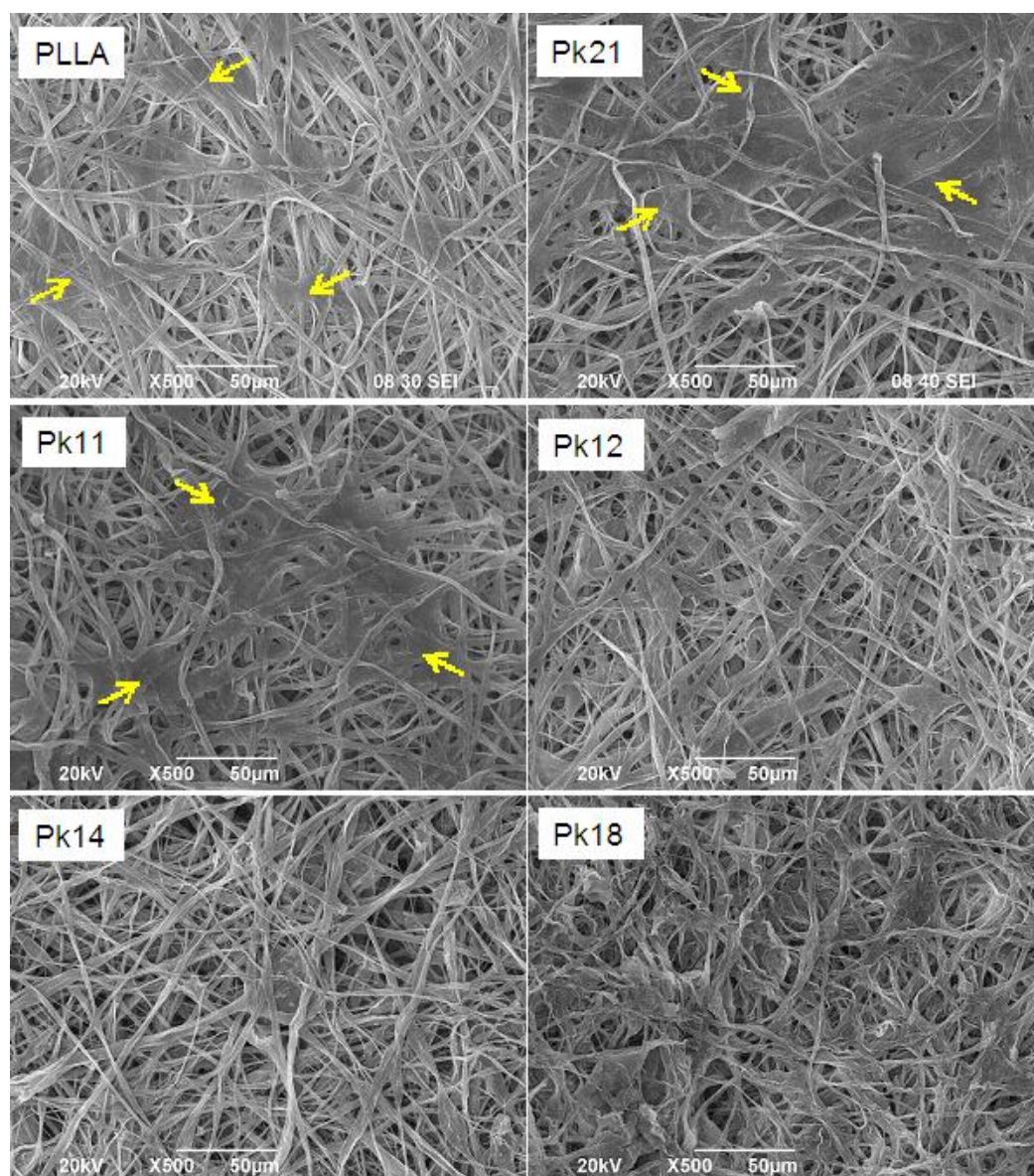


Figure 6.21 SEM images of Pk fibrous membranes with cells cultured for three days. Cells were seen stretched and spread like translucent films on the PLLA, Pk21 and Pk11 membranes (arrows); few cells were seen on the Pk12, Pk14 and Pk18 membranes.

In addition, cells were cultured on the membranes for three days to observe cell adhesion through SEM. In accord with the MTS assay results, confluent cells were seen to stretch and spread spanning across the fibers as translucent films on the PLLA, Pk21 and Pk11 membranes (Figure 6.21, yellow arrows), while confluent cells were hard to be seen on the other Pk membranes.

### 6.5.5 Discussion

In vitro cytotoxicity tests were performed using the extractions of the membranes to determine the cytotoxicity of the membranes. The Pk12, Pk14 and Pk18 membranes were found to inhibit cell proliferation. The cells cultured in the extractions of these three membranes underwent significant morphological changes, and very few cells could be seen through the inverted microscope.

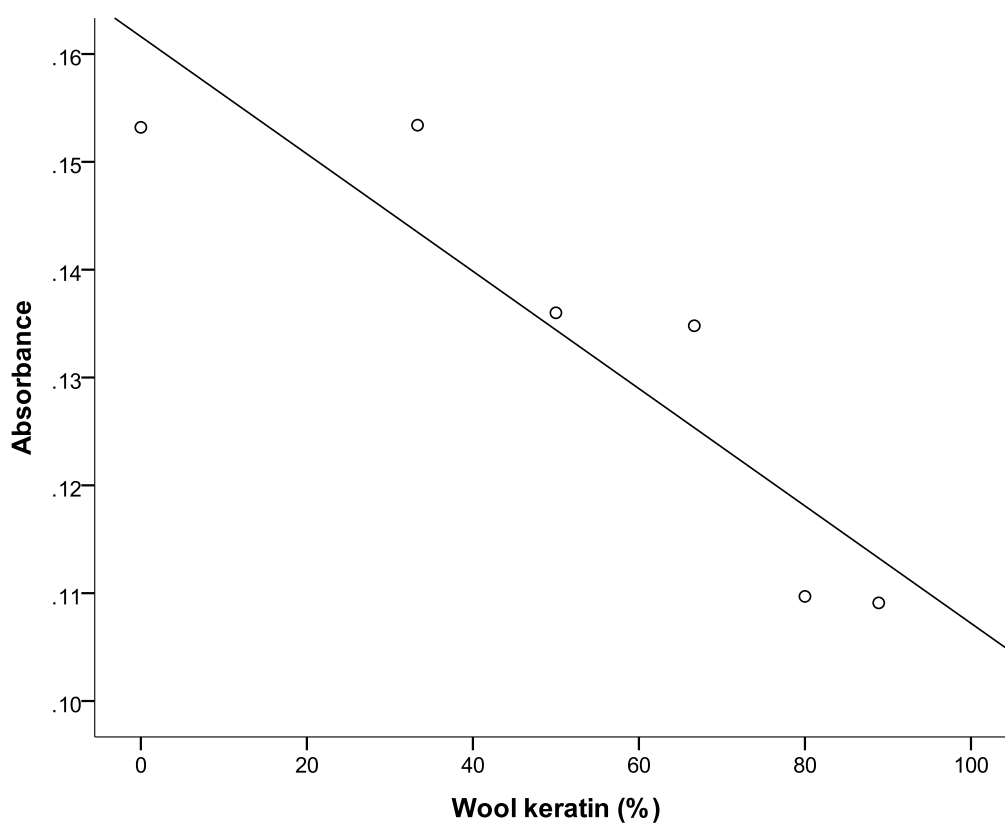


Figure 6.22 The linear relationship between the wool keratin concentration and the cell adhesion of the PLLA and Pk fibrous membranes ( $r = -0.91$ ,  $P < 0.05$ ).

As shown in Figure 6.22, the cell adhesion reduced significantly as the keratin concentration increased. Furthermore, the cell adhesion had a significant negative correlation with the keratin concentration. These findings suggested that the high concentrations of wool keratin could be cytotoxic. In addition, the cell adhesion result for the Pk21 membrane was significantly higher than that of the other Pk

membranes. Although it was not obvious, the Pk11 membrane also showed the potential for cell adhesion in the SEM images. These results implied that a wool keratin concentration higher than Pk11, would be cytotoxic.

On the other hand, according to the results shown in Chapter 4, the Pk membranes had the same contact angle values after sterilization, so, it seems that for Pk membranes, the cytotoxicity had no correlation with their hydrophilicity. However, the cytotoxicity of the Pk membranes had high correlation with some of the other properties of the scaffolds (Figures 23 to 26).

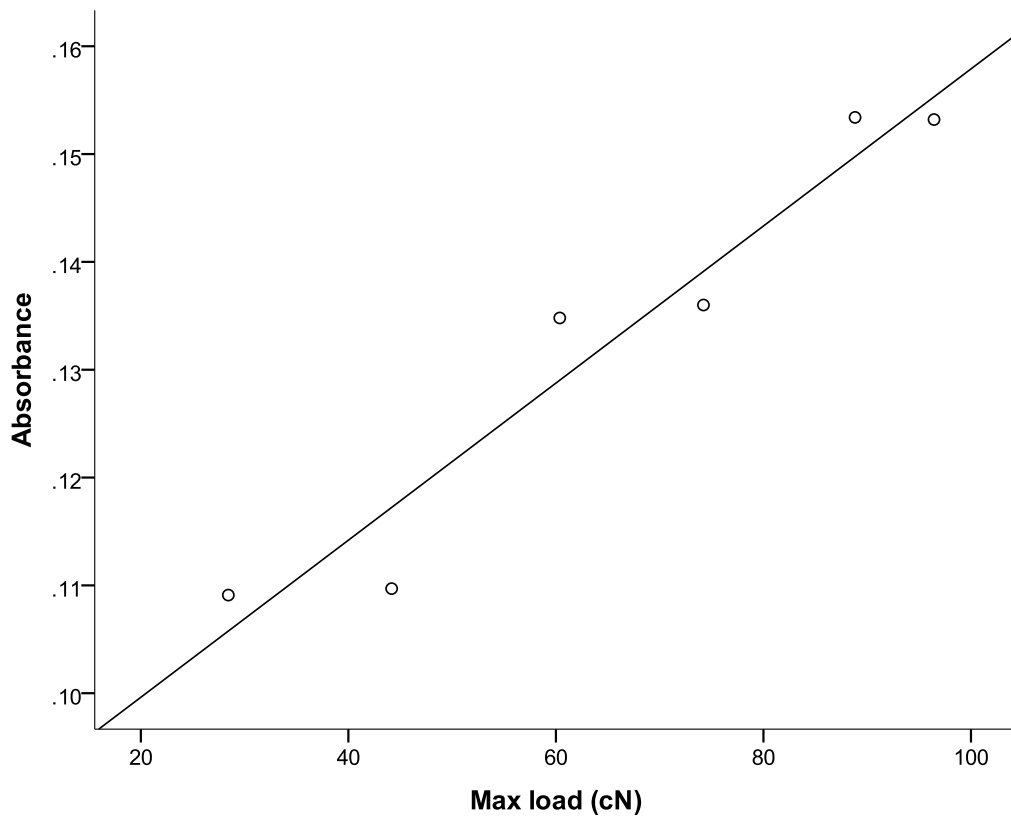


Figure 6.23 The linear relationship between the max load and the cell adhesion of the PLLA and Pk fibrous membranes ( $r = 0.97$ ,  $P < 0.05$ ).

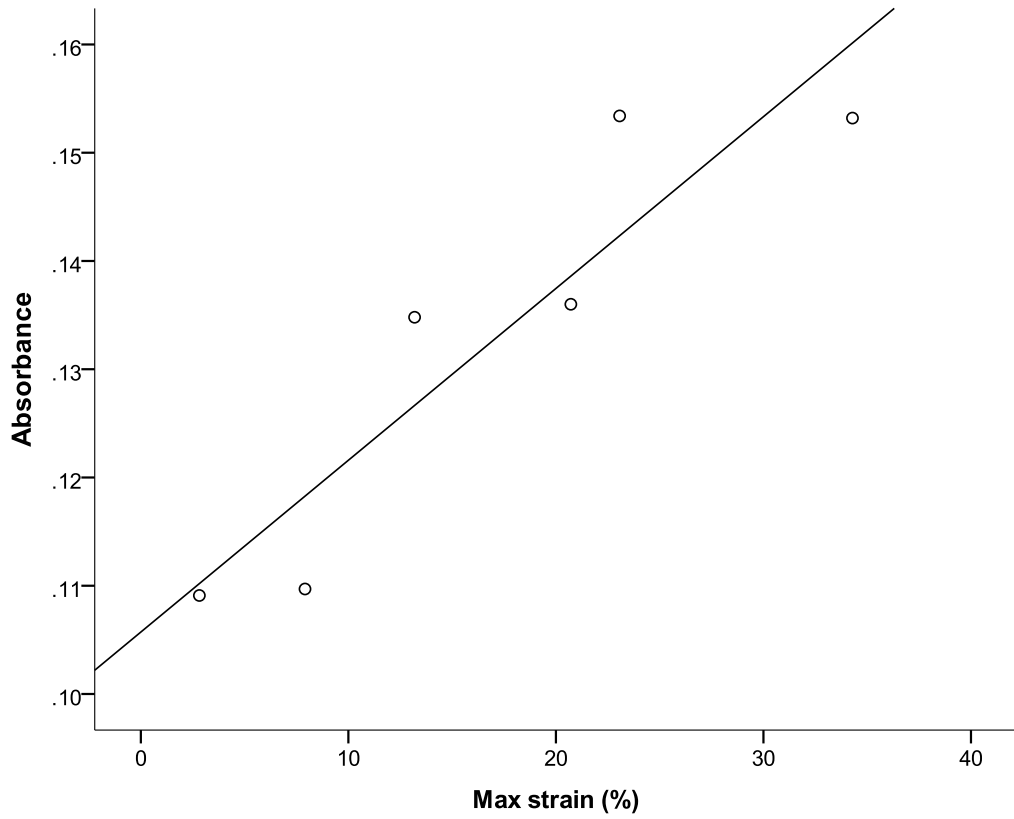


Figure 6.24 The linear relationship between the max strain and cell adhesion of the PLLA and Pk fibrous membranes ( $r = 0.92$ ,  $P < 0.05$ ).

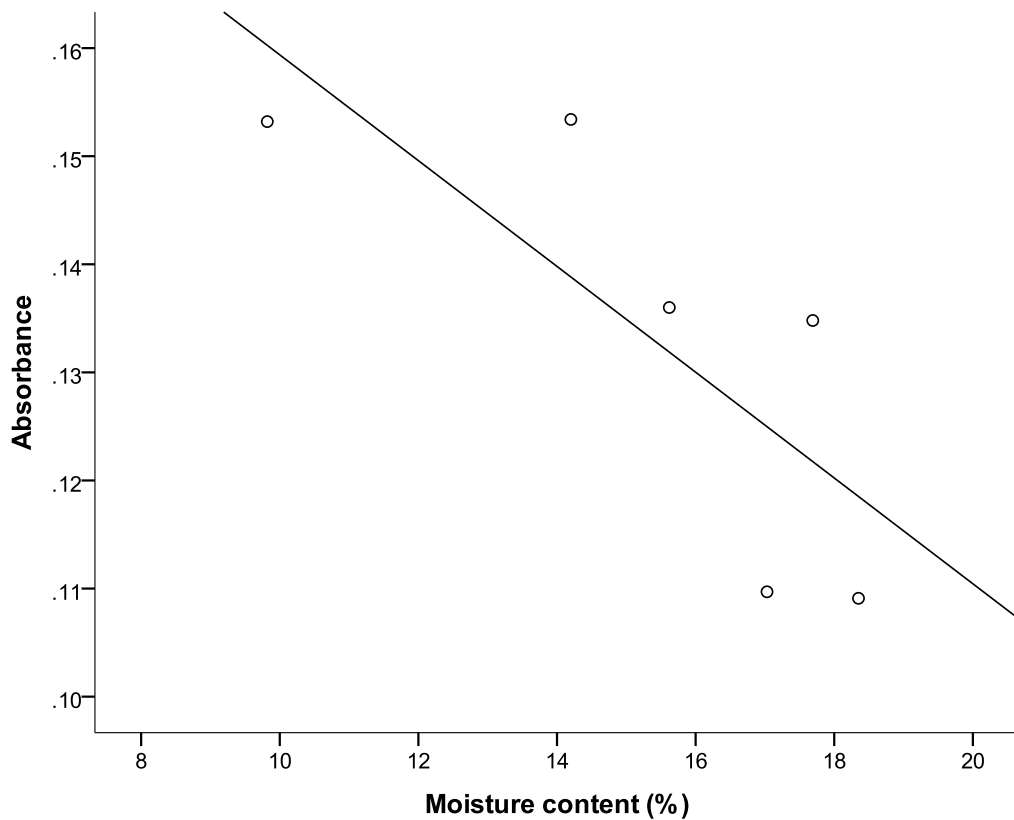


Figure 6.25 The linear relationship between the moisture content and cell adhesion of the PLLA and Pk fibrous membranes ( $r = -0.78$ ,  $P < 0.05$ ).

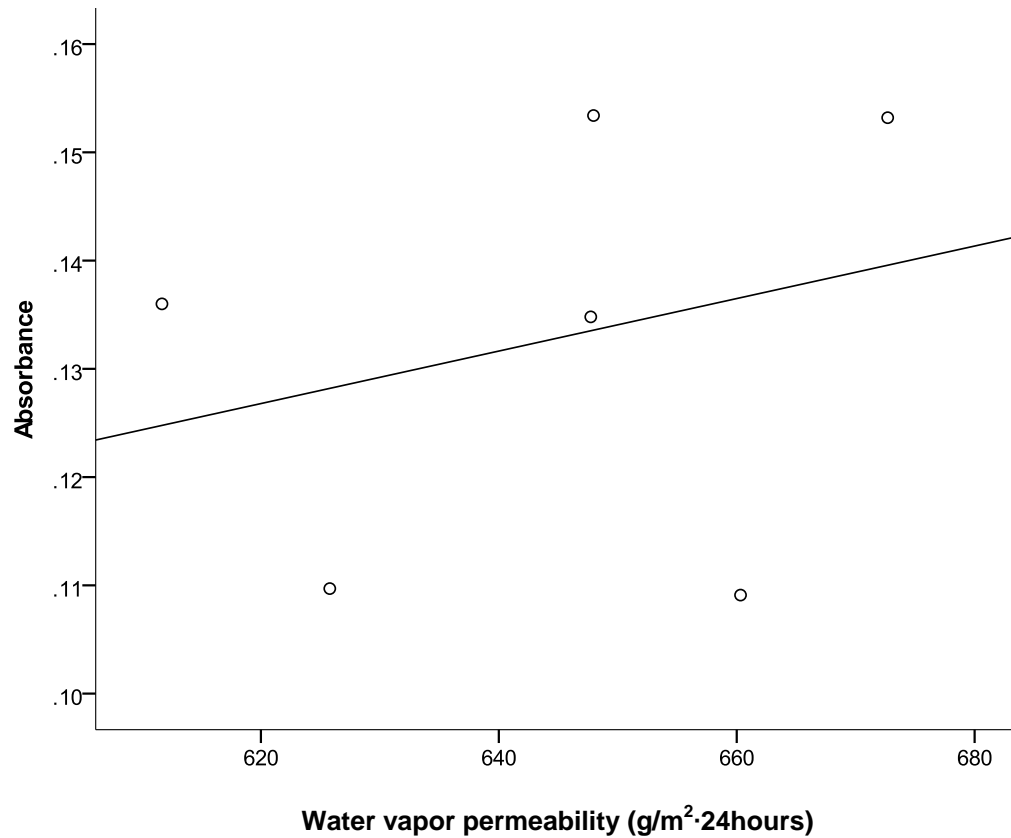


Figure 6.26 The linear relationship between the water vapor permeability and the absorbance of cell adhesion of PLLA and Pk fibrous membranes ( $r = 0.27$ ,  $P > 0.05$ ).

The values of the linear correlation coefficients between the physical properties and cell adhesion of Pk membranes are shown in Figures 6.23 to 6.26. The results showed that the cell adhesion on the Pk membranes had a strong positive linear correlation with the maximum load and maximum strain, while it had a strong negative linear correlation with moisture content. The cell adhesion of these membranes had a very weak positive correlation with water vapor permeability. These results indicated that as the tensile strength decreased or the moisture content increased, fewer cells adhered to the Pk membranes. In other words, the tensile strength and moisture content influenced the cell adhesion of Pk membranes.

McClary et al suggested that the culture surfaces could modulate cell adhesion, which would help the spread and growth of cells [McClary et al, 2000]. From the degradability experiment results in this study, it was found that, after the first three hours of degradation, more than half of the keratin particles were lost from the Pk membranes. Therefore, as the extractions of the Pk membranes were obtained after twenty four hours immersion, the extraction must have contained a considerable amount of wool keratin. This keratin might have covered a part of the culture surface, which would reduce the surface area for cell adhesion, so that the subsequent cell proliferation would be inhibited.

### **6.5.6 Conclusions**

In this Chapter, the third objective was achieved by analyzing the cytotoxicity and the relationship between the cytotoxicity and the properties of the scaffolds. According to the results, the safe concentration of wool keratin must be less than 50%. The cytotoxicity of the Pk membranes had was shown to have a strong correlation with the tensile property and moisture content of the scaffolds and that it was, basically, correlated with the wool keratin concentration. It can be concluded that the raw materials and the structure of the scaffolds are two of the main factors which affect their cytotoxicity. However, the specific mechanism of the scaffold cytotoxicity still needs to be further studied.

---

## CHAPTER 7: CELL PROLIFERATION

7.1 Ag/PLLA films .....	127
7.2 PLLA/keratin fibrous membranes.....	134

### 7.1 Ag/PLLA films

Chapter 7 aims to fulfill the fourth objective by exploring the relationship between cell proliferation and the properties and the raw material concentration of the Ag/PLLA films and Pk fibrous membranes. Cell viability is a necessary parameter for tissue engineering scaffolds and it is affected by the properties of the scaffolds. For example, polymer blending can be used to optimize material properties such as morphology, surface energy and biocompatibility, and, in turn, these properties can affect cell response [Calvert et al, 2000; Meredith et al, 2003; Washburn et al, 2004]. To explore the relationship between the cell proliferation and the properties, raw material concentration of the scaffolds, cell proliferation experiments were performed on the PLLA and Ag/PLLA films, the electrospun PLLA and the PLLA/keratin fibrous membranes.

#### 7.1.1 Cell proliferation

Human foreskin fibroblasts (HFF-1, ATCC) used in this study were maintained in Dulbecco's modified eagle's medium (DMEM) with 10% fetal bovine serum (FBS, Invitrogen, USA) in a 37°C and 5% CO<sub>2</sub> incubator. The medium was changed twice weekly. All of the films were sterilized by ultraviolet irradiation for 20min after immersion in 70% ethanol for 1 hr. Each film was seeded with  $2 \times 10^4$

cells and kept in the incubator. The number of cells was determined by MTS assay with the optical density measurement at 492nm.

### 7.1.2 Statistical analysis

Values were expressed as means  $\pm$  standard deviations. Statistical differences were determined by one-way Analysis of Variance (ANOVA). *P* values of less than 0.05 were considered to be statistically significant.

### 7.1.3 Results

In the primary study, it was found that the adhesion and the proliferation of cells on the PLLA and Ag/PLLA films were lower than that on a normal plate, and that the cells cultured on the PLLA film proliferated more than those on the Ag NP composed PLLA films after one day and seven days culture as shown in Figures 7.1 and 7.2 respectively.

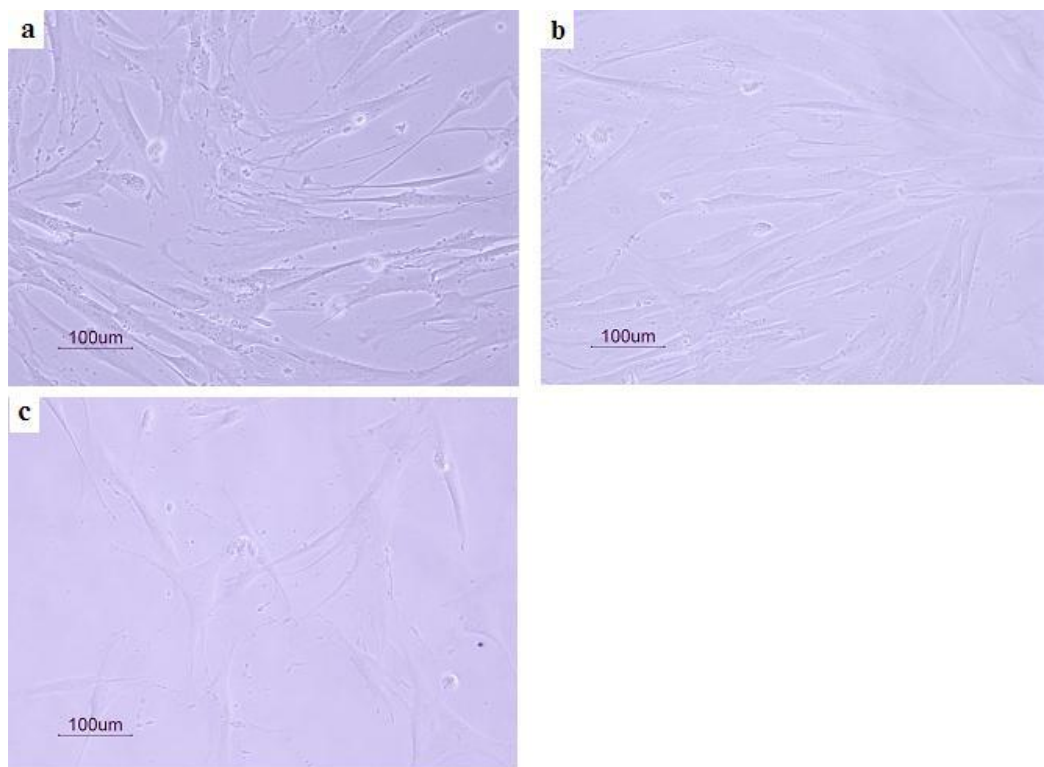


Figure 7.1 Cell adhesion after 1 day culture: (a) Normal plate; (b) PLLA film; (c) Ag/PLLA film.

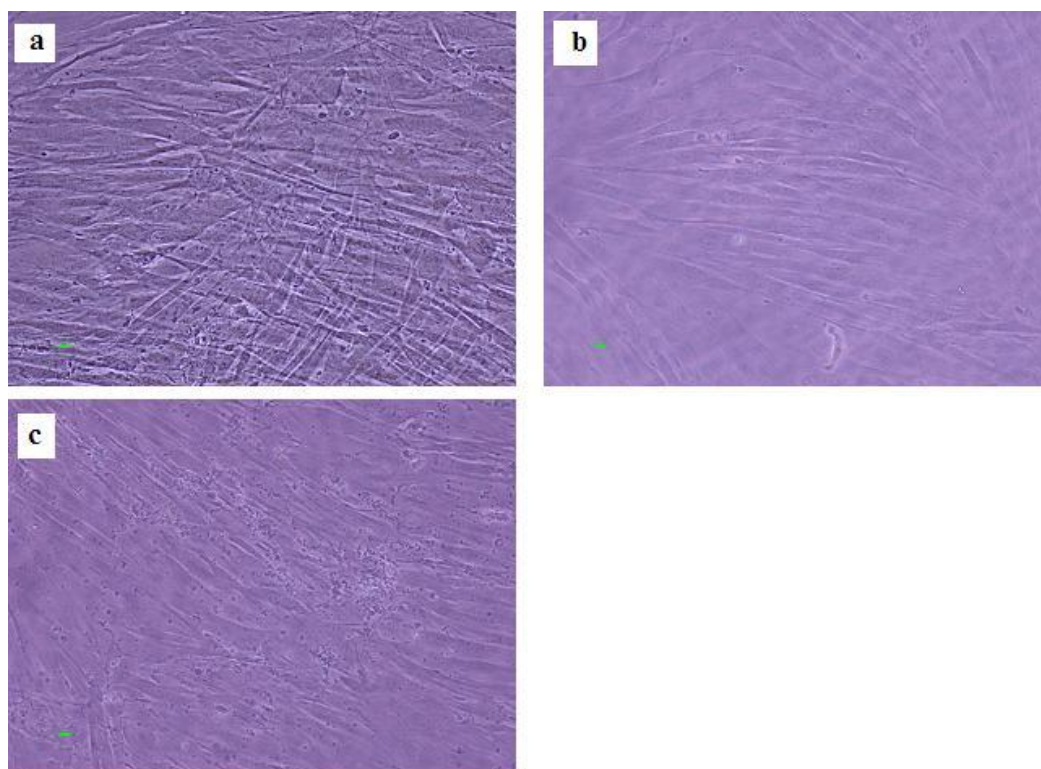


Figure 7.2 Cell proliferation after 7 days culture: (a) Normal plate; (b) PLLA film; (c) Ag/PLLA film.

After observing the above results, five different Ag NP proportions were set at 0.5% Ag/PLLA, 2.5% Ag/PLLA, 5% Ag/PLLA, 7.5% Ag/PLLA and 10% Ag/PLLA (w/w) for the subsequent experiments. Then, cell proliferation experiments were conducted on these films using MTS assay.

A cell proliferation assay was applied to indicate the number of living cells on the films. Following the seeding of  $2 \times 10^4$  cells on each film, the cell number increased with time. After five days of cell culture on the Ag/PLLA films, the cells reached confluence.

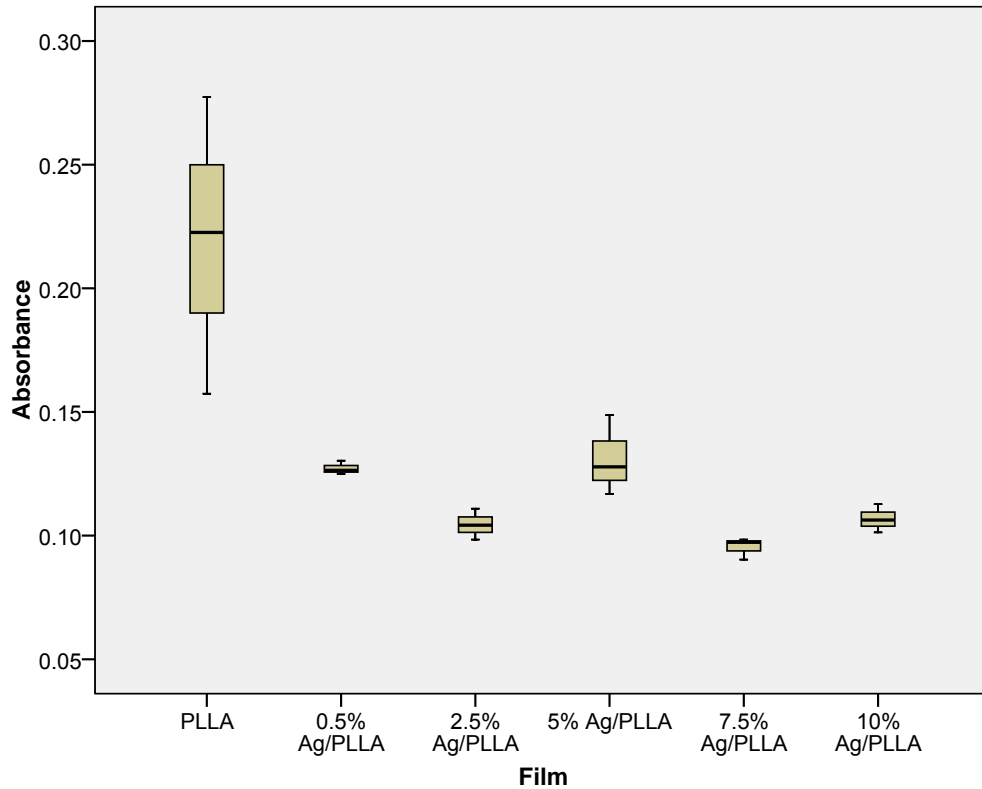


Figure 7.3 Effects of Ag/PLLA films on cell proliferation. Cell proliferation was assessed with MTS reagent and measurement of absorbance at 492nm. The 5% Ag/PLLA film showed slightly higher cell proliferation compared to the other Ag/PLLA films, but there were no significant differences ( $P>0.05$ ).

It can be seen from Figure 7.3 that the cell proliferation was different when the cells were cultured on the PLLA and the Ag/PLLA films; the cell proliferation on the PLLA film was significantly higher than that on the Ag/PLLA films, but there were no significant differences between the 0.5%, 2.5%, 5%, 7.5% and 10% Ag/PLLA films.

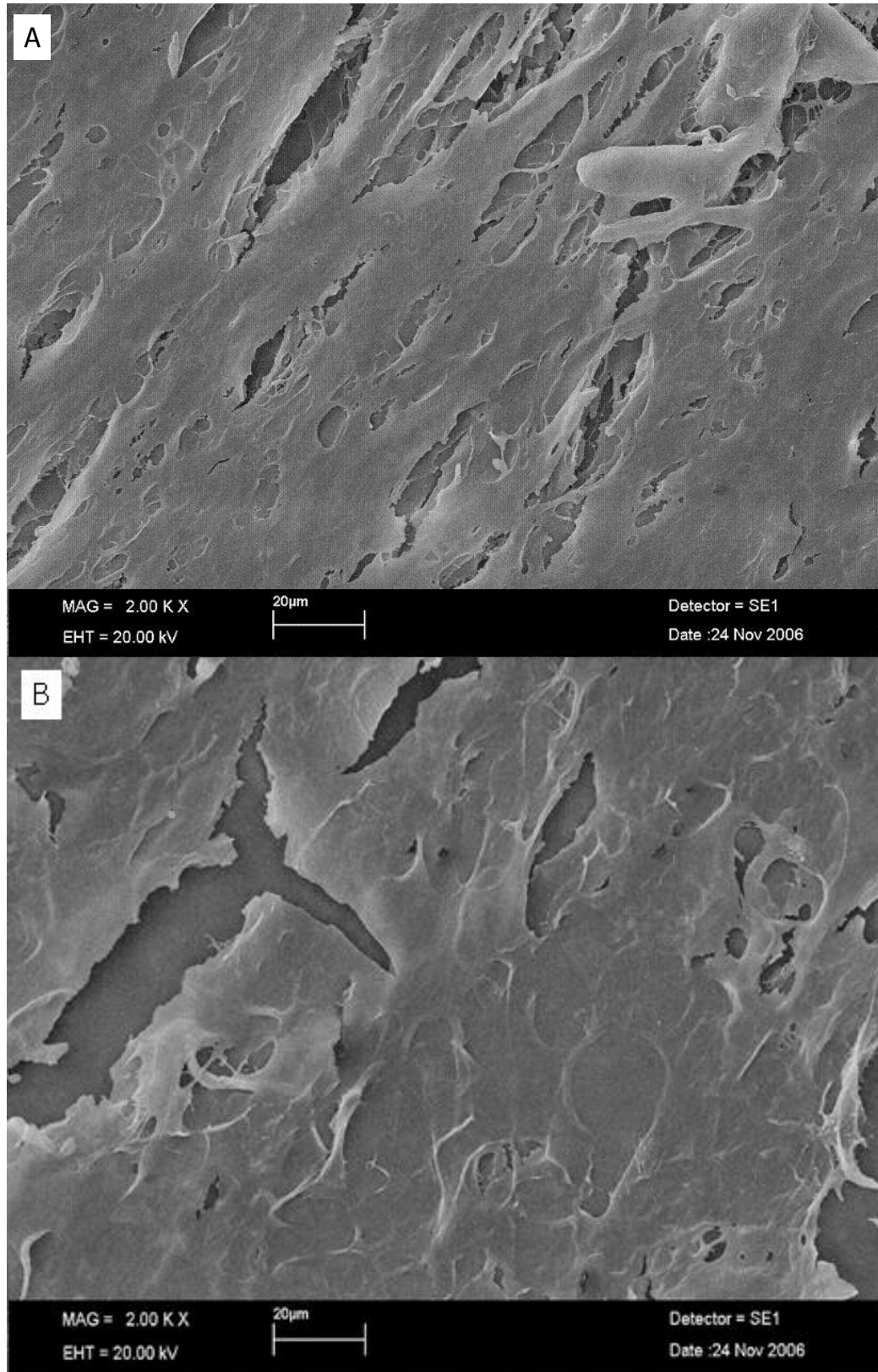


Figure 7.4 SEM images of cell layers on different films after 14 days of culture. Cells already covered the whole films with several layers. (A) PLLA film; (B) 5%Ag/PLLA film.

After 14 days of cell culture, the cells completely covered the films with several layers as the SEM images in Figure 7.4 show. Because there was no significant difference between each Ag/PLLA film, here only the 5% Ag/PLLA film was selected for comparison with the PLLA film. From the images in Figure 7.4, it is evident that the cells had already grown confluent together, and formed several layers, not only on the PLLA film, but also on the Ag/PLLA films. This result implied that although the cell proliferation on the PLLA film was significantly higher than that on the Ag/PLLA films the cells still could be proliferated on the Ag/PLLA membranes.

#### **7.1.4 Discussion**

According to the cytotoxicity test results for the Ag NPs presented in Chapter 6, it is easy to understand that the lower the proportion of Ag NPs to PLLA, the less cytotoxic will be for the Ag/PLLA films. Accordingly, those Ag/PLLA films with an appropriate level of Ag NPs content will be good candidate matrices for tissue engineering. Since the Ag NPs have an antibacterial property, this result implied that the Ag/PLLA films had the potential to be used as non-cytotoxic antibacterial scaffolds for tissue engineering.

Simon et al (2005) did cell proliferation on poly (L-lactic acid)/poly (D, L-lactic acid) blends and found that the proliferation was faster on the smooth, PDLLA-rich end of the gradients rather than on the rough, PLLA-rich end of the gradients. As described in Chapter 4, the main feature of the film surface was its lumpiness = the more the Ag concentration, the lumpier it was. So, the cell

proliferation results shown here might indicate that the cells had a tendency to grow on the smoother surface films with the lower Ag content.

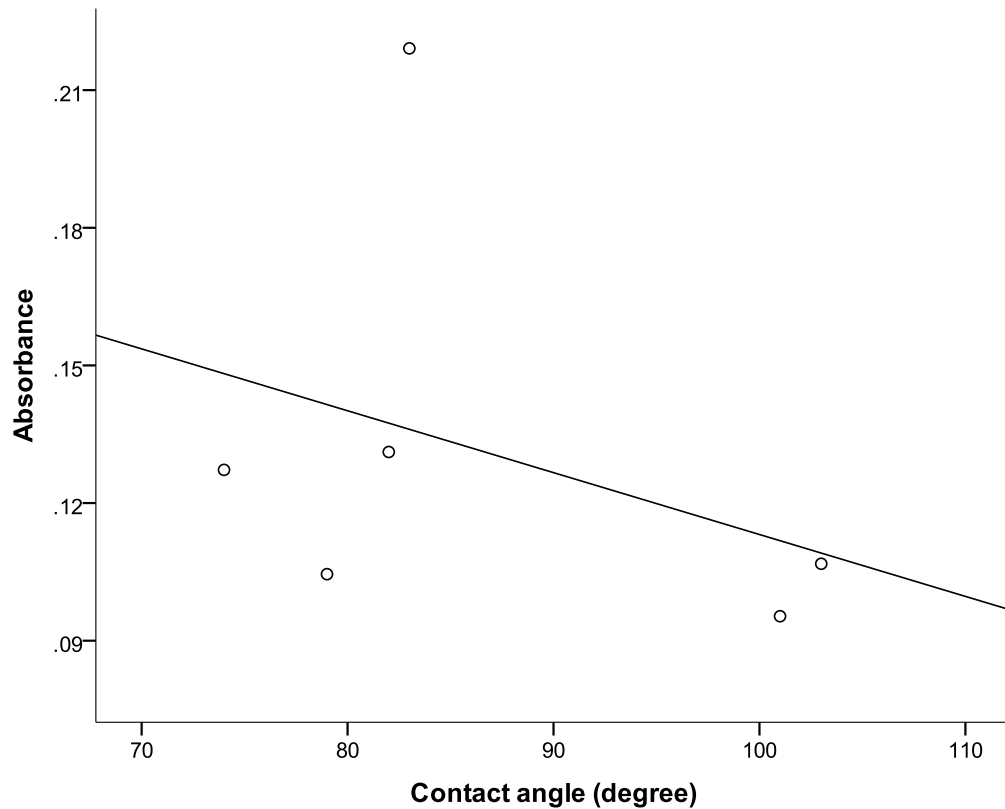


Figure 7.5 The relationship between the contact angle values and the absorbance of cell proliferation in the extractions of the PLLA and Ag/PLLA films ( $r = -0.36$ ,  $P > 0.05$ ).

Furthermore, as shown in Figure 7.5, the correlation coefficient between the contact angle and cell proliferation of the films was  $-0.36$ . This data indicated that the cell proliferation and hydrophilicity of the Ag/PLLA films might have had a negative correlation, although it was not significant.

However, the film structure may not be very suitable as a skin tissue substitute. In contrast, the fibrous structure, which consisted of many fibers, had a larger surface area and more pores than the films. Consequently, Ag/PLLA scaffolds with a fibrous structure may be more suitable for cell proliferation. Thus, more cell

proliferation and other detailed experiments should be performed on the Ag/PLLA fibrous membranes.

### **7.1.5 Conclusions**

This part partially achieved the fourth objective by examining the cell proliferation of the Ag/PLLA films. This study examined the effects of the level of Ag concentration of the Ag/PLLA films on cell proliferation. On the basis of the experimental observations, it can be concluded that the concentration of Ag NPs and the contact angle of Ag/PLLA films affected the cell proliferation on the scaffolds. The optimal proportion of Ag NPs and PLLA for non-cytotoxic should be lower than 5% (w/w).

## **7.2 PLLA/keratin fibrous membranes**

Where the resulting harvest site (donor site) wounds have only partial thickness, the basal cells lining the skin adnexal glands remain in place and repopulate the epidermis over a time period of 7 to 28 days to achieve wound closure [Orgill et al, 2005], so, in the cell proliferation experiments, the cells were cultured on each fibrous membrane for 21 days.

As a rich source of protein, wool keratin has been reported as being suitable for long-term cell cultivation with a high cell density [Tachibana et al, 2002]. Therefore, in this study, PLLA was combined with wool keratin particles (PLLA/keratin) which were expected to improve the cell proliferation. Cell culture experiments were undertaken to assess the effects of the PLLA/keratin composite fibrous scaffolds on cell proliferation.

### **7.2.1 Cell Proliferation**

Osteoblasts (MC3T3, ATCC) used in this study were maintained in Dulbecco's Modified Eagle's Medium (DMEM) with 10% fetal bovine serum (FBS, Invitrogen, USA) in a 37°C and 5% CO<sub>2</sub> incubator. The medium was replaced twice weekly. All of the membranes were sterilized by ultraviolet irradiation for 20 minutes after being immersed in 70% ethanol for 1 hour. Each membrane was seeded with  $2 \times 10^4$  cells and kept in the incubator. MTS assay was employed to assess the cell proliferation.

### **7.2.2 Scanning Electron Microscopy**

Electrospun nanofibrous structures were coated with gold and then their morphologies were observed by SEM (LEICA, Stereoscan 440, 20kV).

### **7.2.3 Statistical Analyses**

Values were expressed as means and standard deviations. Statistical differences were determined by one-way ANOVA. *P* values of less than 0.05 were considered to be statistically significant.

### **7.2.4 Results**

Cell proliferation experiments were performed on the electrospun PLLA and PLLA/keratin fibrous membranes using osteoblasts. The level of cell proliferation was observed by SEM after the cells had been cultured for 3 days (3d), 7 days (7d), 14 days (14d) and 21 days (21d) respectively. SEM images of the PLLA and PLLA/keratin fibrous scaffolds with the cultured cells are shown in Figures 7.6 to 7.11.

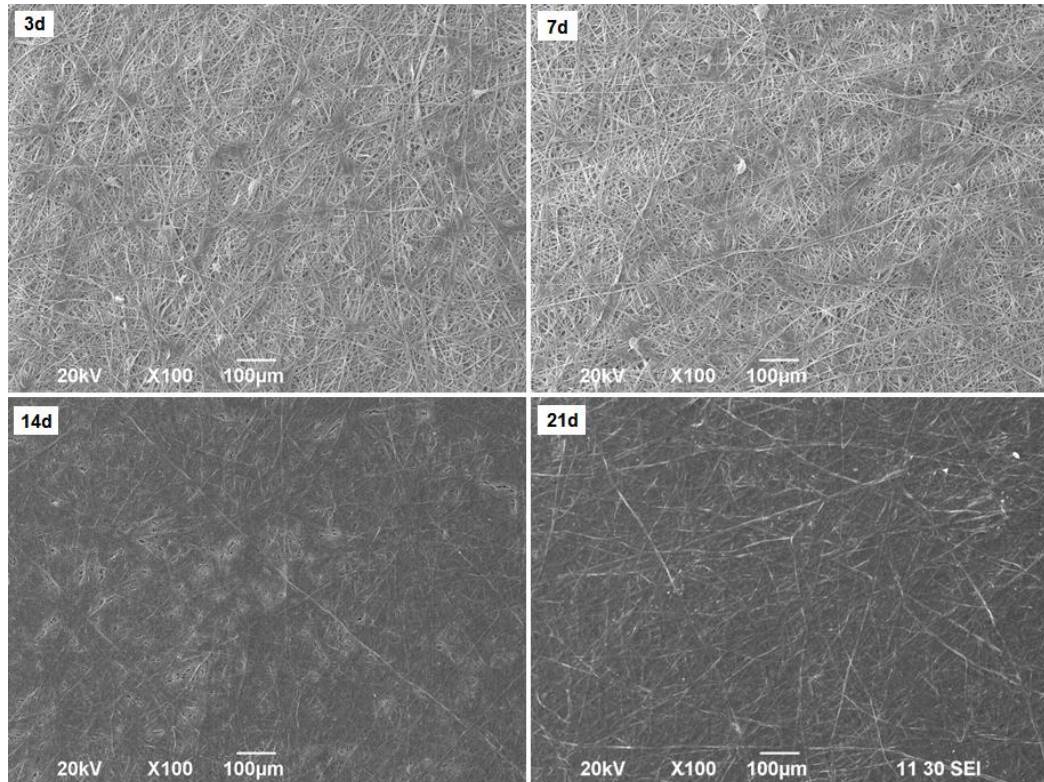


Figure 7.6 SEM images of cells cultured on the PLLA fibrous membrane for 3d, 7d, 14d and 21d. The cells highly proliferated until 21d and covered the whole membrane.

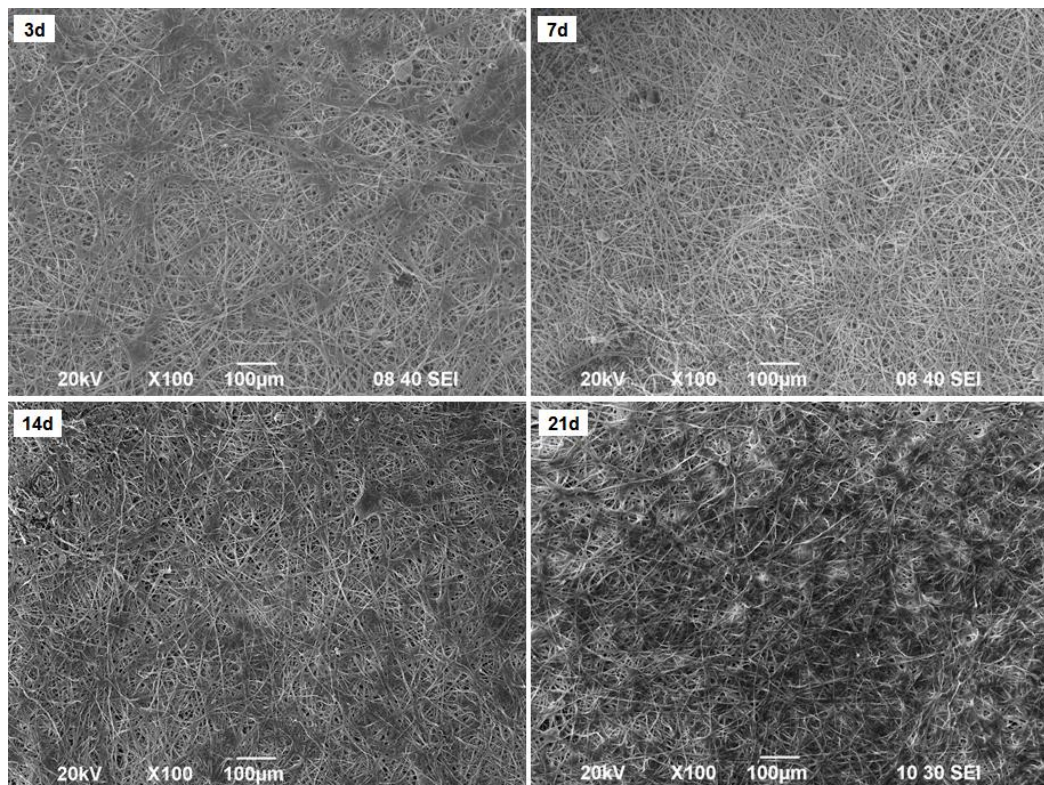


Figure 7.7 SEM images of cells cultured on the Pk21 fibrous membrane for 3d, 7d, 14d and 21d. Cells had obviously proliferated at 21d and were observed on almost the whole membrane.

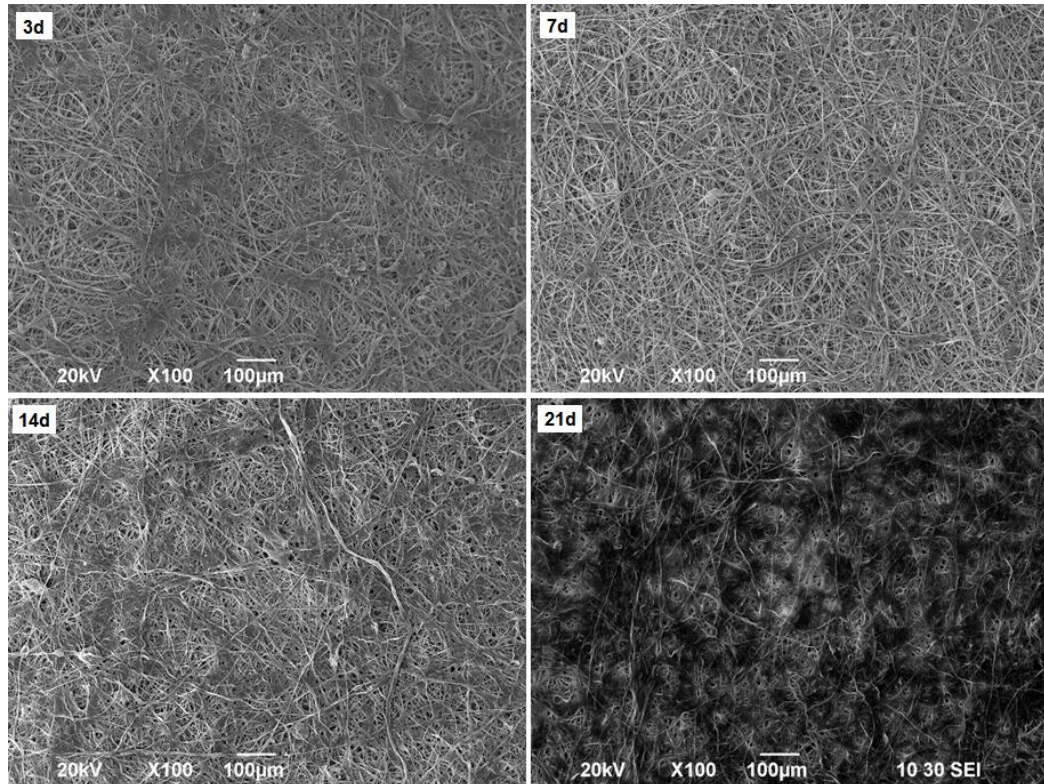


Figure 7.8 SEM images of cells cultured on the Pk11 fibrous membrane for 3d, 7d, 14d and 21d. Cells had obviously proliferated at 21d and were observed on almost the whole membrane.

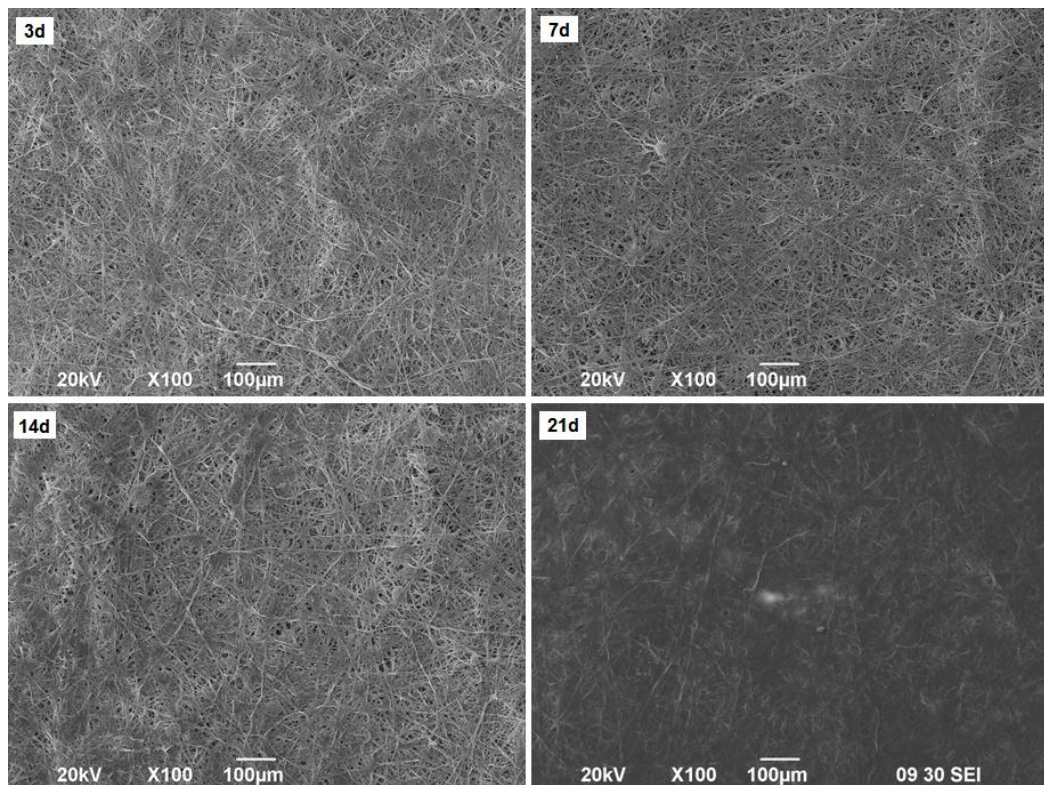


Figure 7.9 SEM images of cells cultured on the Pk12 fibrous membrane for 3d, 7d, 14d and 21d. Cells proliferated gradually and covered almost the whole membrane at 21d.

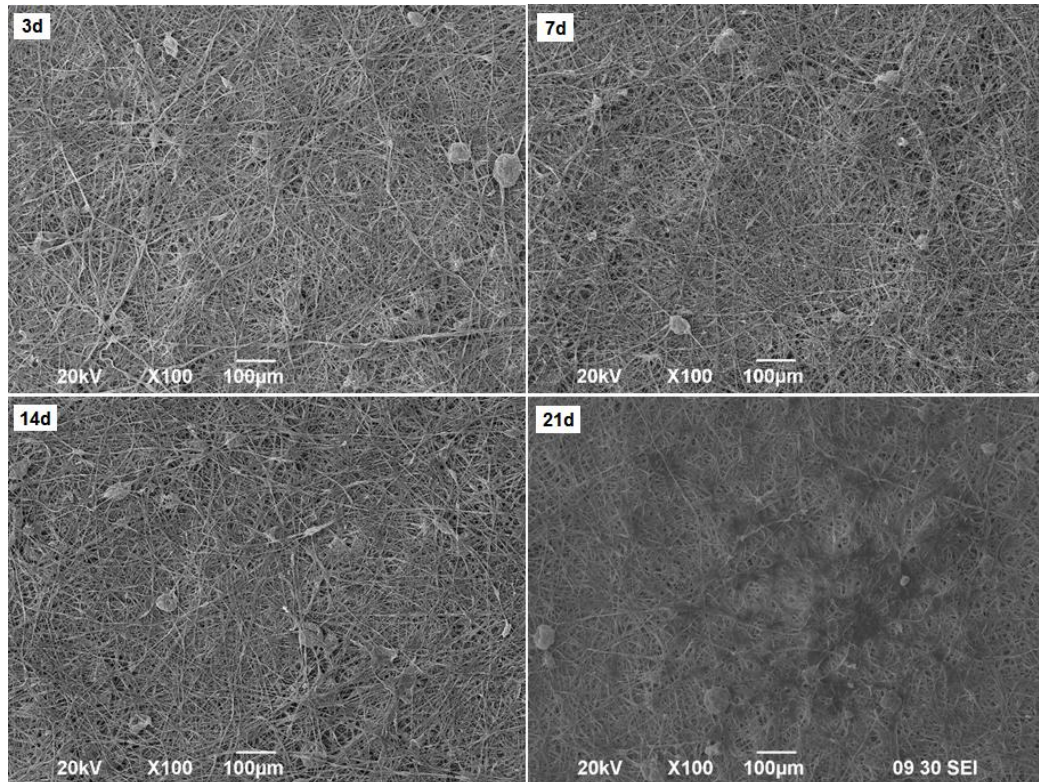


Figure 7.10 SEM images of cells cultured on the Pk14 fibrous membrane for 3d, 7d, 14d and 21d. The proliferation of cells was hardly observed until 14d, only some confluent cells could be observed on the membrane after 21d.

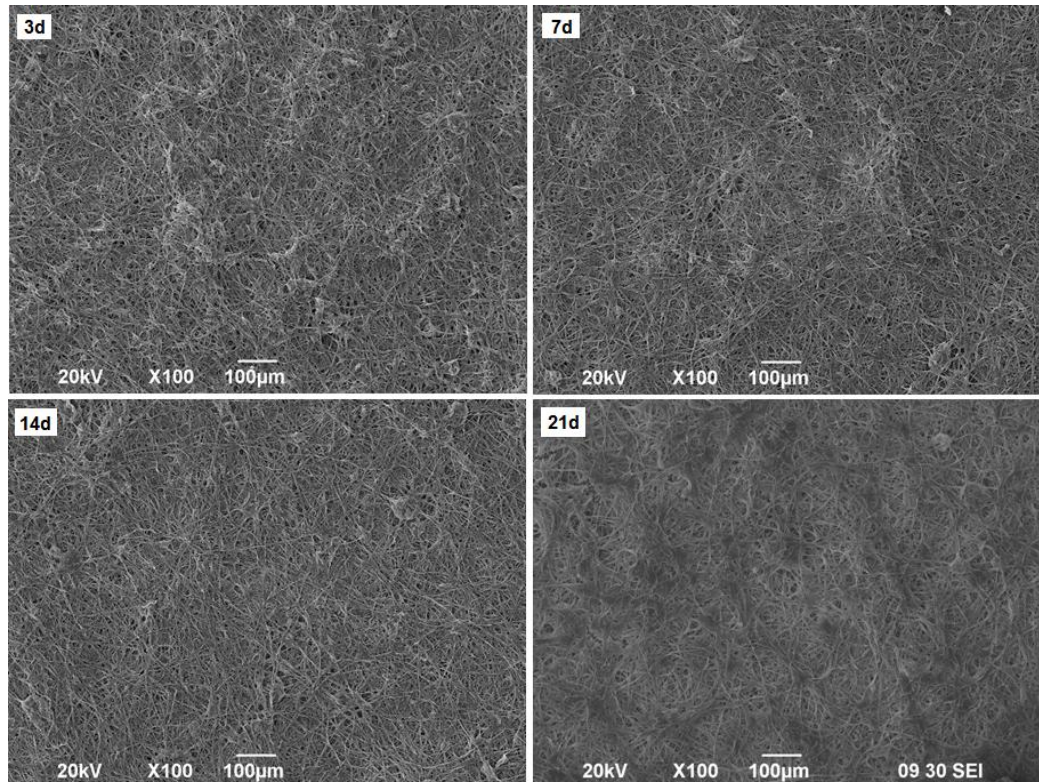


Figure 7.11 SEM images of cells cultured on the Pk18 fibrous membrane for 3d, 7d, 14d and 21d. The proliferation of cells was hardly observed until 14d, only some confluent cells could be observed scattered on the membrane after 21d.

From the Figures above, cells were found to have grown on both the PLLA and PLLA/keratin fibrous membranes. Cells were cultured for 3d, 7d, 14d and 21d respectively. Cells proliferated gradually on the PLLA, Pk21, Pk11 and Pk12 fibrous membranes. Whereas on the Pk14 and Pk18 membranes, scattered cells could be seen only after 21d culture. To derive more information about the cell proliferation on the membranes, the cells were observed under 5000 $\times$  magnification (Figure 7.12).

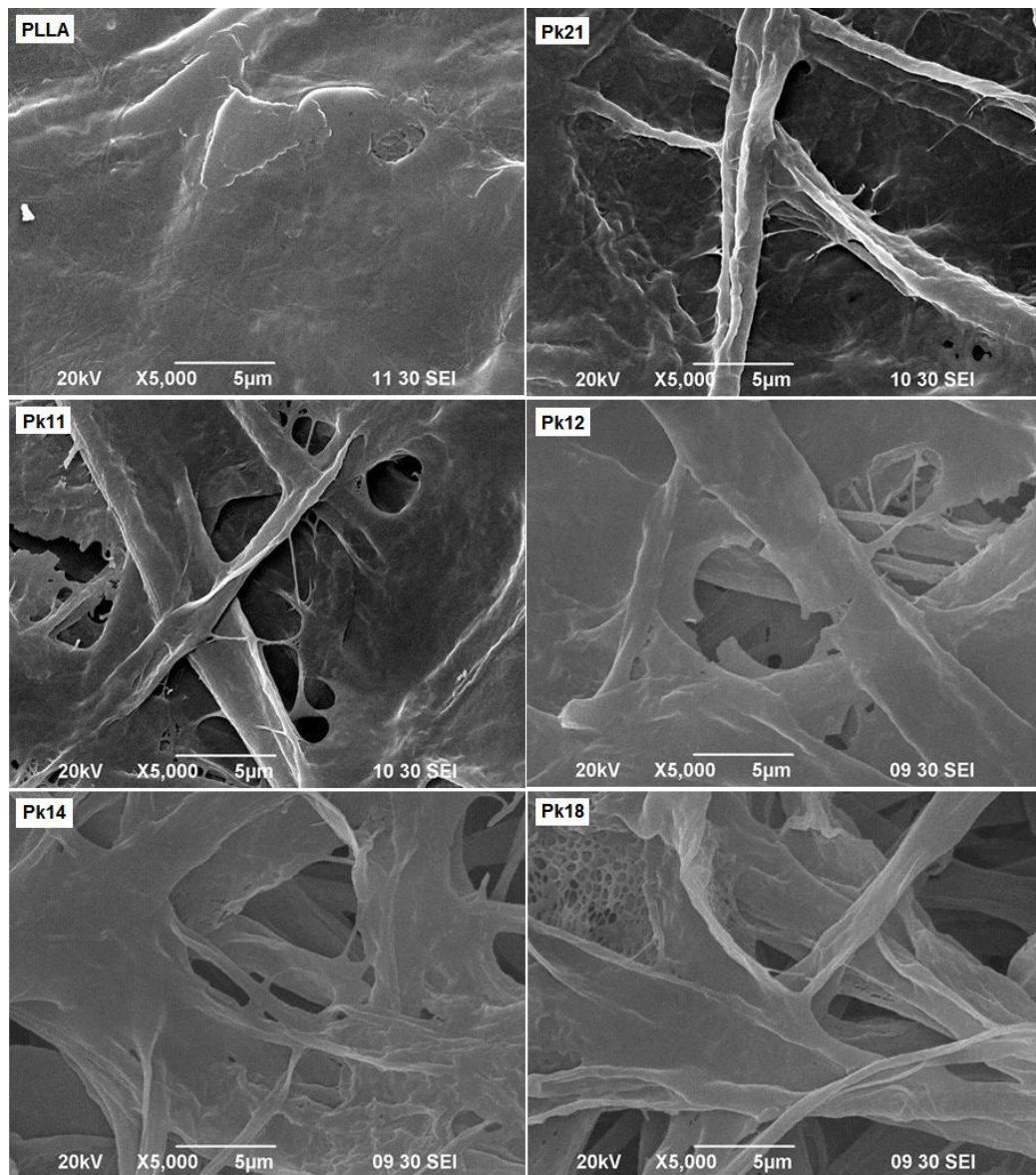


Figure 7.12 SEM images of cells cultured on the PLLA and Pk fibrous membranes for 21d observed under 5000 $\times$  magnification.

Cell proliferation on the PLLA and PLLA/keratin fibrous membranes was simultaneously tested by applying MTS assay (Figure 7.13).

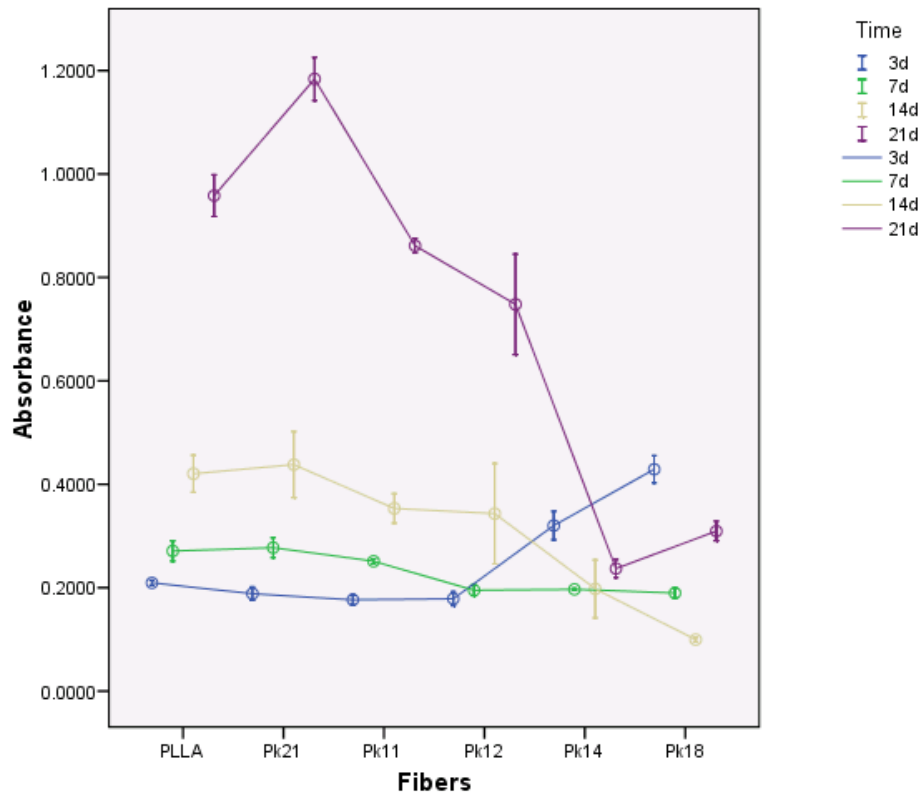


Figure 7.13 MTS assay results for the cell proliferation on the PLLA and Pk fibrous membranes.

As shown in Figure 7.12, after 3 days of culture, the proliferation of cells on the PLLA fibrous scaffolds was slightly higher than that on the PLLA/keratin fibrous scaffolds at the ratios ranging from 2:1 to 1:2, while it was significantly lower than the proliferation on the PLLA/keratin at ratios of 1:4 and 1:8. However, from the 7 day culture, the cell proliferation on the Pk21, Pk11 and Pk12 membranes started to increase, especially in the case of Pk21. After 21 days, the cell proliferation on the Pk14 and Pk18 membranes was higher than the proliferation after 14 days but much lower than the proliferation for the PK11, 12 and 21 the PLLA membranes. , whereas, the cell proliferation on the Pk21 membrane

improved rapidly, and became significantly higher than that on the PLLA. These results suggested that the concentration of wool keratin particles influenced the cell proliferation, particularly after 21 days,

### **7.2.5 Discussion**

Wool keratin, a source of natural proteins, can provide stable structures for cell cultivation [Tachibana et al, 2002]. Keratin films can also provide a good matrix for cell rapid adhesion, spreading and proliferation [Yamauchi et al, 1996]. This result also depended on the proportion of wool keratin in the PLLA/keratin composed fibrous membranes. Another study also found that the Pk membranes improved cell proliferation significantly [Li et al, 2008].

In this study, as the keratin content increased, after 21 days of culturing, the cell proliferation decreased significantly, especially on the Pk14 and Pk18 membranes, while Pk21 indicated the highest cell proliferation compared with PLLA and the other Pk membranes. According to the results discussed in Chapter 6, it may be suggested that the cytotoxicity of the materials should be an important factor that may affect the cell proliferation. Although wool keratin can contribute to support cell proliferation, it needs to be applied in the proper concentration in the composite matrix to be safe for cell culture.

On the other hand, as the proportion of keratin particles increased, more beads formed along the PLLA fibers, which made the surface of the membranes rougher. Since the cells preferred the smoother surface of Ag/PLLA films, the same phenomenon may occur on the Pk membranes. Thus, the roughness of the Pk fibrous membranes may be another factor to affect the cell proliferation. Different results were obtained from the correlation analysis between the properties and the

cell proliferation for 3days, 7days, 14days, and 21days respectively. It was found that the results for the groups after three days were just the opposite to those of the groups for the other durations of culturing. So, in the following Figures (Figures 7.14 to 7.19), the relationship between the properties and cell proliferation of the different membranes over three and fourteen days culture time will be discussed.

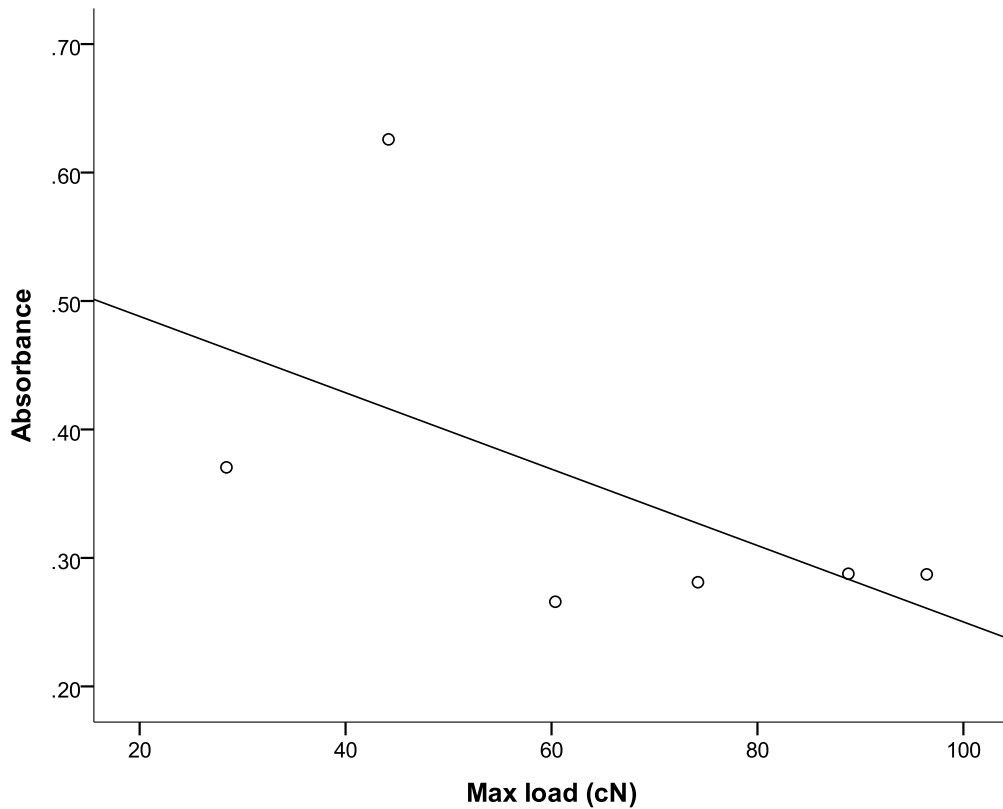


Figure 7.14 The relationship between the maximum load and the 3 days cell proliferation of the PLLA and Pk fibrous membranes ( $r = -0.56$ ,  $P > 0.05$ ).

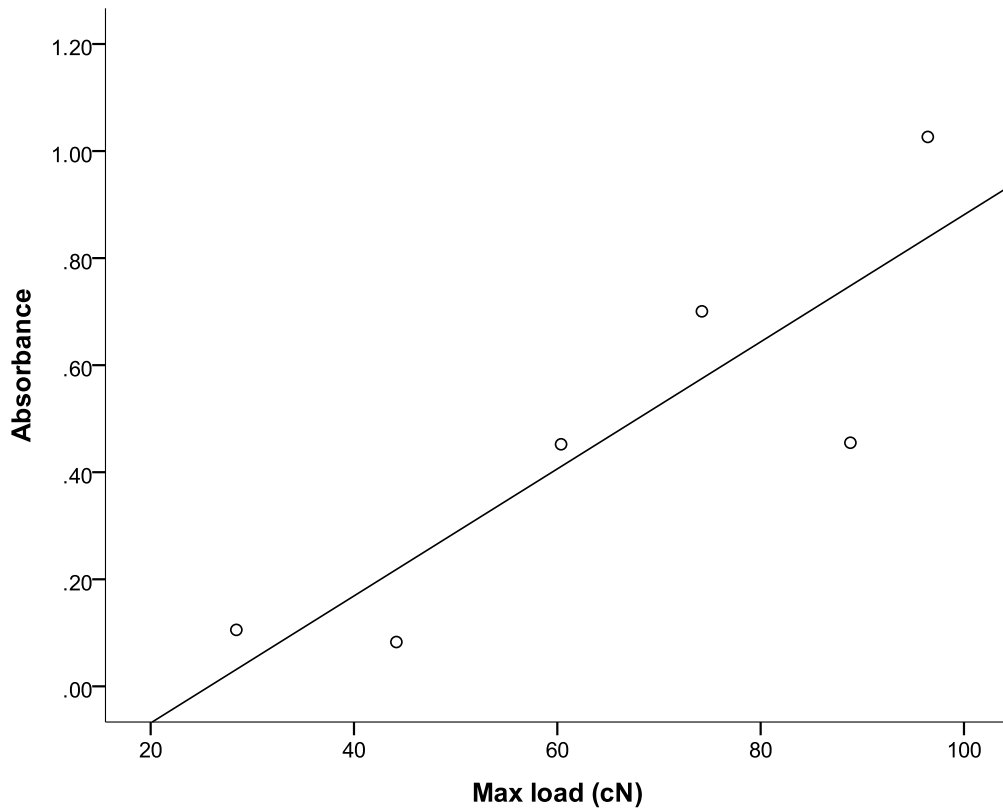


Figure 7.15 The linear relationship between the max load and the 14 days cell proliferation of the PLLA and Pk fibrous membranes ( $r = 0.87$ ,  $P < 0.05$ ).

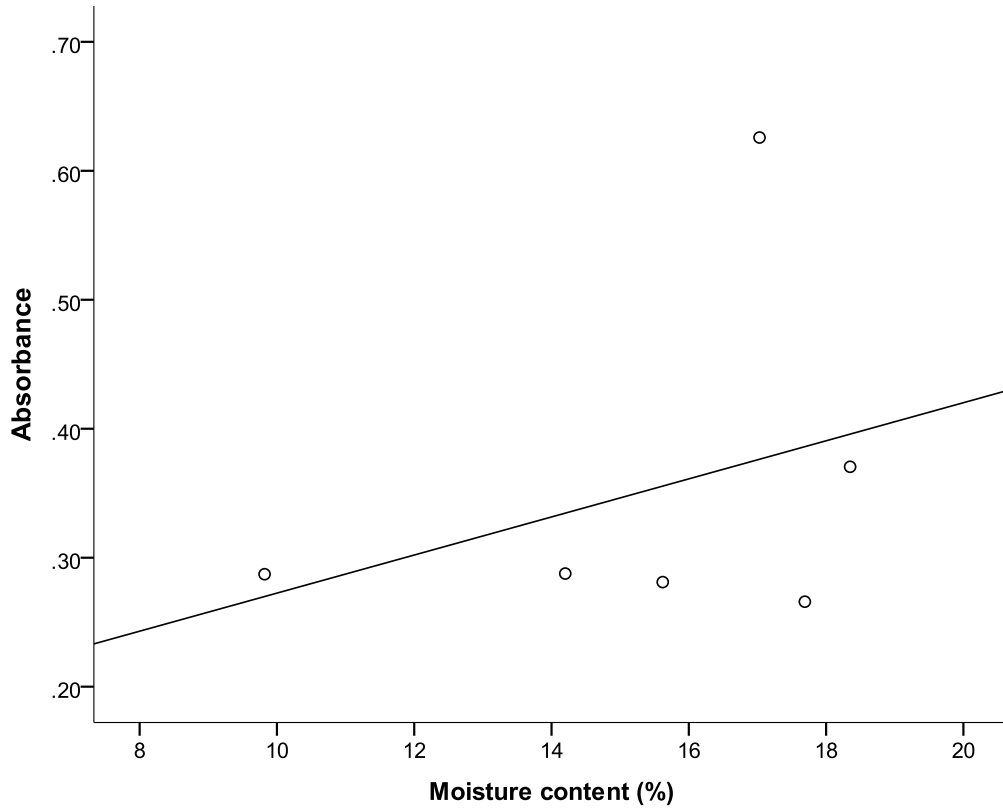


Figure 7.16 The relationship between the moisture content and the 3 days cell proliferation of the PLLA and Pk fibrous membranes ( $r = 0.33$ ,  $P > 0.05$ ).

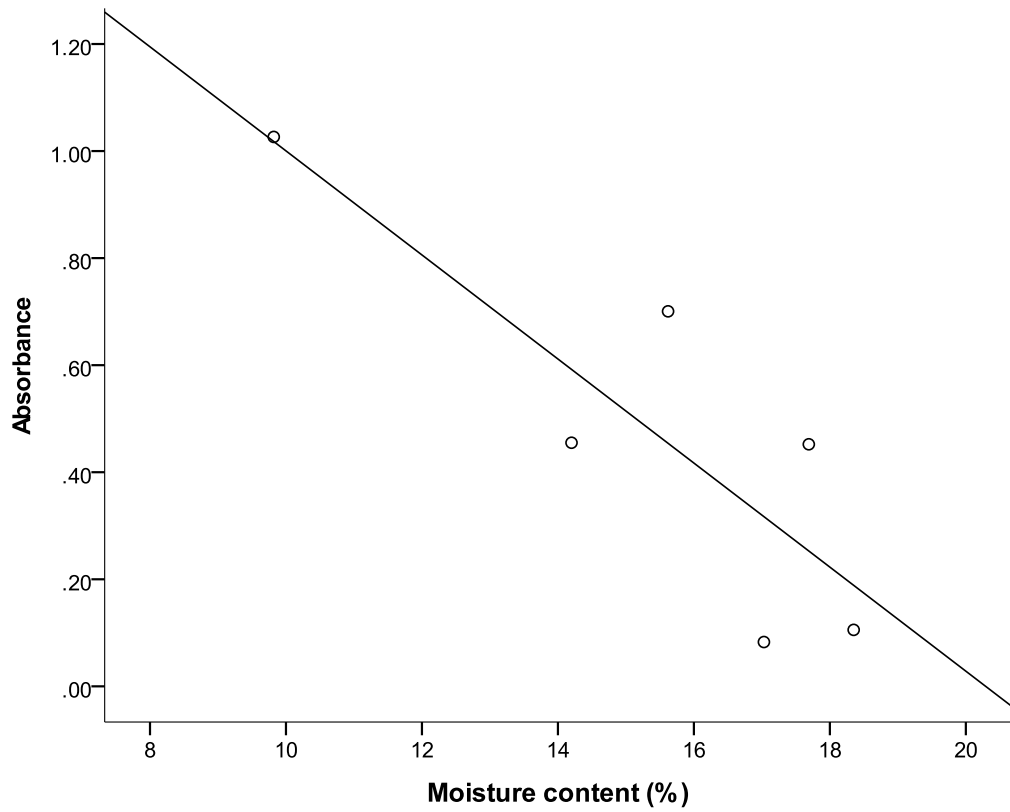


Figure 7.17 The linear relationship between the moisture content and the 14 days cell proliferation of the PLLA and Pk fibrous membranes ( $r = -0.85$ ,  $P < 0.05$ ).

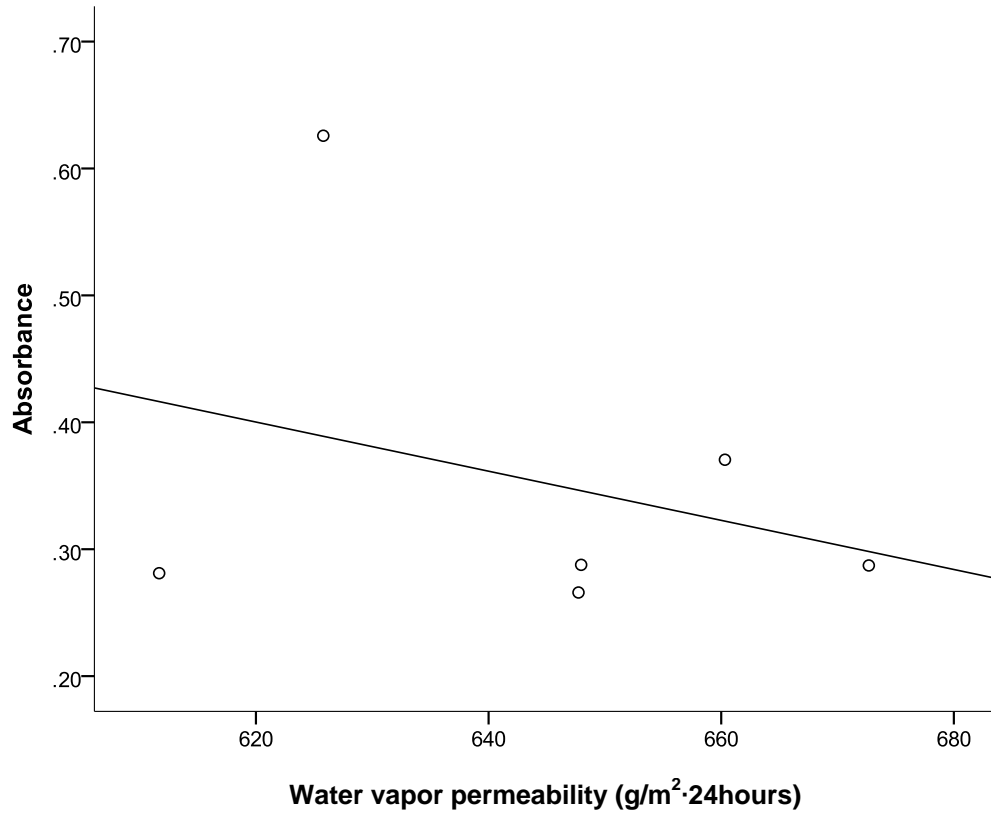


Figure 7.18 The relationship between the water vapor permeability and the 3 days cell proliferation of the PLLA and Pk fibrous membranes ( $r = -0.31$ ,  $P > 0.05$ ).

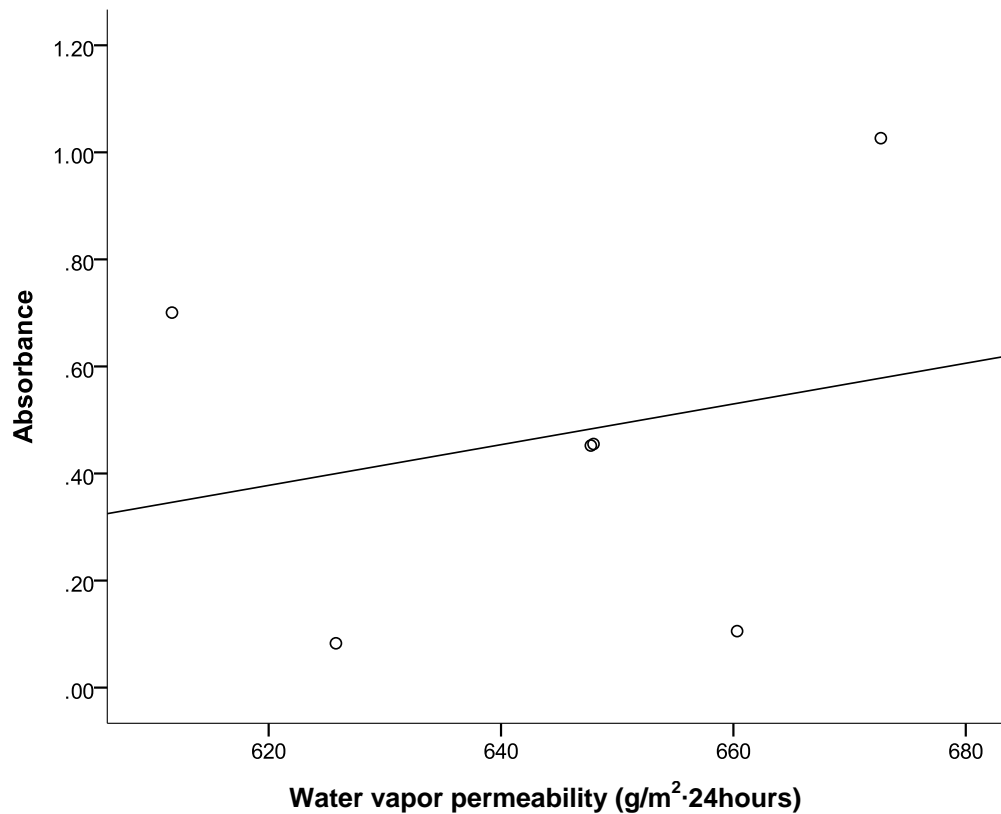


Figure 7.19 The relationship between the water vapor permeability and the 14 days cell proliferation of the PLLA and Pk fibrous membranes ( $r = 0.24$ ,  $P > 0.05$ ).

According to the results shown in the Figures above, for the first three days culture, maximum load, moisture content had no obvious correlation with cell proliferation after 3 days but after 14 days the cell proliferation was observed to increase linearly as the maximum load of the samples increased and decrease as the moisture content increased. Water vapour permeability did not appear to influence the cell proliferation at all. Among the properties of the membranes, the max load and the water content were the most important factors that affected the cell proliferation, whereas the water vapor permeability had no correlation with the cell proliferation. These results may explained by the cytotoxicity of the wool keratin itself as mentioned in Chapter 6, and the roughness formed by the wool keratin particles inside the electrospun fibers. Li et al (2009) reported that more than 80% of the keratin could be released from Pk fibers during the first three days of culturing.

The released keratin may have covered a part of the culture surface, which may have reduced the surface area available for cell adhesion, so that the subsequent cell proliferation will be inhibited. Therefore, after the culture medium was changed, the cell proliferation will have been less affected by the rough surface, so that they could grow normally on the membranes in the subsequent culture period.

### **7.2.6 Conclusions**

In this Chapter, the fourth objective was achieved by studying the cell proliferation and the relationship between the cell proliferation and the properties of the scaffolds. The wool keratin was shown to improve the cell proliferation when it was incorporated into the PLLA. For example, Pk21 increased cell proliferation significantly, whereas other Pk/PLLA composite fiber ratios decreased cell proliferations compared to the 100% PLLA membrane after 21 days culturing. The physical properties had strong correlation with the cell proliferation of the scaffolds.

**CHAPTER 8: ANTIBACTERIAL ACTIVITY**

8.1 Introduction .....	147
8.2 Antibacterial activity of Ag/PLLA films .....	148
8.3 Antibacterial activity of Ag/PLLA fibrous membranes .....	152
8.4 Discussion .....	158
8.5 Conclusions .....	160

**8.1 Introduction**

Chapter 8 aims to fulfill the fifth objective by investigating the antibacterial activity of the scaffolds. In the development of TE scaffolds for medical applications, the risk of infection requires the TE scaffolds to have antibacterial properties [Chen and Schluesener, 2008; Gaonkar et al, 2003; Morris et al, 1998; Walder et al, 2002]. For example, during the treatment of a wound, infection is a common risk which needs to be prevented for good healing of the wound. Due to their strong antibacterial properties and low toxicity, Ag and its compounds have been studied for many years, not only for their low cytotoxicity, but also for their antibacterial activity [Alt et al, 2004; Crabtree et al, 2003; Furno et al, 2004; Galeano et al, 2003; Lai and Fontecchio, 2002; Riley et al, 1995; Thomas et al, 2007; You et al, 2012].

Nanotechnology has provided a most promising field for new developments of biomedical materials. For example, nano-scale particles of silver (Ag NPs), provide larger interface to the environment than that of micro-scale silver particles. Li et al (2006) reported that very small amounts of Ag NPs had strong antibacterial efficacy against bacteria. So, the use of nano-sized silver enables the

usual quantity of silver needed to be reduced, whilst maintaining a good level of antibacterial activity.

To investigate the bacterial activity and mechanism of Ag NP composed scaffolds, antibacterial tests were performed using *E. coli* and *Staphylococcus* which often infect skin wounds and other tissues [Yeo et al, 2003]. In order to investigate the antibacterial activity of the scaffolds with low or no cytotoxicity, the 0.5%, 2.5% and 5% Ag/PLLA films as well as the 5% electrospun Ag/PLLA fibrous membranes were selected for the antibacterial experiments, on the basis of their cytotoxicity test results reported in Chapter 6.

## **8.2 Antibacterial activity of Ag/PLLA films**

### **8.2.1 Preparation of PLLA and Ag/PLLA films**

As described in Chapter 3, PLLA was dissolved in chloroform to produce a 1% (w/w) solution. Ag NPs were then added to the solution and stirred evenly to prepare the 0.5%, 2.5%, 5% Ag/PLLA (w/w) films.

### **8.2.2 Antibacterial test**

*Escherichia coli* ATCC25922 and *Staphylococcus aureus* ATCC25923 were used for this test as these are common micro-organisms involved in hospital-acquired infections. The strains were cultured overnight in 10mL of nutrient broth to achieve a turbidity of  $10^8$  colony forming units (CFU)/mL.

#### ***Minimum inhibitory concentration (MIC) assay***

The MIC was assayed using a two-fold microdilution broth method [Shan et al, 2008]. Dilutions were used to dispense 1mL into each well of a sterile 24-well

plate. Each well contained  $5 \times 10^5$  CFU/mL of test bacteria and the serially diluted extractions. Negative controls were prepared with uninoculated medium and the positive control wells contained inoculated PLLA extraction. After incubation at  $37^\circ\text{C}$  for 20hr, the turbidity of each extraction was assessed by the naked eye to detect the inhibition of bacterial growth. Fifty microlitres of the medium were taken from each well that had no visible turbidity and spread evenly on freshly prepared nutrient agar plates before being incubated at  $37^\circ\text{C}$  for 24hr to determine the minimum bactericidal concentration (MBC). The tests were performed in triplicate for each extraction.

#### ***Maximum antibacterial activity (MAA) assay***

The maximum antibacterial activity assay was a method referred to in a previous study [Li et al, 2006] which was used to determine the highest concentration of bacteria which can be inhibited by the original extractions. Ten micro liters of the serially diluted inoculated broth were added to each well of the 24-well plates, which contained 1mL of the original extractions, to obtain the bacterial concentrations from  $1 \times 10^6$  to  $1 \times 10^1$  CFU/mL. Then, the plates were incubated at  $37^\circ\text{C}$  for 24hr. Following the same procedure as in the MIC assay, 50 $\mu\text{L}$  of the medium were taken from those wells which were visibly clear, spread evenly on freshly prepared nutrient agar plates, and incubated at  $37^\circ\text{C}$  for 24hr to determine the MAA. The tests were again performed in triplicate.

#### **8.2.3 Scanning electron microscopy (SEM)**

Films with and without cultured cells were sputter coated with gold and then observed by scanning electron microscopy (LEICA, Stereoscan 440, 20kV).

### 8.2.4 Statistical analysis

Values were expressed as means  $\pm$  standard deviations. Statistical differences were determined by one-way Analysis of Variance (ANOVA). *P* values of less than 0.05 were considered to be statistically significant.

### 8.2.5 Results

#### *Antibacterial properties of Ag/PLLA films*

The extractions of the 0.5%, 2.5% and 5% Ag/PLLA films were used to test the antibacterial properties of the Ag/PLLA films against *Escherichia coli* and *Staphylococcus*. As shown in Table 8.1, the extractions of the 0.5% and 2.5% Ag/PLLA films were revealed to have antibacterial properties and the extraction of the 5% Ag/PLLA film showed the strongest antibacterial effect.

Table 8.1 Assessment of the antibacterial activity of the extractions of the Ag/PLLA films

Assay	Extractions		
	0.5% Ag/PLLA	2.5% Ag/PLLA	5% Ag/PLLA
MIC: <i>Escherichia coli</i> ( $1 \times 10^5$ CFU/mL)	-	-	+ (original)
<i>Staphylococcus aureus</i> ( $1 \times 10^5$ CFU/mL)	-	-	-
MAA: <i>Escherichia coli</i> (CFU/mL) *	0	$1 \times 10^4$	$1 \times 10^5$
<i>Staphylococcus aureus</i> (CFU/mL)	0	$1 \times 10^1$	$1 \times 10^3$

\* See Figure 8.1 and Figure 8.2.

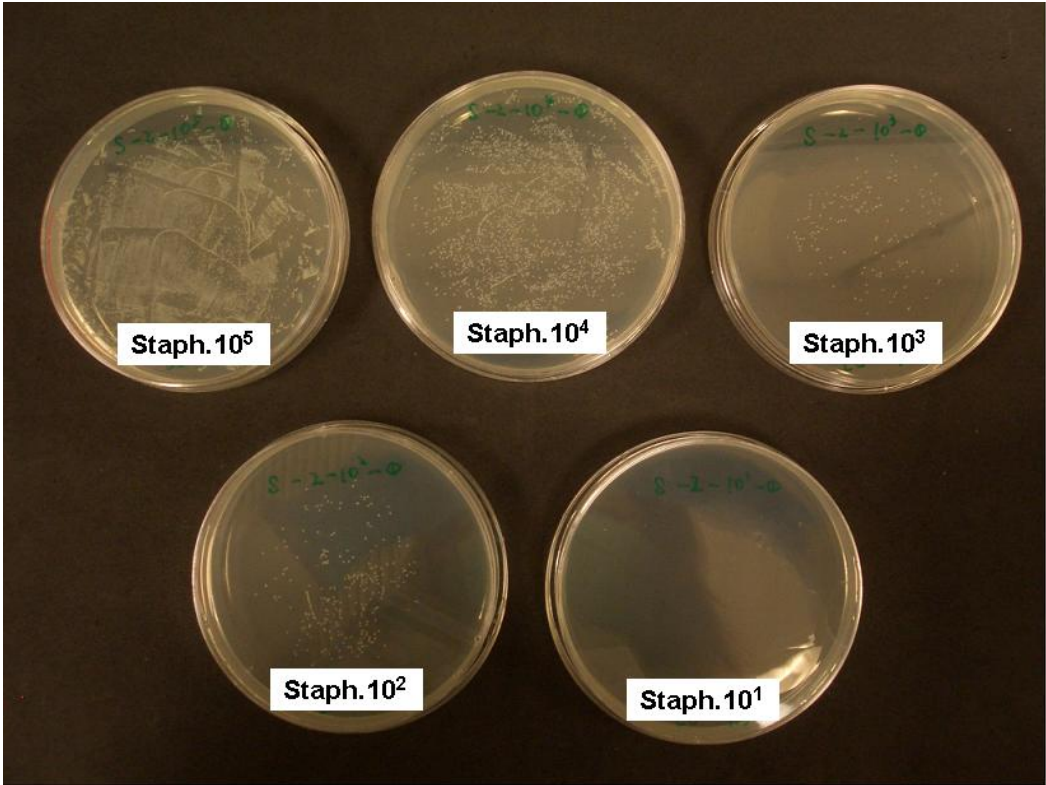


Figure 8.1 Results of the antibacterial activity for the extraction of the 2.5% Ag/PLLA film using Staph. at different bacteria concentrations: 10<sup>1</sup>, 10<sup>2</sup>, 10<sup>3</sup>, 10<sup>4</sup> and 10<sup>5</sup> CFU/mL after 24hr incubation at 37°C. The highest concentration of Staph., which could be inhibited by the original extraction of the 2.5% Ag/PLLA film, was 10<sup>1</sup> CFU/mL.

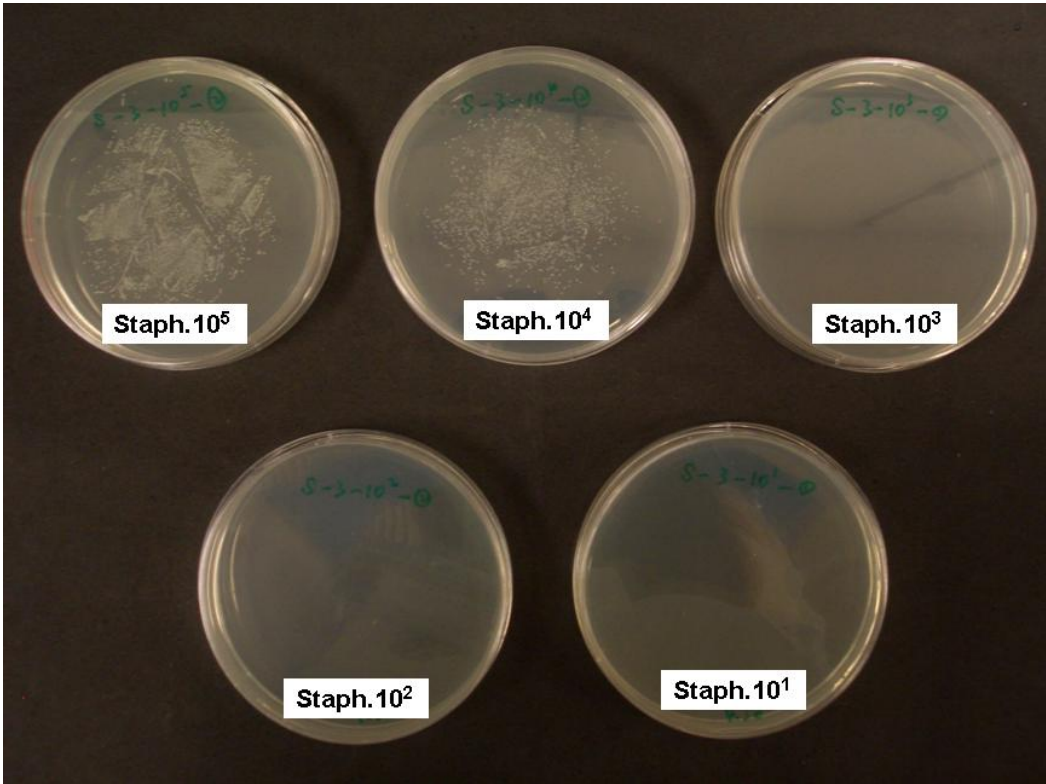


Figure 8.2 Results of the antibacterial activity for the extraction of the 5% Ag/PLLA film using Staph. at different bacteria concentrations:  $10^1$ ,  $10^2$ ,  $10^3$ ,  $10^4$  and  $10^5$  CFU/mL after 24hr incubation at  $37^\circ\text{C}$ . The highest concentration of Staph., which could be inhibited by the original extraction of the 5% Ag/PLLA film, was  $10^3$  CFU/mL.

As shown in Figures 8.1 and 8.2, after 24hr incubation at  $37^\circ\text{C}$ , the highest concentration of Staph. which could be inhibited by the original extraction of the 2.5% Ag/PLLA film was  $10^1$  CFU/mL, whereas the highest concentration of Staph. inhibited by the extraction of the 5% Ag/PLLA film was  $10^3$  CFU/mL. Accordingly, it can be observed in Figure 8.1 that the petri dish labeled as *Staph. 10<sup>1</sup>* was very clean, whereas in Figure 8.2, the petri dishes labeled *Staph. 10<sup>3</sup>*, *Staph. 10<sup>2</sup>* and *Staph. 10<sup>1</sup>* were all very clean, which indicated that no bacteria had been grown in them.

### 8.3 Antibacterial activity of Ag/PLLA fibrous membranes

#### 8.3.1 Electrospinning of PLLA and Ag/PLLA fibrous membranes

The electrospinning method used to produce the fibrous membranes was that used in a previous study [Li et al, 2009] and has already been described in section 3.3 PLLA was dissolved at a weight ratio of 1% in an organic solvent mixed with a composition of chloroform and N, N-dimethylformamide (DMF) (10:1, w/w). Ag NPs were then added to the solution and stirred evenly to prepare a 5% Ag/PLLA solution for electrospinning. The PLLA and Ag/PLLA solutions were deposited into a syringe with a blunt needle, and ejected by the syringe plunger at a feeding rate of 0.3 mL/min. A grounded metal rotating drum wrapped with aluminum foil was located at a fixed distance of 10 cm away from the tip of the needle to collect the fibers. A high electric voltage field (13KV) was applied to the continuous stream of droplets as it emerged from the nozzle.

This converted the solution stream into continuous filaments which assembled on the rotating drum to form PLLA and Ag/PLLA fibrous membranes.

### **8.3.2 Antibacterial test**

The antibacterial test method was performed in accordance with AATCC147-2004. *Escherichia coli* (E.coli, ATCC25922) and *Staphylococcus aureus* (Staph., ATCC25923) were used, again because they are the common micro-organisms involved in hospital-acquired infections [Li et al, 2006]. Each test was repeated three times for every specimen.

#### ***Procedure***

The strains were cultured overnight in 10mL of nutrient broth to achieve a turbidity of  $10^8$  colony forming units (CFU)/mL. Sterilized nutrient agar was dispensed by pouring  $15\pm 2$ mL into separate standard (15×100 mm) flat bottom petri dishes to obtain firm, solid agar before inoculating. Using a 4mm inoculating loop, one loopful was loaded with the 10 times diluted inoculums and transferred to the surface of the sterile agar, by making five streaks covering the central area of a petri dish. A specimen of each Ag/PLLA membrane was gently pressed onto the agar surface to ensure intimate contact with it. Then it was incubated at 37°C for 24hr. A PLLA membrane was used as a negative control. All the membrane specimens were cut to a diameter of 5mm for the antibacterial test.

#### ***Evaluation***

The incubated plates were examined for the interruption of growth along the streaks of inoculum beneath the specimen and for a clear zone of inhibition

beyond its edge. The average width of the zone of inhibition along a streak on either side of the test specimen was calculated using the following equation:

$$W = (T-D)/2 \quad (\text{eq. 8.1})$$

where:

$W$  = the width of the clear zone of inhibition in mm

$T$  = the total diameter of the test specimen and the clear zone in mm

$D$  = the diameter of the test specimen in mm

### 8.3.3 Scanning electron microscopy (SEM)

The PLLA and Ag/PLLA fibrous membranes with bacteria were sputter coated with gold and then observed using scanning electron microscopy (LEICA, Stereoscan 440, 20kV).

### 8.3.4 Statistical analysis

Values were expressed as means  $\pm$  standard deviations. Statistical differences were determined by one-way ANOVA.  $P$  values of less than 0.05 were considered to be statistically significant.

### 8.3.5 Results

#### *Antibacterial activities of Ag/PLLA fibrous membranes*

E.coli and Staph. were used for this test to evaluate the antibacterial capability of Ag/PLLA fibrous membranes. The bacteria were cultured overnight in 10mL nutrient broth to achieve a turbidity of  $10^8$  colony forming units (CFU)/mL. A loop of each kind of bacteria at a concentration of  $10^8$  CFU/mL was taken to evenly streak the agar filled petri dishes. Each of the 5mm diameter circular

fibrous membrane specimens with was gently pressed onto the inoculated agar surface before incubation at 37°C for 24hr.

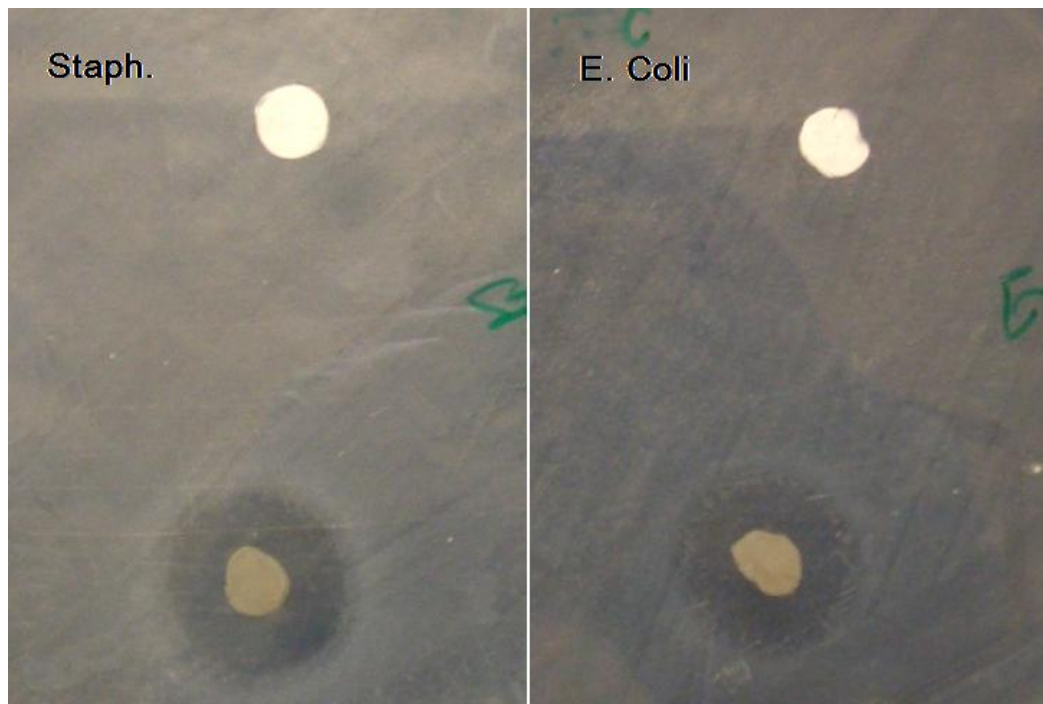


Figure 8.3 Antibacterial test results for the Ag/PLLA using Staphylococcus (Left) and E. coli (right). Bacteria inhibited, clear zones for both the E.coli and Staph. can be observed around the Ag/PLLA membranes (lower specimen) with an average width of 5mm after 24hr incubation.

In Figure 8.3, the upper specimens are the PLLA membranes, and the lower specimens are the Ag/PLLA membranes. All the membranes were freshly prepared. After 24hr incubation, obvious bacteria inhibited, clear zones around the Ag/PLLA membranes could be seen, the average width of the zones was  $5.5 \pm 0.1$ mm. Conversely, no clear zone of inhibition was seen around the PLLA membranes. Both the Staph. and E.coli had the same results which indicated the strong antibacterial activity of the Ag/PLLA.

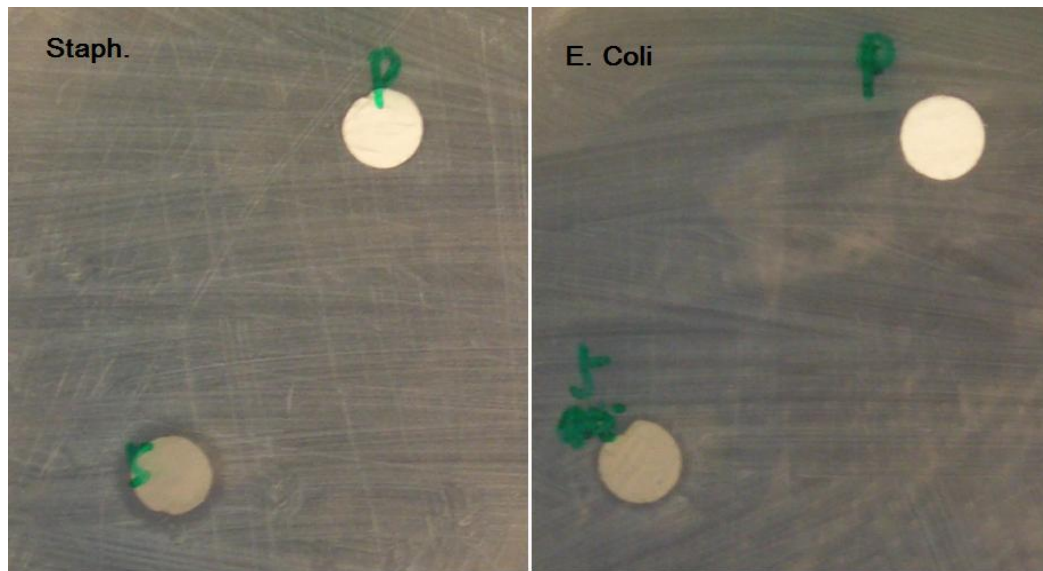


Figure 8.4 Antibacterial activity of the Ag/PLLA fibrous membrane (lower specimen) was reduced after exposure in air for 8 weeks. The average width of the E.coli and Staph. inhibition clear zones decreased to 1.2mm and 1.5mm respectively after 24hr incubation.

After exposure in air for 8 weeks, the Ag/PLLA membranes were still observed to provide antibacterial activity. The average widths of the bacterial inhibition zones for the Ag/PLLA membranes were  $1.2 \pm 0.1$ mm for the E.coli and  $1.5 \pm 0.1$ mm for the Staph (Figure 8.4). According to Table 8.2, the antibacterial activity was found to have decreased significantly.

Table 8.2 Assessment of the antibacterial activity of the extractions of the Ag/PLLA membranes

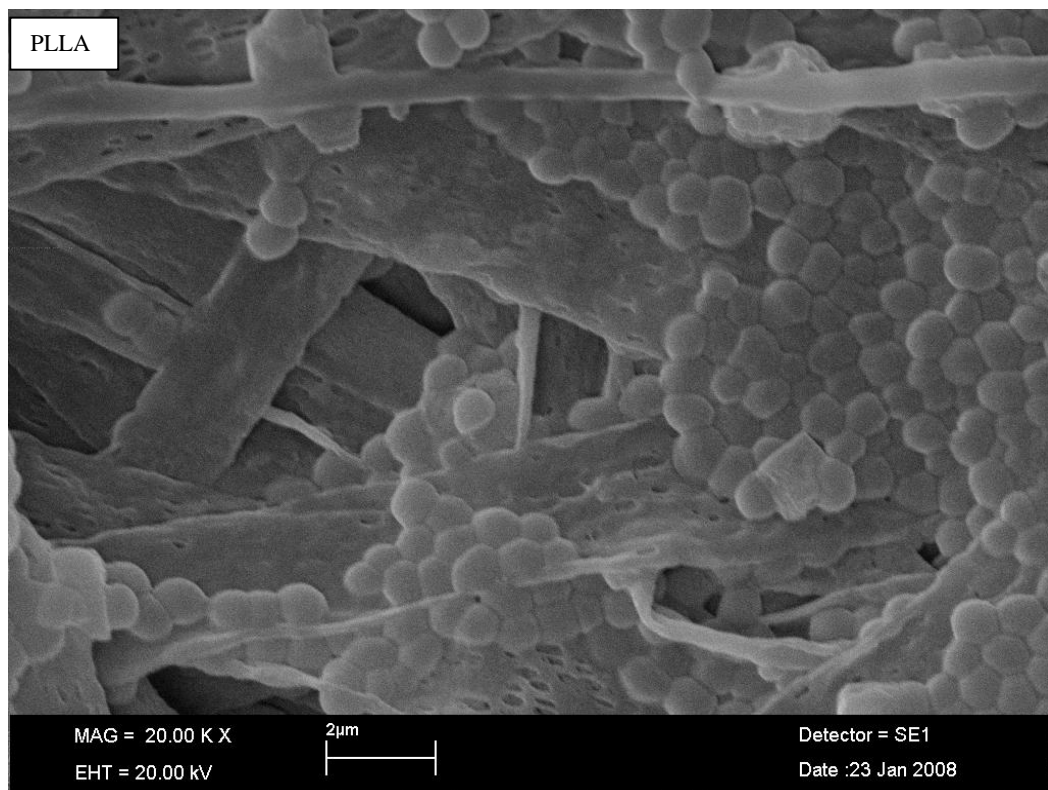
Bacteria	Average width of bacteria inhibition clear zone (mm)	
	PLLA	5% Ag/PLLA
Before: Escherichia coli	0	$5.0 \pm 0.1^*$
Staphylococcus aureus	0	$5.0 \pm 0.1^*$
After: Escherichia coli	0	$1.2 \pm 0.1^*$
Staphylococcus aureus	0	$1.5 \pm 0.1^*$

\* The mean values were shown for means  $\pm$  SD.  $P < 0.05$  vs PLLA membranes.

These results showed that the Ag/PLLA membranes had strong antibacterial capability. Furthermore, after exposure in air for a long term, they were still antibacterial. This result does not exclude the possibility that, if the antibacterial activity test had been sustained for a longer period, the Ag/PLLA membranes could possibly have released more Ag NPs to prolong their antibacterial activity.

***SEM observation of Staph. on the PLLA and Ag/PLLA fibrous membranes***

The morphological changes in the bacteria were also observed through SEM using Staph.. 20 $\mu$ L of diluted inoculum of Staph. at a concentration of 10<sup>7</sup> CFU/mL were spread on the PLLA and Ag/PLLA membranes respectively before being incubated at 37°C for 2hr. SEM observations were then performed.



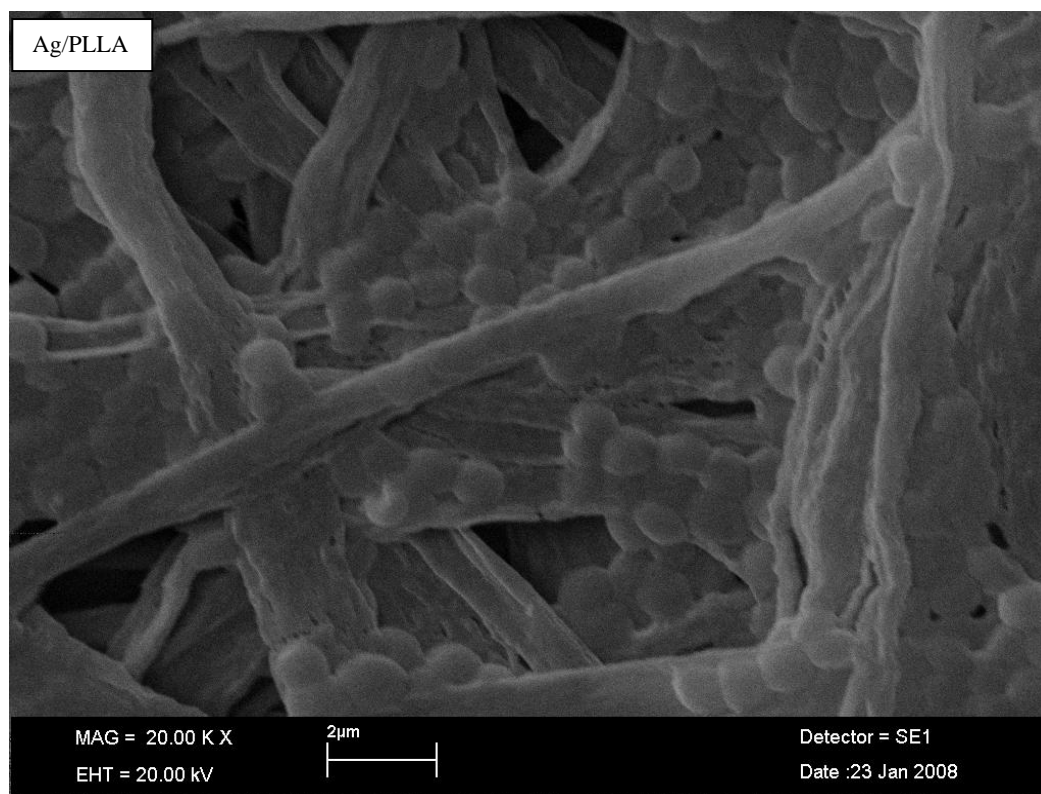


Figure 8.5 SEM images showing Staph. on the PLLA and Ag/PLLA fibrous membrane magnified 20 thousand times (20kV). (1) The number of Staph. on the PLLA membranes were more than that on the Ag/PLLA membrane. (2) Staph. on the PLLA membrane had a smooth surface, whereas those on the Ag/PLLA membrane were not very smooth.

As shown in Figure 8.5, the number of Staph. spread over the PLLA membrane was obviously more than that on the Ag/PLLA membrane. Also, the surface of the Staph. on the PLLA membrane was smoother than that on the Ag/PLLA membrane. This result indicated that there might be less destruction of the bacteria spread over the PLLA membrane than that on the Ag/PLLA membrane.

#### 8.4 Discussion

TE scaffolds that are effective in reducing the possibility of infections will be more acceptable for medical applications. Skin is the first protective barrier for all the tissues and organs, a wound on the skin will easily weaken the

anti-infection capability of the human body. Thus, antibacterial skin TE scaffolds will be more beneficial for wound recovery than other TE scaffolds.

The Ag NPs were observed to be cytotoxic to bacterial cells, but less harmful to normal cells. This finding suggested an exploration of the intersection of the low cytotoxicity and antibacterial activity of the various Ag NPs concentrations [Chen and Ma, 2006; Chen and Schluesener, 2008; Crabtree et al, 2003; Furno et al, 2004]. In 2004, Alt et al reported that bone cement with 1% of Ag NPs showed high antibacterial activity against most of the tested strains. Yeo et al (2003) found that fibers containing Ag NPs showed excellent antibacterial property. Furthermore, electrospun fibers can produce permeable fibrous membranes with a wide interface area for them to perform their antibacterial activity more effectively.

Some researchers have suggested that, when dissolved in water, the Ag NPs convert to silver ions ( $\text{Ag}^+$ ), which can kill pathogens [Park et al, 2009]. However, other scientists found that the Ag NPs played the role of antibiosis independently [Li et al, 2010; Gupta et al, 2001]. In this study, the Ag/PLLA composite films and fibrous membranes with an appropriate level of Ag content were found to inhibit the proliferation of *E. coli* and *Staphylococcus* significantly, whilst allowing good cell proliferation. This result seemed to support the independent antibacterial role of Ag NPs. In terms of the degradability of the PLLA, the Ag NPs were presumed to be released from the PLLA fibers gradually along with the degradation of the PLLA, thus sustaining the Ag/PLLA scaffold's antibacterial capability for a prolonged period. After eight-week exposure to air, the antibacterial activity of the Ag/PLLA fibrous membranes

reduced. This result may have been caused by the oxidation of the air or other reactions during the exposure.

The morphological changes in the bacteria were observed by SEM. More Staph. were seen on the PLLA membrane than were on the Ag/PLLA membrane and the surface of the Staph. on the PLLA membranes was smoother than that on the Ag/PLLA membranes. These findings imply that the Ag NPs may affect the structure of the bacterial membrane, thereby causing the defunctionalization of the bacteria. Choi et al observed that the Ag NPs were absorbed onto the bacterial cell surface and caused cell surface depression [2008]. Many researchers have attributed the highly efficient antibacterial effect of Ag NPs to their super miniature size and larger surface area that help the Ag NPs to easily damage the bacteria membrane [Pal et al, 2007]. However, the specific mechanism of antibacterial activity of Ag/PLLA scaffolds needs further investigation.

## 8.5 Conclusions

In this Chapter, the fifth objective was achieved by examining the antibacterial activity of the scaffolds. On the basis of the observations and findings above, it can be concluded that Ag/PLLA scaffolds can provide a strong antibacterial function. Furthermore, the fibrous structure, which consists of many fibers, has larger surface area and more pores than that of the films. Thus, an Ag/PLLA fibrous membrane will be more effective and economical than the films as an antibacterial scaffold. However, the factors which influence the antibacterial effect need further investigation to clarify the mechanism of antibacterial activity of Ag/PLLA membranes.

## CHAPTER 9: CONCLUSIONS AND SUGGESTIONS FOR FUTURE RESEARCH

9.1 Conclusions .....	161
9.2 Suggestions for future research.....	164

This thesis has described a systematic study carried out to establish an understanding of functionality of tissue engineering scaffolds suitable as skin substitutes. The research gaps identified in the literature review have been filled by fulfilling the objectives summarized below. The limitation of the work is pointed out and future work is suggested.

### 9.1 Conclusions

In Chapter 4, the first objective was achieved by studying the physical properties of the scaffolds. As the concentration of wool keratin increased, the diameter of the nano fibres increased linearly, not only for the wool keratin-PEO, but also for the PLLA/keratin fibrous membranes. As the proportion of keratin increased, the tensile strength and elongation of the Pk fibrous membranes decreased, while their moisture content increased. Their water vapor permeability was not influenced by keratin content significantly. The Pk21 membrane had the best moisture one-way transport property. Thus, based on the results of the tests, in particular the tensile property and the moisture related properties, it can be suggested that the Pk fibrous membranes with a suitable proportion of keratin particles can, possibly, provide an optimal matrix for skin substitutes.

In Chapter 5, the second objective was achieved by examining the *in vitro* degradation of the PLLA and PLLA/keratin membranes. The keratin

encapsulated structure and the wool keratin proportion affected the degradability of the PLLA/keratin fibrous membranes. The decreasing tensile strength and elongation may have been responsible for the faster degradability the PLLA/keratin fibers. Furthermore, because wool keratin-PEO fibrous membranes can be easily dissolved in water, combining PEO with the Pk or Ag/PLLA scaffolds may preferably help control the degradability of these two kinds of TE scaffolds.

In Chapter 6, the third objective was fulfilled by examining the cytotoxicity of the scaffolds. According to the cytotoxicity test results, the safe wool keratin concentration must be less than 50%. The cytotoxicity of the Pk membranes had a close relationship with the tensile property and moisture content of the scaffolds. Basically, the cytotoxicity was most correlated to the wool keratin concentration. The concentration of the Ag NPs affected the cytotoxicity of the scaffolds proportionally. The higher the concentration of Ag NPs, the more was the cytotoxicity of the scaffolds. Furthermore, the hydrophilicity and cell proliferation of the scaffolds had a strong negative linear correlation. Thus, the optimal proportion of the Ag NPs and PLLA for non-cytotoxicity was determined to be 5% (w/w) for the films, and 0.5% (w/w) for the Ag/PLLA fibrous membranes. However, in the extraction of the 2.5% Ag/PLLA membrane, some living cells were still evident, and in the extraction of the 5% Ag/PLLA membrane, although there were not many, there were still a few stretched living cells visible. So, it is concluded that the Ag NPs concentration in the Ag/PLLA membranes should be less than 5% (w/w) at most. Additionally, the probable release rate of the Ag NPs in the different scaffolds was also found, and the Ag/PLLA fibrous membranes were shown to have a much higher release rate of

Ag NPs than the Ag/PLLA films. This implied that, compared with the films, the Ag/PLLA fibrous membranes could use less Ag NPs for a comparable antibacterial activity, with the same level of cytotoxic effects on the cells. Thus, the conclusion is reached that the Ag/PLLA fibrous membrane will be more effective and economical than the films as an antibacterial scaffold. This finding has also provided an indication of the Ag NPs dosage required to fabricate scaffolds for medical applications. However, the mechanism of the Ag NPs' action on the cells was not elucidated. Therefore, further investigation into the effects of Ag NPs on cells needs to be pursued in subsequent studies.

In Chapter 7, the fourth objective was achieved by examining the cell proliferation of the scaffolds. The results showed that, by incorporating appropriate wool keratin content, Pk membranes can improve the cell proliferation. For example, the Pk21 membrane increased the cell proliferation significantly, while the other Pk composite fibers decreased the cell proliferations compared to the 100% PLLA membrane. This result implied that not all the good substance can be used without any limitation. Otherwise, it may bring out an even worse result. On the other hand, the physical properties of the membranes had a strong correlation with the cell proliferation of the scaffolds. It can be concluded that the raw materials and the properties of the scaffolds are the two main factors which affect the cytotoxicity, but the specific mechanism of the scaffold cytotoxicity still needs further studies.

In Chapter 8, the fifth objective was achieved by studying the antibacterial activity of the scaffolds. As mentioned in Chapter 2, the graft-wound bed interface, which often becomes the location for bacterial proliferation, can inhibit

this by keeping the wound bed wet. However, according to this study, it was not “the wetter, the better”, so, the appropriate moisture content in the wound bed must be determined for optimum healing. This role can be achieved by combining the Pk and Ag/PLLA fibrous membranes together. In other words, wool keratin can make the Ag/PLLA scaffolds more appropriate for use as antibacterial scaffolds.

In summary, the Pk fibrous membranes may help to detach less skin from the limited donor sites of the patients, while the Ag NPs composed TE scaffolds will provide a good antibacterial property to reduce the risk of infection. Thus, to apply TE scaffolds composed of wool keratin and Ag NPs to the skin may be more effective and less traumatic to the patients who suffer multiple skin injuries.

## **9.2 Suggestions for future research**

### **9.2.1 Cell proliferation and antibacterial function**

Cell-biomaterial combinations for scaffold-based tissue engineering are multifactorial. Based on the review of silver toxicity studies and the cytotoxicity experimental results, the Ag NPs composed scaffolds have a strong antibacterial activity, but their cytotoxicity is a non-negligible problem. Fortunately, Posgai et al found that vitamin C can reduce the cytotoxicity of Ag NPs [2011]. Thus, in a future study, vitamin C may be incorporated into the Ag/PLLA scaffolds to produce less cytotoxic antibacterial skin TE scaffolds. Before that, it will be better to combine wool keratin, Ag NPs, and PLLA together to fabricate Ag/Pk fibrous membranes in order to get the biomechanical properties closer to those of

human skin. In addition, after proliferating fibroblasts on existing skin TE scaffolds, keratinocytes will be cultured on the top of the fibroblasts proliferated scaffolds to fabricate epidermal/dermal skin substitutes for subsequent study.

On the other hand, , some materials have an inherent antibacterial property, such as chitosan. Eaton et al (2008) studied the antibacterial effects of chitosan on *Escherichia coli* and *Staphylococcus aureus*, and found that these effects were related to the molecular weight of chitosan. Therefore, for example, if these antibacterial matrices were composited with Ag NPs or any other antibacterial substances, the TE scaffolds would be more efficient and acceptable for reducing the possibility of infections. Furthermore, considering both the cytotoxicity of Ag NPs, and some studies related to the antibacterial activity of traditional Chinese medicine (TCM) [Tan et al, 2011; Wu et al, 2008], it may be possible for TCM to play an important role as an effective and eco-friendly skin TE scaffold.

### **9.2.2 Composing TCM into scaffolds**

As has been gradually realised, TCM has relatively complex components which makes it difficult for the bacteria to acquire drug resistance [Tan et al, 2011]. To date, it has been identified that more than four hundred kinds of TCM indicate a wide spectrum of antibacterial and antiviral function. So, if the TCM can be combined into the scaffolds for tissue engineering, it may open a much wider area to develop more effective scaffolds for clinic biomaterials with less drug resistance.

Furthermore, in an initial study, one of the antibacterial TCMs, dang gui, was found to obviously improve cell proliferation after being composited into PLLA fibers. This result indicated that TCM has the potential to proliferate cells too.

In modern society, TCM has become more popular and acceptable because of its low toxicity and few side effects with very low drug resistance. Thus, to produce skin TE scaffolds with TCM would be another good direction for further clinical applications.

### **9.2.3 Animal model experiments**

The development of a TE scaffold requires the evaluation of its biocompatibility prior to the application of the scaffold in human subjects. The next step for this research work will be to apply the scaffolds to small animals first, then, proceeding to larger animals, if the results are positive. Experiments on animals, such as rats, may be done as follows:

1. wound healing animal model preparation: anaesthetize the rat first, shaving the dorsal skin and sterilize the skin, then cut a 2cm long wound.
2. experimental groups: use both female and male rats. Negative control, positive control (gauze), and scaffolds groups will be set-up, with 20 rats for each group.
3. observation indicators: 1) wound healing time; 2) change of wound size; 3) morphological observation: tissue structure recovery, inflammatory reaction, immunological rejection; 4) Immune-Histochemical observation.

In conclusion, this investigation has suggested that a non-cytotoxic, antibacterial, nano-technology, wool keratin composed Ag/PLLA scaffold will have very good potential for tissue engineering.

---

**References**

**Agic A**, Nikitovic M, Mijovic B. Design of dermal electrospun replacement. *Periodicum Biologorum* 2010; 112 (1): 63-68.

**Alt V**, Bechert T, Steinrucke P, Wagener M, Seidel P, Dingeldein E, Domann E, Schnettler R. An in vitro assessment of the antibacterial properties and cytotoxicity of nanoparticulate silver bone cement. *Biomaterials* 2004; 25: 4383-4391.

**Andreassi A**, Bilenchi R, Biagioli M, D'Aniello C. Classification and pathophysiology of skin grafts. *Clinics in Dermatology* 2005; 23: 332-337.

**Andrei G**, Duraffour S, Van den Oord J, Snoeck R. Epithelial raft cultures for investigations of virus growth, pathogenesis and efficacy of antiviral agents, *Antiviral Research* 2010; 85: 431-449.

**Annaih AN**, Ottenio M, Bruyere K, Destrade M and Gilchrist MD. Mechanical properties of excised human skin. *WCB 2010, IFMBE Proceedings* 2010; 31: 1000-1003.

**Aroca AS**, Fernández AJC, Ribelles JLG, Pradas MM, Ferrer GG, Pissis P. Porous poly(2-hydroxyethyl acrylate) hydrogels prepared by radical polymerisation with methanol as diluent. *Polymer* 2004; 45 (26): 8949-8955.

**Arora S**, Jain J, Rajwade JM, Paknikar KM. Cellular responses induced by silver nanoparticles: In vitro studies. *Toxicology Letters* 2008; 179(30): 93-100.

**Blackwood KA**, Mckean R, Canton I, Freeman CO, Franklin KL, Cole D, Brook I, Farthing P, Rimmer S, Haycock JW, Ryan AJ, Macneil S. Development of biodegradable electrospun scaffolds for dermal replacement. *Biomaterials* 2008; 29(21): 3091-3104.

**Blank IH**. Factors which influence the water content of the stratum corneum. *The Journal of Investigative Dermatology* 1952; 18: 433-440.

**Blanpain C**, Lowry WE, Geoghegan A, Polak L, Fuchs E. Self-renewal, multipotency, and the existence of two cell populations within an epithelial stem cell niche. *Cell* 2004; 118: 635-648.

**Braydich-Stolle L**, Hussain S, Schlager JJ, Hofmann MC. In vitro cytotoxicity of nanoparticles in mammalian germline stem cells. *Toxicological Sciences* 2005; 88 (2): 412-419.

**Campoccia D**, Doherty P, Radice M, Brun P, Abatangelo G, Williams DF. Semisynthetic resorbable materials from hyaluronan esterification. *Biomaterials* 1998; 19: 2101-2127.

**Calvert JW**, Marra KG, Cook L, Kumta PN, DiMilla PA, Weiss LE. Characterization of osteoblast-like behavior of cultured bone marrow stromal

cells on various polymer surfaces. *Journal of Biomedical Materials Research* 2000; 52(2): 279-284.

**Cao Y**, Zhou YM, Shan Y, Ju HX, Xue XJ. Triple-helix scaffolds of grafted collagen reinforced by Al<sub>2</sub>O<sub>3</sub>-ZrO<sub>2</sub> nanoparticles. *Advanced Materials* 2006; 18(14): 1838-1841.

**Caravaggi C**, De Giglio R, Pritelli C, Sommaria M, Dalla Noce S, Faglia E, Mantero M, Clerici G, Fratino P, Dalla Paola L, Mariani G, Mingardi R, Morabito A. HYAFF 11-based autologous dermal and epidermal grafts in the treatment of noninfected diabetic plantar and dorsal foot ulcers: a prospective, multicenter, controlled, randomized clinical trial. *Diabetes Care* 2003; 26: 2853-2859.

**Chaloupka K**, Malam Y, Seifalian AM. Nanosilver as a new generation of nanoparticle in biomedical applications. *Trends in Biotechnology* 2010; 28: 580-588.

**Chen VJ**, Ma PX. The effect of surface area on the degradation rate of nano-fibrous poly (L-lactic acid) foams. *Biomaterials* 2006; 27 (20): 3708-3715.

**Chen X**, Schluesener HJ. Nanosilver: A nanoparticle in medical application. *Toxicology Letters* 2008; 176: 1-12.

**Chen Y**, Mak AFT, Wang M, Li JS, Wong MS. PLLA scaffolds with biomimetic apatite coating and biomimetic apatite/collagen composite coating to enhance osteoblast-like cells attachment and activity. *Surface and Coatings Technology* 2006; 201(3-4): 575-580.

**Cheng L**, Zhang SM, Chen PP, Huang SL, Liu L, Zhou W, Liu J, Gong H, Luo QM. Fabrication and characterization of fluorohydroxyapatite nanocrystals/poly (D, L-lactide) composite scaffolds. *Current Applied Physics* 2007; 7S1: 71-74.

**Chiu JB**, Luu YK, Fang DF, Hsiao BS, Chu B, Hadjiargyrou M. Electrospun nanofibrous scaffolds for biomedical applications. *Journal of Biomedical Nanotechnology* 2005; 1(2): 115-132.

**Choi OK**, Deng KK, Kim NJ, Ross Jr. L, Surampalli RY, Hu ZQ. The inhibitory effects of silver nanoparticles, silver ions, and silver chloride colloids on microbial growth. *Water Research* 2008; 42: 3066-3074.

**Choi YS**, Hong SR, Lee YM, Song KW, Park MH, Nam YS. Study on gelatin-containing artificial skin: I. Preparation and characteristics of novel gelatin-alginate sponge. *Biomaterials* 1999; 20(5): 409-417.

**Clark RA**, K. Ghosh, M.G. Tonnesen, Tissue engineering for cutaneous wounds. *Journal of Investigative Dermatology*. 2007; 127: 1018-1029.

**Converse JM**, Smahel J, Ballantyne DL, Jr Harper AD. Inosculation of vessels of skin graft and host bed: a fortuitous encounter. *British Journal of Plastic Surgery* 1975; 28: 274-282.

**Coolen** NA, Vlig M, van den Bogaardt AJ, Middelkoop E, Ulrich MM. Development of an in vitro burn wound model. *Wound Repair and Regeneration*. 2008; 16: 559-567.

**Crabtree** JH, Burchette RJ, Siddiqi RA, Huen LL, Hadnott LL, Fishman A. Efficacy of silver-ion implanted catheters in reducing peritoneal dialysis-related infections. *Peritoneal Dialysis International* 2003; 23: 368-374.

**Derler** S, Gerhardt LC. Tribology of skin: review and analysis of experimental results for the friction coefficient of human skin. *Tribology Letter* 2012; 45:1-27.

**Doshi** J, Reneker DH. Electrospinning process and applications of electrospun fibers. *Journal Electrostatics* 1995; 35(2-3): 151-160.

**Eaton** P, Fernandes JC, Pereira E, Pintado ME, Xavier Malcata F. Atomic force microscopy study of the antibacterial effects of chitosans on *Escherichia coli* and *Staphylococcus aureus*. *Ultramicroscopy* 2008; 108: 1128-1134.

**Edwards** C, Marks R. Evaluation of biomechanical properties of human skin. *Clinics in Dermatology* 1995; 13: 375-380.

**Ellis-Behnke** RG, Liang YX, You SW, Tay DKC, Zhang SG, So KF, Schneider G.E. Nano neuro knitting: Peptide nanofiber scaffold for brain repair and axon regeneration with functional return of vision. *Proceedings of the national academy of sciences of the United States of American* 2006; 103(13): 5054-5059.

**Flasza-Baron** M, Kemp P, Shering D, Marshall D, Denham Z, Johnson PA. Development and manufacture of a human living dermal equivalent (ICX-SKN). *European Cells and Materials* 2008; 16 (S3): 3.

**Furno** F, Morley KS, Wong B, Sharp BL, Arnold PL, Howdle SM, Bayston R, Brown PD, Winship PD, Reid HJ. Silver nanoparticles and polymeric medical devices: a new approach to prevention of infection? *Journal of Antimicrobial Chemotherapy* 2004; 54:1019-1024.

**Galeano** B, Korff E, Nicholson WL. Inactivation of vegetative cells, but not spores, of *Bacillus anthracis*, *B-cereus*, and *B-subtilis* on stainless steel surfaces coated with an antimicrobial silver- and zinc-containing zeolite formulation. *Applied and Environmental Microbiology* 2003; 69: 4329-4331.

**Gaonkar** TA, Sampath LA, Modak SM. Evaluation of the antimicrobial efficacy of urinary catheters impregnated with antiseptics in an in vitro urinary tract model. *Infection Control and Hospital Epidemiology* 2003; 24: 506-513.

**Gefen** A. *Bioengineering research of chronic wounds* 2009: 343-362; ISBN 978-3-642-00533-6.

**George** ML, Eccles SA, Tutton MG, Abulafi AM, Swift RI. Correlation of plasma and serum vascular endothelial growth factor levels with platelet count in colorectal cancer: clinical evidence of platelet scavenging? *Clinical Cancer Research* 2000; 6: 3147-3152.

**Green CB.** RT-PCR detection of *Candida albicans* ALS gene expression in the reconstituted human epithelium (RHE) model of oral candidiasis and in model biofilms. *Microbiology* 2004; 150: 267-275.

**Groeber F, Holeiter M, Hampel M, Hinderer S, Schenke-Layland K.** Skin tissue engineering - In vivo and in vitro applications. *Advanced Drug Delivery Reviews* 2011; 128: 352–366.

**Gopal R, Kaur S, Maa Z, Chanc C, Ramakrishna S, Matsuura T.** Electrospun nanofibrous filtration membrane. *Journal of Membrane Science* 2006; 281: 581–586.

**Hendriks FM.** Mechanical behaviour of human epidermal and dermal layers in vivo. 2005; ISBN 90-386-2896-X.

**Herndon DN, Barrow RE, Rutan RL, Rutan TC, Desai MH, Abston S.** A comparison of conservative versus early excision. Therapies in severely burned patients. *Annals of Surgery* 1989; 209(5): 547-552.

**Hill P, Brantley H, Van Dyke M.** Some properties of keratin biomaterials: Kerateines. *Biomaterials* 2010; 31: 585–593.

**Holder WD, Gruber HE, Moore AL, Culberson CR, Anderson W, Burg KJL, Mooney DJ.** Cellular ingrowth and thickness changes in poly-L-lactide and polyglycolide matrices implanted subcutaneously in the rat. *Journal of Biomedical Materials research* 1998; 41(3): 412-421.

**Hosseinkhania H, Hosseinkhanib M, Tian F, Kobayashi H, Tabata Y.** Ectopic bone formation in collagen sponge self-assembled peptide-amphiphile nanofibers hybrid scaffold in a perfusion culture bioreactor. *Biomaterials* 2006; 27(29): 5089-5098.

**Hosseinkhani H, Hosseinkhani M, Khademhosseini A, Kobayashi H.** Bone regeneration through controlled release of bone morphogenetic protein-2 from 3-D tissue engineered nano-scaffold. *Journal of Controlled Release* 2007; 117(3): 380-386.

**Hosseinkhani H, Hosseinkhani M, Tian FR, Kobayashi H, Tabata Y.** Bone regeneration on a collagen sponge self-assembled peptide-amphiphile nanofiber hybrid scaffold. *Tissue Engineering* 2007; 13 (1): 11-19.

**Hu JY, Li Y, Yeung KW, Wong ASW, Xu WL.** Moisture management tester: a method to characterize fabric liquid moisture management properties. *Textile Research Journal* 2005; 75:57-62.

**Hussain SM, Hess KL, Gearhart JM, Geiss KT, Schlager JJ.** In vitro toxicity of nanoparticles in BRL 3A rat liver cells. *Toxicology In Vitro* 2005; 19: 975-983.

**Jayaraman K, Kotaki M, Zhang YZ, Mo XM, Ramakrishna S.** Recent advances in polymer nanofibers. *Journal of Nanoscience and Nanotechnology* 2004; 4: 52-65.

**Ji Y**, Ghosh K, Shu XZ, Li BQ, Sokolov JC, Prestwich GD, Clark RAF, Rafailovich MH. Electrospun three-dimensional hyaluronic acid nanofibrous scaffolds. *Biomaterials* 2006; 27: 3782-3792.

**Jordan BJ**, Hong R, Gider B, Hill J, Emrick T, Rotello VM. Stabilization of  $\alpha$ -chymotrypsin at air-water interface through surface binding to gold nanoparticle scaffolds. *Soft Matter* 2006; 2(7): 558-560.

**Katti DS**, Robinson KW, Ko FK, Cato T, Laurencin. Bioresorbable nanofiber-based systems for wound healing and drug delivery: optimization of fabrication parameters. *Journal of Biomedical Materials Research Part B: Applied Biomaterials* 2004; 70B (2): 286-296.

**Kidambi S**, Bruening ML. Multilayered polyelectrolyte films containing palladium nanoparticles: synthesis, characterization, and application in selective hydrogenation. *Chemistry of Materials* 2005;17:301-307.

**Kim K**, Luu YK, Chang C, Fang DF, Hsiao BS, Chu B, Hadjiargyrou M. Incorporation and controlled release of a hydrophilic antibiotic using poly(lactide-co-glycolide)-based electrospun nanofibrous scaffolds. *Journal of Controlled Release* 2004; 98 (1): 47-56.

**Kim K**, Yu M, Zong XH, Chiu J, Fang DF, Seo YS, Hsiao BS, Chu B, Hadjiargyrou M. Control of degradation rate and hydrophilicity in electrospun non-woven poly(D, L-lactide) nanofiber scaffolds for biomedical applications. *Biomaterials* 2003; 24 (27): 4977-4985.

**Kim YS**, Kim JS, Cho HS, Rha DS, Kim JM. Twenty-eight-day oral toxicity, genotoxicity, and gender-related tissue distribution of silver nanoparticles in Sprague-Dawley rats. *Inhalation Toxicology* 2008; 20: 575-583.

**Kong LJ**, Gao Y, Cao WL, Gong YD, Zhao NM, Zhang XF. Preparation and characterization of nano-hydroxyapatite/chitosan composite scaffolds. *Journal of Biomedical Materials Research* 2005; 75A(2): 275-282.

**Kong LJ.**, Gao Y, Lu GY, Gong YD, Zhao NM, Zhang XF. A study on the bioactivity of chitosan/nano-hydroxyapatite composite scaffolds for bone tissue engineering. *European Polymer Journal* 2006; 42(12): 3171-3179.

**Kubo K**, Kuroyanagi Y. Development of a cultured dermal substitute composed of a spongy matrix of hyaluronic acid and atelo-collagen combined with fibroblasts: fundamental evaluation. *Journal of Biomaterials Science, Polymer Edition* 2003; 14: 625-641.

**Kvitek L**, Panacek A, Prucek R, Soukupova J, Vanickova M, Kolar M and Zboril R. Antibacterial activity and toxicity of silver - nanosilver versus ionic silver. *Journal of Physics: Conference Series* 2011; 304: 012029.

**Kwon IK**, Kidoaki S, Matsuda T. Electrospun nano- to microfiber fabrics made of biodegradable copolyesters: structural characteristics, mechanical properties and cell adhesion potential. *Biomaterials* 2005; 26(18): 3929-3939.

- Lafrance H**, Guillot M, Germain L, Auger FA. A method for the evaluation of tensile properties of skin equivalents. *Medical Engineering and Physics* 1995; 17 (7): 537-543.
- Lai KK**, Fontecchio SA. Use of silver-hydrogel urinary catheters on the incidence of catheter-associated urinary tract infections in hospitalized patients. *American Journal of Infection Control* 2002; 30: 221-225.
- Langer R**, Vacanti JP. Tissue engineering (cover story). *Science* 1993; 260(5110): 920-926.
- Li HT**, Li LN, Wang L. The Study on the Preparation and Anti-Bacteria Functions for Nano-AgI, Nano-CuI and Nano-Ag Particles. *Hans Journal of Nanotechnology* 2011; 1: 17-21.
- Li JX**, He AH, Han CC, Fang DF, Hsiao B, Chu B. Electrospinning of hyaluronic acid (HA) and HA/Gelatin blends. *Macromolecular Rapid Communications* 2006; 27: 114-120.
- Li JS**, Mak AFT. Hydraulic permeability of polyglycolic acid scaffolds as a function of biomaterials degradation. *Journal of Biomaterials Applications* 2005; 19 (3): 253-266.
- Li JS**, Li Y, Li L, Mak AFT, Ko F and Qin L. Fabrication of poly(L-lactic acid) scaffolds with wool keratin for osteoblast cultivation. *Composites Part B: Engineering* 2009; 40 (7): 664-667.
- Li L**, Li Y, Li JS Mak AFT, Ko F, Qin L. The effects of PLLA/keratin composite fibrous scaffolds on the proliferation of osteoblasts, *TBIS Proceedings, International Symposium of Textile Bioengineering and Informatics, Hong Kong, China, 2008*, pp 696-699.
- Li MY**, Mondrinos MJ, Gandhi MR, Ko FK, Weiss AS, Lelkes PI. Electrospun protein fibers as matrices for tissue engineering. *Biomaterials* 2005; 26(30): 5999-6008.
- Li WJ**, Laquerriere P, Laurencin CT, Caterson EJ, Tuan RS, Ko FK. Electrospun nanofibrous structure: A novel scaffold for tissue engineering. *Journal of Biomedical Materials Research* 2002; 60: 613-621.
- Li WJ**, Tuli R, Huang XX, Laquerriere P, Tuan RS. Multilineage differentiation of human mesenchymal stem cells in a three-dimensional nanofibrous scaffold. *Biomaterials* 2005; 26(25): 5158-5166.
- Li WJ**, Mauck RL, Tuan RS. Electrospun nanofibrous scaffolds: Production characterization, and applications for tissue engineering and drug delivery. *Journal of Biomedical Nanotechnology* 2005; 1(3): 259-275.
- Li WR**, Xie XB, Shi QS. Antibacterial activity and mechanism of silver nanoparticles on *Escherichia coli*. *Applied Microbial and Cell Physiology* 2010; 85: 1115-1122.

- Li Y**, Leung P, Yao L, Song QW, Newton E. Antimicrobial effect of surgical masks coated with nanoparticles. *Journal of Hospital Infection* 2006; 62: 58-63.
- Li Y**, Xu T, Hu JY, Yang GR. Preparation of nano functional wool protein crystallites (colloid crystal) by nano- emulsification method. *China Patent* 2004; CN1693371.
- Liang DH**, Luu YK, Kim KS, Hsiao BS, Hadjiargyrou M, Chu B. In vitro non-viral gene delivery with nanofibrous scaffolds. *Nucleic Acids Research* 2005; 33 (19): e170.
- Liu H**, Chen D, Tang F, Du G, Li L, Meng X, Liang W, Zhang Y, Teng X, Li Y. Photothermal therapy of Lewis lung carcinoma in mice using gold nanoshells on carboxylated polystyrene spheres. *Nanotechnology* 2008; 19: 455101.
- Liu HC**, Lee IC, Wang JH, Yang SH, Young TH. Preparation of PLLA membranes with different morphologies for culture of MG-63 cells. *Biomaterials* 2004; 25(18): 4047-4056.
- Liu J**, Cui XM, Zhang Y, Zhao ML, Gu QY, Wu XH, Xu LH, Yang YY, Yu SX, Wang DW. Study on the artificial dermal skin built by different scaffolds. *Chinese Journal of Reparative and Reconstructive Surgery* 2003; 7(2): 104-107.
- MacArthur BD**, Oreffo ROC. Bridging the gap. *Nature* 2005; 433(7021): 19.
- MacNeil S**. Progress and opportunities for tissue-engineered skin. *Nature* 2007; 445: 874-880.
- Manjubala I**, Scheler S, Bossert J, Jandt KD. Mineralisation of chitosan scaffolds with nano-apatite formation by double diffusion technique. *Acta Biomaterialia* 2006; 2(1): 75-84.
- Martin P**, Leibovich SJ. Inflammatory cells during wound repair: the good, the bad and the ugly. *Trends in Cell Biology* 2005; 15: 599-607.
- McClary KB**, Ugarova T, Grainger DW. Modulating fibroblast adhesion, spreading, and proliferation using self-assembled monolayer films of alkylthiolates on gold. *Journal of Biomedical Materials Research* 2000; 50 (3): 428-239.
- Meredith JC**, Sormana JL, Keselowsky BG, Garcia AJ, Tona A, Karim A, Amis EJ. Combinatorial characterization of cell interactions with polymer surfaces. *Journal of Biomedical Materials Research* 2003; 66A(3): 483-490.
- Morris NS**, Stickler DJ. Encrustation of indwelling urethral catheters by *Proteus mirabilis* biofilms growing in human urine. *Journal of Hospital Infection* 1998; 39: 227-234.
- Myers SR**, Grady J, Soranzo C, Sanders R, Green C, Leigh IM, Navsaria HA. A hyaluronic acid membrane delivery system for cultured keratinocytes: clinical "take" rates in the porcine kerato-dermal model, *Journal of Burn Care and Rehabilitation* 1997; 18: 214-222.

**Nagai Y**, Unsworth LD, Koutsopoulos S, Zhang SG. Slow release of molecules in self-assembling peptide nanofiber scaffold. *Journal of Controlled Release* 2006; 115(1): 18-25.

**Noh HK**, Lee SW, Kim JM, Oh JE, Kim KH, Chung CP, Choi SC, Park WH, Min BM. Electrospinning of chitin nanofibers: Degradation behavior and cellular response to normal human keratinocytes and fibroblasts. *Biomaterials* 2006; 27(21): 3934-3944.

**Nomi M**, Atala A, Coppi PD, Soker S. Principals of neovascularization for tissue engineering, *Molecular Aspects of Medicine* *Molecular Aspects to Medicine* 2002; 23: 463-483.

**Pal S**, Tak YK, Song JM. Does the antibacterial activity of silver nanoparticles depend on the shape of the nanoparticle? A study of the gram-negative bacterium *Escherichia coli*. *Applied and Environmental Microbiology* 2007; 73(6): 1712-1720.

**Papini R**. Management of burn injuries of various depths. *British Medical Journal* 2004; 329; 158-160.

**Park A.**, Baddiel C. Rheology of stratum corneum i. a molecular interpretation of the stress-strain curve. *Journal of the Society of Cosmetic Chemists* 1972; 23: 3-12.

**Park HJ**, KIm JY, Kim J, Lee JH, Hahn JS, Gu MB, Yoon J. Silver-ion-mediated reactive oxygen species generation affecting bactericidal activity. *Water Research* 2009; 43: 1027-1032.

**Park KE**, Jung SY, Lee SJ, Min BM, Park WH. Biomimetic nanofibrous scaffolds: Preparation and characterization of chitin/silk fibroin blend nanofibers. *International Journal of Biological Macromolecules* 2006; 38(3-5): 165-173.

**Park KE**, Kang HK, Lee SJ, Min BM, Park WH. Biomimetic nanofibrous scaffolds: Preparation and characterization of PGA/Chitin blend nanofibers. *Biomacromolecules* 2006; 7(2): 635-643.

**Pattison MA**, Webster TJ, Haberstroh KM. Select bladder smooth muscle cell functions were enhanced on three-dimensional, nano-structured poly (ether urethane) scaffolds. *Journal of Biomaterials Science, Polymer Edition* 2006; 17 (11): 1317-1332.

**Pham QP**, Sharma U, Mikos AG. Electrospinning of polymeric nanofibers for tissue engineering applications: A review. *Tissue Engineering* 2006; 12 (5): 1197-1211.

**Ponec M**. Skin constructs for replacement of skin tissues for in vitro testing. *Advanced Drug Delivery Review* 2002; 54 (Suppl 1): 19-S30.

**Posgai R**, Cipolla-McCulloch CB, Murphy KR, Hussain SM, Rowe JJ. Differential toxicity of silver and titanium dioxide nanoparticles on *Drosophila*

melanogaster development, reproductive effort, and viability: Size, coatings and antioxidants matter. *Chemosphere* 2011; 85: 34-42.

**Putthanarat S**, Eby RK, Kataphinan W, Jones S, Naik R, Reneker DH, Farmer BL. Electrospun Bombyx mori gland silk. *Polymer* 2006; 47 (15): 5630-5632.

**Ramalingam M**, Seeram R. Nano-featured scaffolds for tissue engineering: a review of spinning methodologies. *Tissue Engineering* 2006; 12(3): 437-447.

**Ramay HR**, Li ZS, Shum E, Zhang MQ. Chitosan-Alginate porous scaffolds reinforced by hydroxyapatite nano- and micro-particles: Structural, mechanical, and biological properties. *Journal of Biomedical Nanotechnology* 2005; 1(2): 151-160.

**Reneker DH**, Chun I. Nanometre diameter fibres of polymer, produced by electrospinning. *Nanotechnology* 1996; 7(3): 216-223.

**Riley DM**, Classen DC, Stevens LE, Burke JP. A large randomized clinical trial of a silver-impregnated urinary catheter: lack of efficacy and staphylococcal superinfection. *American Journal of Medicine* 1995; 98:349-356.

**Robinson MK**, R. Osborne, M.A. Perkins, Strategies for the assessment of acute skin irritation potential. *Journal of Pharmacology and Toxicological Methods* 1999; 42: 1-9.

**Sachlos E**, Gotora D, Czernuszka JT. Collagen scaffolds reinforced with biomimetic composite nano-sized carbonate-substituted hydroxyapatite crystals and shaped by rapid prototyping to contain internal microchannels. *Tissue Engineering* 2006; 12 (9): 2479-2487.

**Saiag P**, Coulomb B, Lebreton C, Bell E, Dubertret L. Psoriatic fibroblasts induce hyperproliferation of normal keratinocytes in a skin equivalent model in vitro. *Science* 1985; 230: 669-672.

**Sangsanoh P**, Supaphol P. Stability improvement of electrospun chitosan nanofibrous membranes in neutral or weak basic aqueous solutions. *Biomacromolecules* 2006; 7(10): 2710-2714.

**Senador AE**, Shaw MT, Mather PT. Electrospinning of polymeric nanofibers: Analysis of jet formation. *Materials Research Society Symposium Proceedings* 2001; 661: 591-596.

**Shan B**, Cai YZ, Brooks JD, Corke H. Antibacterial properties of Polygonum cuspidatum roots and their major bioactive constituents. *Food Chemistry* 2008; 109: 530-537.

**Sheila M**. progress and opportunities for tissue-engineered skin. *Nature* 2007; 445 (7130): 874-880.

**Shimizu K**, Ito A, Honda H. Enhanced cell-seeding into 3D porous scaffolds by use of magnetite nanoparticles. *Journal of Biomedical Materials Research Part B: Applied Biomaterials* 2006; 77B(2): 265-272.

**Shin** YM, Hohman MM, Brenner MP, Rutledge GC. Experimental characterization of electrospinning: The electrically forced jet and instabilities. *Polymer* 2001; 42(25): 9955-9967.

**Shum** AWT, Mak AFT. Morphological and biomechanical characterization of in vitro degradation of PGA scaffolds. *Polymer Degradability and Stability* 2003; 81(1): 141-149.

**Simon** CG, Eidelman N, Kennedy SB, Sehgal A, Khatri CA, Washburn NR. Combinatorial screening of cell proliferation on poly (L-lactic acid)/poly (D, L-lactic acid) blends. *Biomaterials* 2005; 26(34): 6906-6915.

**Singh** A, Hede S, Sastry M. Spider silk as an active scaffold in the assembly of gold nanoparticles and application of the gold-silk bioconjugate in vapor sensing. *Small* 2007; 3(3): 466-473.

**Sukigara** S, Gandhi M, Ayutsede J, Micklus M, Ko F. Regeneration of Bombyx mori silk by electrospinning - part 1: processing parameters and geometric properties. *Polymer* 2003; 44(19): 5721-5727.

**Sukigara** S, Gandhi M, Ayutsede J, Micklus M, Ko F. Regeneration of Bombyx mori silk by electrospinning. Part 2. Process optimization and empirical modeling using response surface methodology. *Polymer* 2004; 45(11): 3701-3708.

**Tachibana** A, Furuta Y, Takeshima H et al. Fabrication of wool keratin sponge scaffolds for long-term cell cultivation. *Journal of Biotechnology* 2002; 93:165-170.

**Tan** EPS, Lim CT. Characterization of bulk properties of nanofibrous scaffolds from nanomechanical properties of single nanofibers. *Journal of Biomedical Materials Research* 2006; 77A(3): 526-533.

**Tan** PX, Liu XX, Li JC, He JH. Study on the inhibit mechanism primarily of extracts from coptis on clinical resistant the medicine of Staphylococcus aureus. *Journal of Chinese Medicinal Materials* 2011; 34(10): 1575-1579.

**Thomas** V, Yallapu MM, Sreedhar B, Bajpai SK. A versatile strategy to fabricate hydrogel-silver nanocomposites and investigation of their antimicrobial activity. *Journal of Colloid and Interface Science* 2007; 315: 389-395.

**Torres** FG, Nazhat SN, Fadzullah SHSM, Maquet V, Boccaccini AR. Mechanical properties and bioactivity of porous PLGA/TiO<sub>2</sub> nanoparticle-filled composites for tissue engineering scaffolds. *Composites Science and Technology* 2007; 67(6): 1139-1147.

**Tumbar** T. Epithelial skin stem cells. *Methods in Enzymology* 2006; 419: 73-99.

**Tumbar** T, Guasch G, Greco V, Blanpain C, Lowry WE, Rendl M, Fuchs E. Defining the epithelial stem cell niche in skin. *Science* 2004; 303: 359-363.

**Uccioli L.** A clinical investigation on the characteristics and outcomes of treating chronic lower extremity wounds using the TissueTech Autograft System. *The International Journal of Lower Extremity Wounds* 2003; 2: 140-151.

**Vacanti CA, Mikos AG.** Letter from the editors. *Tissue Engineering* 1995; 1: 1-2.

**Venugopal JR, Zhang YZ, Ramakrishna S.** In vitro culture of human dermal fibroblasts on electrospun polycaprolactone collagen nanofibrous membrane. *Artificial Organs* 2006; 30 (6): 440-446.

**Walder B, Pittet D, Tramer MR.** Prevention of bloodstream infections with central venous catheters treated with anti-infective agents depends on catheter type and insertion time: evidence from a meta-analysis. *Infection Control and Hospital Epidemiology* 2002; 23:748-756.

**Washburn NR, Yamada KM, Simon CG, Kennedy SB, Amis EJ.** High-throughput investigation of osteoblast response to polymer crystallinity: Influence of nanometer-scale roughness on proliferation. *Biomaterials* 2004; 25(1-2): 1215-1224.

**Wei GB, Jin QM, Giannobile WV, Ma PX.** Nano-fibrous scaffold for controlled delivery of recombinant human PDGF-BB. *Journal of Controlled Release* 2006; 112 (1): 103-110.

**Welss T, D.A. Basketter, K.R. Schroder,** In vitro skin irritation: facts and future. State of the art review of mechanisms and models, *Toxicology In Vitro* 2004; 18: 231-243.

**Wong JJ, Bronzino JD.** *Biomaterials.* CRC press. Taylor & Francis Group, LLC. 2007; *Biomaterials, Biocompatibility:* pp 3-20; *Biodegradation, Tissue Engineering:* pp6-16.

**Woodfield TBF, Malda J, de Wijn J, Peters F, Riesle J, van Blitterswijk CA.** Design of porous scaffolds for cartilage tissue engineering using a three-dimensional fiber-deposition technique. *Biomaterials* 2004; 25: 4149-4161.

**Wu R, Xu LF, Ye S.** The experimental observation of the inhibitory effect of ten traditional Chinese medicine (TCM) preparation on enteropathogenic E.coli O86:H2 in vitro. *Journal of Practical Medical Techniques* 2008; 15(8): 1008-1010.

**Xie Y, S.C. Rizzi, R. Dawson, E. Lynam, S. Richards, D.I. Leavesley, Z. Upton,** Development of a three-dimensional human skin equivalent wound model for investigating novel wound healing therapies, *Tissue Engineering Part C: Methods* 2010; 16: 1111-1123.

**Yamauchi K, Maniwa M, Mori T.** Cultivation of fibroblast cells on keratin-coated substrata. *Journal of Biomaterials Science, Polymer Edition* 1998; 9 (3): 259-270.

**Yannas IV and Burke JF.** Design of an artificial skin. I. Basic design principles. *Journal of Biomedical Materials Research* 1980; 14: 65-81.

- Yarin** AL, Koombhongse S, Reneker DH. Taylor cone and jetting from liquid droplets in electrospinning of nanofibers. *Journal of Applied Physics* 2001; 90(9): 4836-4846.
- Ye** P, Xu ZK, Wu J, Innocent C, Seta P. Nanofibrous poly (acrylonitrile-co-maleic acid) membranes functionalized with gelatin and chitosan for lipase immobilization. *Biomaterials* 2006; 27(22): 4169-4176.
- Yeo** SY, Lee HJ, Jeong SH. Preparation of nanocomposite fibers for permanent antibacterial effect. *Journal of Materials Science* 2003; 38: 2143-2147.
- Yoon** K, Kim K, Wang XF, Fang DF, Hsiao BS, Chu B. High flux ultrafiltration membranes based on electrospun nanofibrous PAN scaffolds and chitosan coating. *Polymer* 2006; 47(7): 2434-2441.
- You** CG, Han CM, Wang XG, Zheng YR, Li QY, Hu XL, Sun HF. The progress of silver nanoparticles in the antibacterial mechanism, clinical application and cytotoxicity. *Molecular Biology Report* 2012; 39: 9193-9201.
- Yuan** XY, Mak AFT, Yao KD. Comparative observation on accelerated degradation of poly (L-lactic acid) fibers in phosphate buffered saline and a dilute alkaline solution. *Polymer Degradability and Stability* 2002; 75(1): 45-53.
- Yuan** XY, Mak AFT, Yao KD. In vitro degradation of poly (L-lactic acid) fibers in phosphate buffered saline. *Journal of Applied Polymer Science* 2002; 85(5): 936-943.
- Yuan** XY, Mak AFT, Yao KD. Surface degradation of poly (L-lactic acid) fibers in a concentrated alkaline solution. *Polymer Degradability and Stability* 2003; 79(1): 45-52.
- Zacchi** V, Soranzo C, Cortivo R, Radice M, Brun P, Abatangelo G. In vitro engineering of human skin like tissue. *Journal of Biomedical Materials Research* 1998; 40 (2): 187-194.
- Zhong** SP, Teo WE, Zhu X, Beuerman R, Ramakrishna S, Yung LYL. Formation of collagen-glycosaminoglycan blended nanofibrous scaffolds and their biological properties. *Biomacromolecules* 2005; 6(6): 2998-3004.
- Zong** S, Cao Y, Zhou Y, Ju H. Zirconia nanoparticles enhanced grafted collagen tri-helix scaffold for unmediated biosensing of hydrogen peroxide. *Langmuir* 2006; 22(21): 8915-8919.